

EMB 50 Series

REPORTS

UNCLASSIFIED

AD 2 2 4 7 6 1

DEFENSE DOCUMENTATION CENTER

FOR

SCIENTIFIC AND TECHNICAL INFORMATION

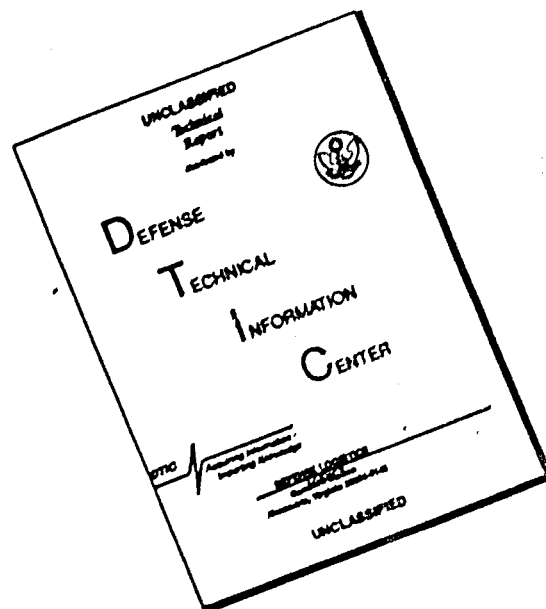
CAMERON STATION, ALEXANDRIA, VIRGINIA



UNCLASSIFIED

NOTICE: When government or other drawings, specifications or other data are used for any purpose other than in connection with a definitely related government procurement operation, the U. S. Government thereby incurs no responsibility, nor any obligation whatsoever; and the fact that the Government may have formulated, furnished, or in any way supplied the said drawings, specifications, or other data is not to be regarded by implication or otherwise as in any manner licensing the holder or any other person or corporation, or conveying any rights or permission to manufacture, use or sell any patented invention that may in any way be related thereto.

DISCLAIMER NOTICE



THIS DOCUMENT IS BEST QUALITY AVAILABLE. THE COPY FURNISHED TO DTIC CONTAINED A SIGNIFICANT NUMBER OF PAGES WHICH DO NOT REPRODUCE LEGIBLY.

NAVY DEPARTMENT
THE DAVID W. TAYLOR MODEL BASIN
Washington 7, D. C.

DDC

1976

TESTS OF TWENTY RELATED MODELS OF
V-BOTTOM MOTOR BOATS
EMB SERIES 50

DDC
RECEIVED
JUN 20 1964
DDC-IRA B

MARCH 1949

Revised Edition

REPORT R-47

Tests of Twenty Related Models
of
V-Bottom Motor Boats

E.M.B. SERIES 50

for

The David Taylor Model Basin

REPORT NO. 170

by

Kenneth S. M. Davidson
and
Anthony Suarez

October 28, 1941

Revised December 1948

EXPERIMENTAL TOWING TANK
Stevens Institute of Technology
Hoboken, New Jersey

FOREWORD

This report is a revision of a former report, bearing the same title and number, published by the David Taylor Model Basin in October 1941. The original report was compiled by the Stevens Institute of Technology and dealt with a series of tests conducted in the Stevens Experimental Towing Tank at the request of Taylor Model Basin. The revision, based on subsequent work done at Stevens, consisted principally in the addition of charts showing running trim and a drawing of the parent form, together with conversion factors for the other models. The original text has also been modified slightly to include suitable references to the new data.

C O N T E N T S

	Page
Introduction	1
Results	3
Resistances	3
Charts	Pages 12 to 45
Contours of Running Trim	6
Charts	Pages 46 to 79
Longitudinal Centers of Gravity	6
Charts	Pages 80 to 83
Wetted Surfaces	6
Charts	Pages 84 to 94
Porpoising	7
Charts	Pages 95 to 103

INTRODUCTION

This report presents the principal results of an investigation of the effects on the performance of V-bottom boats of variations in proportions and loading, in a form for ready use by designers. Tabulations of the complete test data are on file for reference at the Experimental Towing Tank, Stevens Institute of Technology, Hoboken, New Jersey, and at the David W. Taylor Model Basin, Carderock, Maryland.

Tests were made of a series of twenty models derived from a single parent form. The models were designed at the United States Experimental Model Basin, Washington, D. C., and are designated U.S.E.M.B. Series 50.

The models were 40 inches in length and had:

displacement-length ratios, $\Delta / \left(\frac{L}{100}\right)^3$ 40, 80, 120, 160

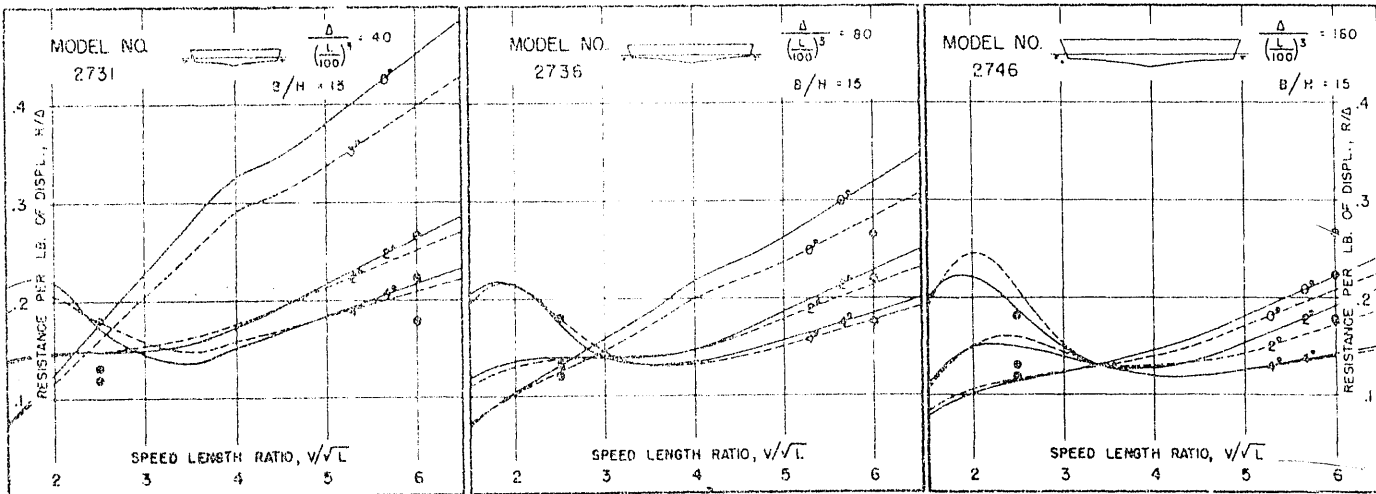
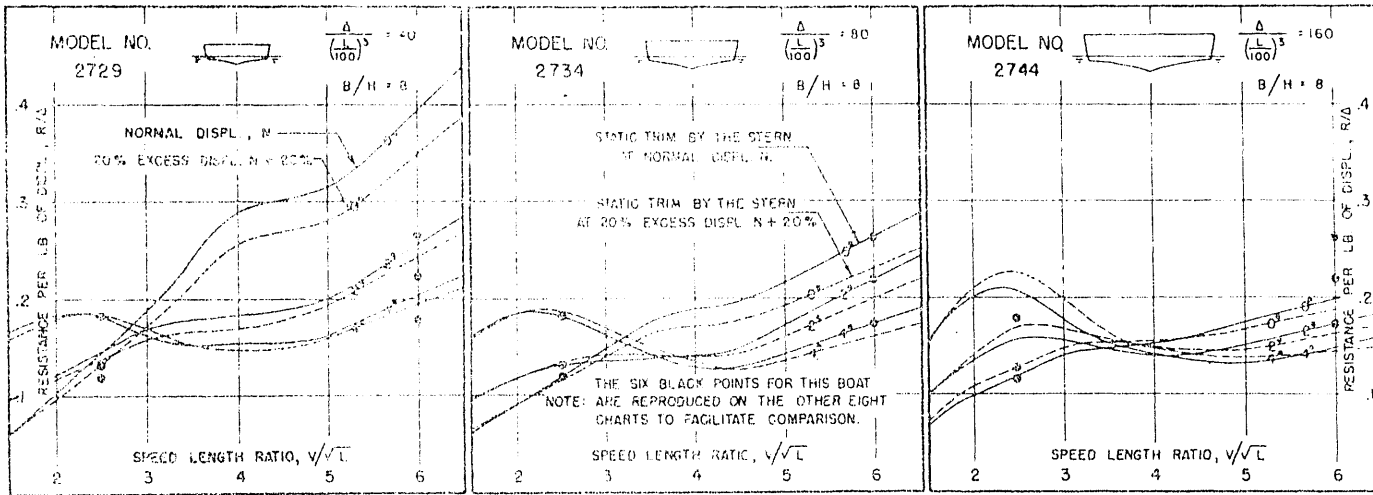
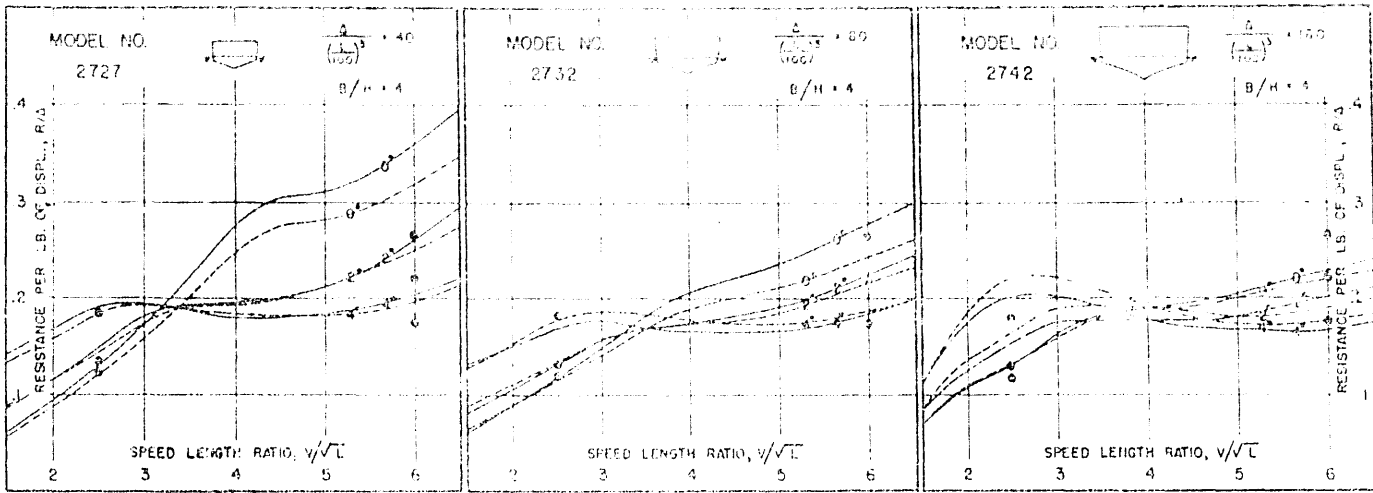
beam-draft ratios, B/H 4, 6, 8, 11, 15

Page 8 gives the dimensions and particulars of the twenty models together with the multipliers used to obtain the offsets of the series models from the parent model. The lines and offsets of the parent design,

$\left[\Delta / \left(\frac{L}{100}\right)^3 = 110; B/H = 5.3\right]$, are shown on page 9. A photograph of the twenty models is included, page 11.

The tow point for all models was 1/2 inch above the designed L.W.L. and at the midlength.

The investigation was made for the David W. Taylor Model Basin, Carderock, Maryland, under United States Navy Contracts Nos. N171s-50126 and N171s-54701.



$\frac{R_{TOTAL}}{\Delta}$ vs. $\frac{V}{\sqrt{L}}$ FOR THE CENTRAL AND THE EIGHT EXTREME MODELS OF THE SERIES
SIX LOADING CONDITIONS ARE SHOWN FOR EACH MODEL.

Resistances

The chart on page 2 provides a comprehensive overall view of the resistances. This chart brings out clearly:

- 1) the major importance of static trim,
- 2) the pronounced importance of displacement-length ratio,
- 3) the relatively lesser importance of both beam-draft ratio and excess displacement.

The contour charts on pages 13-45, incl., define the resistances in detail. These charts provide a broad system of resistance data for V-bottom forms, comparable in general to that provided for steamship forms by the contour charts for Taylor's Standard Series in THE SPEED AND POWER OF SHIPS.

There are three sets of contour charts:

for normal displacement, N	pages 13-23
for 10% excess displacement, N + 10%	pages 24-34
for 20% excess displacement, N + 20%	pages 35-45

The three charts on each page are for three values of static trim by the stern, τ , at constant speed-length ratio, V/\sqrt{L} .

It will be seen that, in laying out the Series 50 models, the procedure for systematically varying the model proportions followed the precedent established by Taylor's Standard Series of steamship forms in that variations were made in displacement-length ratio and beam-draft ratio, both factors being based upon the designed L.W.L. of the parent form. This procedure, with the logical extension of the test program to include given angular changes of static trim, fixed the form of presentation for the resistance contour charts.

In the actual design of a V-bottom boat, however, the factors most readily fixed in the early stages will usually be:

- | | |
|-----------------------------------|------------|
| a) Length | L, |
| b) Displacement | Δ , |
| c) Longitudinal Center of Gravity | L.C.G., |
| d) Beam | B; |

a) and b) emerging first, followed by c) when a preliminary weight distribution has been worked out, and then by d). These factors fix:

$$\Delta / \left(\frac{L}{100} \right)^3, \text{ L.C.G./L, and } B/L;$$

but they do not fix:

$$B/H \text{ or } \tau$$

both of which necessarily appear as parameters on the resistance contour charts. Hence, to make a preliminary estimate of power required, on the basis of the Series 50 resistance contours, it will usually be necessary, first, to transform

given values of B/L and $L.C.G./L$ into the equivalent values of B/H and τ for the Series 50 form.

The same problem may often arise in selecting the Series 50 form which corresponds to a given finished design, for the purpose of comparing the power requirements. For V-bottom forms in general, neither B/H nor τ has the simple, straightforward significance either has for steamship forms; H depends upon the amount and longitudinal variation of the deadrise, and τ upon the transom beam and the up-sweep of the buttocks aft. It will usually be desirable, then, to define correspondence between the two forms in terms of the same basic factors, a), b), c), d), listed in the previous paragraph.

The following notes relate to the transformation of B/L to B/H , and of $L.C.G./L$ to τ , for Series 50 forms.

B/L to B/H

Writing Volume = $K_1 \times B \times H \times L$, where K_1 is the block coefficient
for the Series 50 form = 0.407

$$\text{and } H = \frac{B}{B/H}$$

$$\text{then Volume} = K_1 \frac{B^2}{B/H} L$$

$$\text{or } B/H = \frac{K_1 B^2 L}{\text{Volume}}$$

dividing the righthand side by L^3/L^3

$$B/H = K_1 \frac{(B/L)^2}{\text{Volume}/L^3}$$

$$\text{or } B/H = K_2 \frac{(B/L)^2}{4 \left(\frac{L}{100} \right)^3}, \text{ where } K_2 = 1.16 \times 10^4.$$

This formula contains the necessary factors for the transformation.

L.C.G./L to τ

The static trim can be obtained by interpolation from the contour charts of L.C.G. described in the next section. Although an equation could be worked out for this relationship, it would be much less simple to use than the contour charts.

Example of E.H.P. Estimate. Suppose it is desired to find the E.H.P. of a Series 50 form having the following particulars (or of the Series 50 form corresponding to a given form having the same particulars), at the indicated speed:

V = 35 knots	
L	60.00 feet
A (sea water)	{ 23.75 tons, designed 26.13 tons, actual (10% excess)
L.C.G.	64% of L from F.P.
B	13.45 feet

$F_y = k \tan \alpha \delta$. The effect of this force is both to decrease the displacement and to shift the L.C.G. aft to $(L.C.G.)'$.* Convert the new displacement to a per cent of the normal displacement (73.75 tons in the example given in the previous paragraph). Determine, by interpolation from the L.C.G. contour charts, a new static trim angle τ' corresponding to the new $(L.C.G.)'$ at the new percentage of normal displacement. A new value of resistance, corresponding to the changed conditions, can now be found by the procedure in (6) on page 5. A second approximation can be made if necessary.

Contours of Running Trim

The contour charts on pages 47-79 give running trims for the whole series. Running trim is defined as the change of trim, $(\Delta\tau)$, due to the forward motion of the model.

Again, there are three sets of contour charts:

for normal displacement, N	pages 47-57
for 10% excess displacement, N + 10%	pages 58-68
for 20% excess displacement, N + 20%	pages 69-79

As for the resistance contours, there are three charts on each page for three values of static trim by the stern.

Longitudinal Centers of Gravity

The contour charts on pages 81-83 define the relationship between the static trim by the stern, τ , and the position of the longitudinal center of gravity, L.C.G., for all of the models of the series. The purpose of these charts is explained in the preceding section, page 4.

There are three sets of contour charts:

for normal displacement, N	page 81
for 10% excess displacement, N + 10%	page 82
for 20% excess displacement, N + 20%	page 83

Wetted Surfaces

The contour charts on pages 85-94 define the wetted surfaces. These charts are included to permit making expansions to full size by treating the friction and residual components independently (as is usual for displacement-type vessels), if this is desired. They are necessary, in the case of V-bottom forms, because of the large variation of the wetted surface with speed.

There are two sets of contour charts:

for normal displacement, N	pages 85-89
for 20% excess displacement, N + 20%	pages 90-94

* $(L.C.G.)'$ is the position of the resultant of δ and F_y .

Once the wetted surface is determined, the expansion to full size can be carried out by the usual procedures employed for large ships, except that a friction formulation which provides satisfactory turbulent friction data for 40-inch models, such as the Schoenherr, must necessarily be adopted.

Porpoising.

It was found in the course of the resistance tests that, in many instances, a longitudinal instability developed with increase of speed, similar in character to that ordinarily described in connection with seaplanes as porpoising. Damped out for the resistance tests, this condition was subsequently studied more carefully in a separate series of tests on seven selected models of the series.

The results of these tests are summarized in the charts on page 96, which indicate limiting speed-length ratios for longitudinal stability. They are shown in detail in the graphical records of the porpoising motion of each model tested, on pages 97-103.

There is no evidence that these porpoising tests for Series 50 forms necessarily describe the porpoising characteristics of other forms of different shapes. It is believed, however, that they are reasonably indicative for most forms.

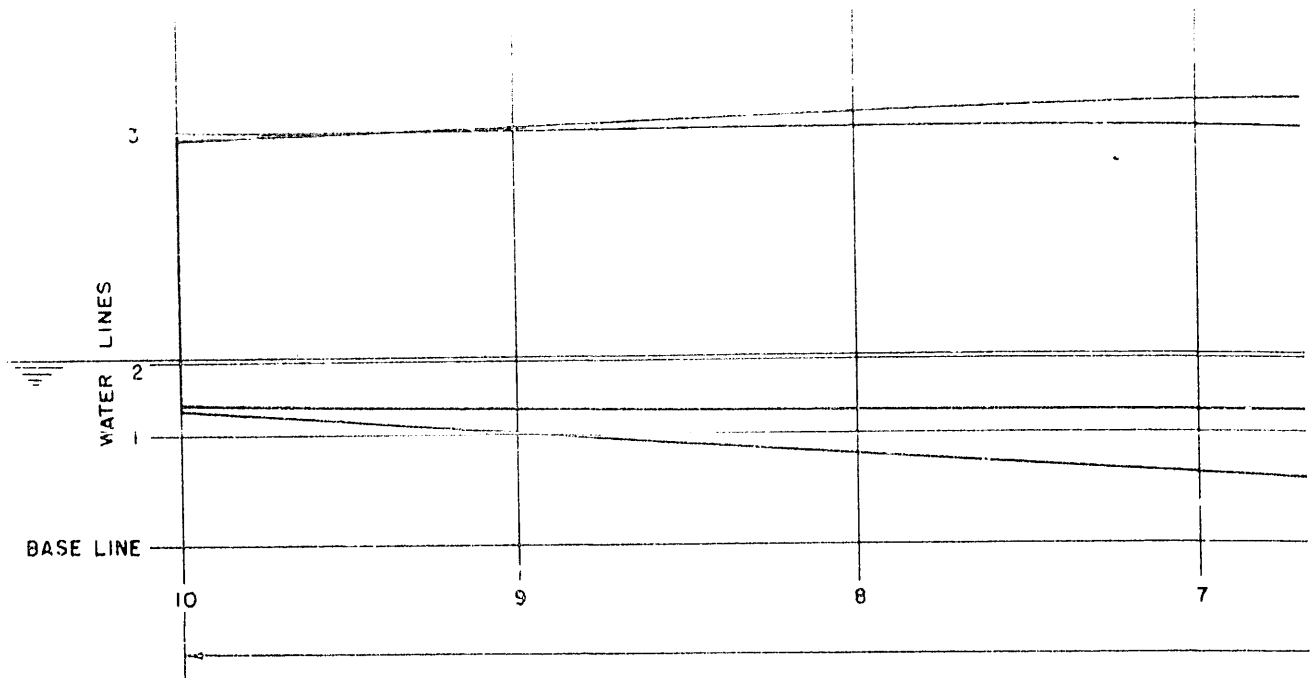
PARTICULARS AND DIMENSIONS

$\Delta / \left(\frac{L}{100}\right)^3$	Displacement pounds	B/H	4	8	11	15	
40	3.24	Model	2727	2728	2729	2730	2731
		Beam	4.760	5.827	6.725	7.890	9.215
		Draft	1.190	0.97	0.841	0.717	0.614
80	6.48	Model	2732	2733	2734	2735	2736
		Beam	6.730	8.240	9.518	11.160	13.040
		Draft	1.682	1.373	1.190	1.014	0.869
120	9.73	Model	2737	2738	2739	2740	2741
		Beam	8.240	10.100	11.650	13.660	15.960
		Draft	2.060	1.683	1.457	1.242	1.064
160	12.97	Model	2742	2743	2744	2745	2746
		Beam	9.515	11.660	13.460	15.780	18.440
		Draft	2.379	1.943	1.683	1.435	1.229

Values of beam and draft in inches.
 Beam of LWL, and draft to the rabbet.
 Model Length, 40 inches.

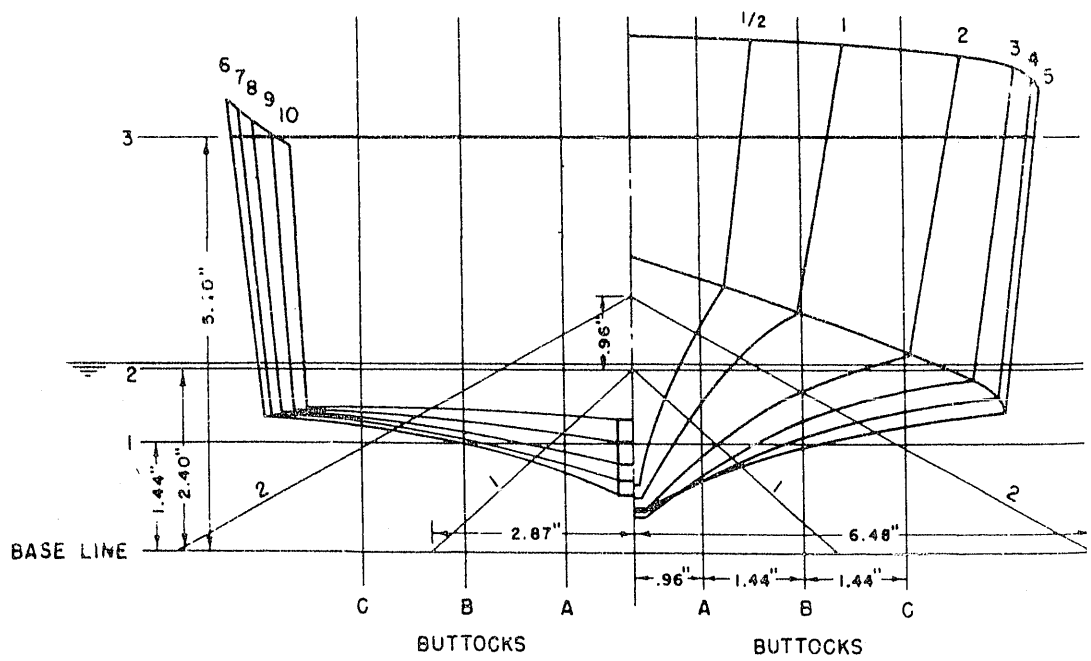
ENLARGEMENTS FROM PARENT MODEL

Model	Enlargement		Model	Enlargement	
	Beam	Draft		Beam	Draft
2727	0.4444	0.5765	2737	0.7694	0.9989
2728	0.5447	0.4705	2738	0.9431	0.8160
2729	0.6280	0.4075	2739	1.0880	0.7063
2730	0.7365	0.3475	2740	1.2760	0.6022
2731	0.8600	0.2976	2741	1.4900	0.5158
2732	0.6282	0.8160	2742	0.8884	1.1535
2733	0.7695	0.6655	2743	1.0884	0.9420
2734	0.8887	0.5770	2744	1.2570	0.8159
2735	1.0420	0.4916	2745	1.4740	0.6958
2736	1.2177	0.4213	2746	1.7220	0.5958



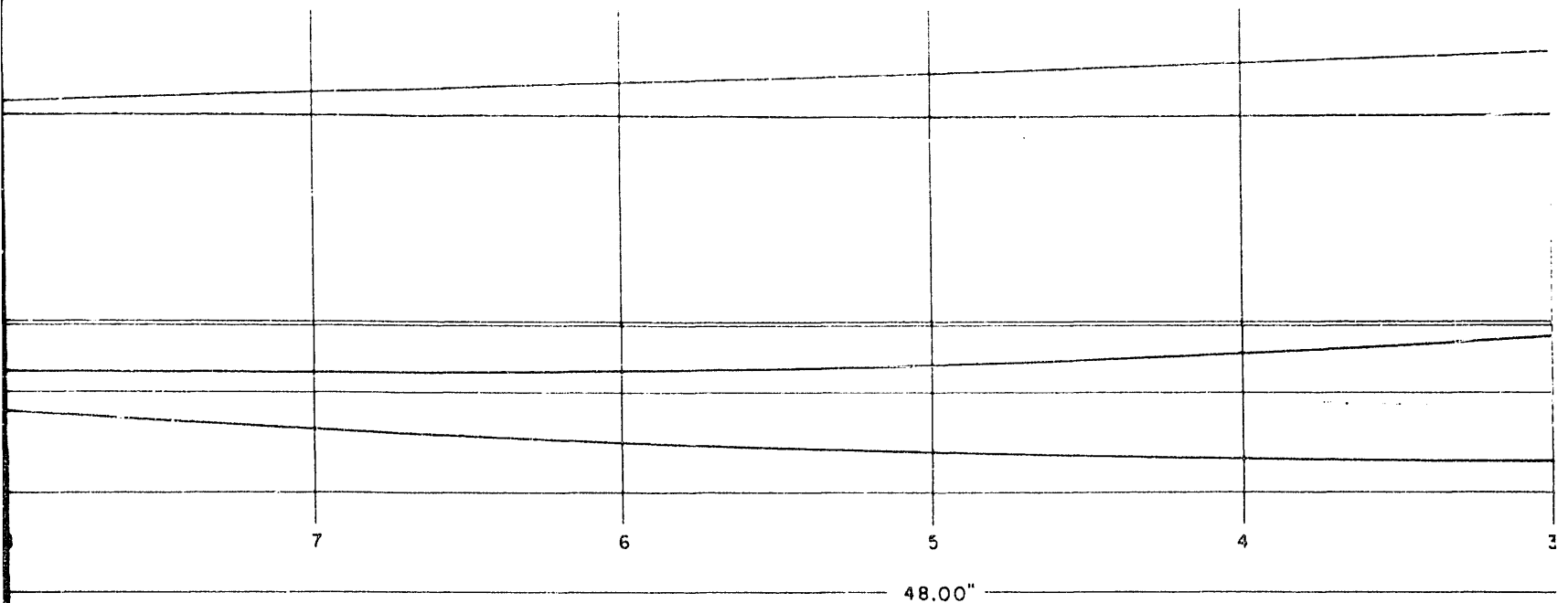
NOTE: DESIGNED L.W.L. CORRESPONDS TO STATIC TRIM BY THE STERN, $\gamma = 0^\circ$

1



9

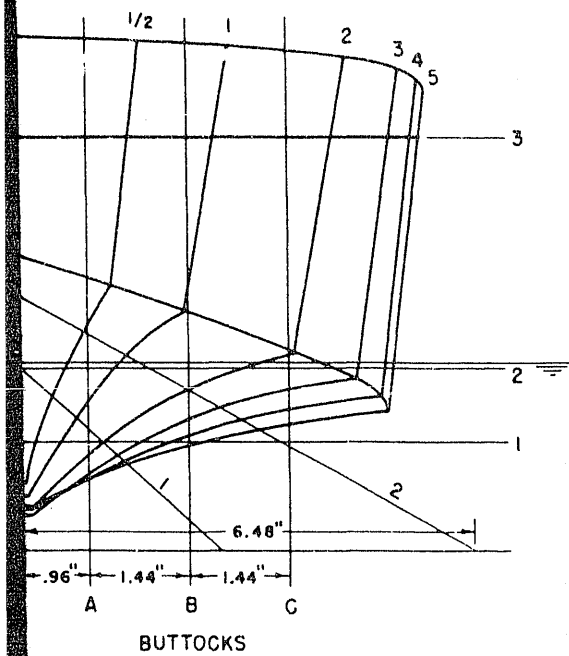
SERIES 50 PARENT LINES



THE STERN, $\gamma = 0^\circ$

TABLE OF

STATION	HALF-BREADTHS						DIAGO 1
	KEEL	WATER-LINES			CHINE	DECK	
		1	2	3			
1/2	0.15	0.24	0.63	1.55	1.285	1.72	0.595
1	0.175	0.57	1.36	2.77	2.34	2.99	1.015
2	0.195	1.23	3.22	4.44	3.915	4.64	1.54
3	0.22	1.77	4.83	5.28	4.80	5.415	1.80
4	0.23	2.21	5.225	5.59	5.175	5.685	1.93
5	0.235	2.54	5.345	5.71	5.28	5.78	1.98
6	0.24	2.61	—	5.67	5.24	5.73	1.95
7	0.24	2.32	—	5.54	5.13	5.57	1.81
8	0.24	1.68	—	5.34	4.995	5.35	1.61
9	0.24	0.24	—	5.08	4.82	5.075	1.325
10	0.24	—	—	4.81	4.63	4.81	0.985



2

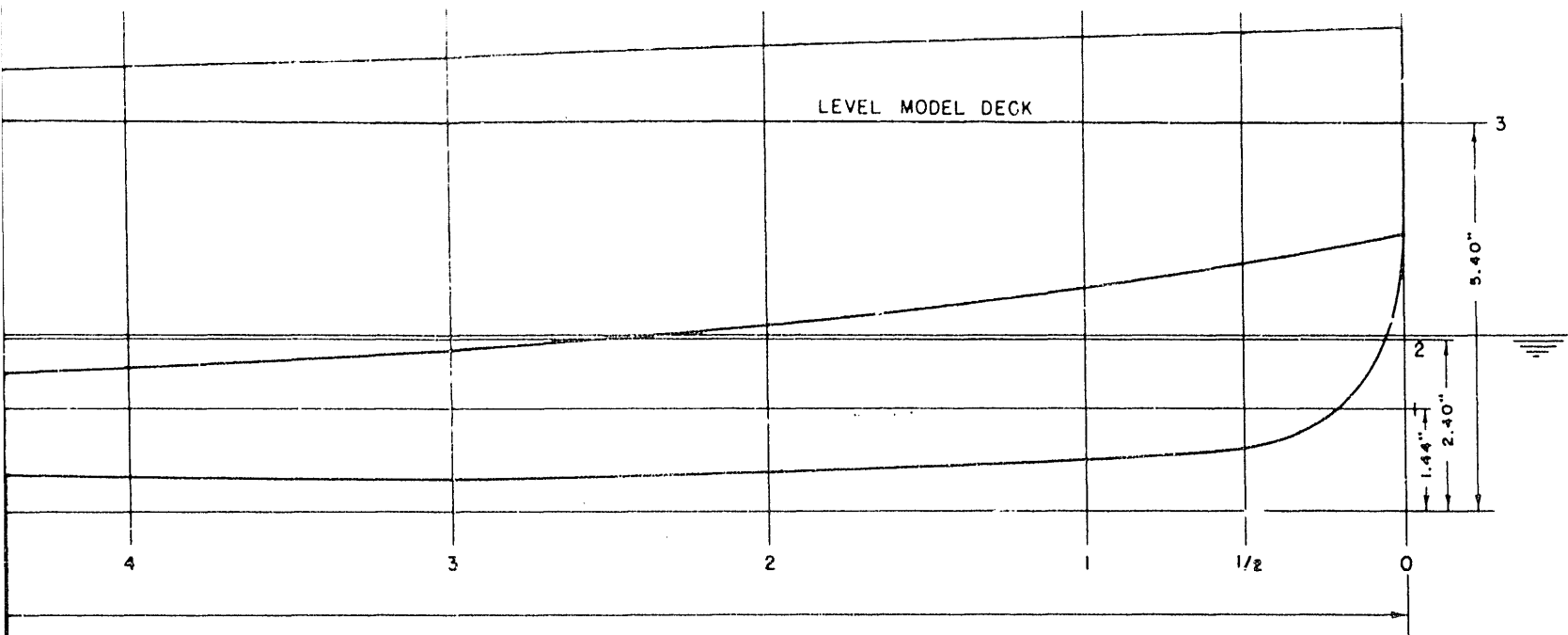
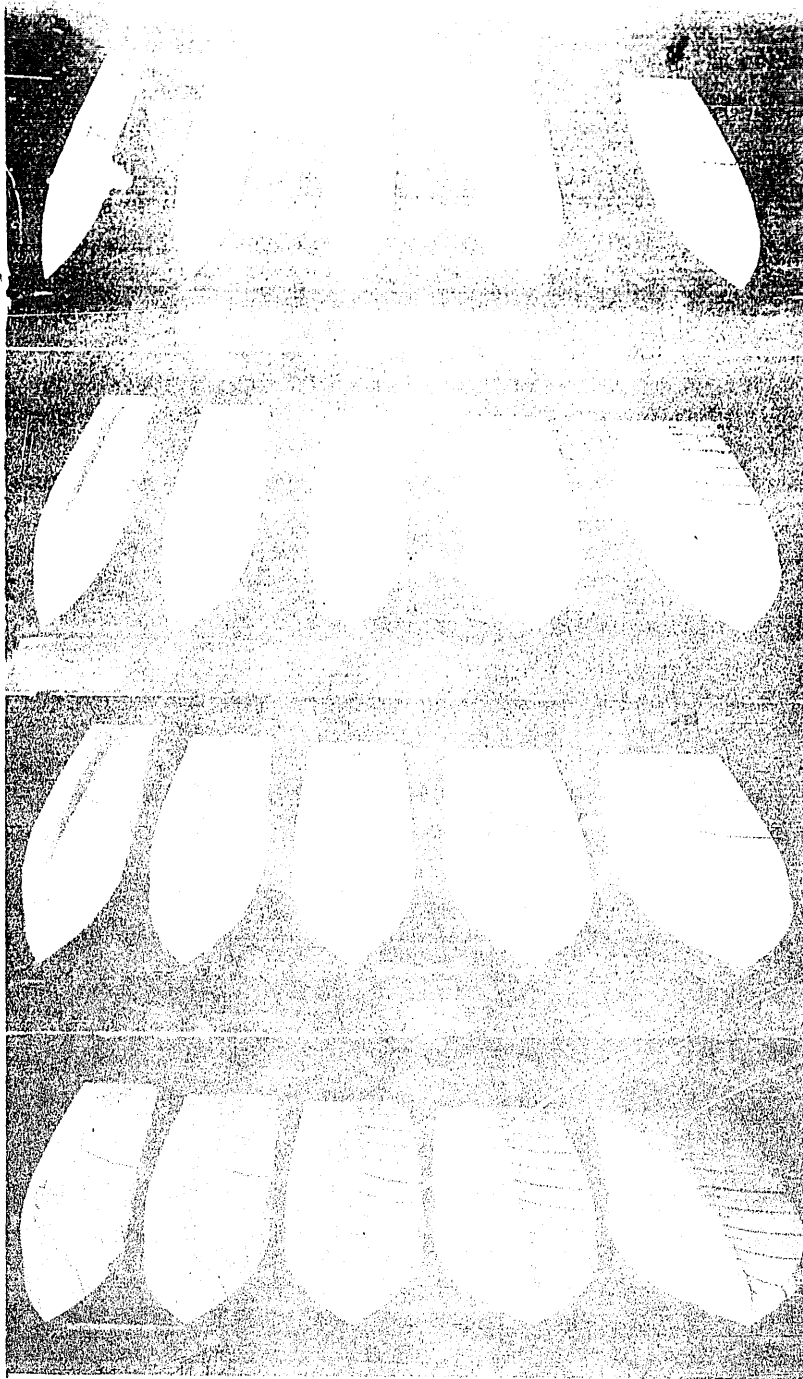


TABLE OF OFFSETS

-BREADTHS			DIAGONALS		HEIGHTS						STATION	
LINES	CHINE	DECK	1	2	KEEL	BUTTOCKS			CHINE	DECK		
						A	B	C				
3												
1.55	1.285	1.72	0.595	1.01	0.89	2.99	—	—	3.46	6.65	1/2	
2.77	2.34	2.99	1.015	1.73	0.71	1.98	—	—	3.14	6.58	1	
4.44	3.915	4.64	1.54	2.70	0.53	1.23	2.12	2.57	2.58	6.43	2	
5.28	4.80	5.415	1.80	3.235	0.46	0.985	1.705	2.095	2.22	6.29	3	
5.59	5.175	5.685	1.93	3.575	0.485	0.92	1.50	1.835	1.99	6.14	4	
5.71	5.28	5.78	1.98	3.77	0.57	0.90	1.405	1.70	1.83	6.00	5	
5.67	5.24	5.73	1.95	3.84	0.73	0.975	1.39	1.645	1.765	5.96	6	
5.54	5.13	5.57	1.81	3.785	0.94	1.125	1.46	1.665	1.745	5.71	7	
5.34	4.995	5.35	1.61	3.70	1.17	1.310	1.55	1.705	1.765	5.57	8	
5.08	4.82	5.075	1.325	3.525	1.44	1.535	1.68	1.775	1.81	5.42	9	
4.81	4.63	4.81	0.985	3.28	1.73	1.775	1.835	1.865	1.865	5.28	10	

3



40

80

120

160

Displacement-Length Ratio

4

6

8

11

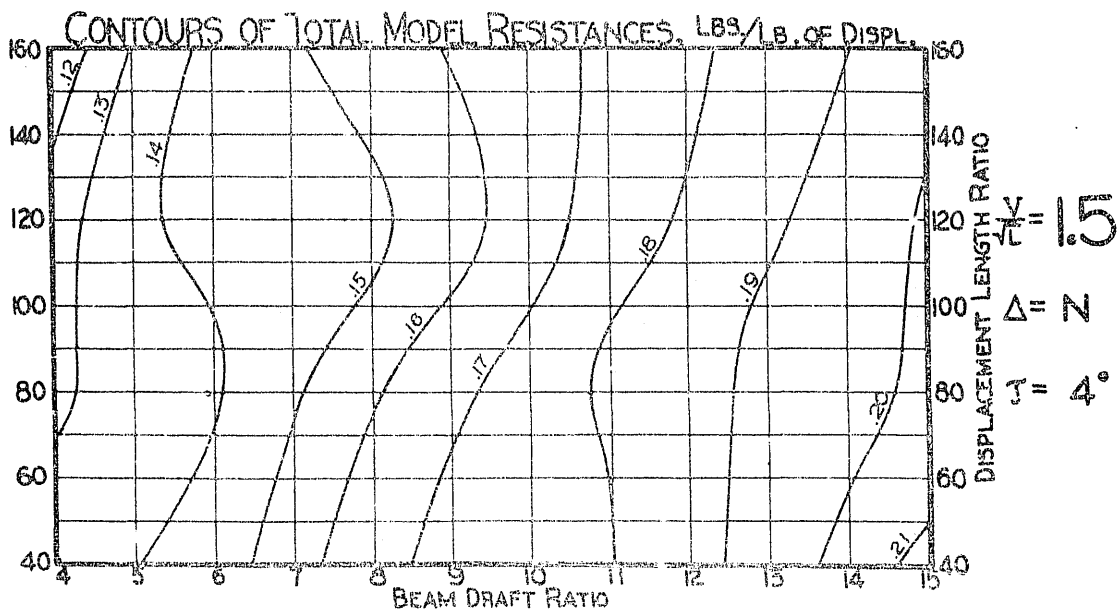
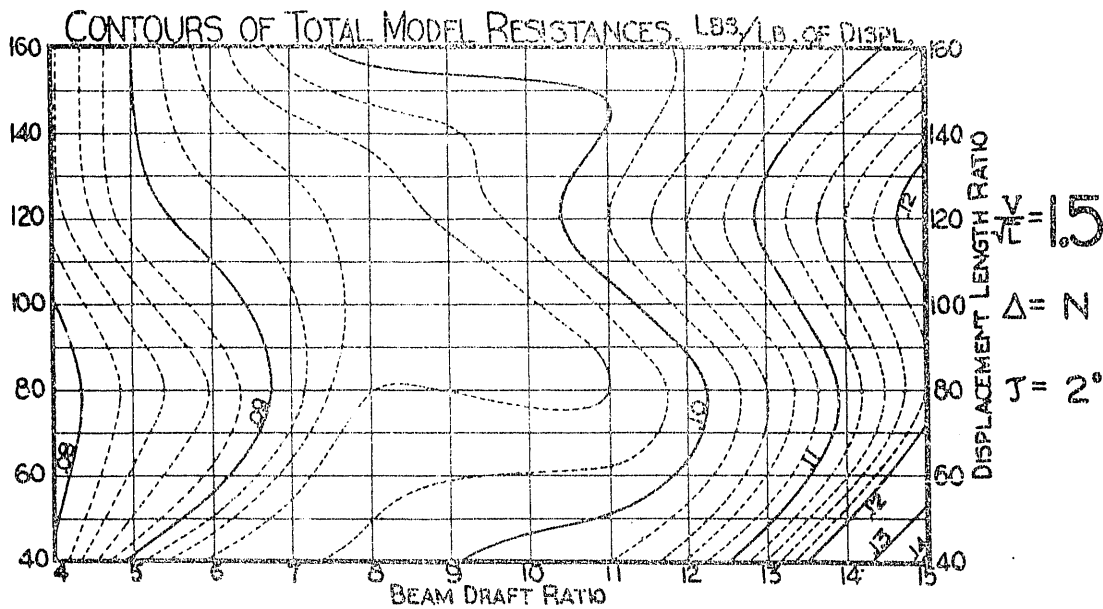
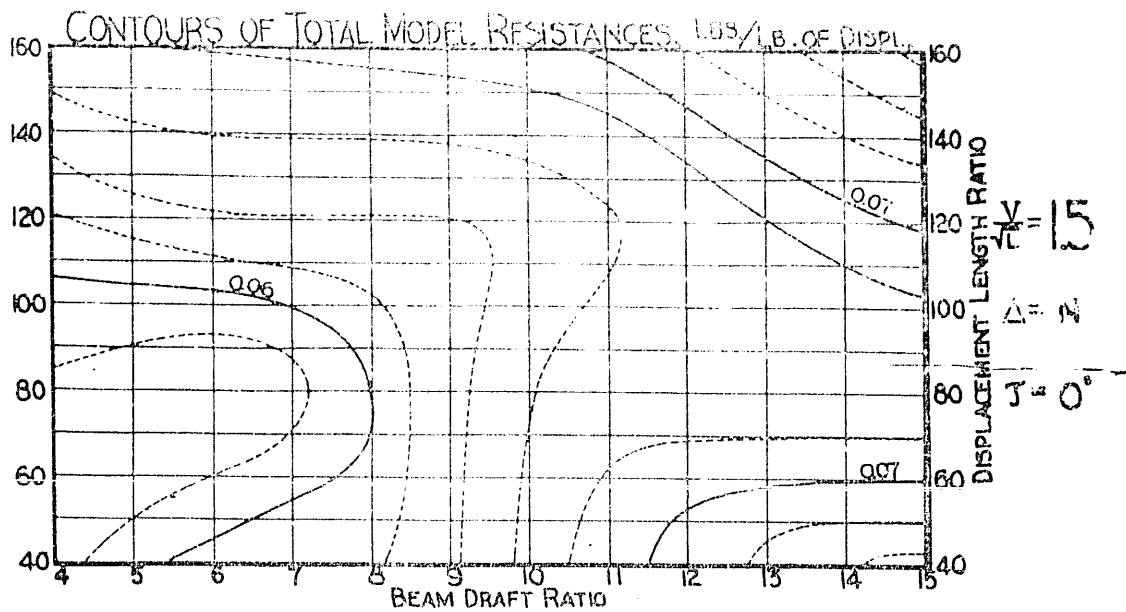
15

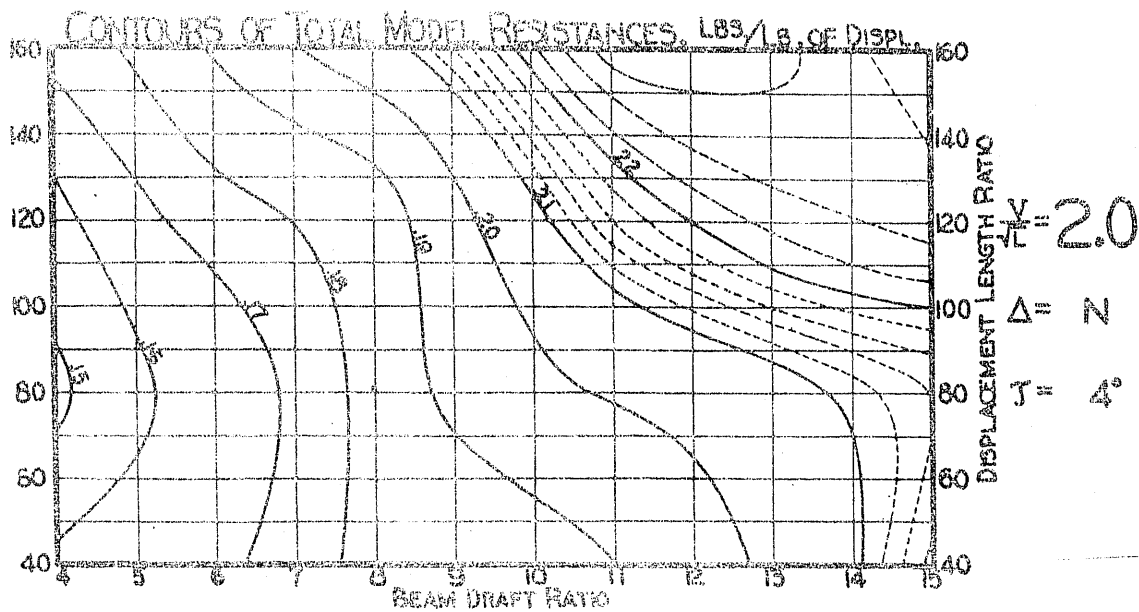
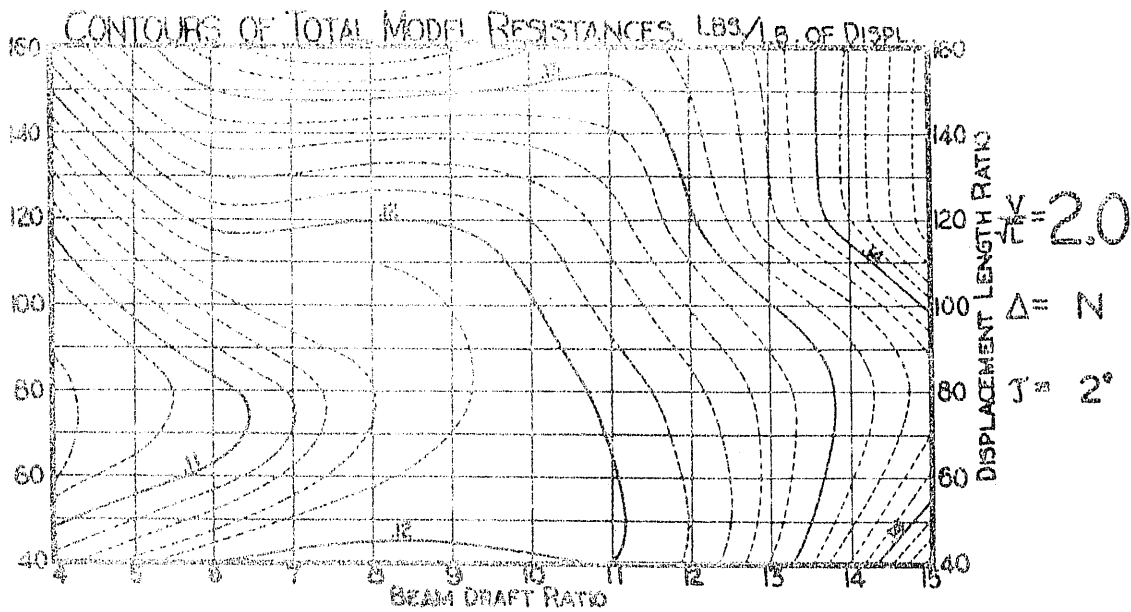
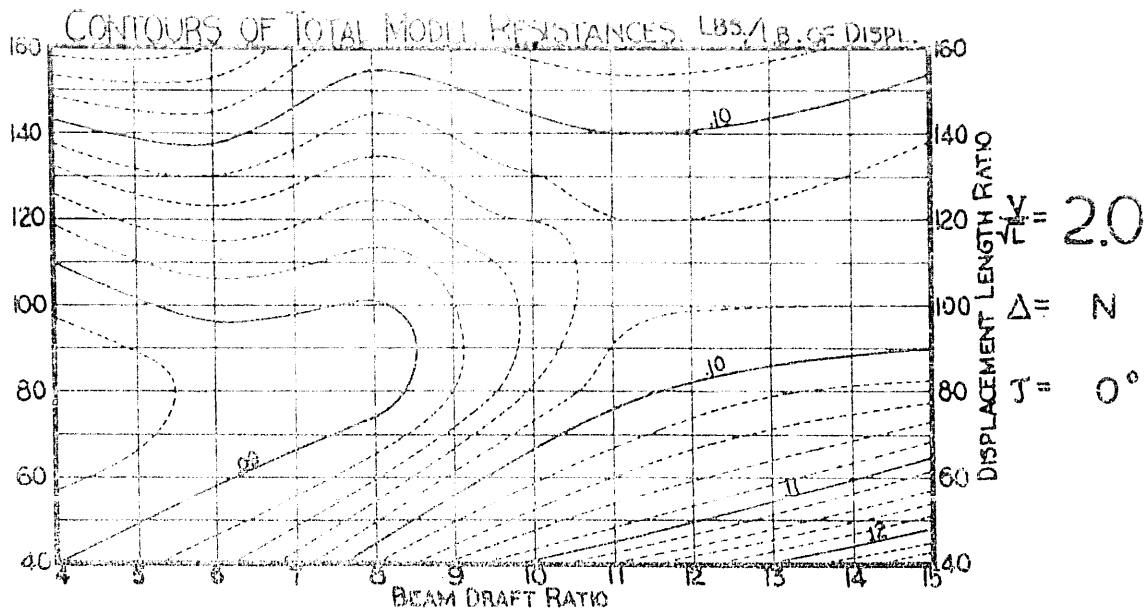
Beam-Draft Ratio

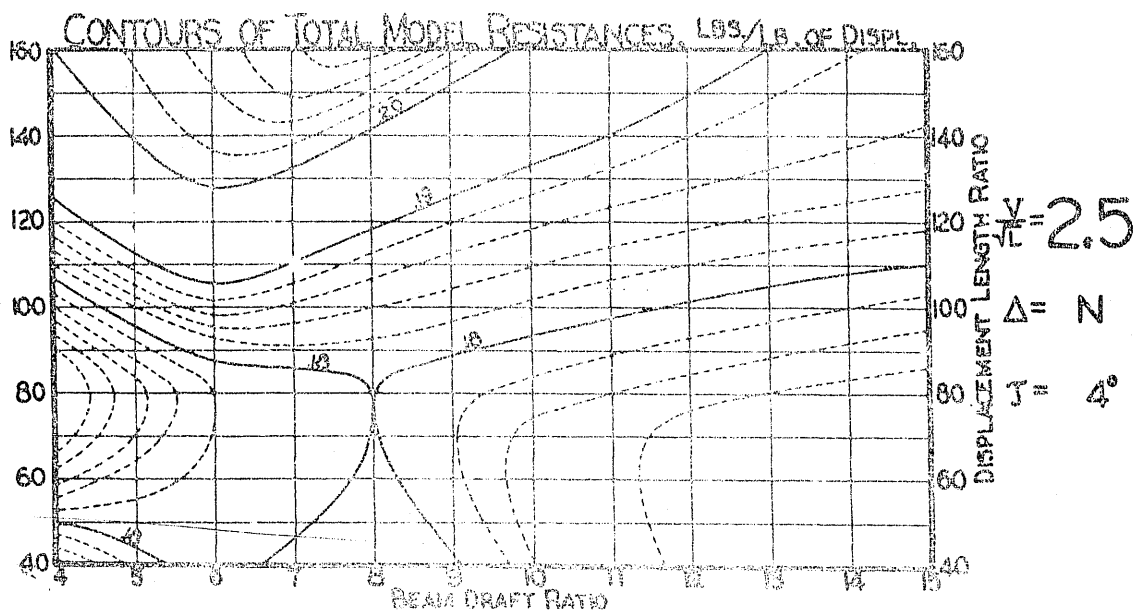
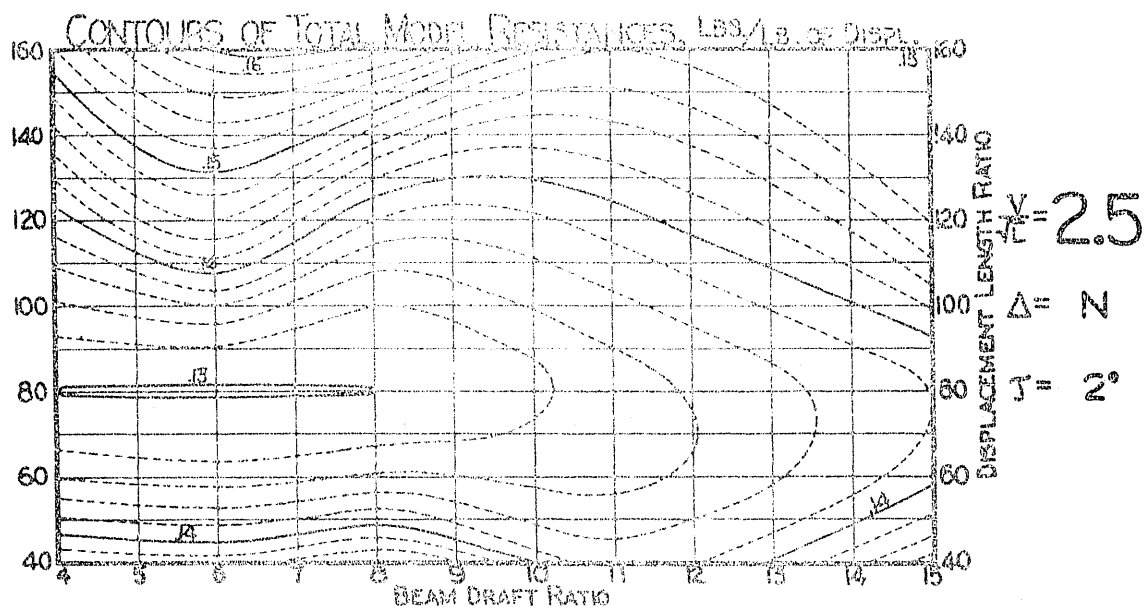
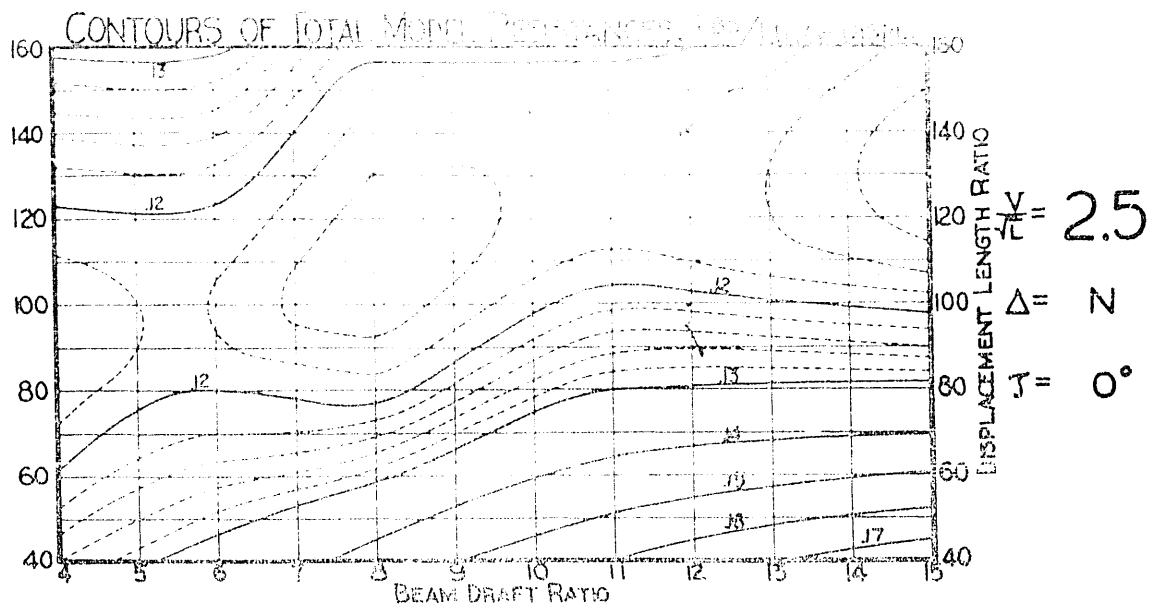
CONTOURS
OF
RESISTANCE
PER POUND OF DISPLACEMENT

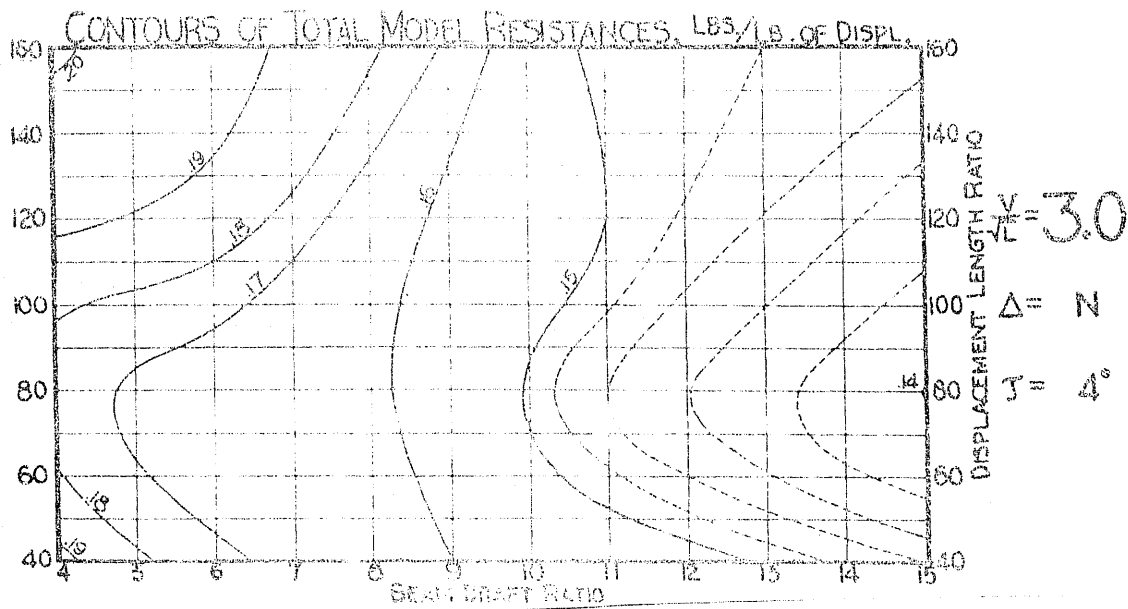
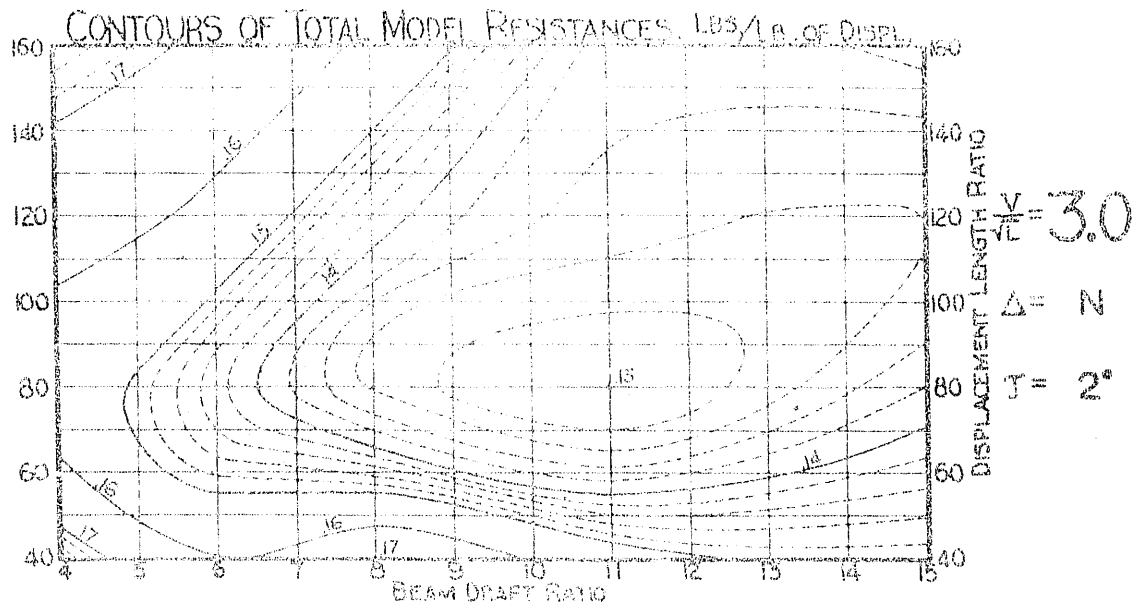
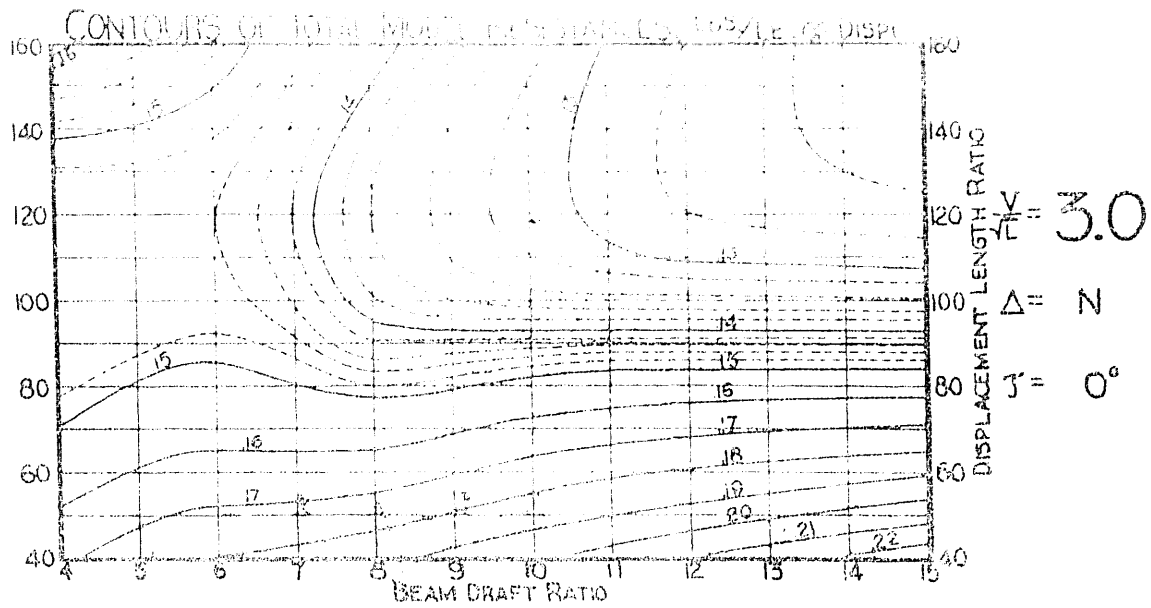
Speed-Length Ratios 1.5-6.5 in Steps of 0.5

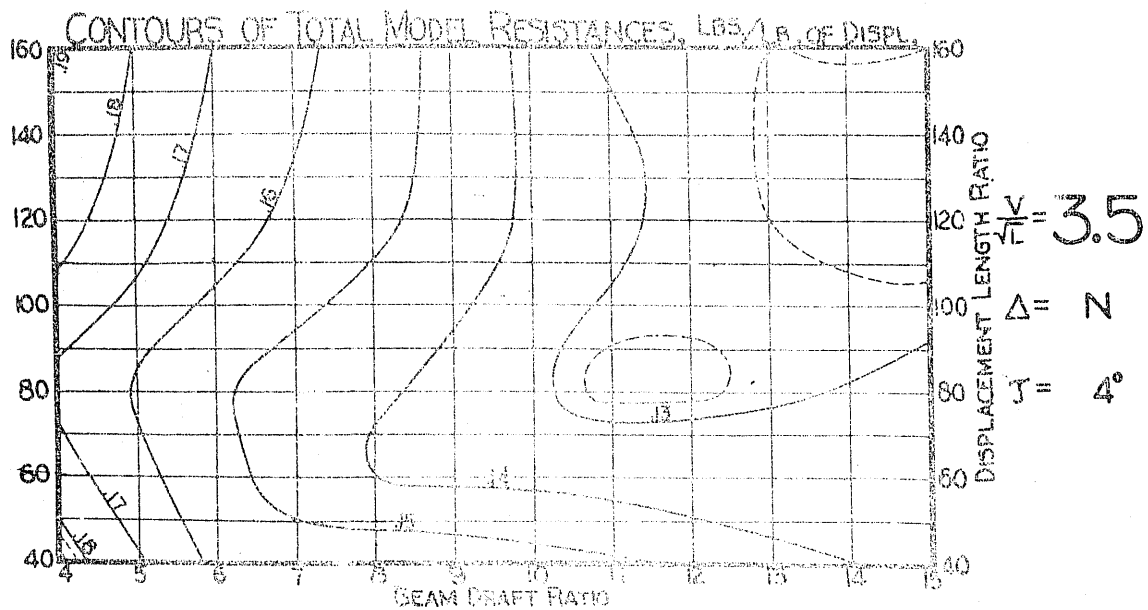
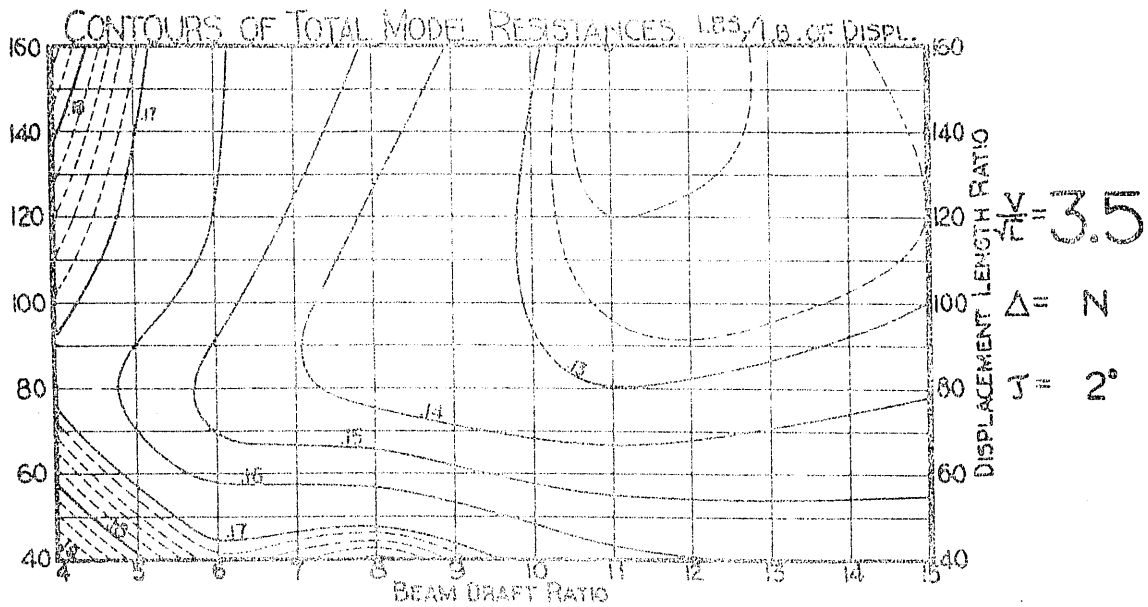
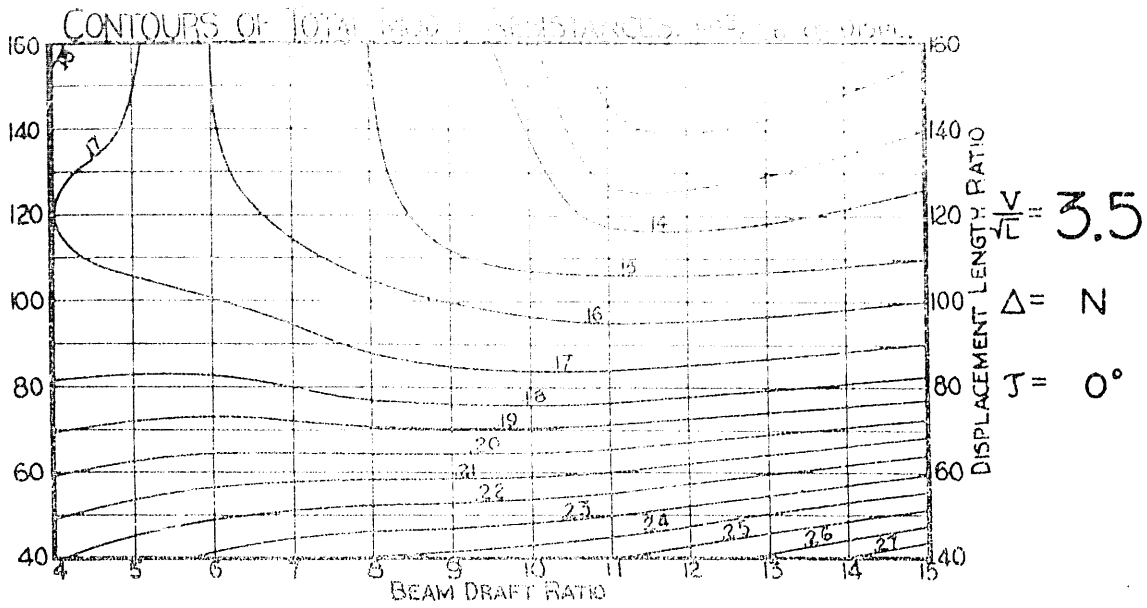
	Pages
100% Displacement (N)	13 to 23
110% " (N + 10%)	24 to 34
120% " (N + 20%)	35 to 45

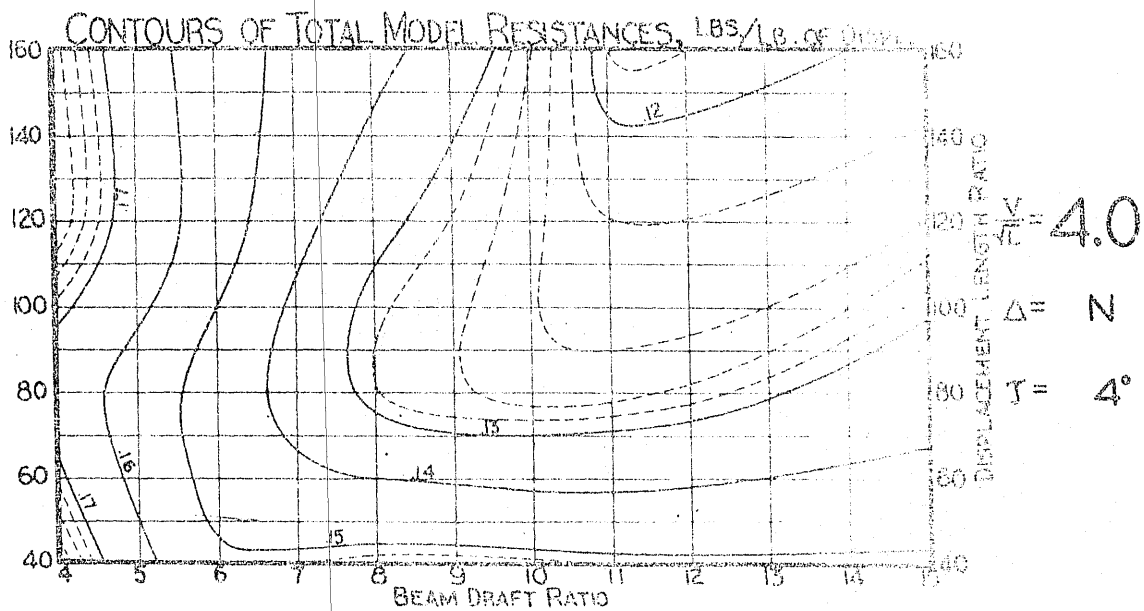
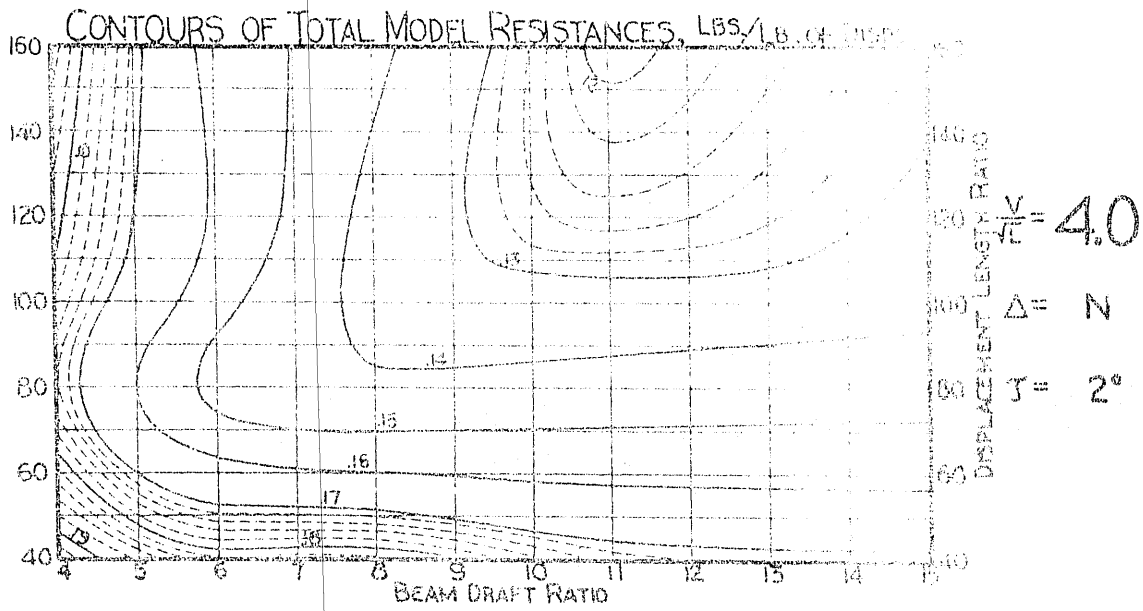
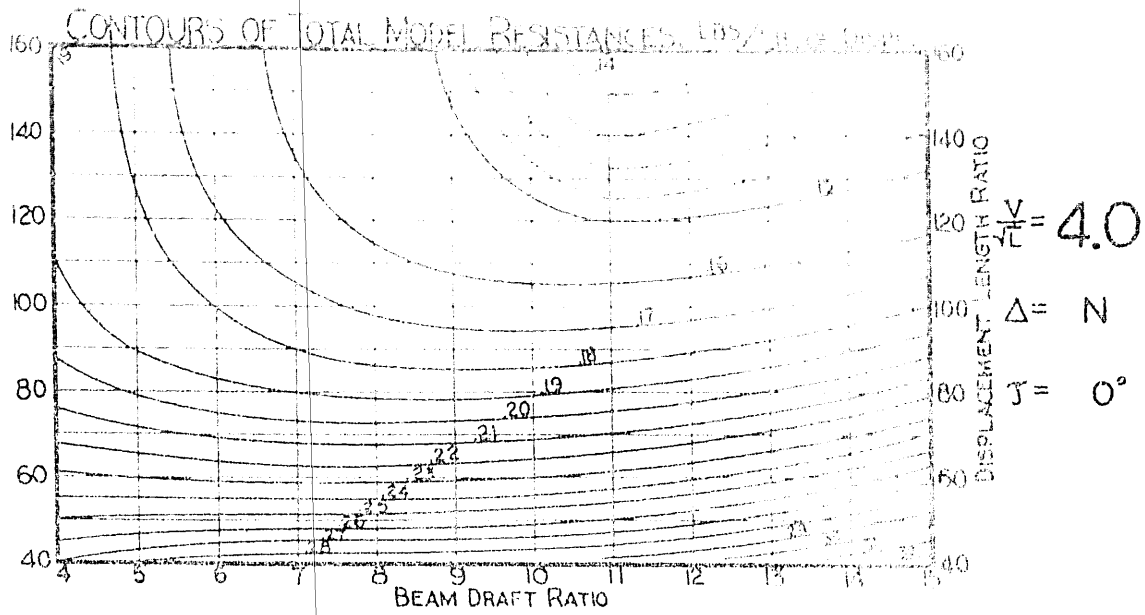


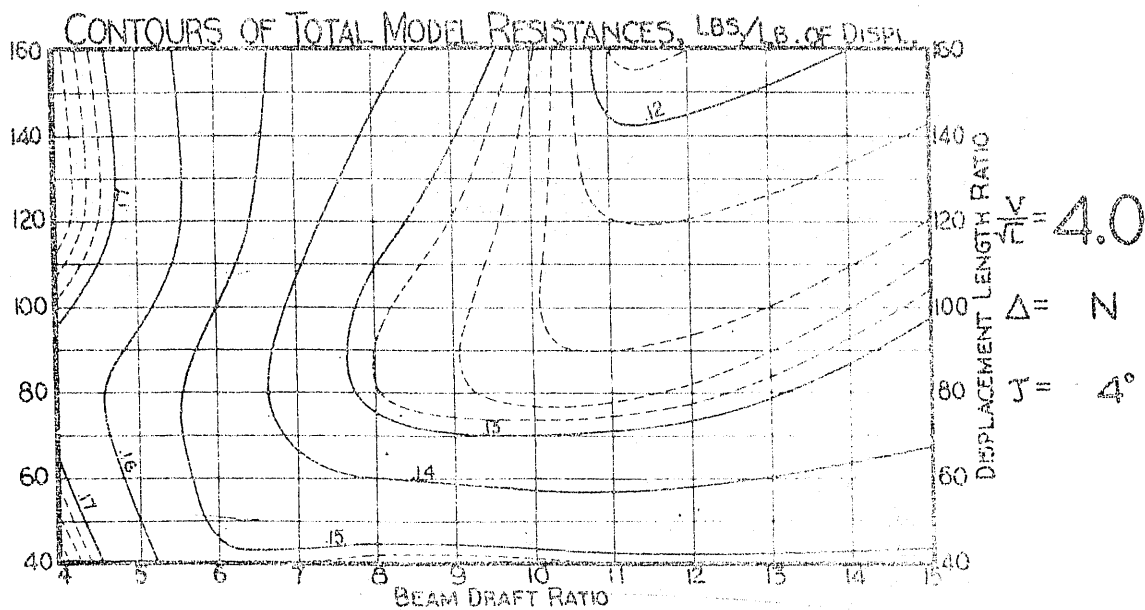
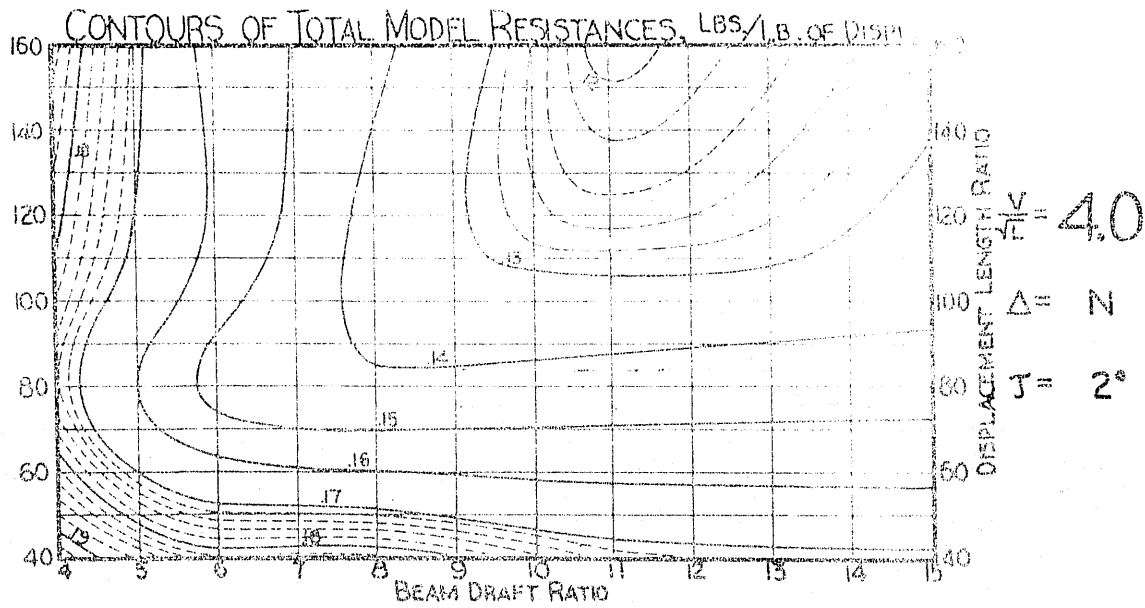
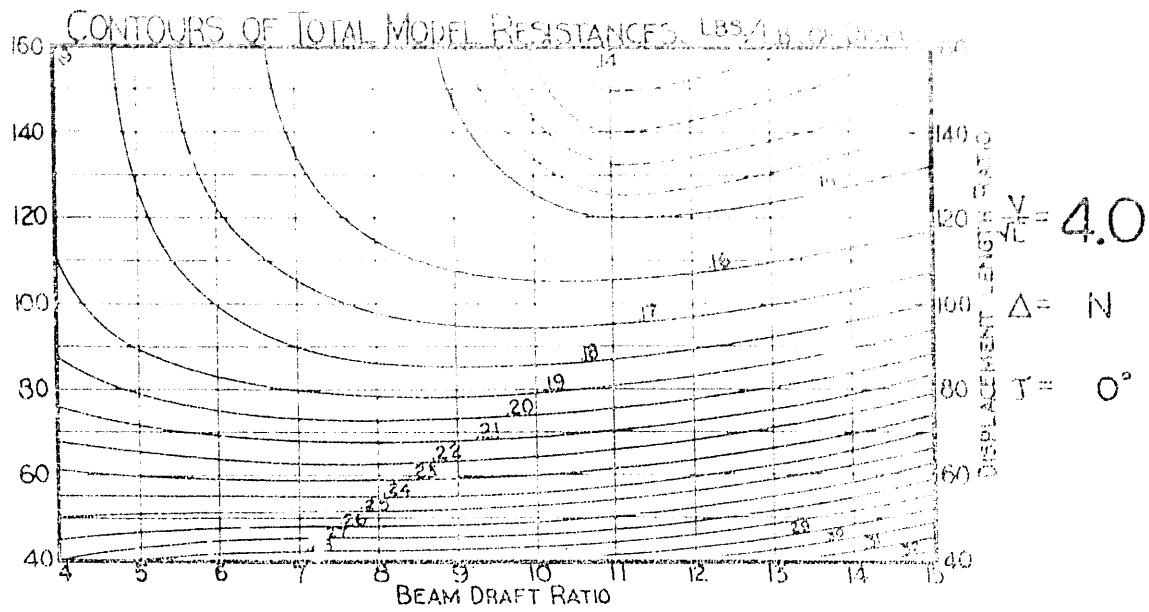


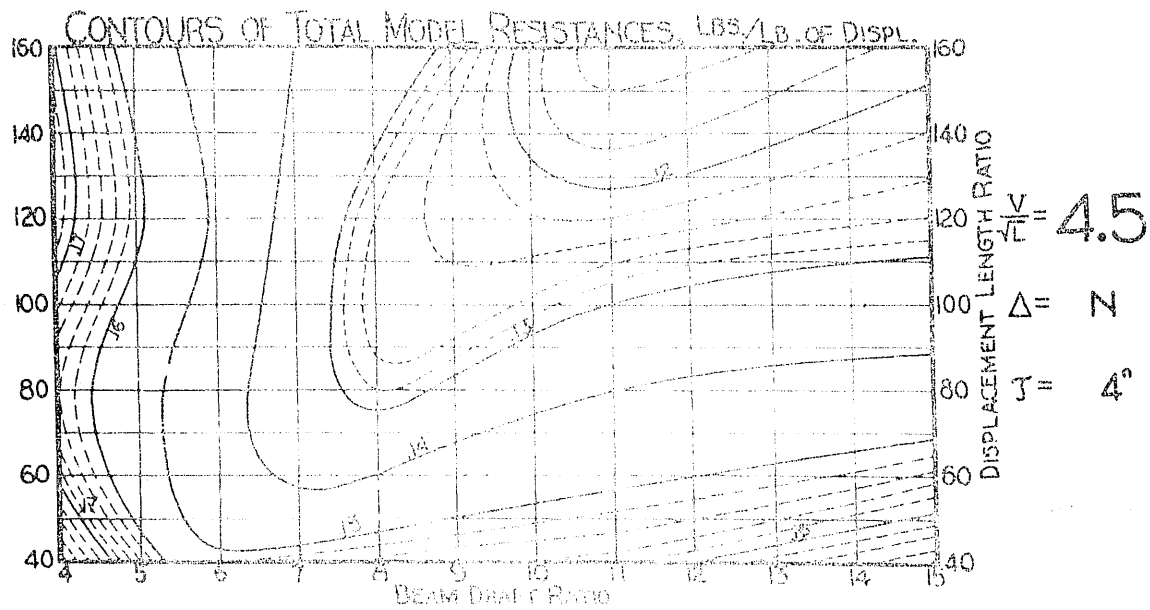
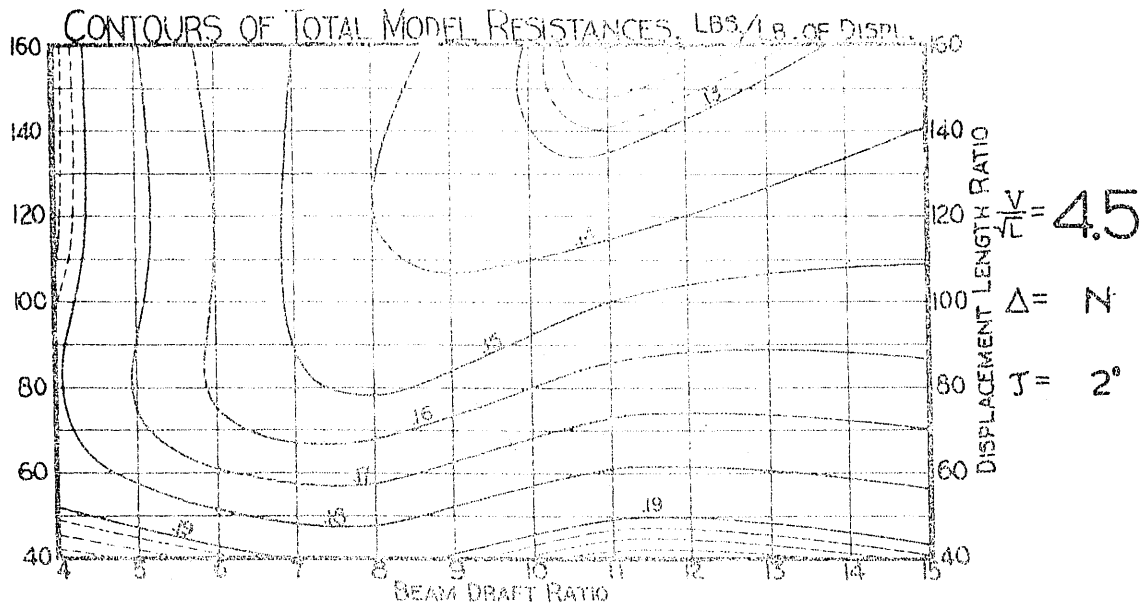
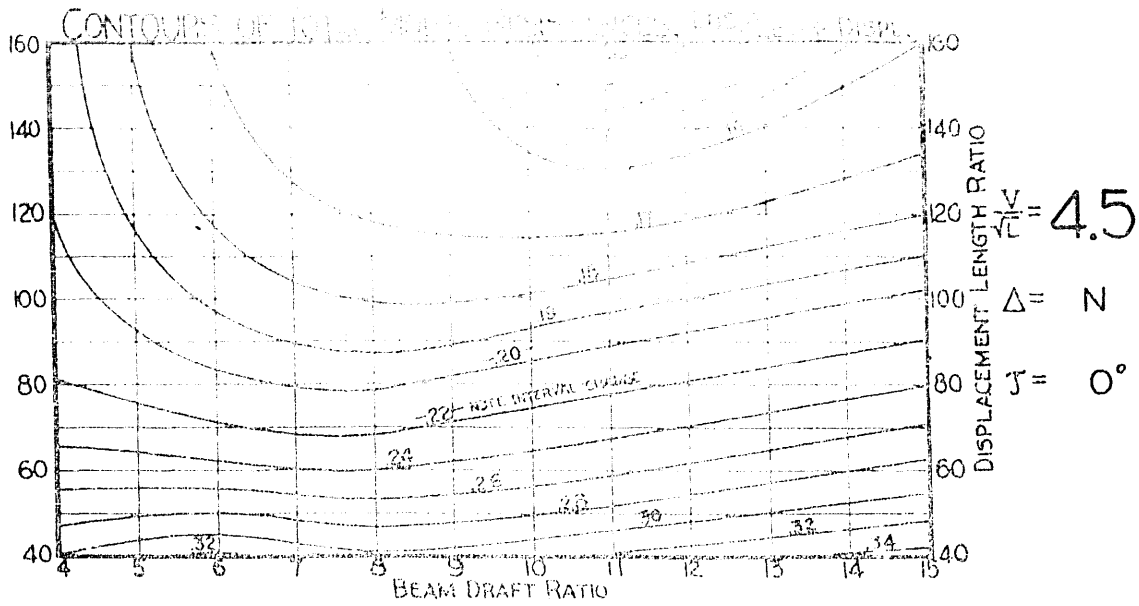


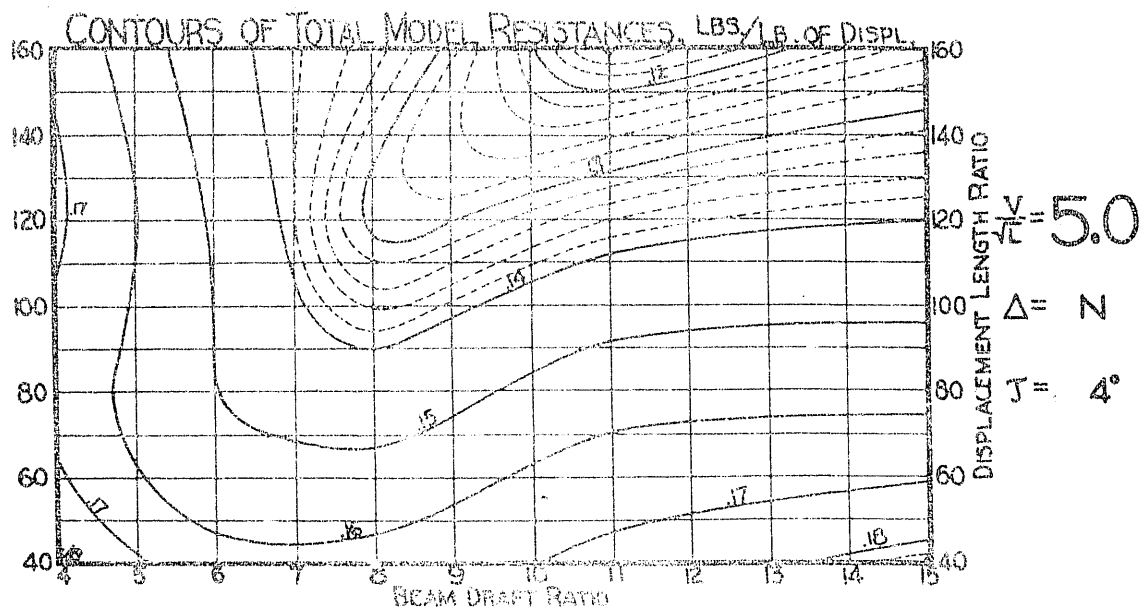
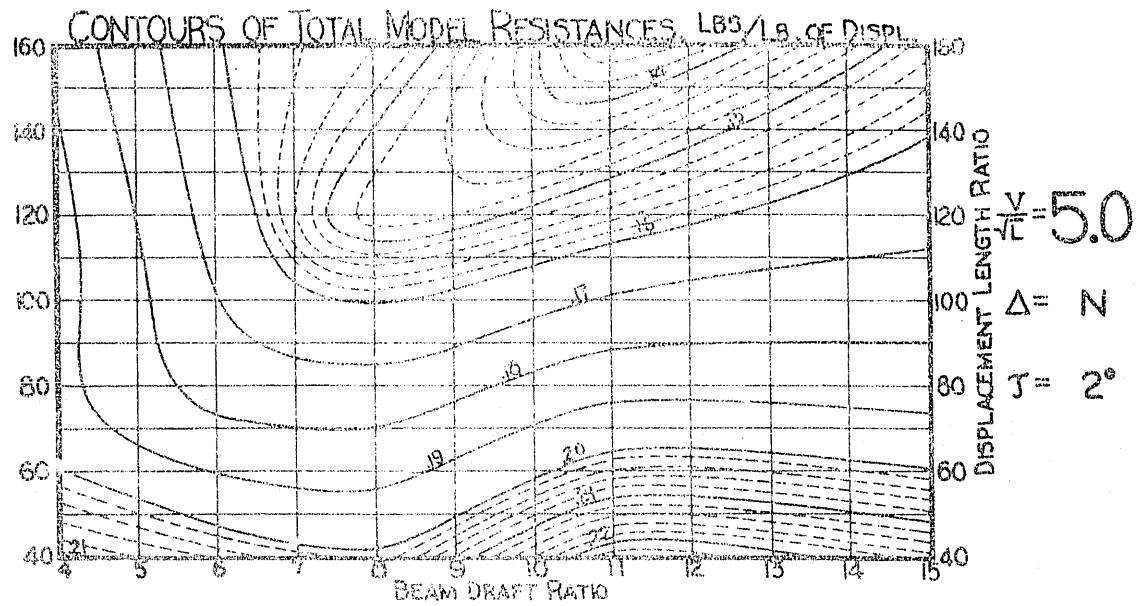
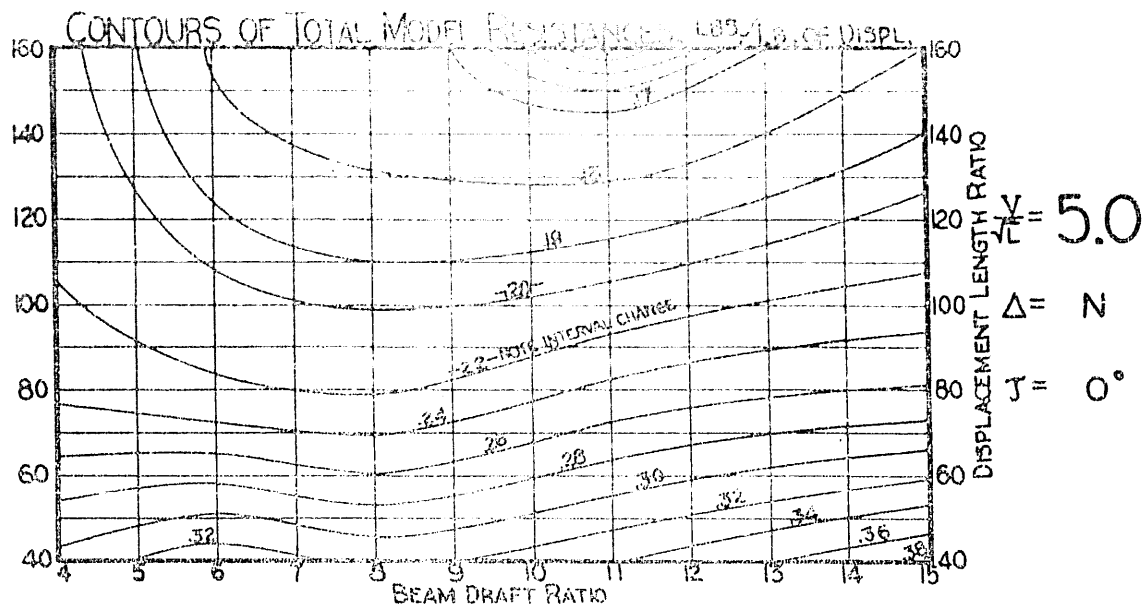


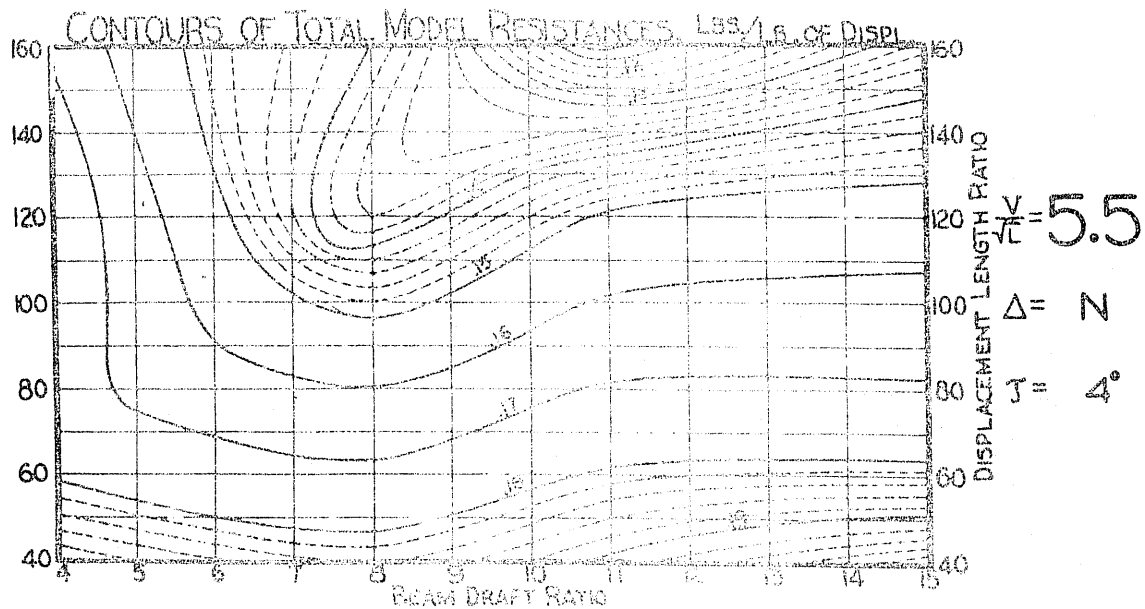
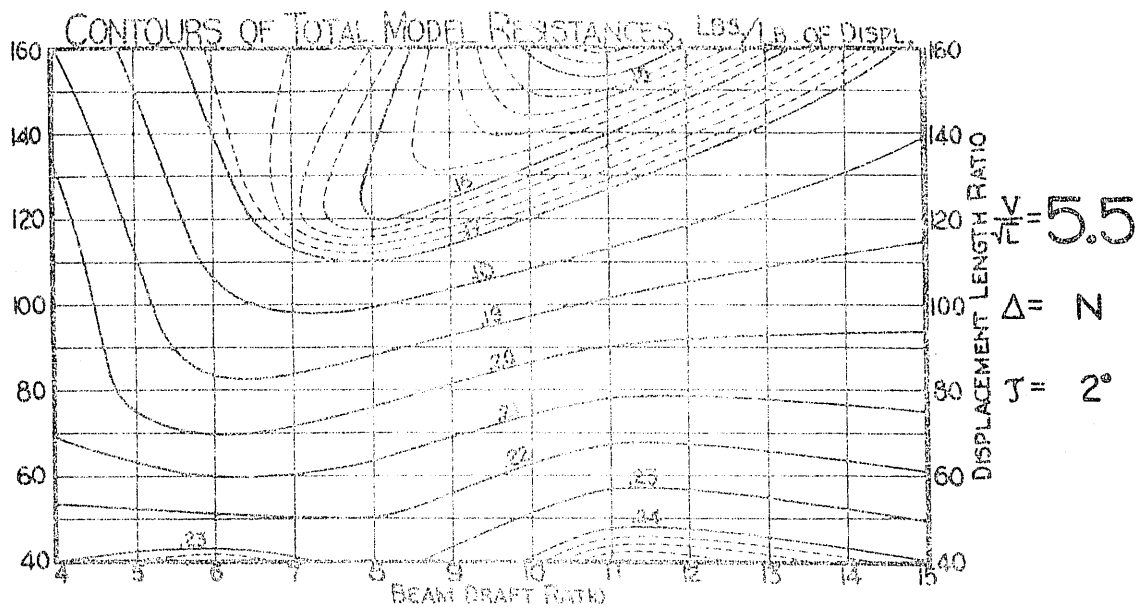
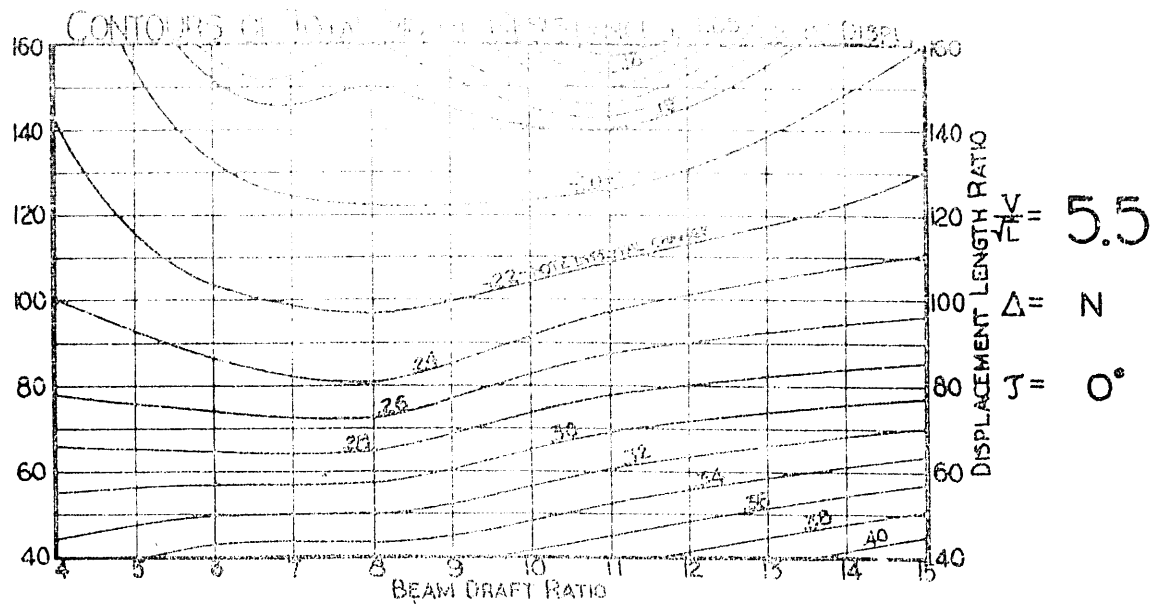


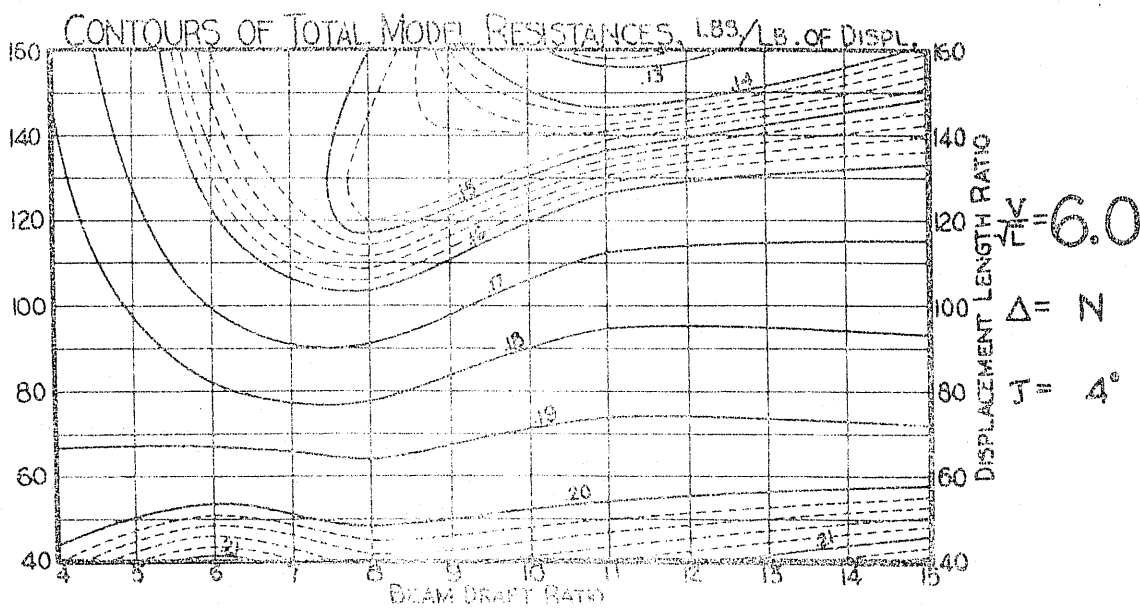
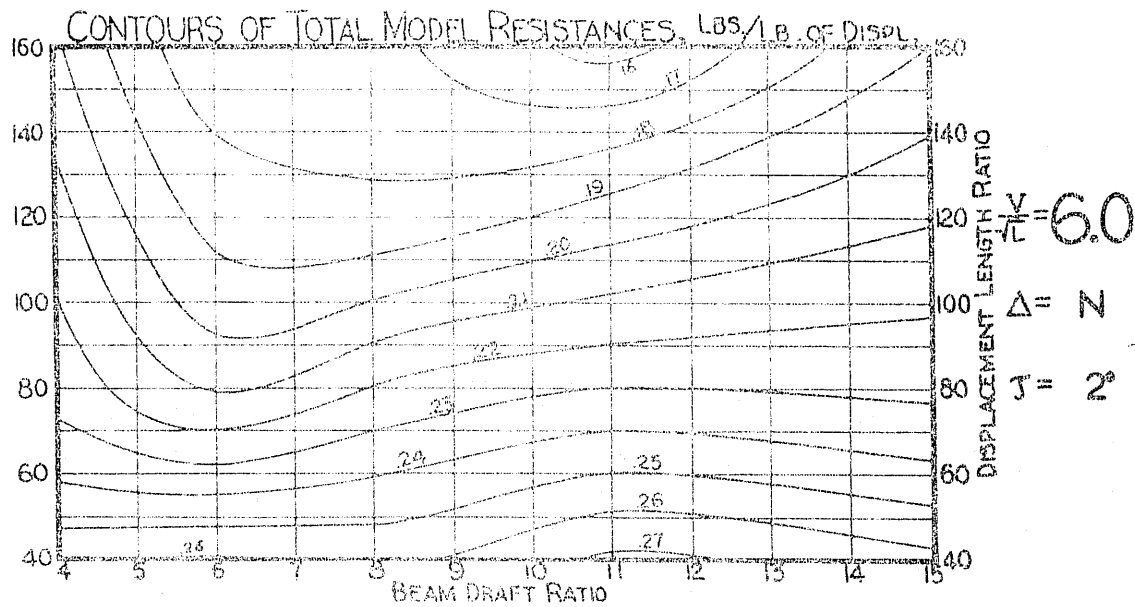
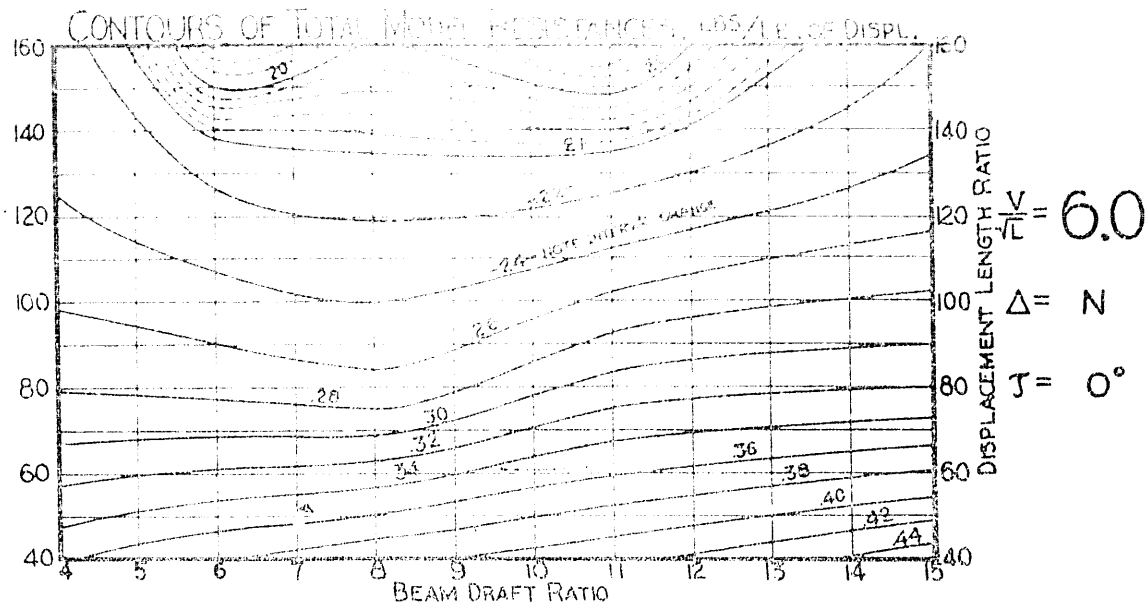


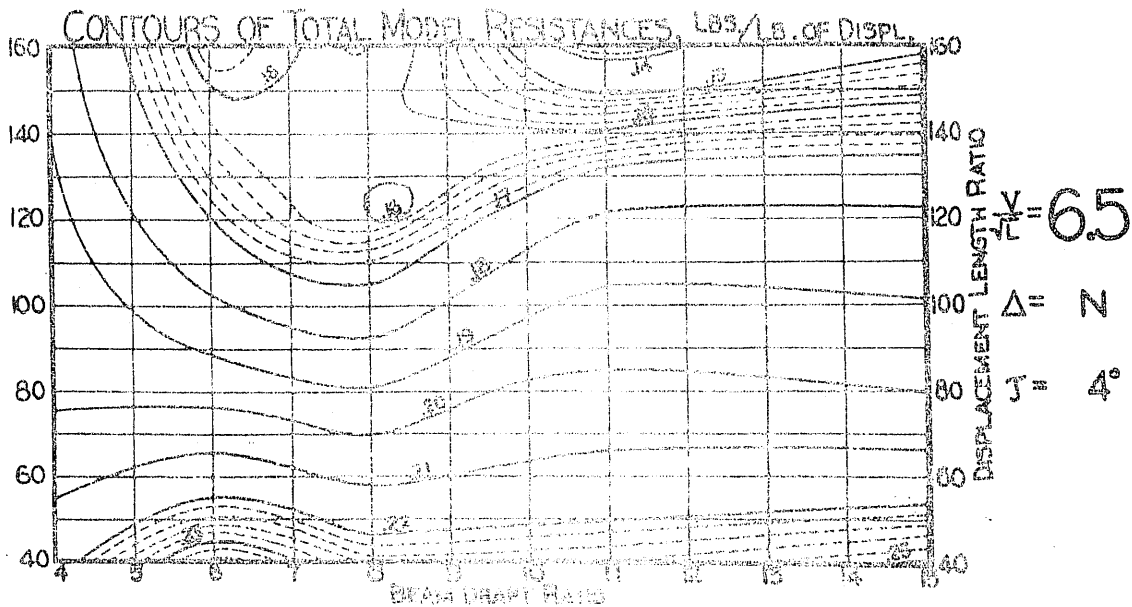
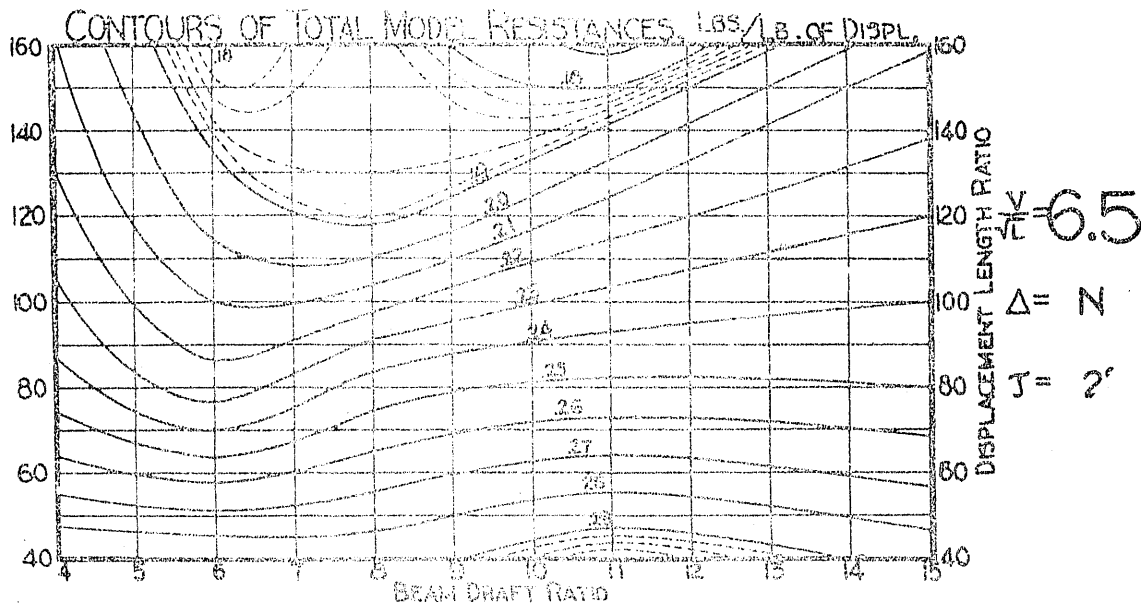
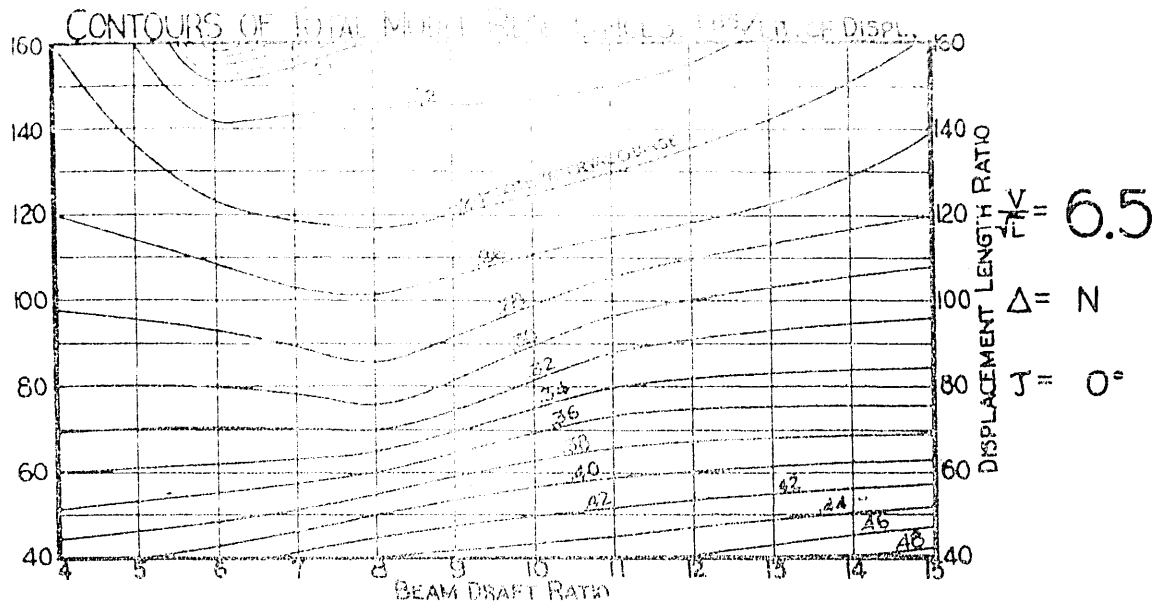


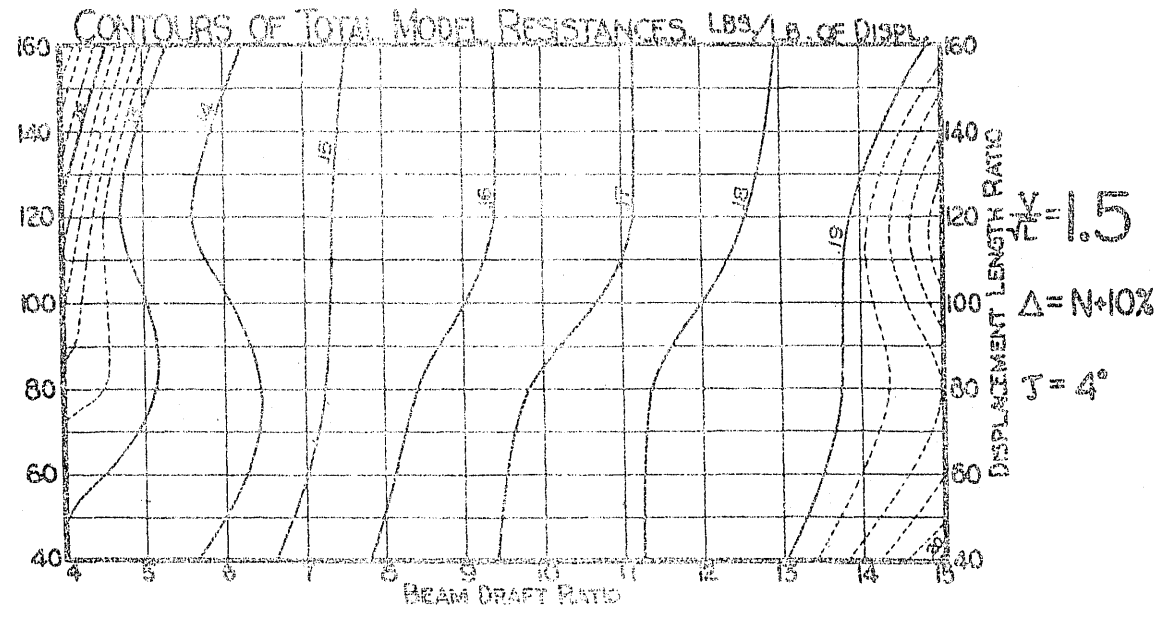
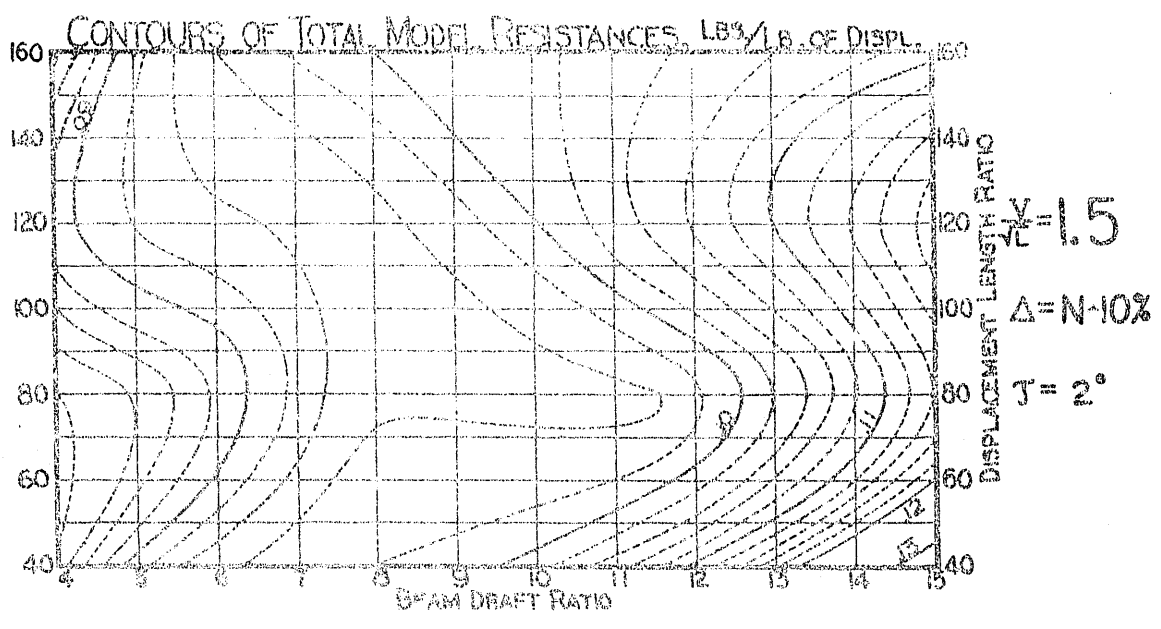
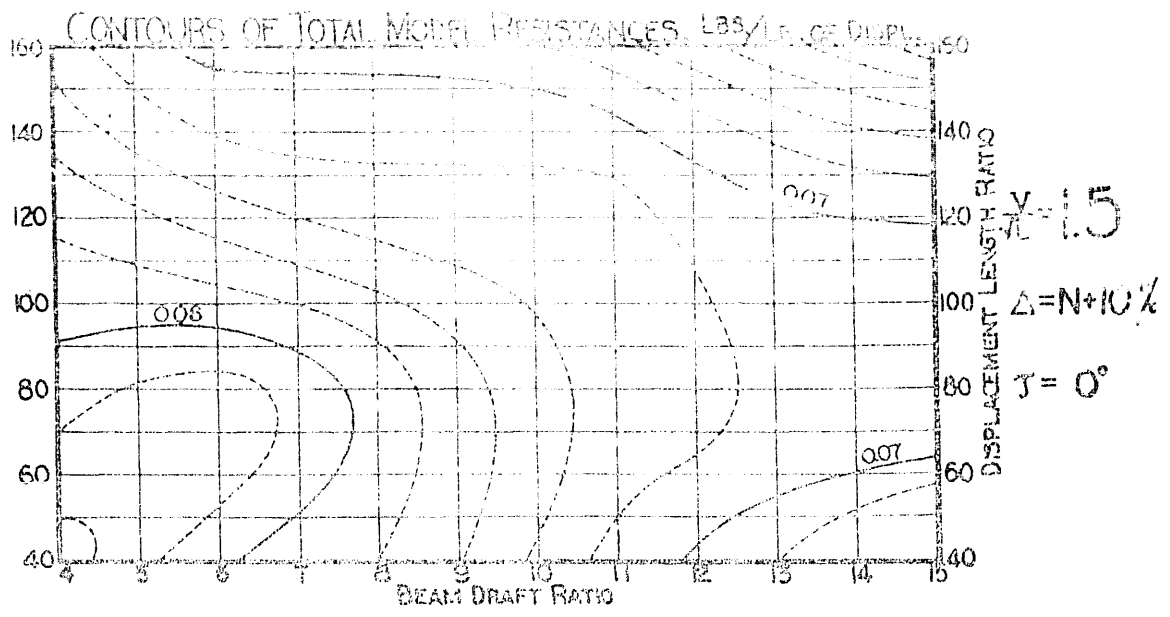


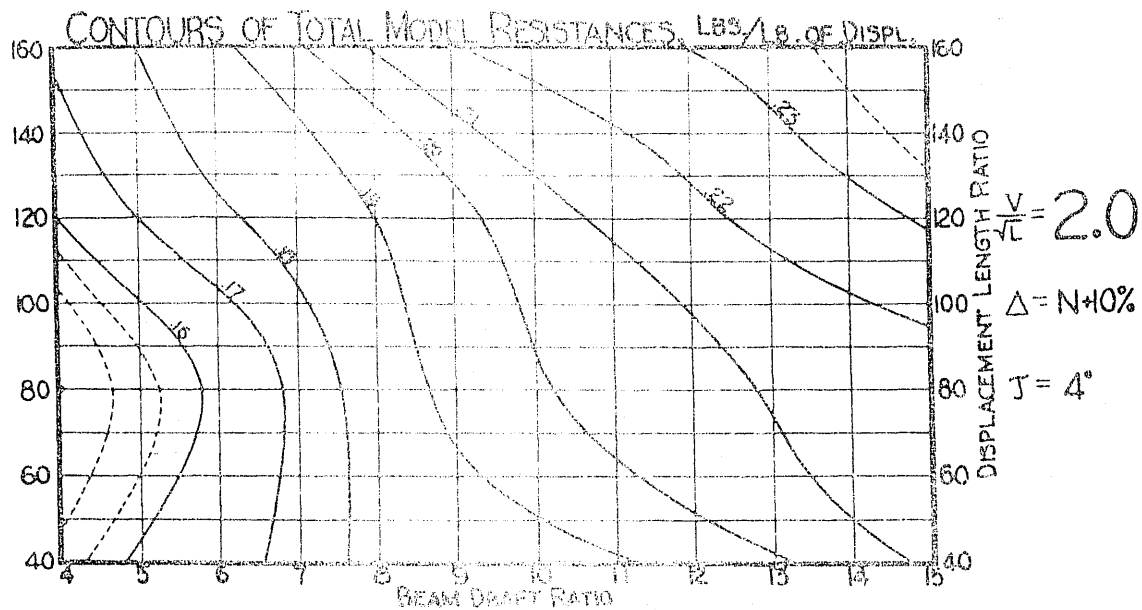
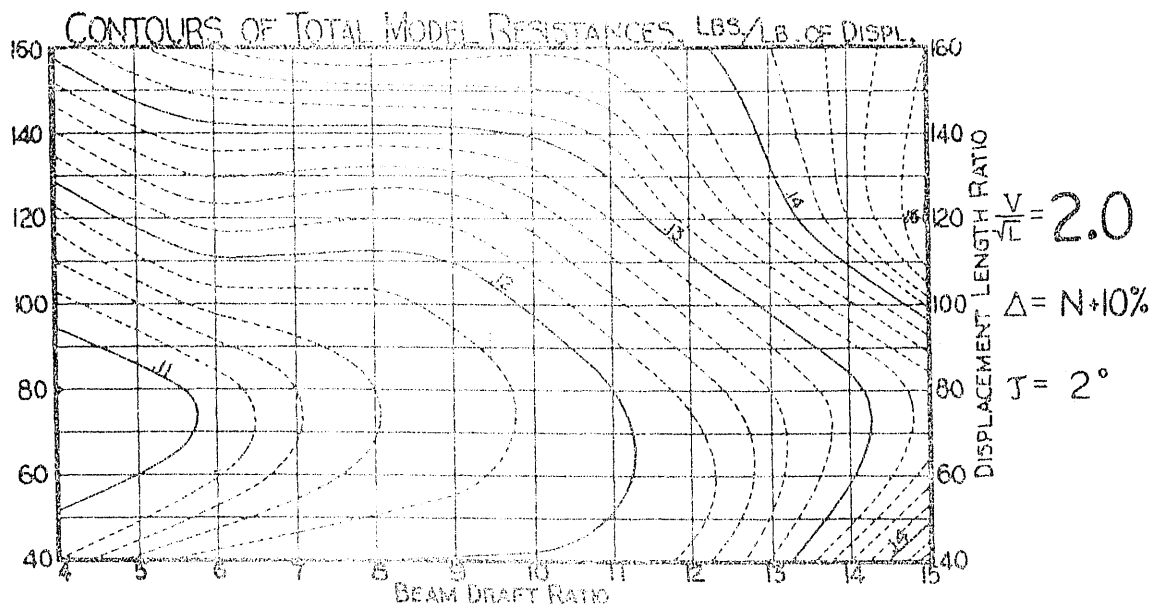
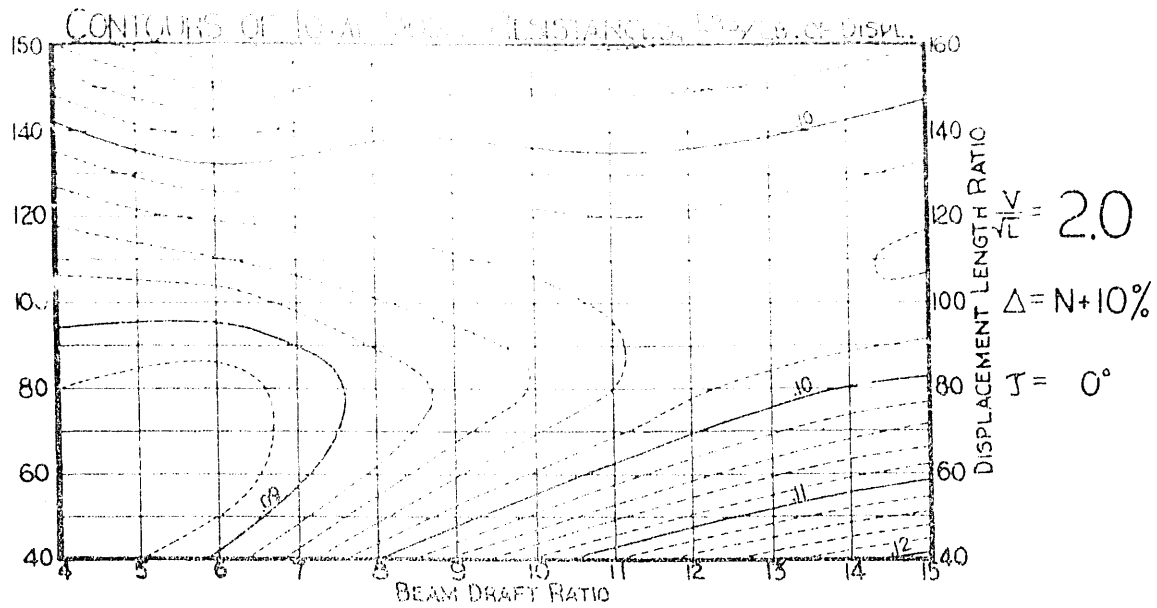


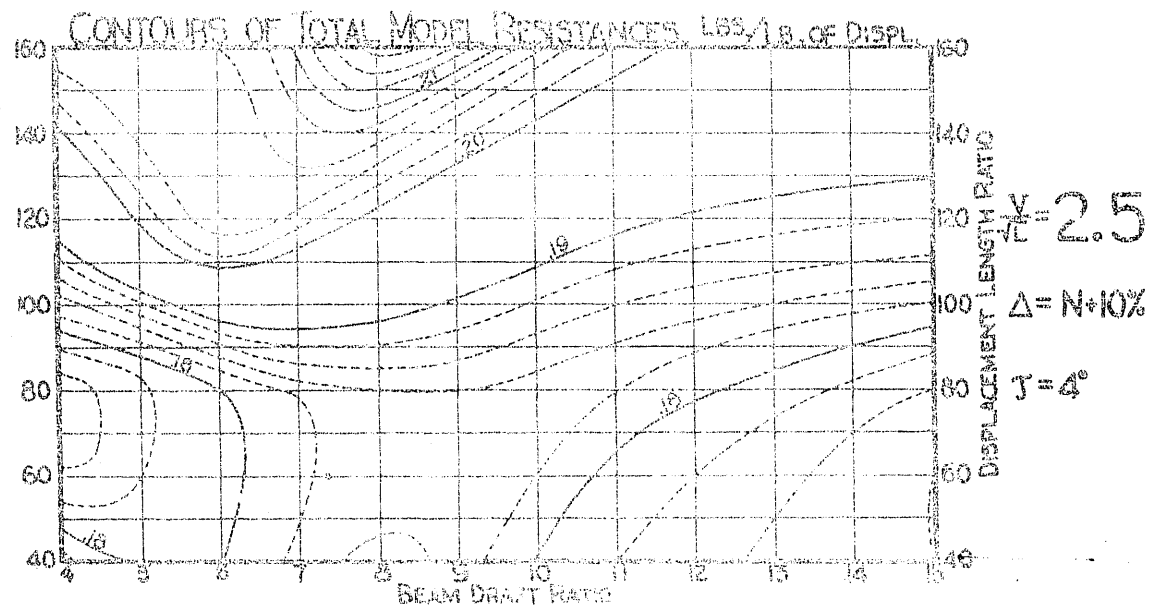
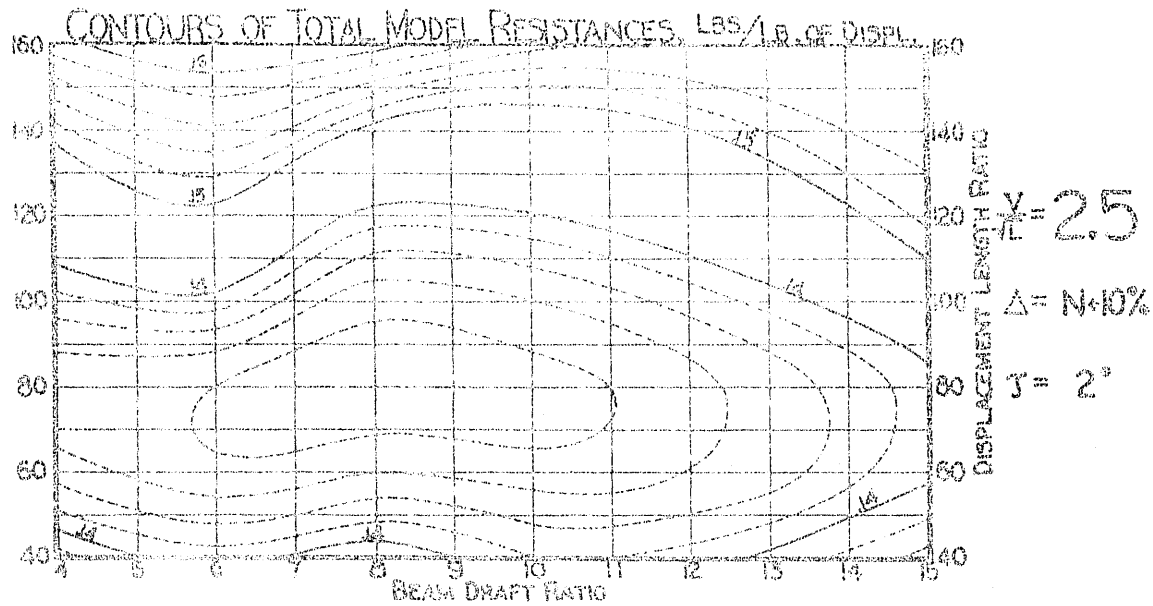
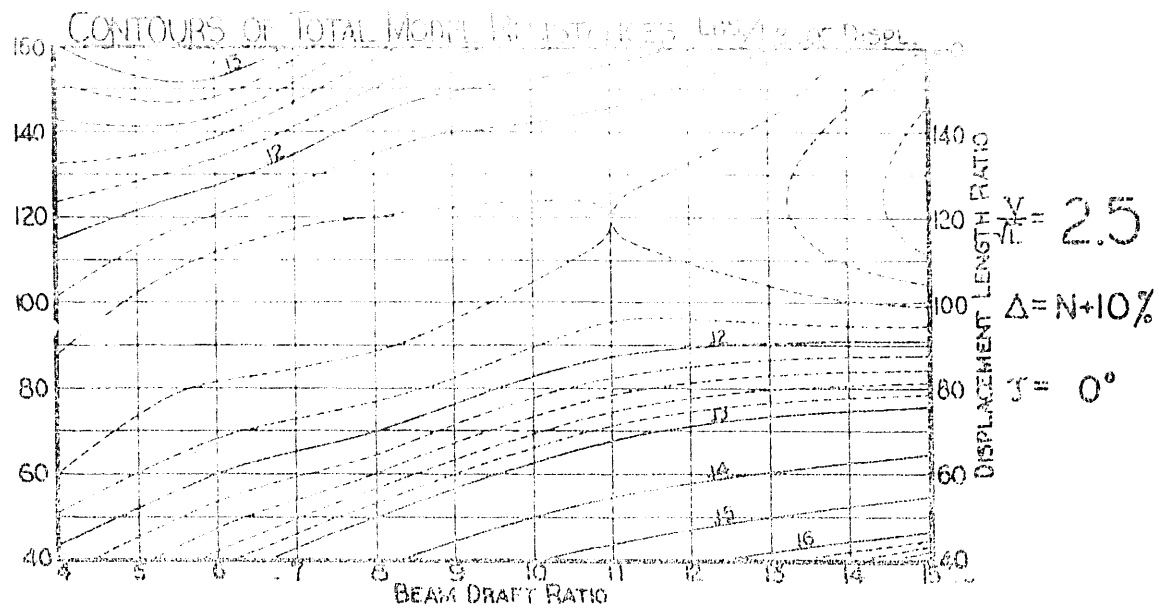


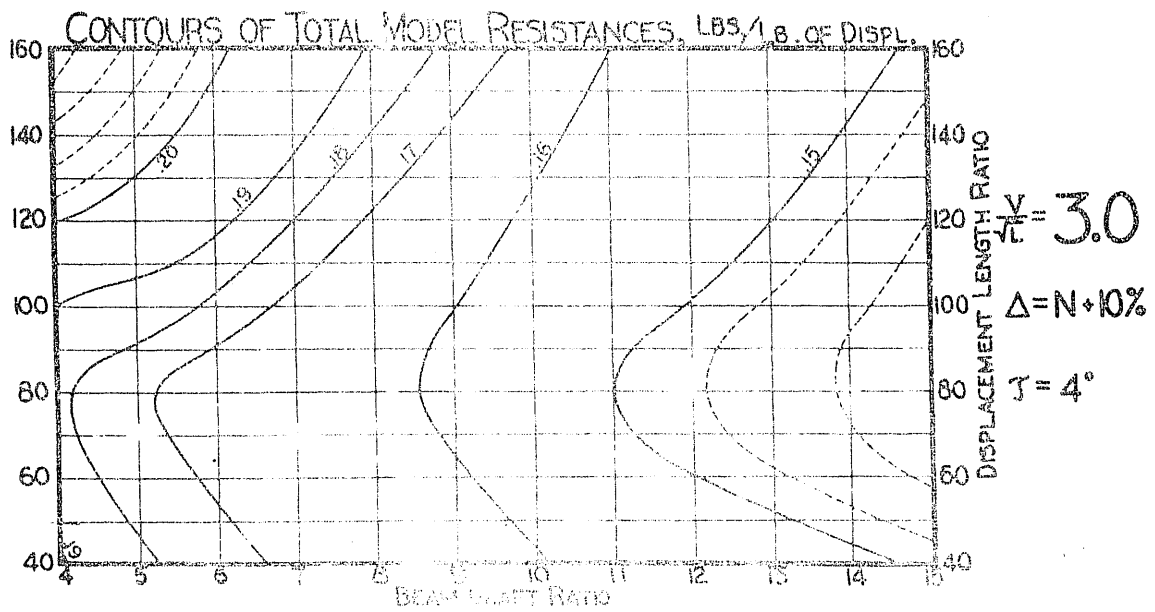
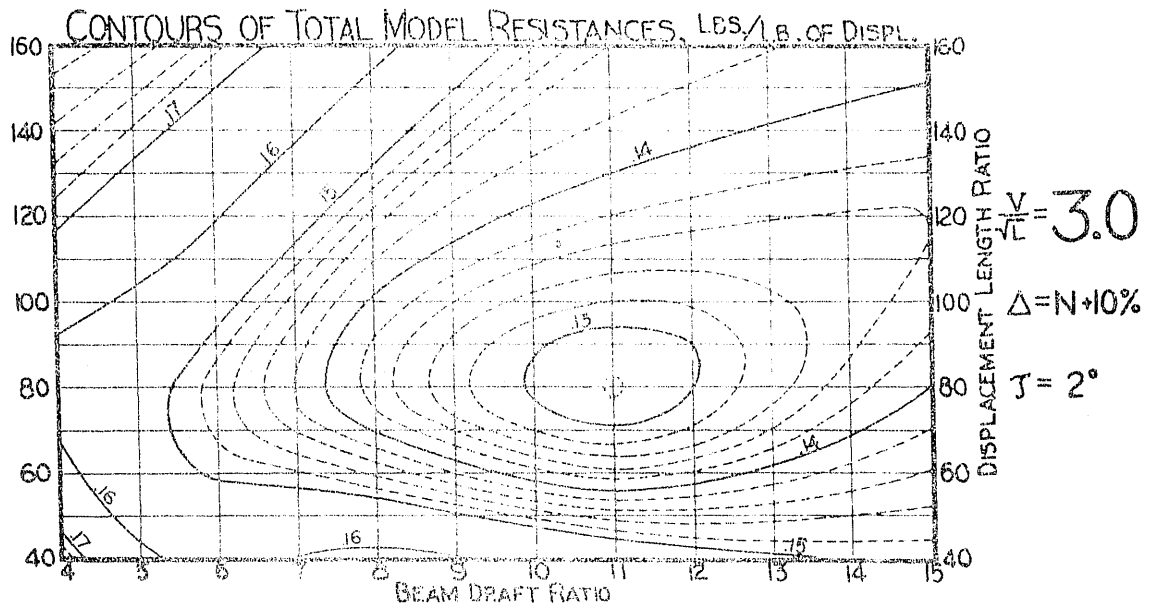
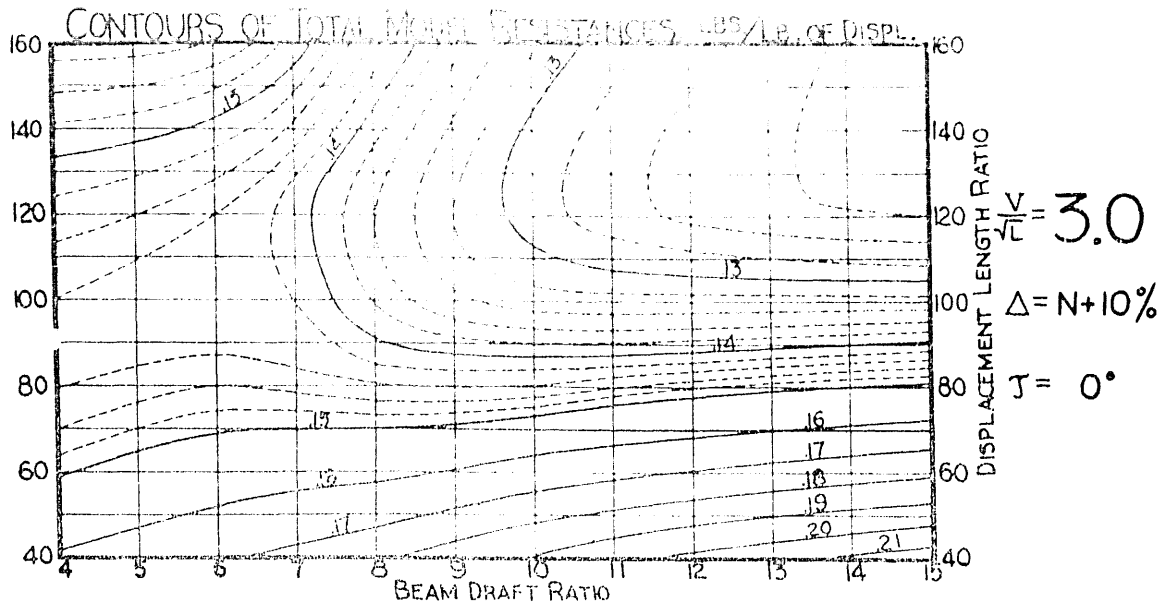


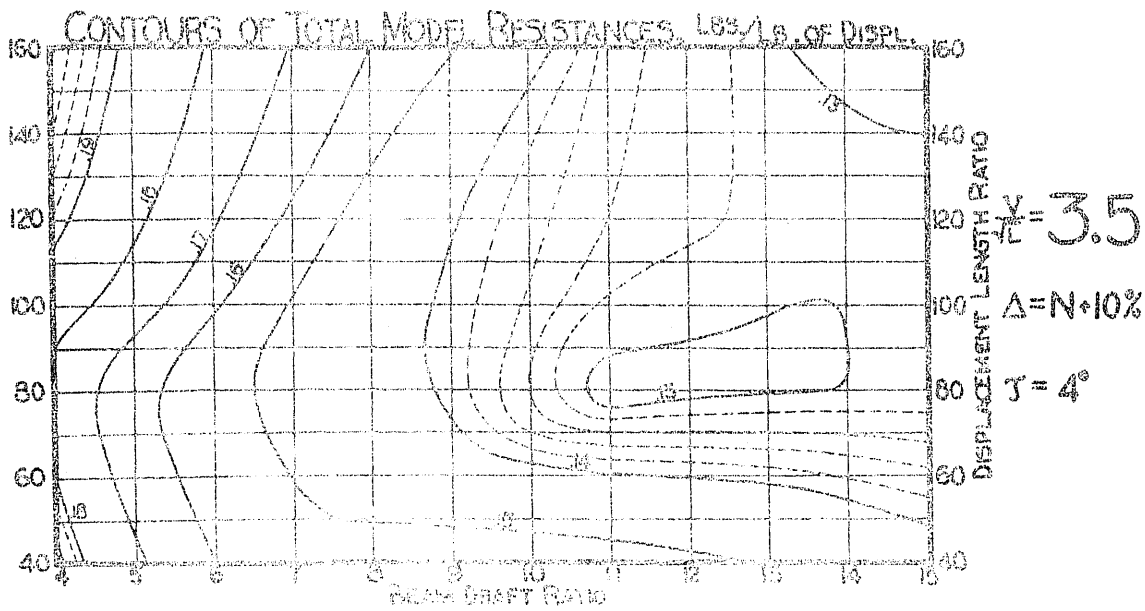
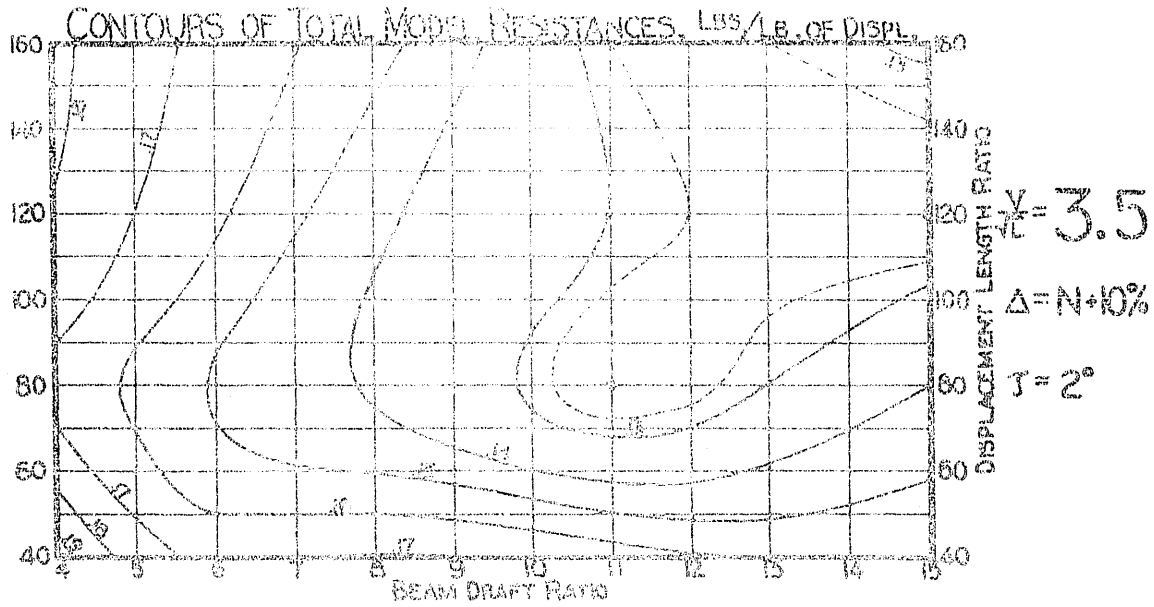
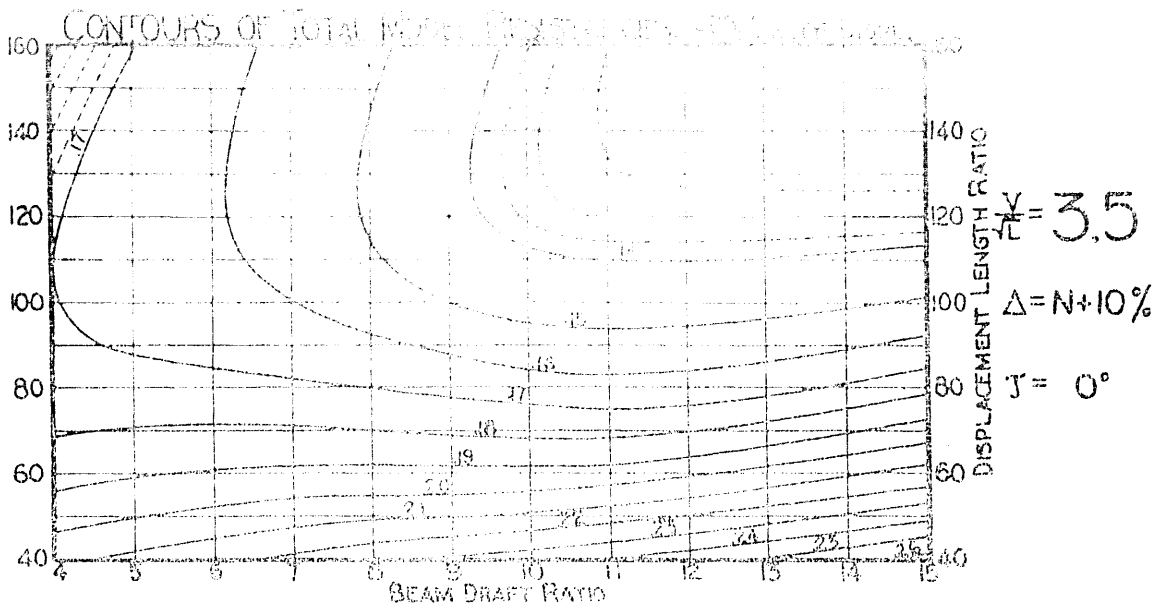


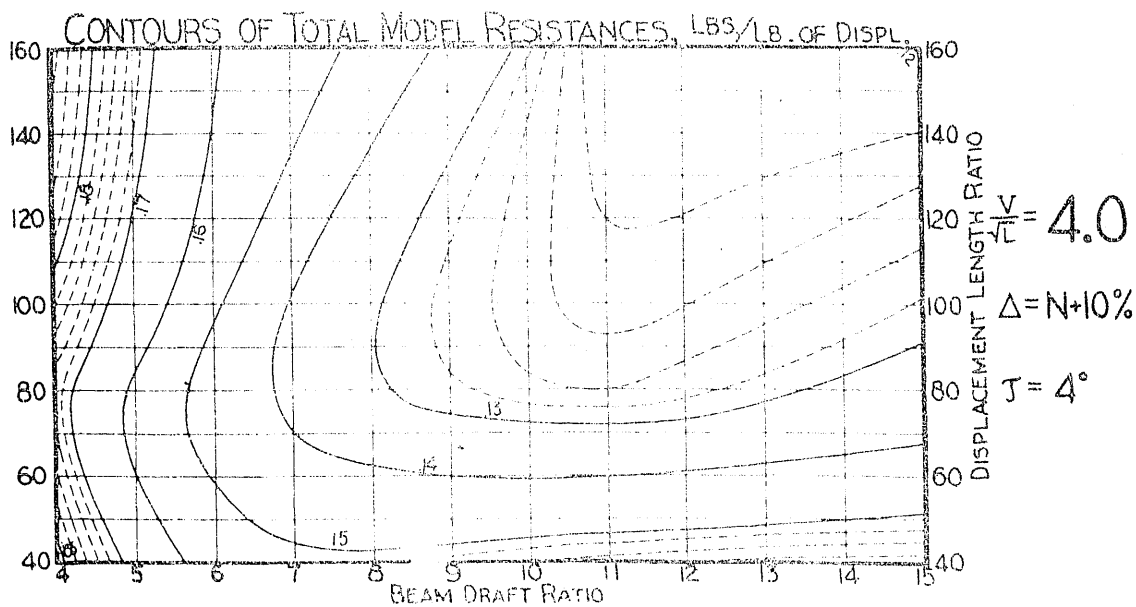
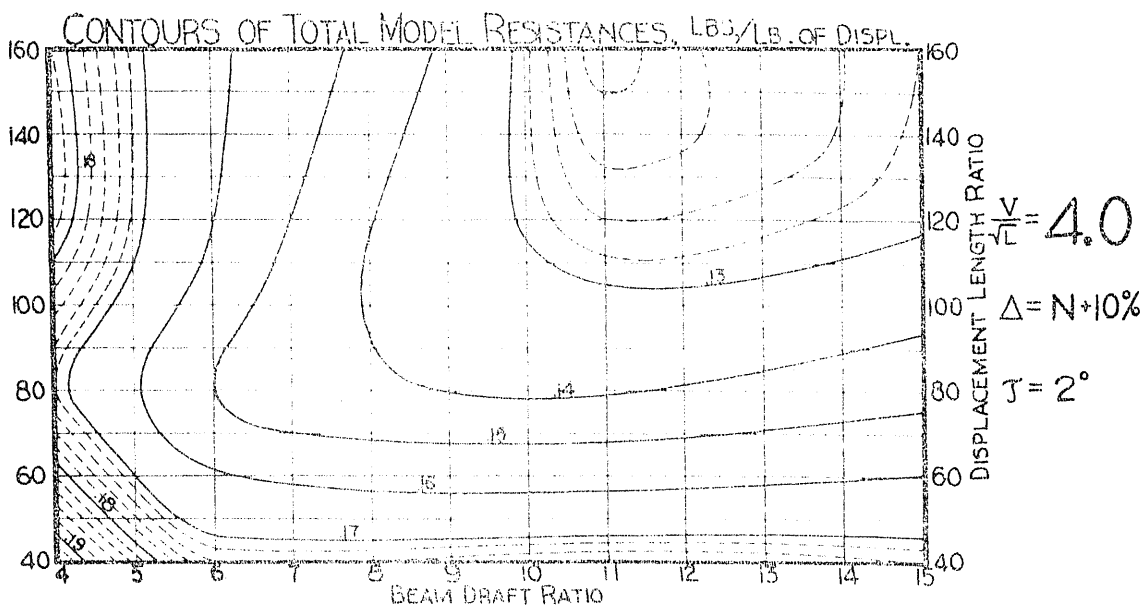
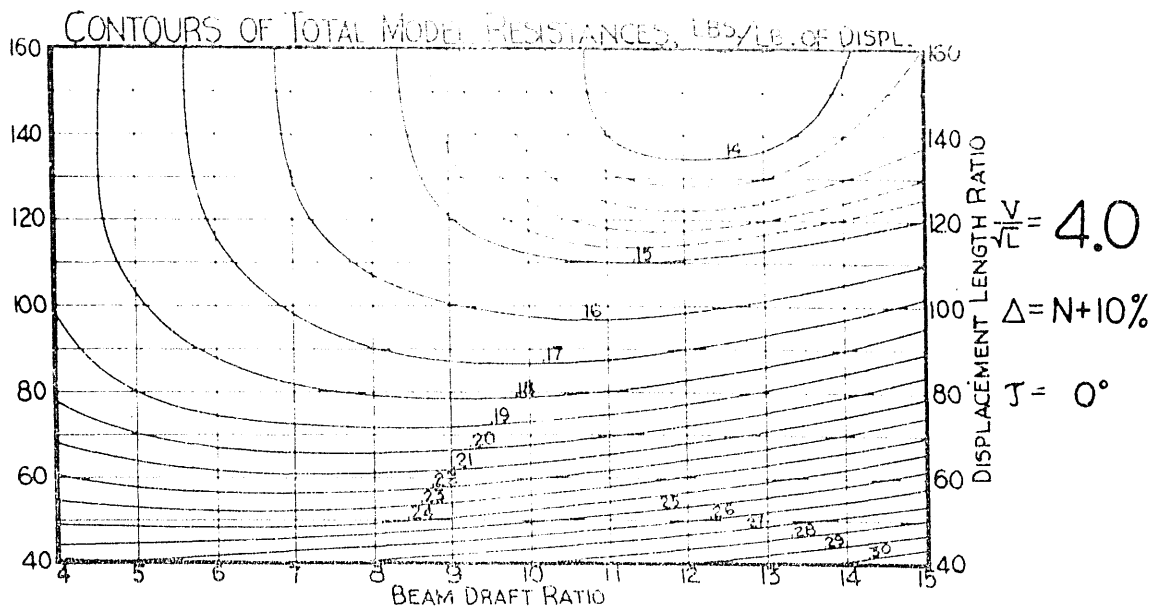


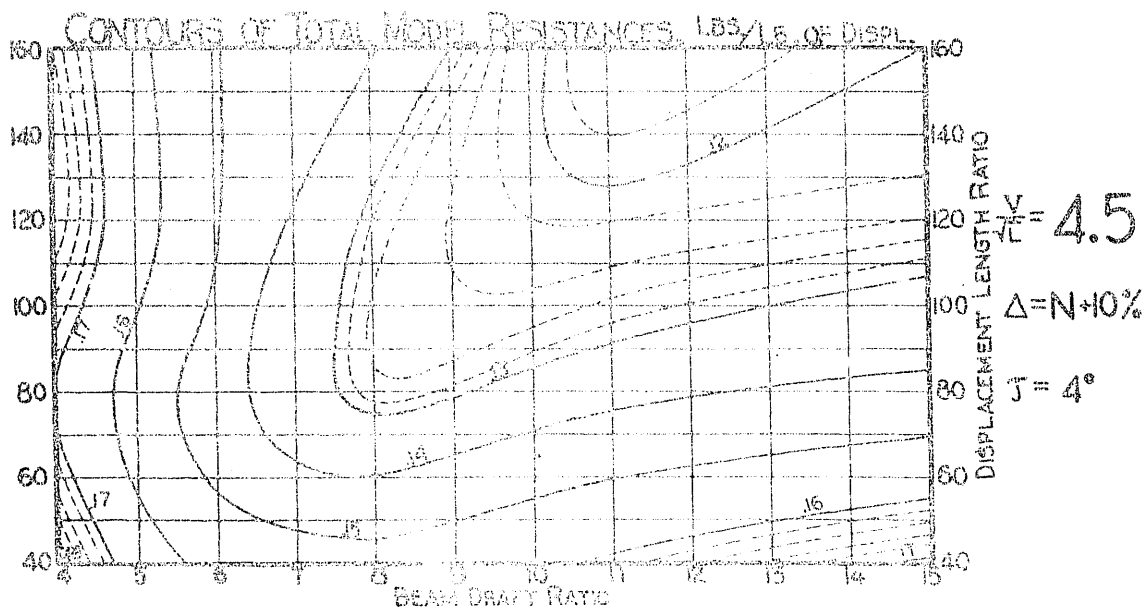
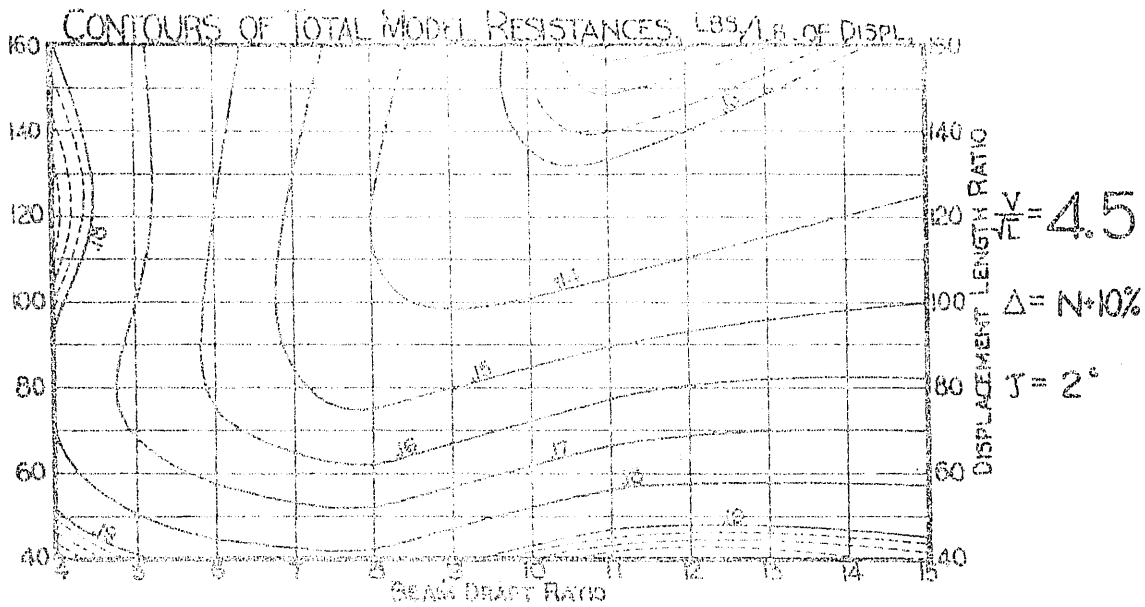
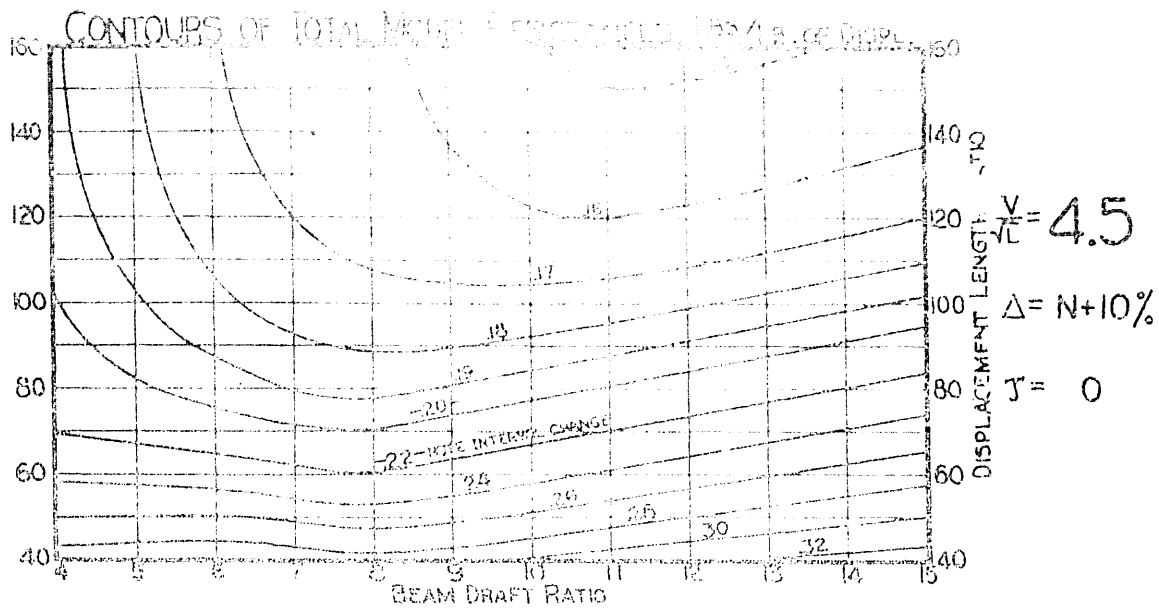


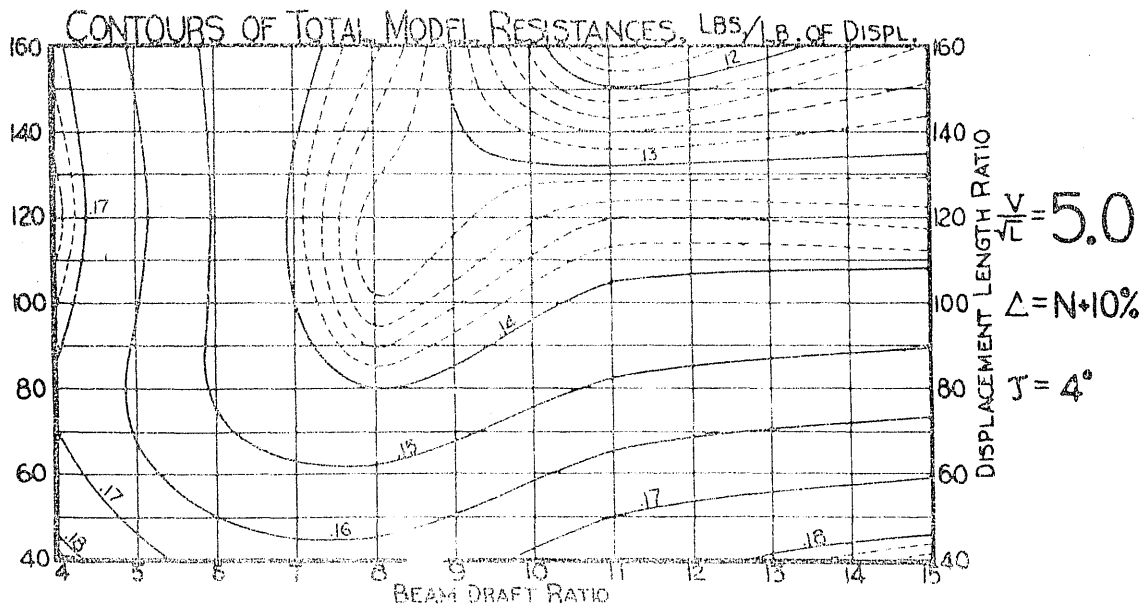
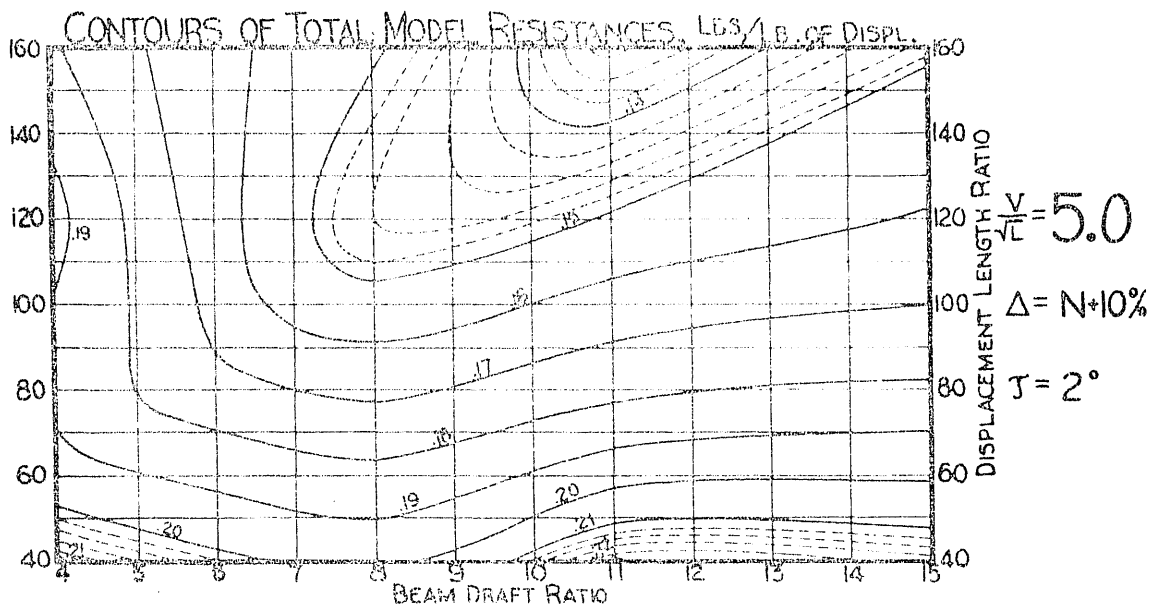
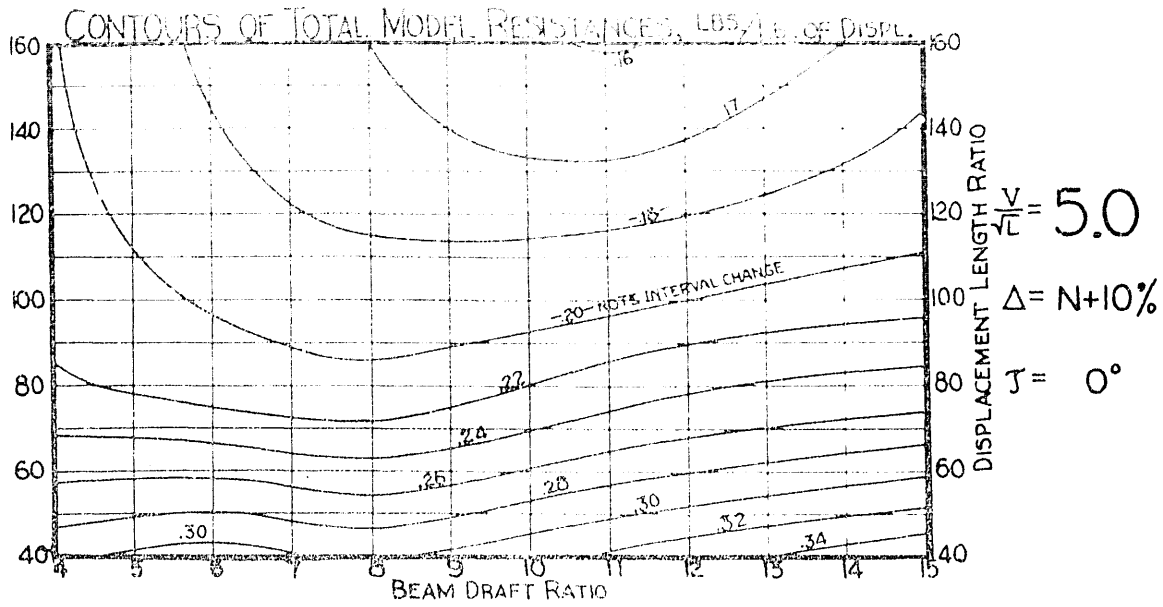


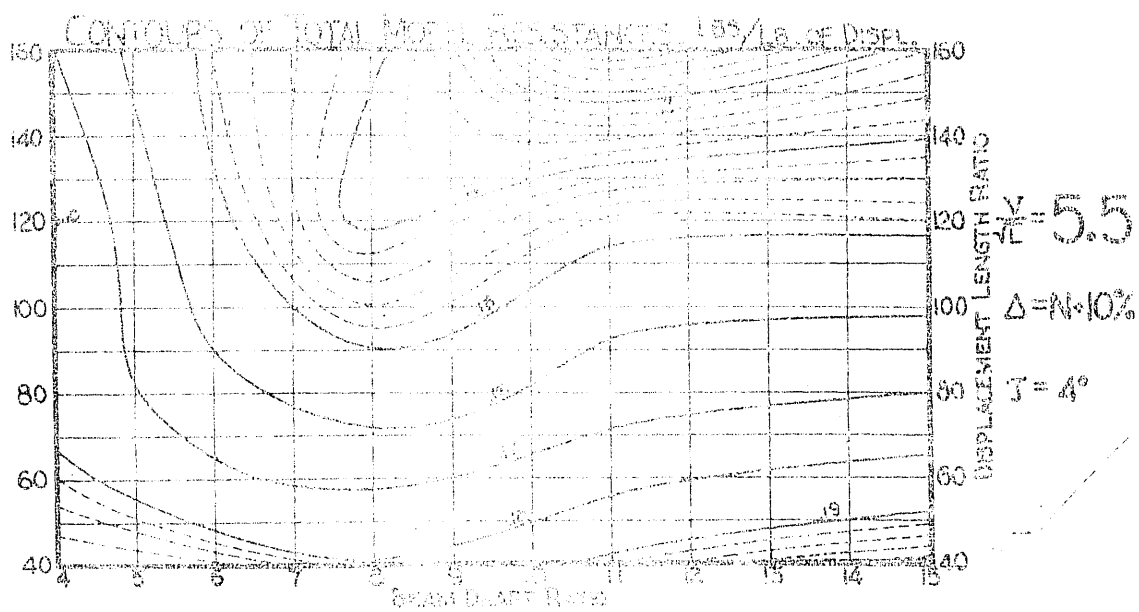
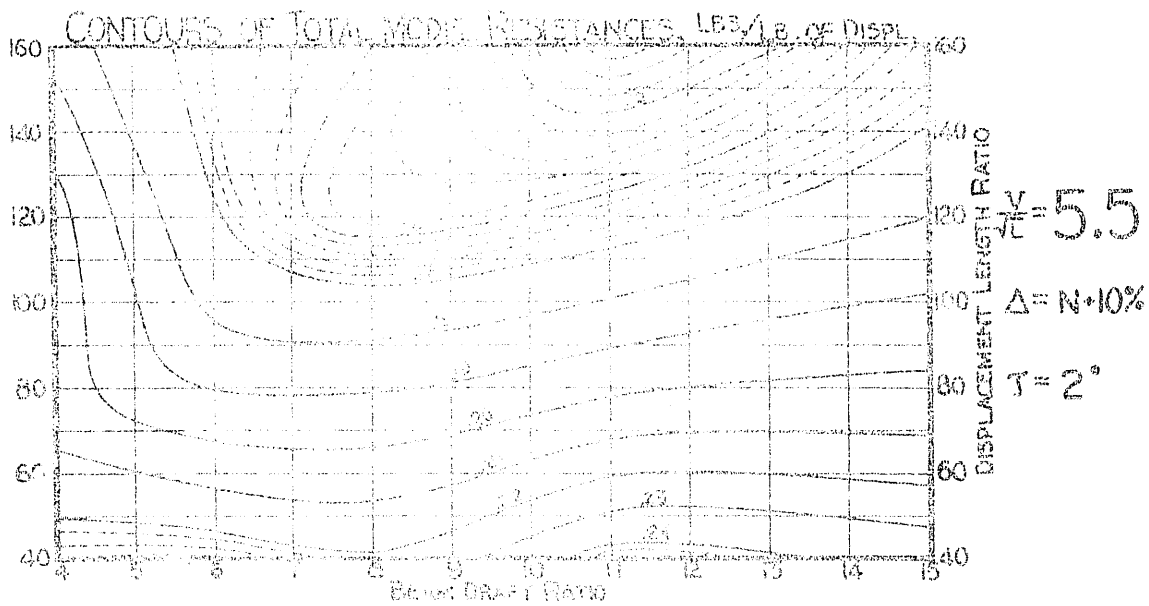
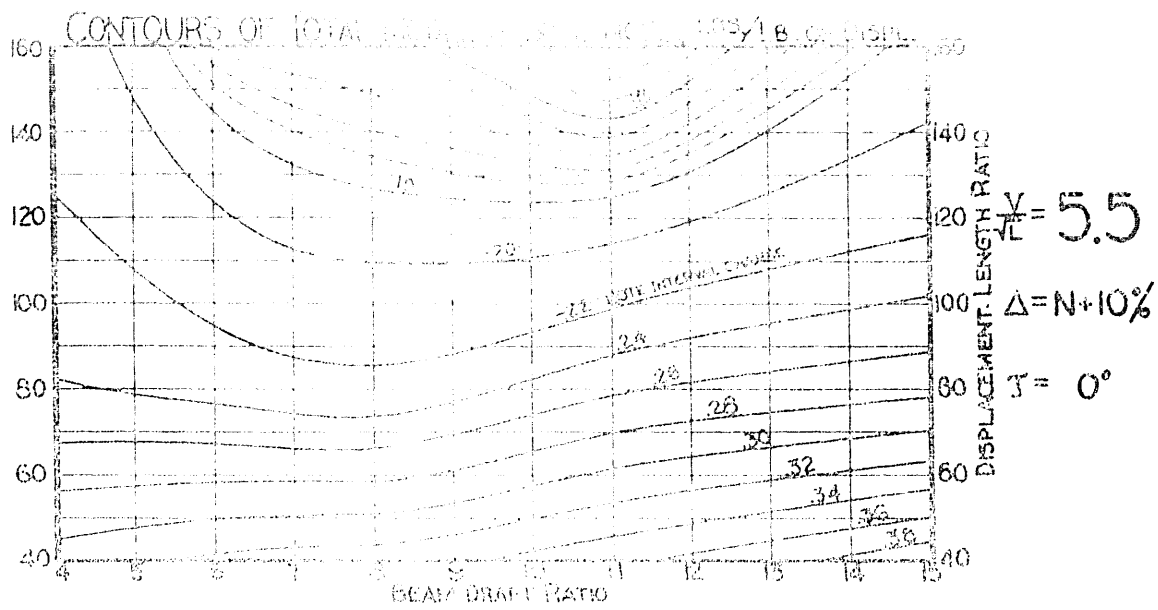


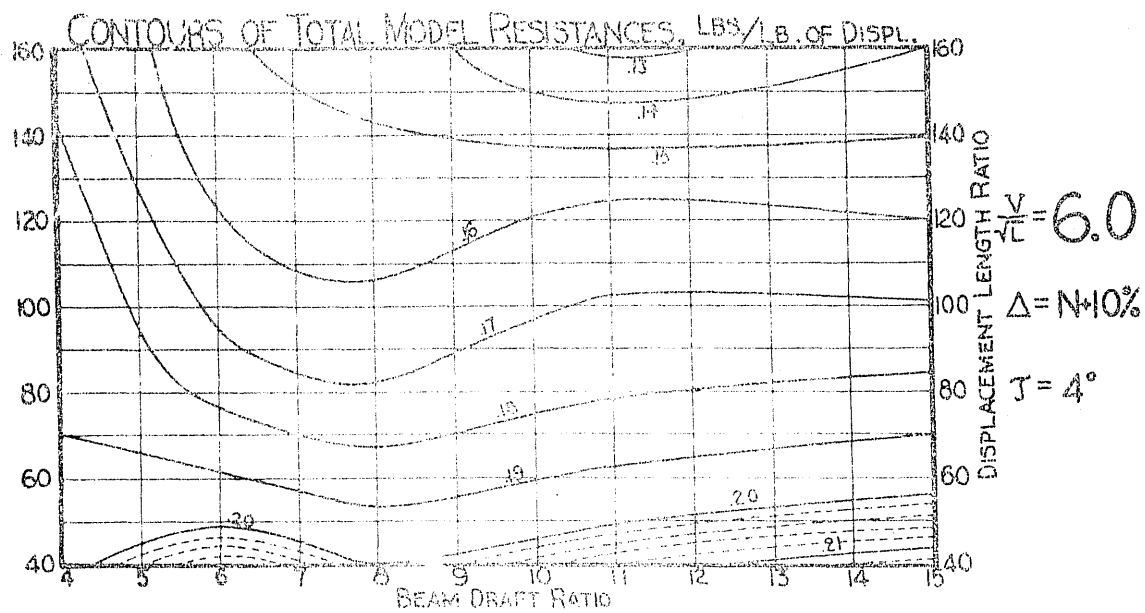
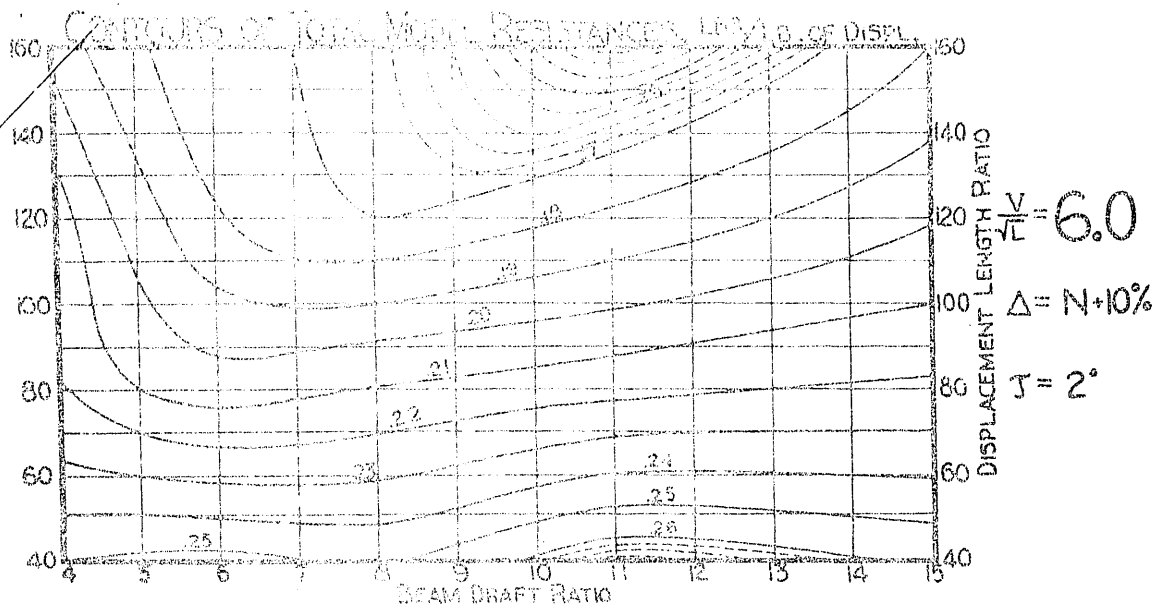
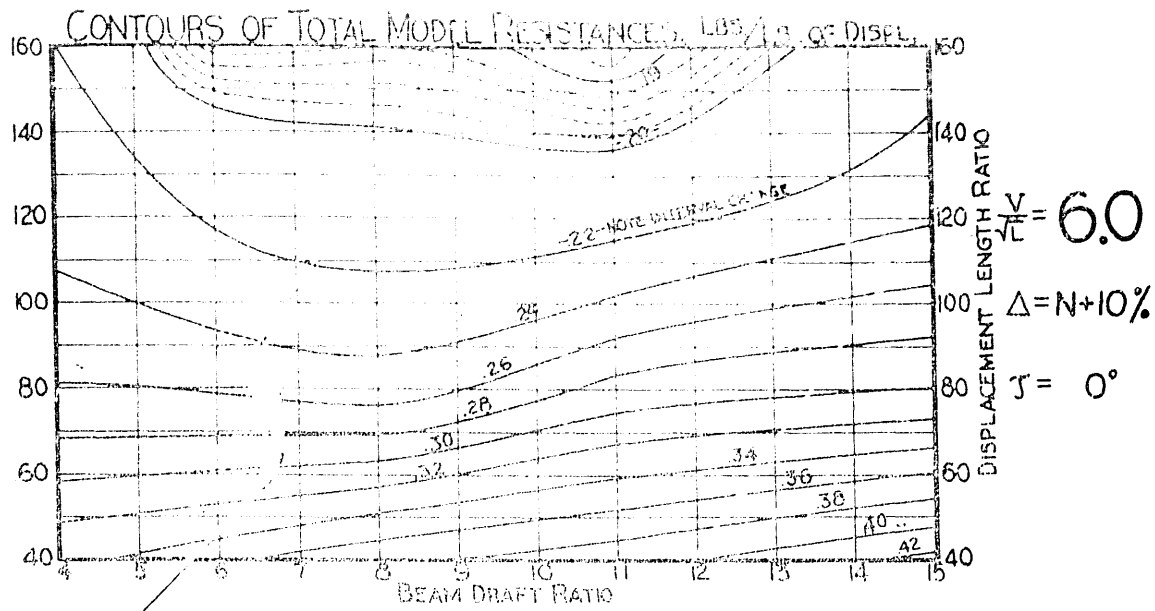


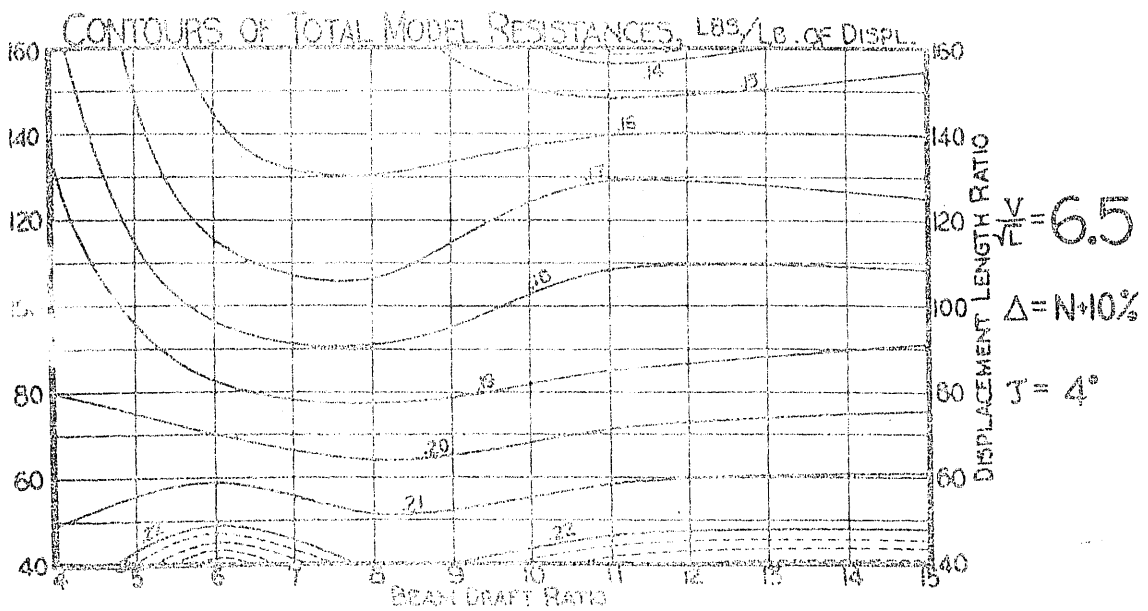
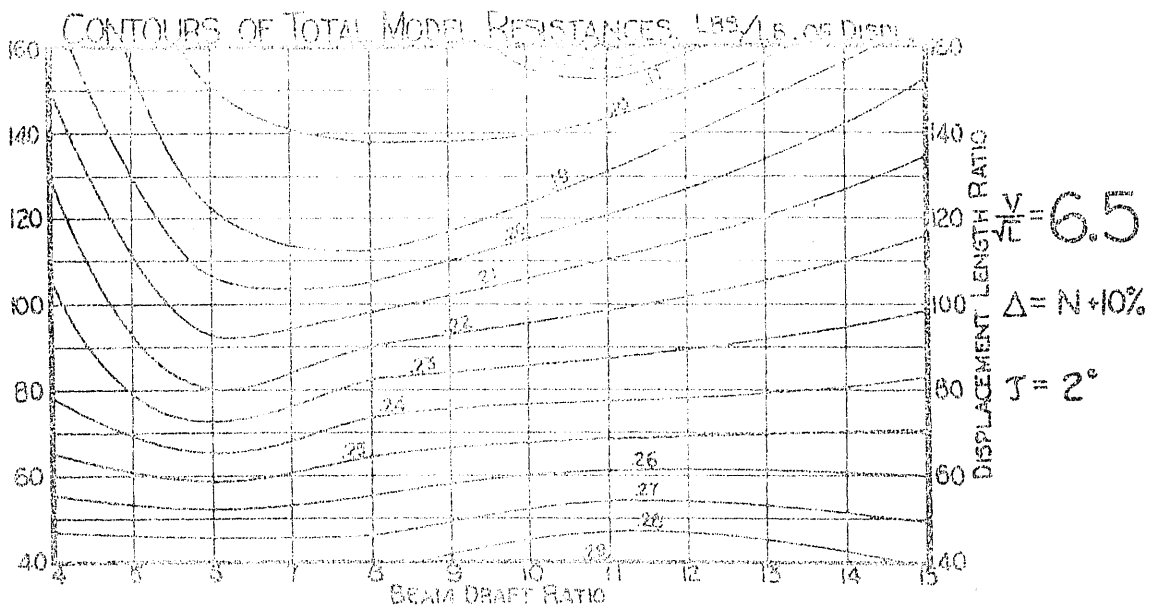
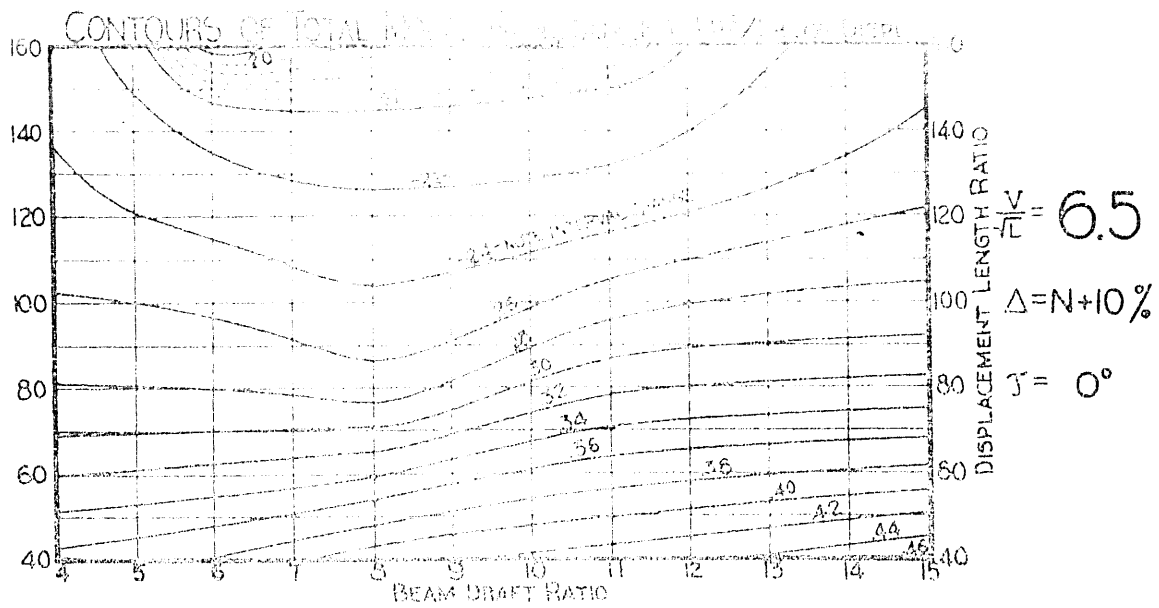


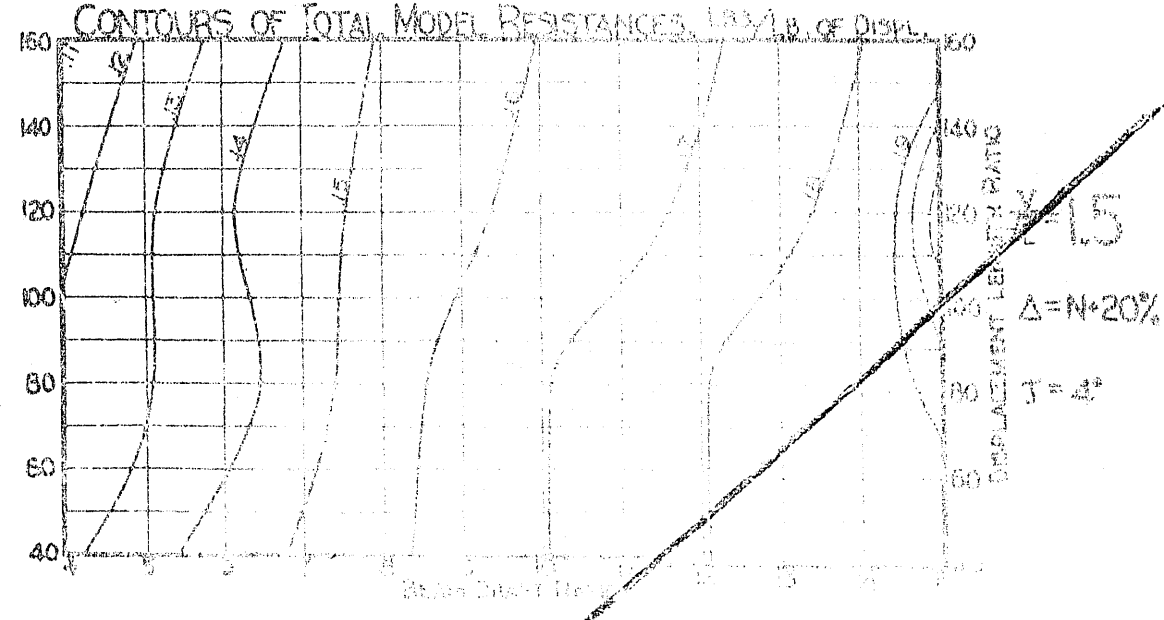
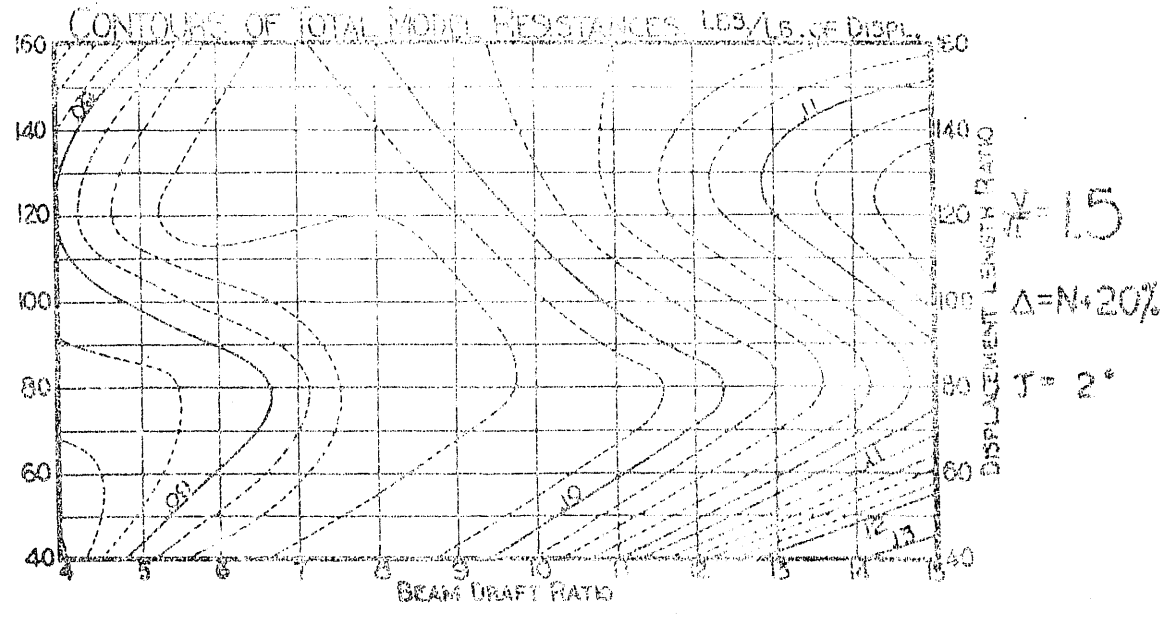
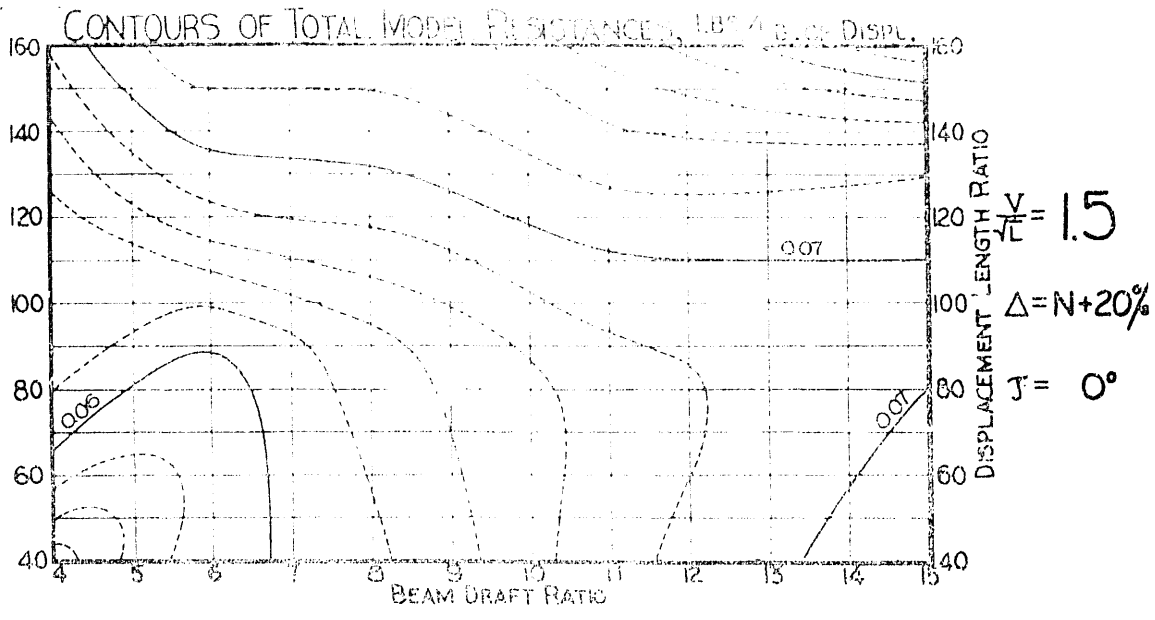


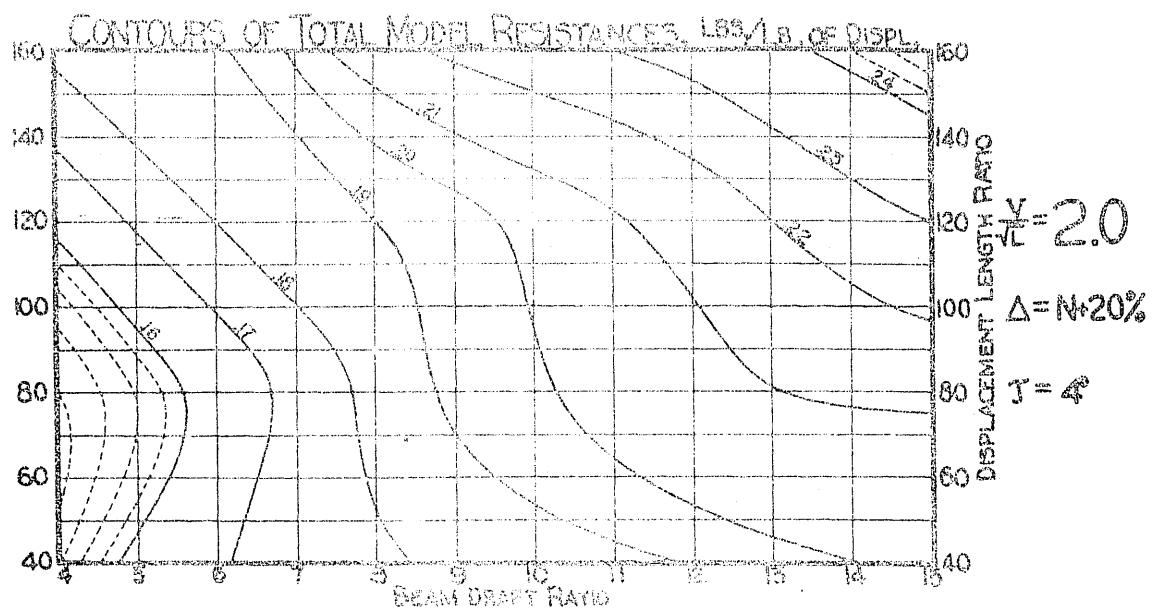
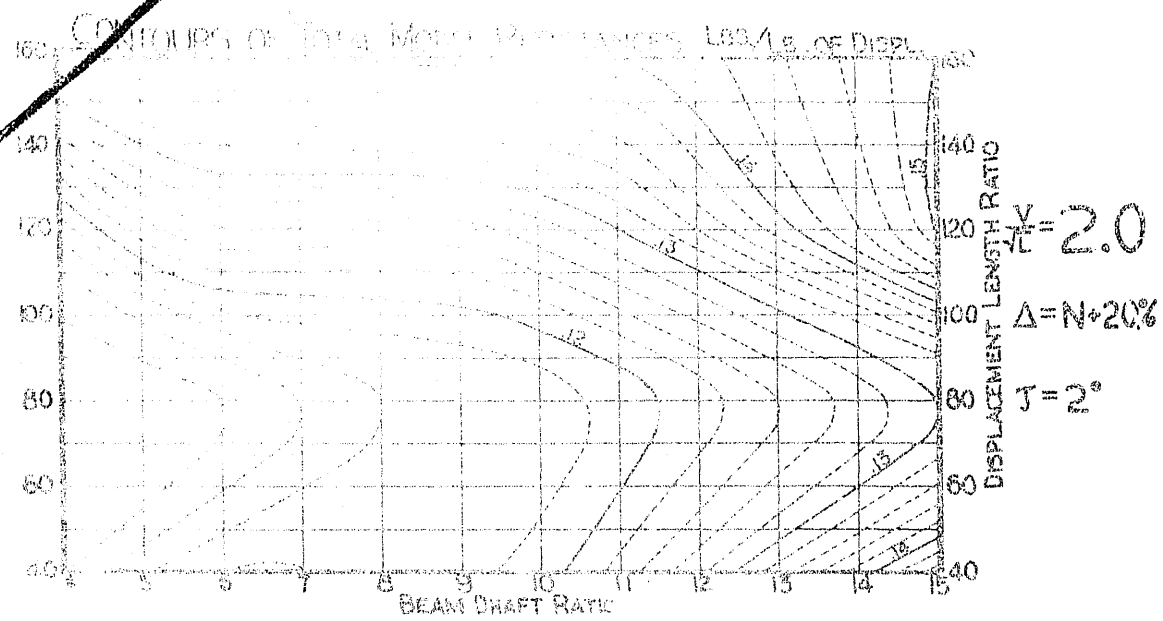
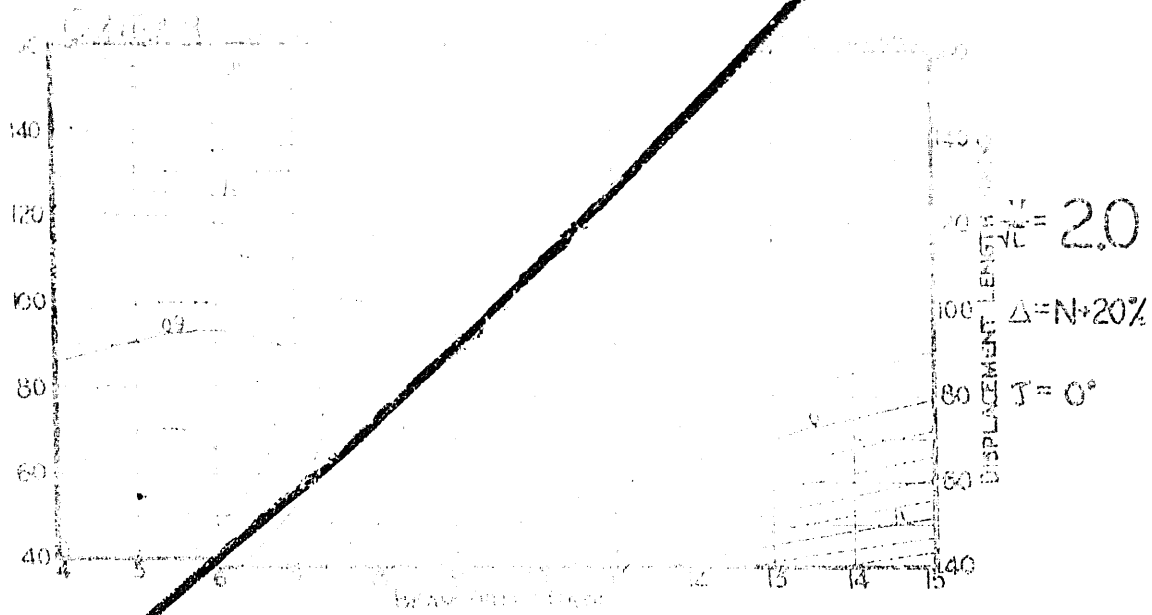


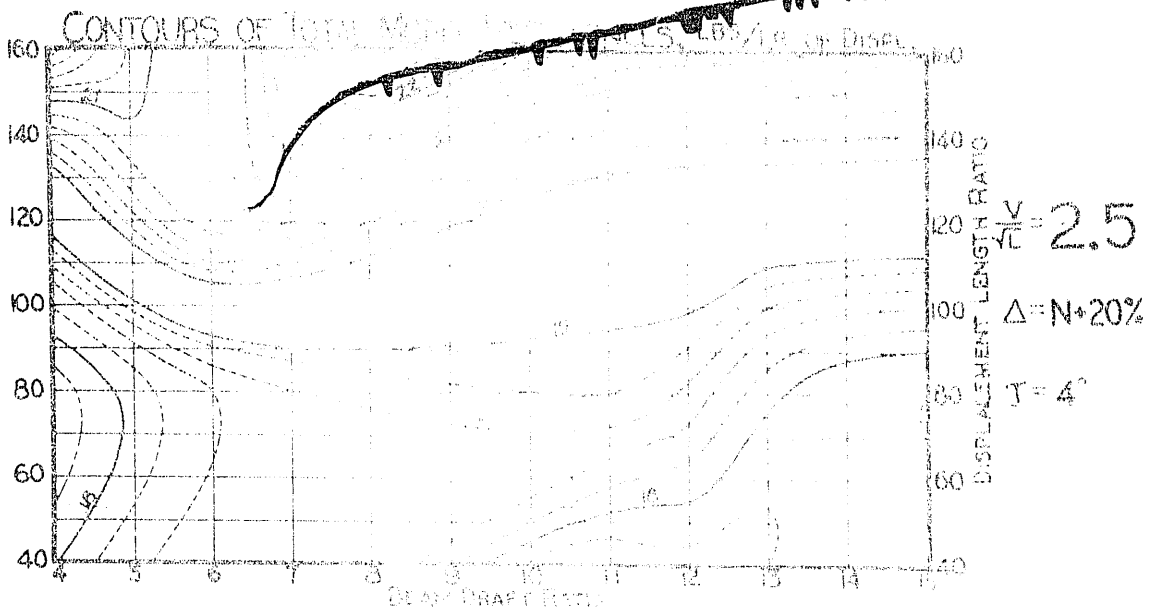
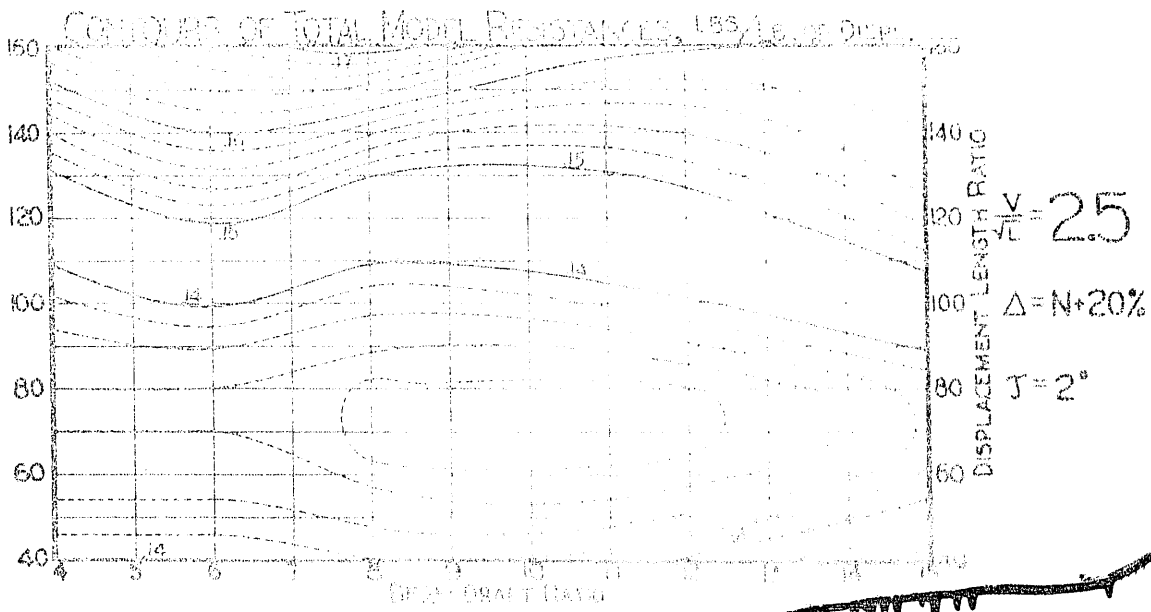
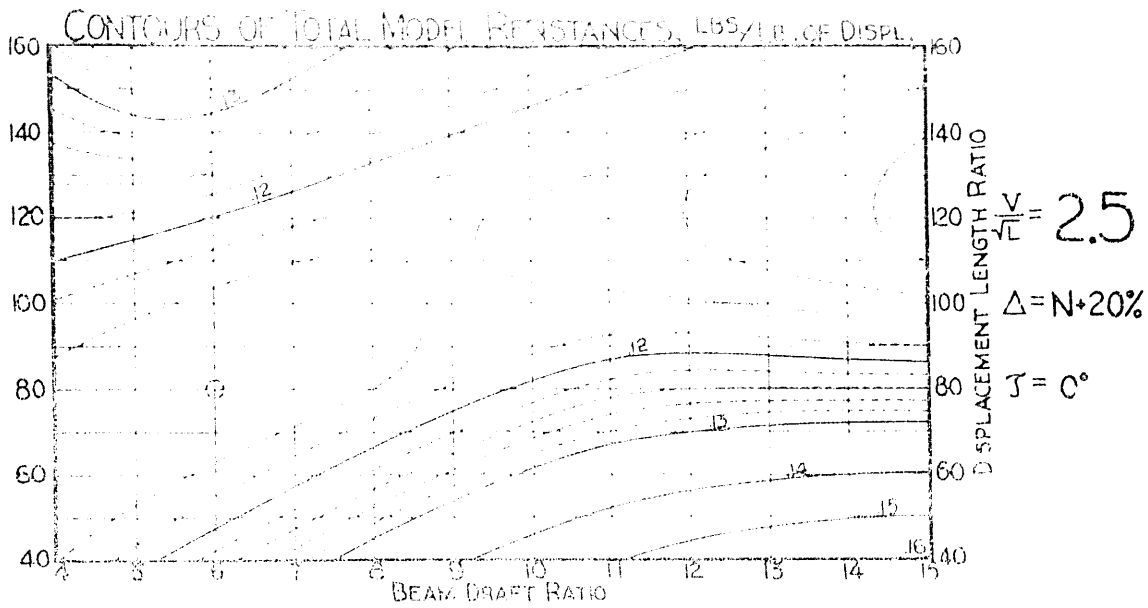


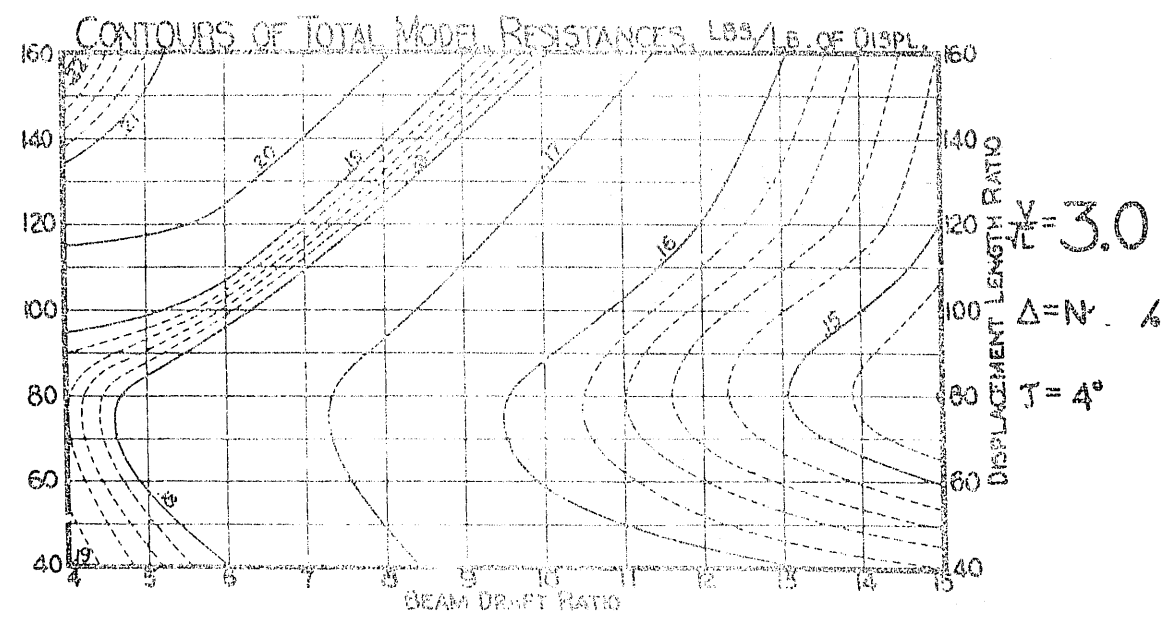
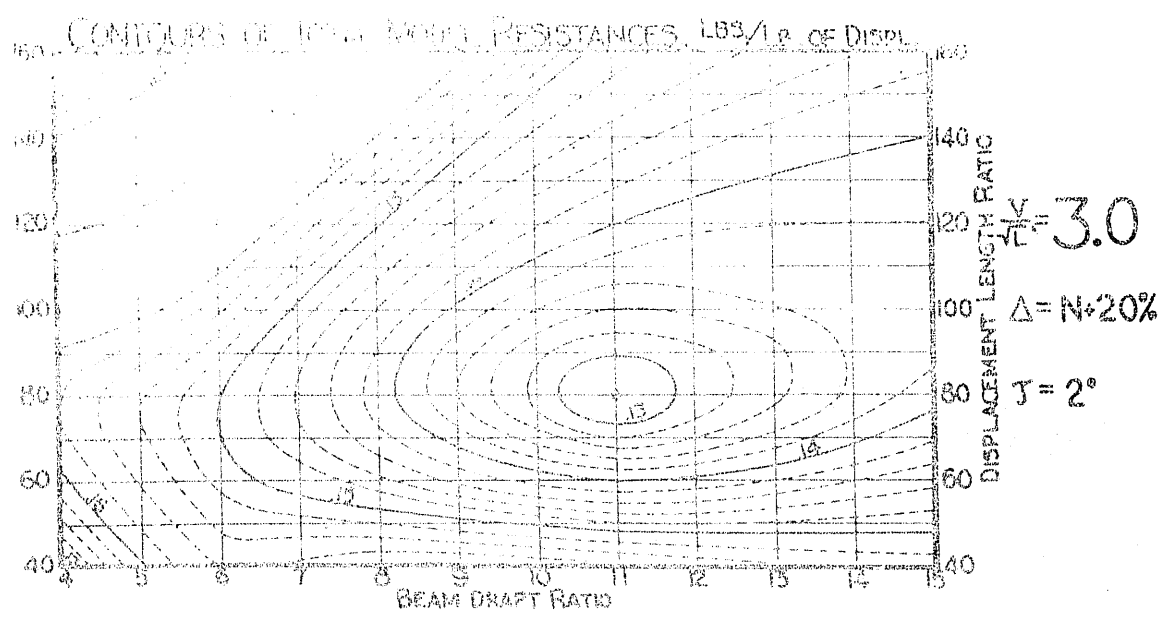
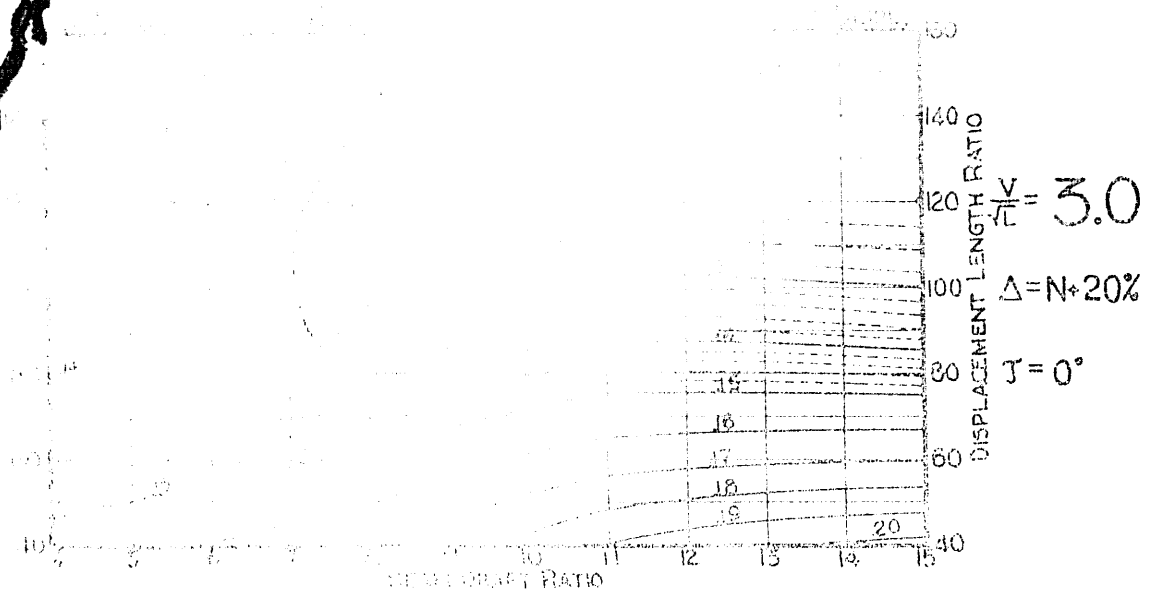


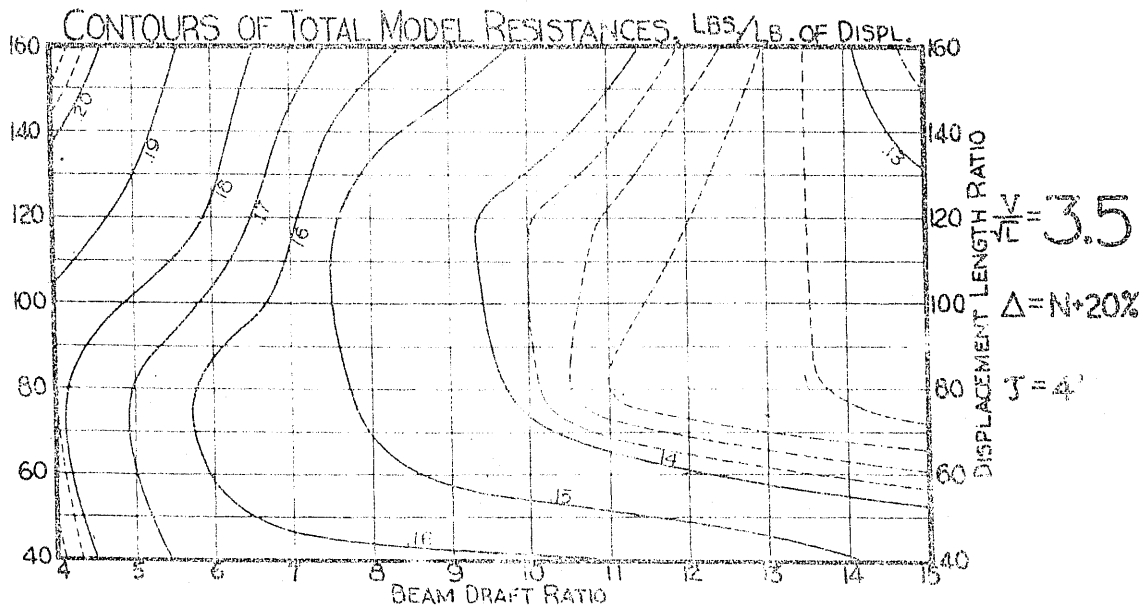
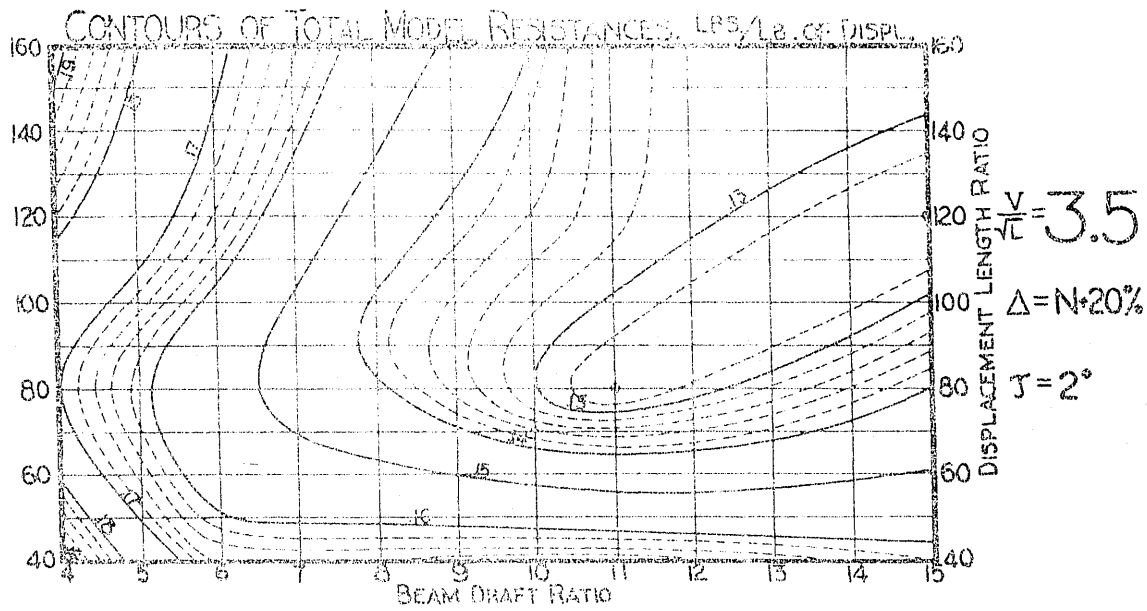
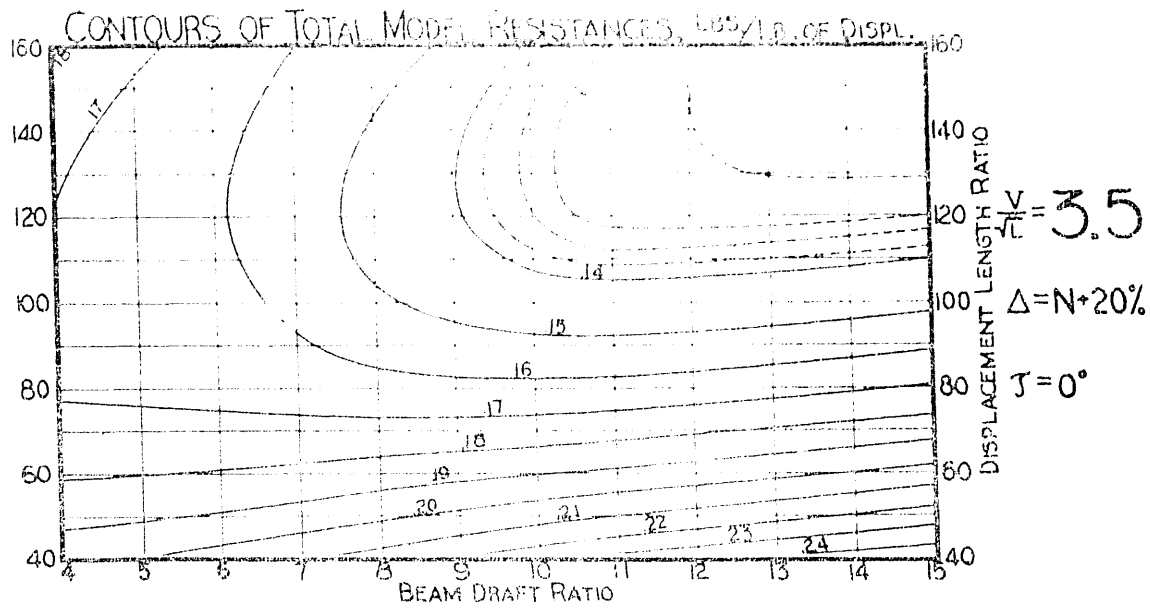


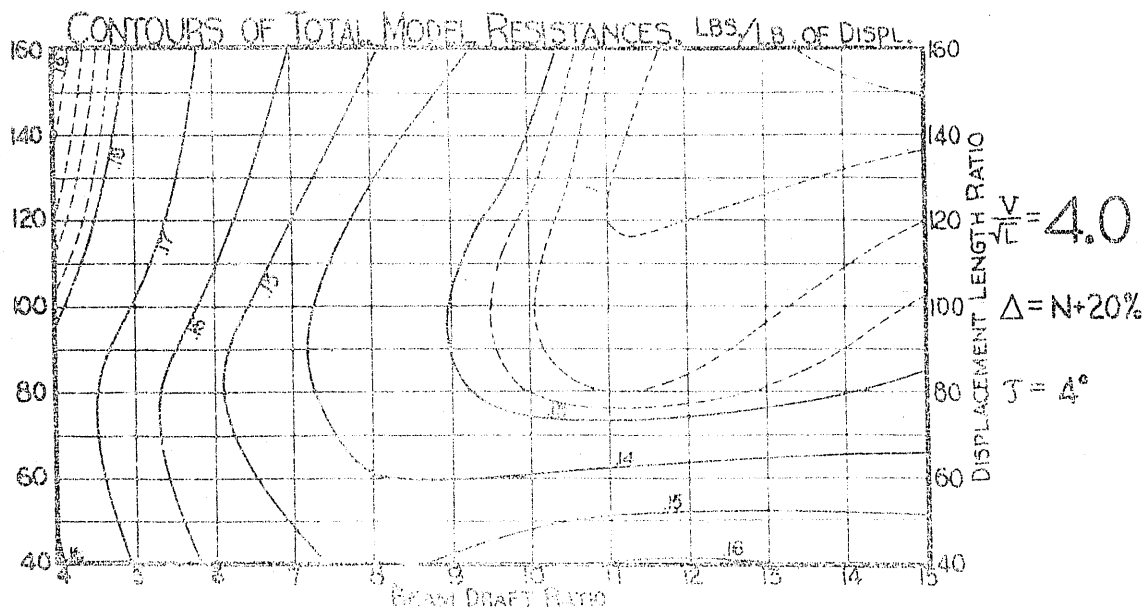
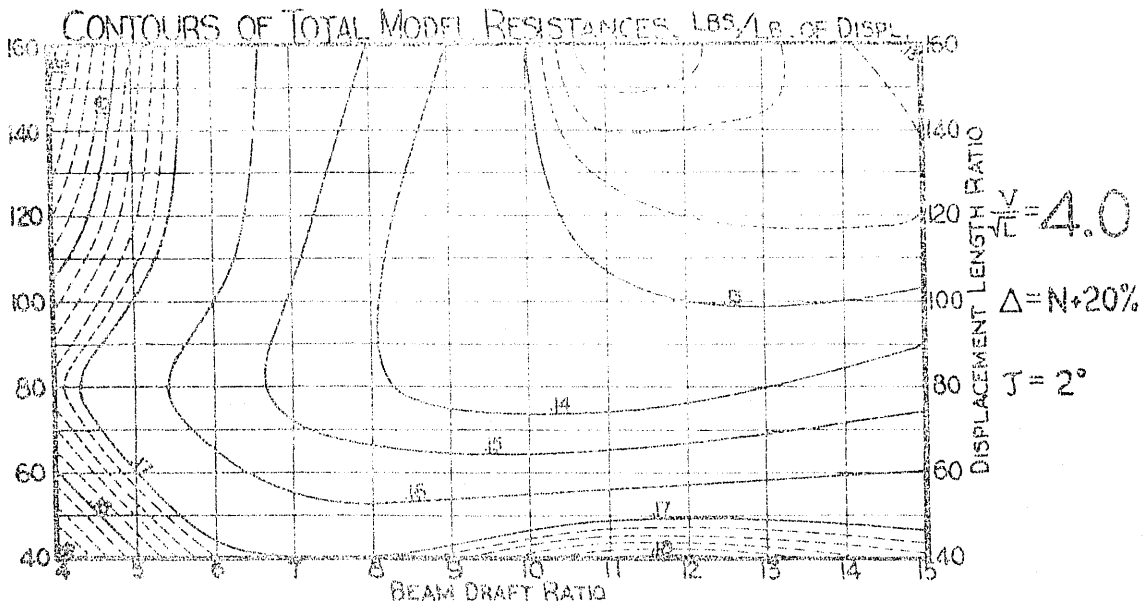
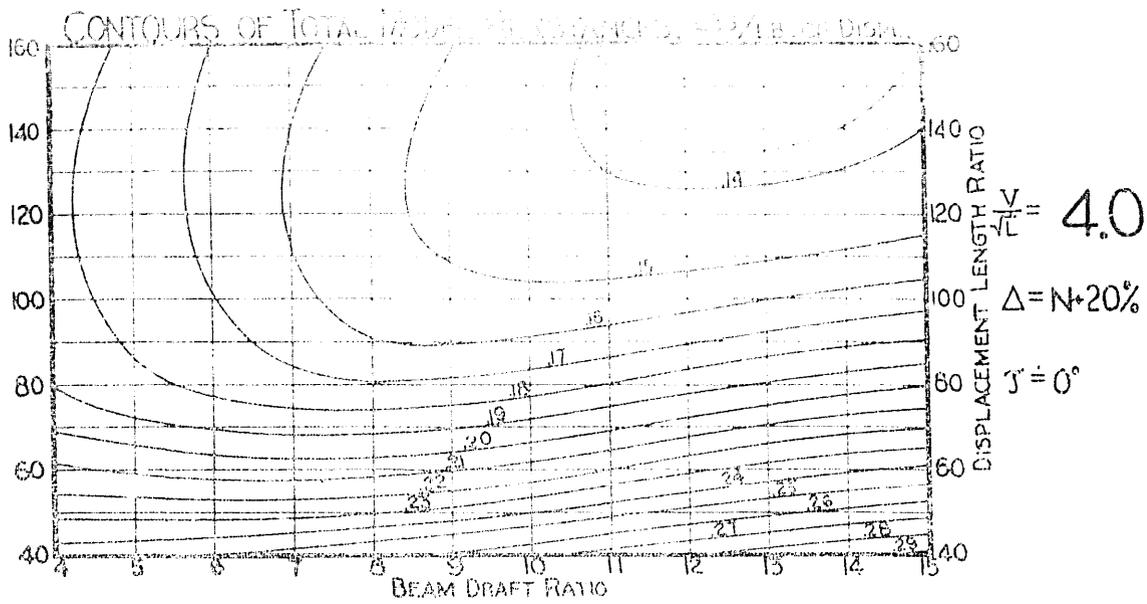


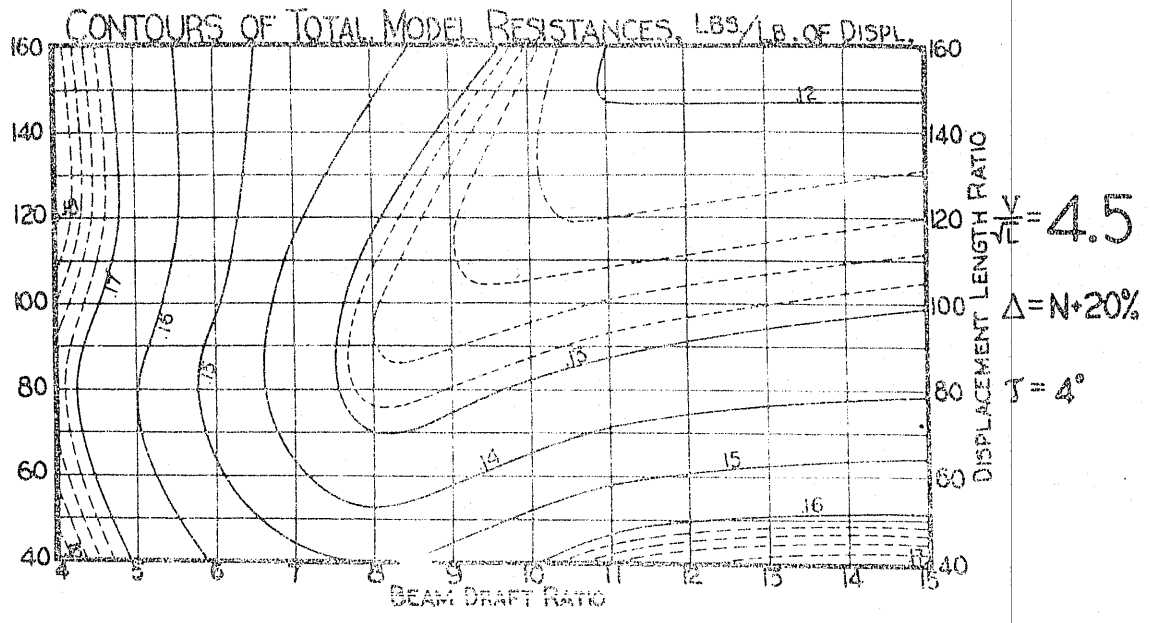
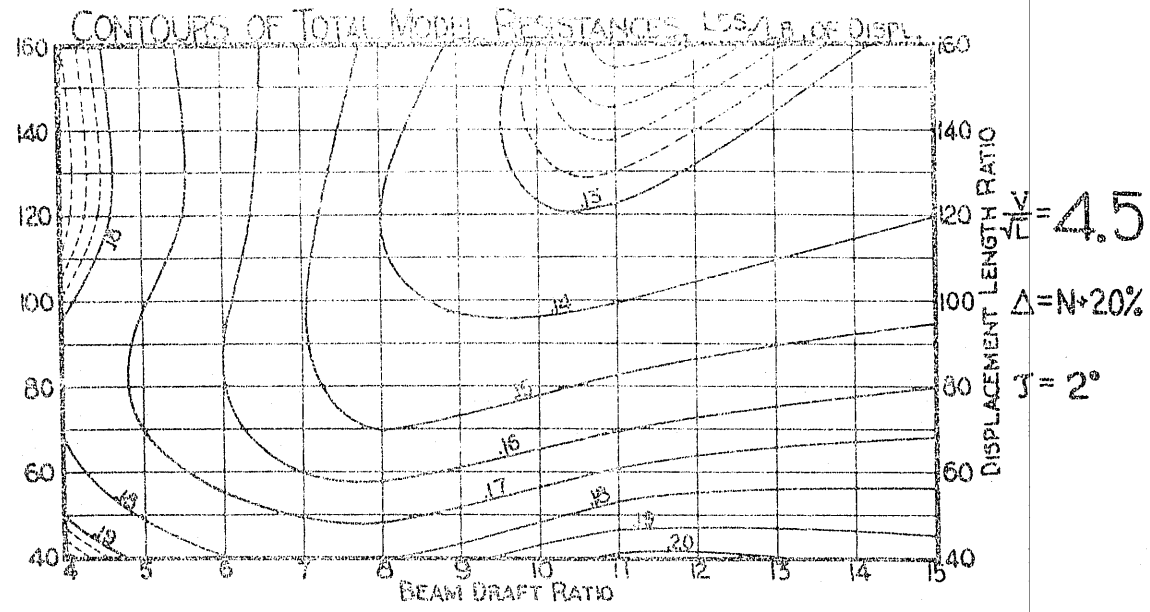
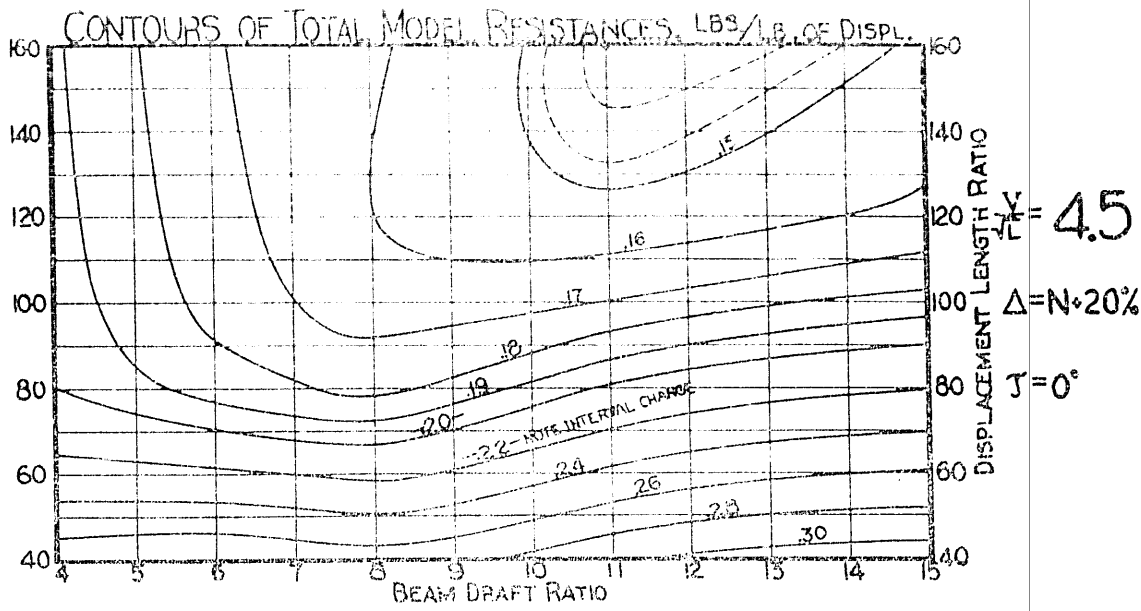


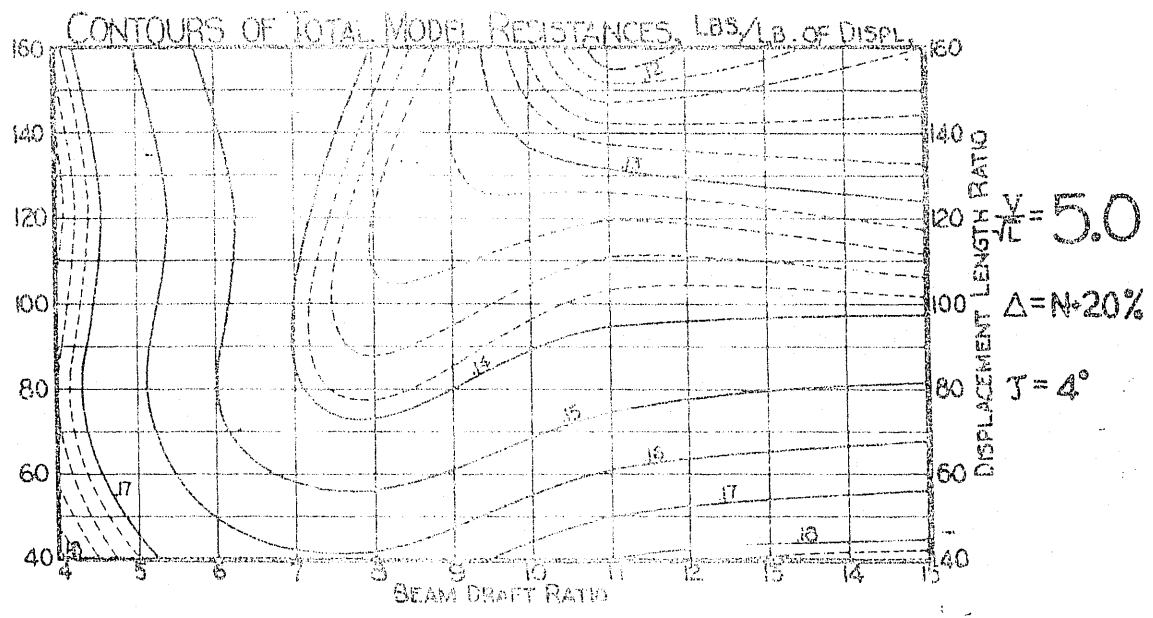
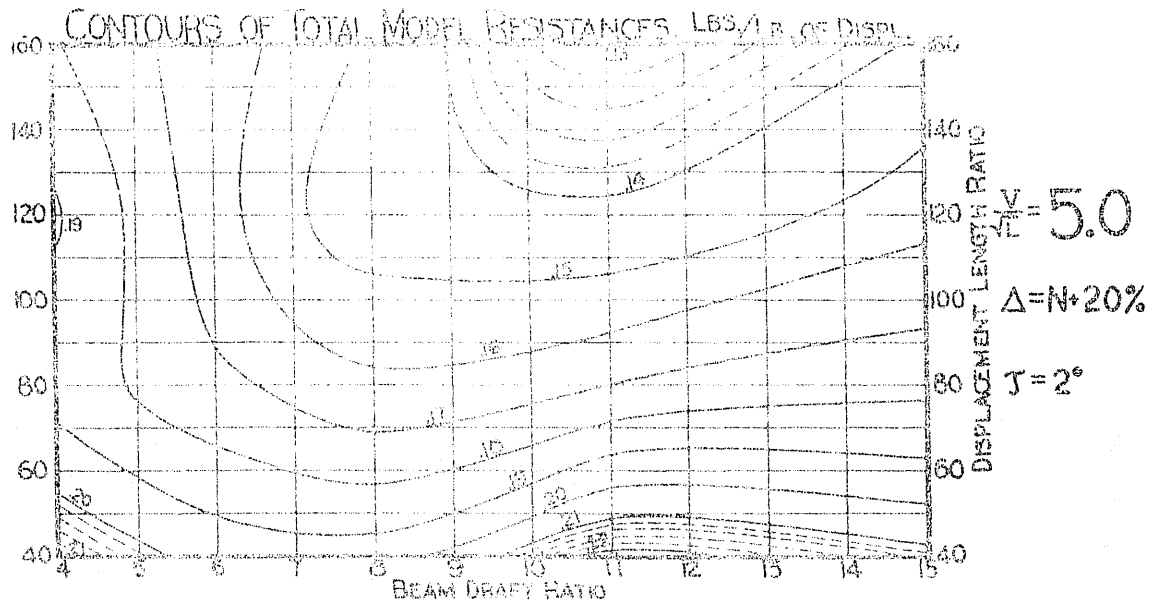
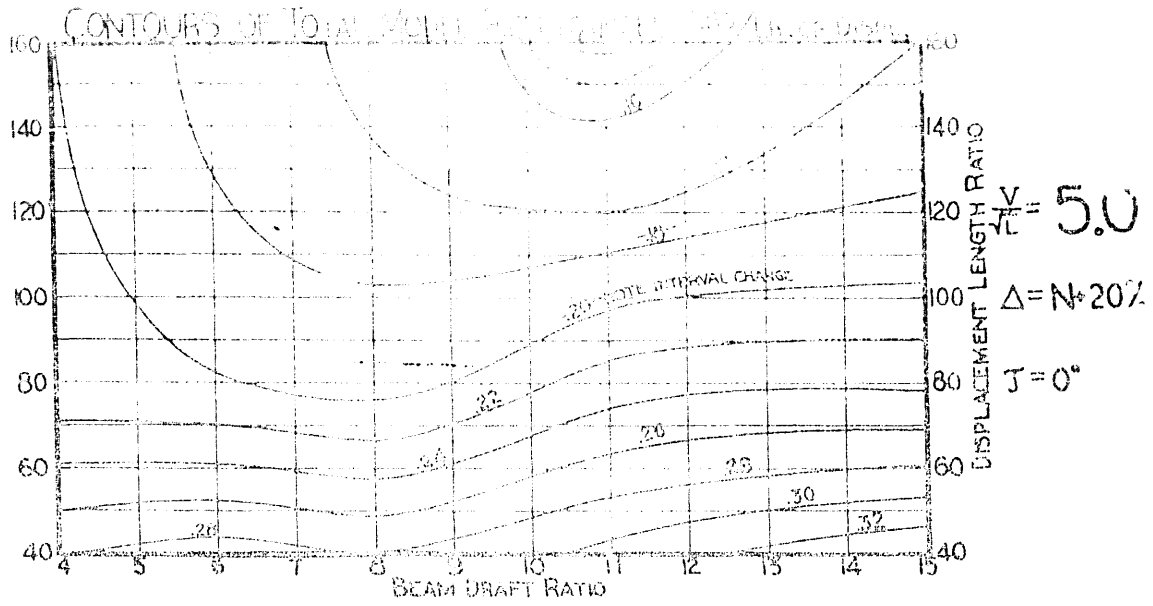


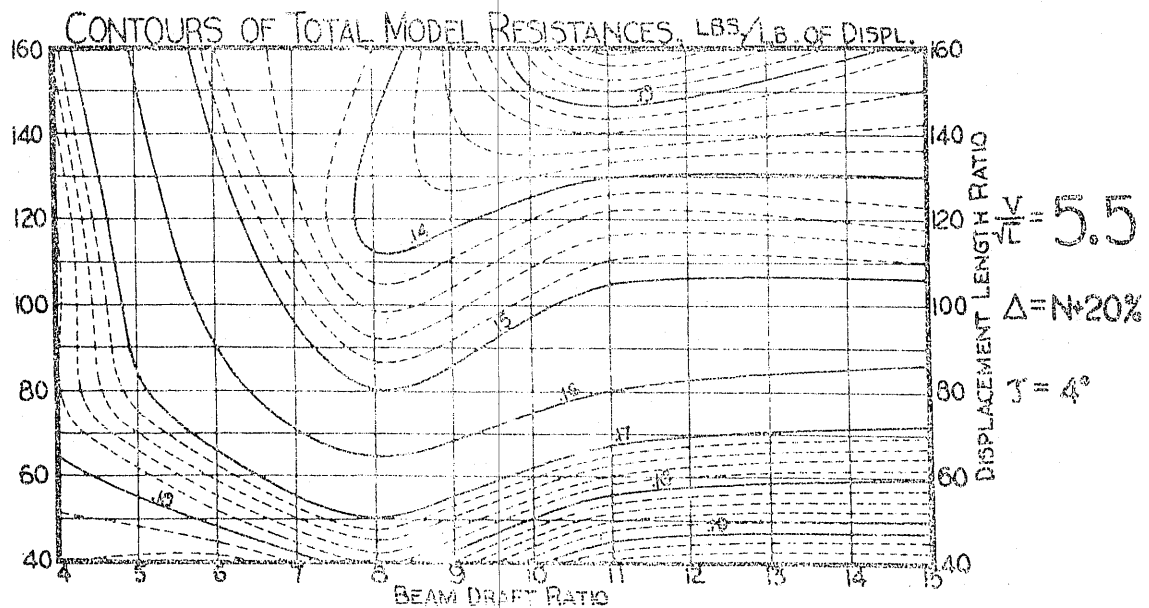
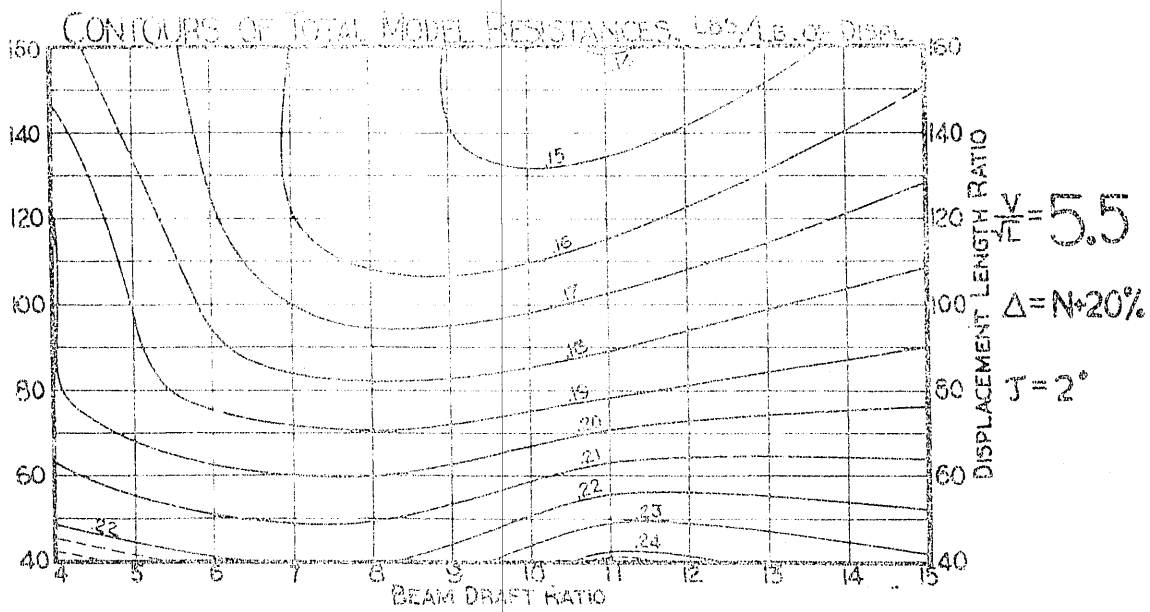
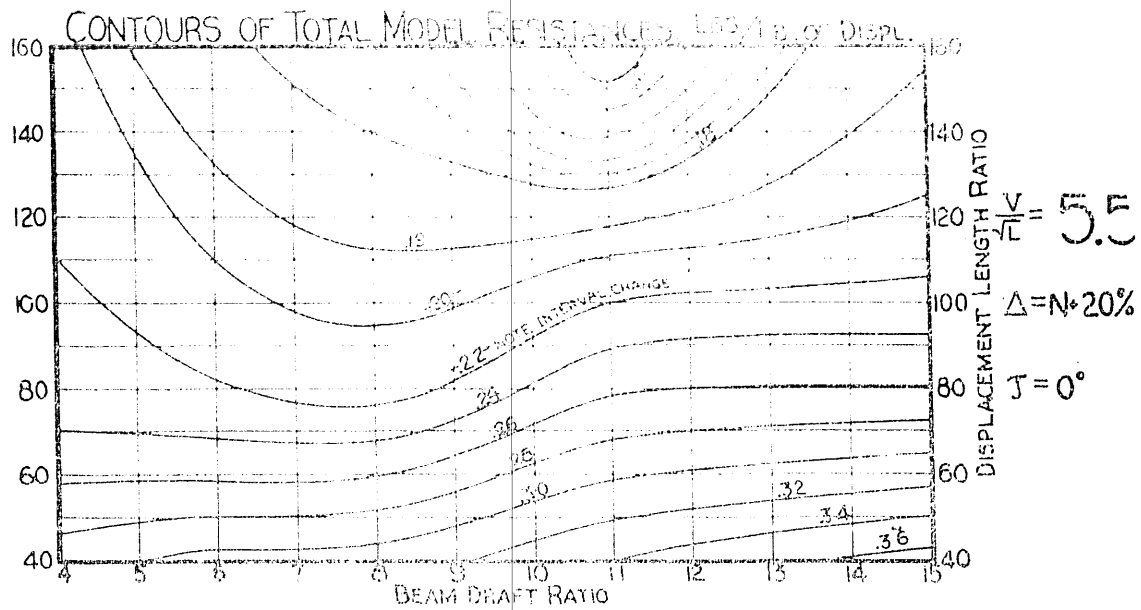


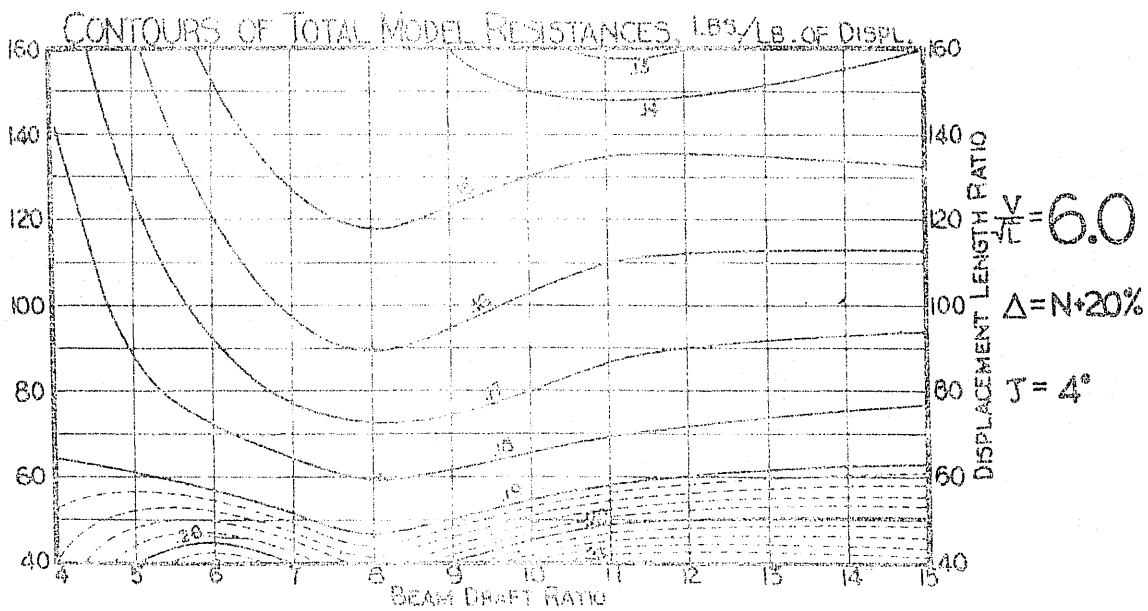
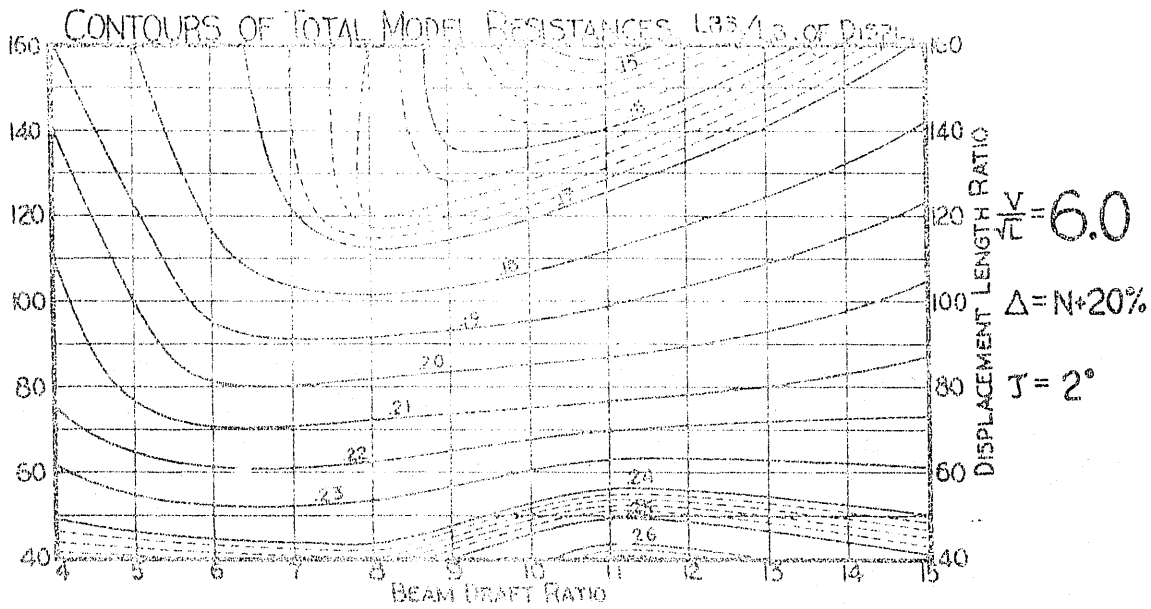
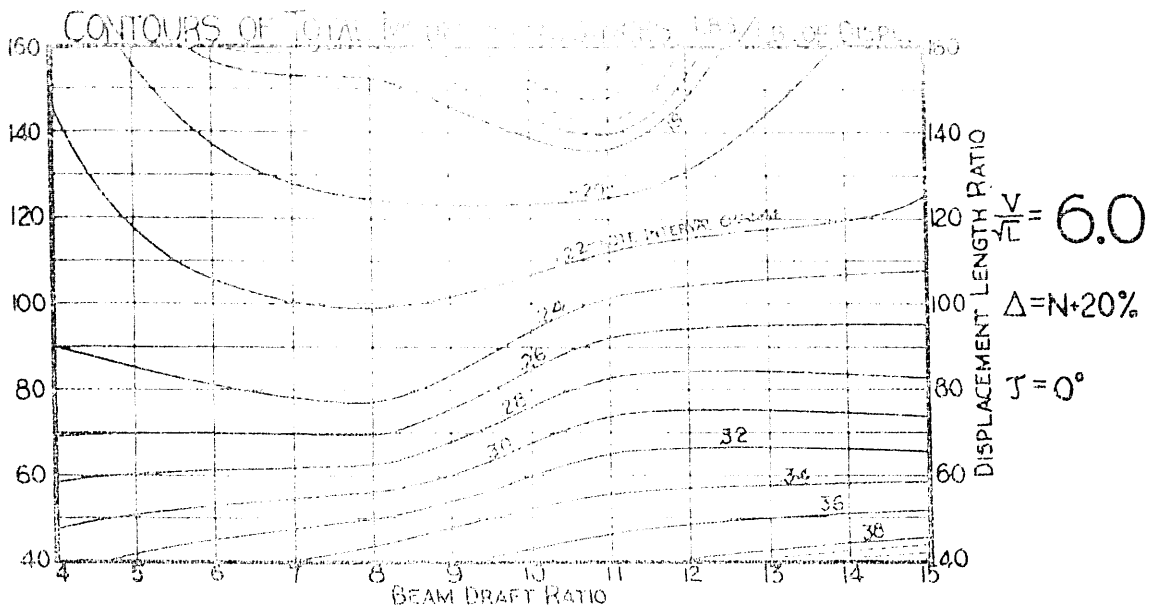


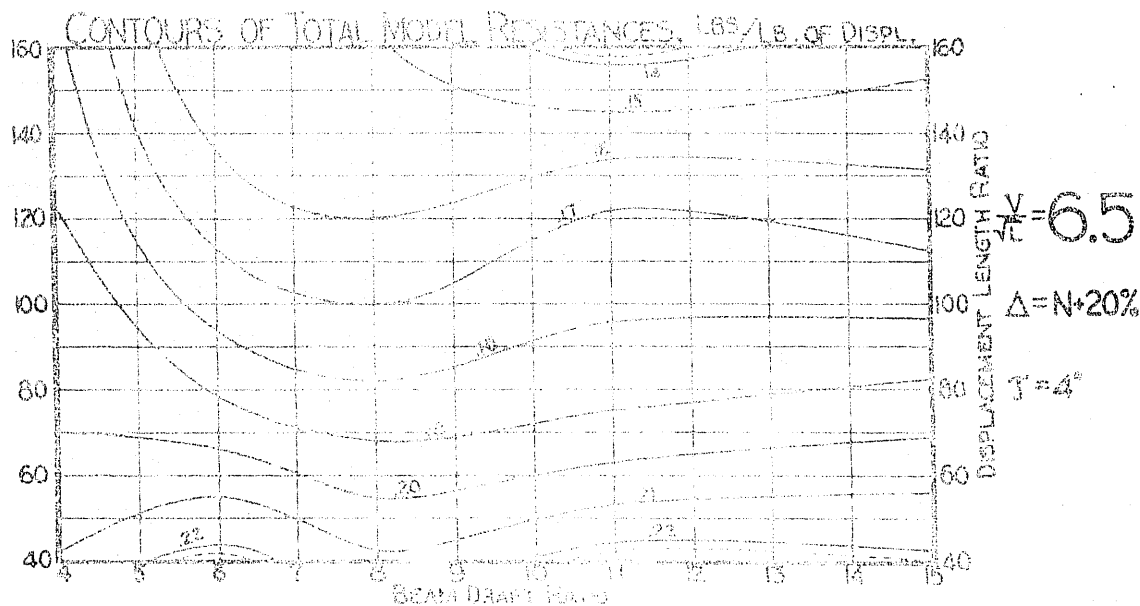
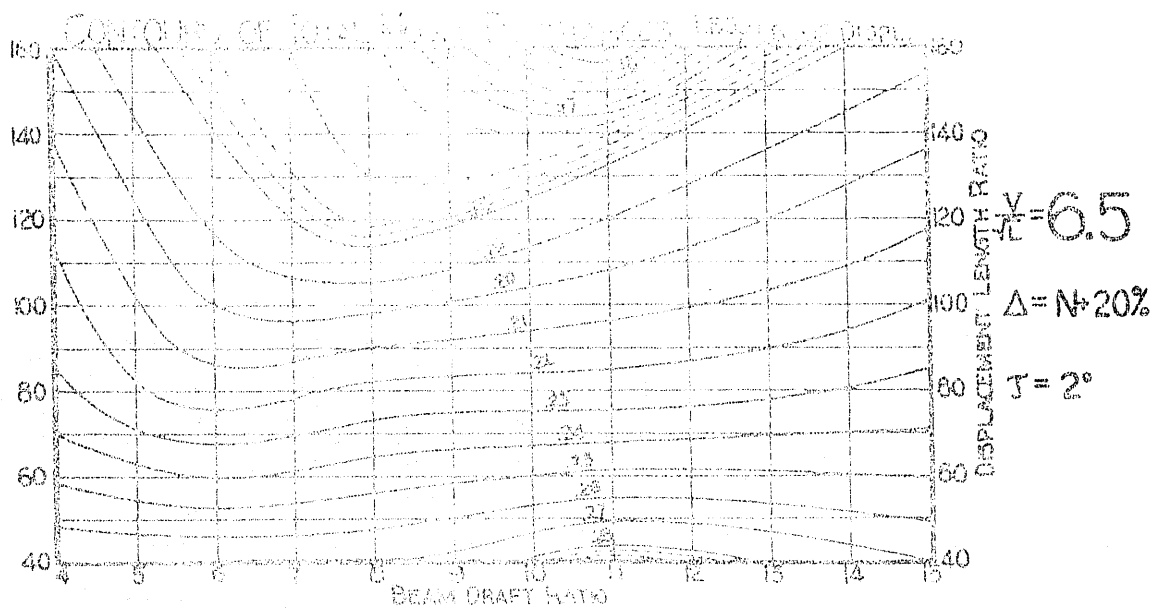
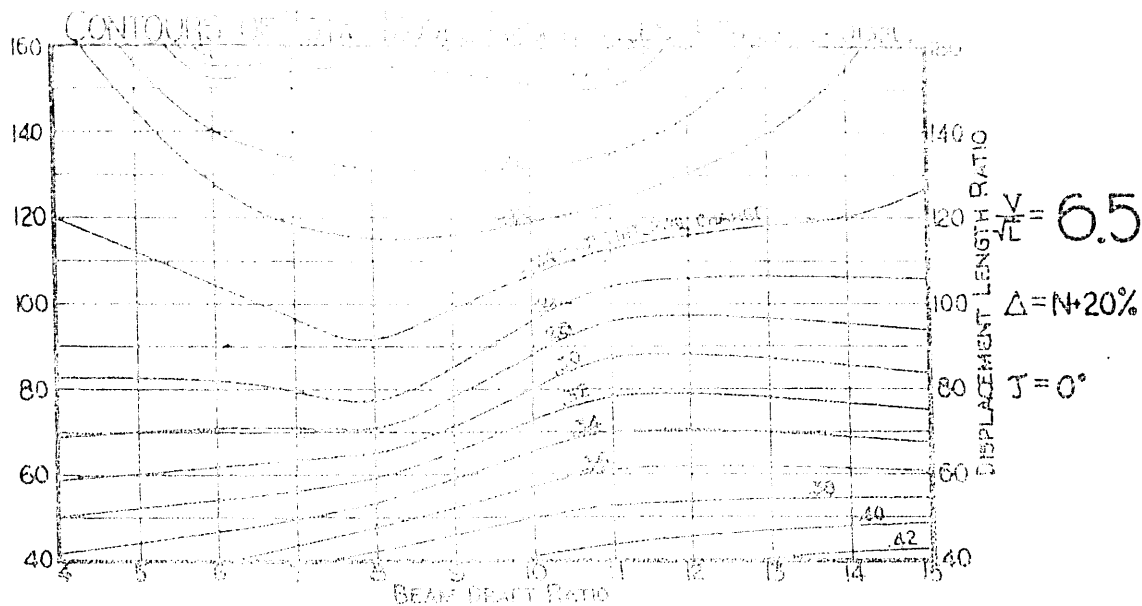










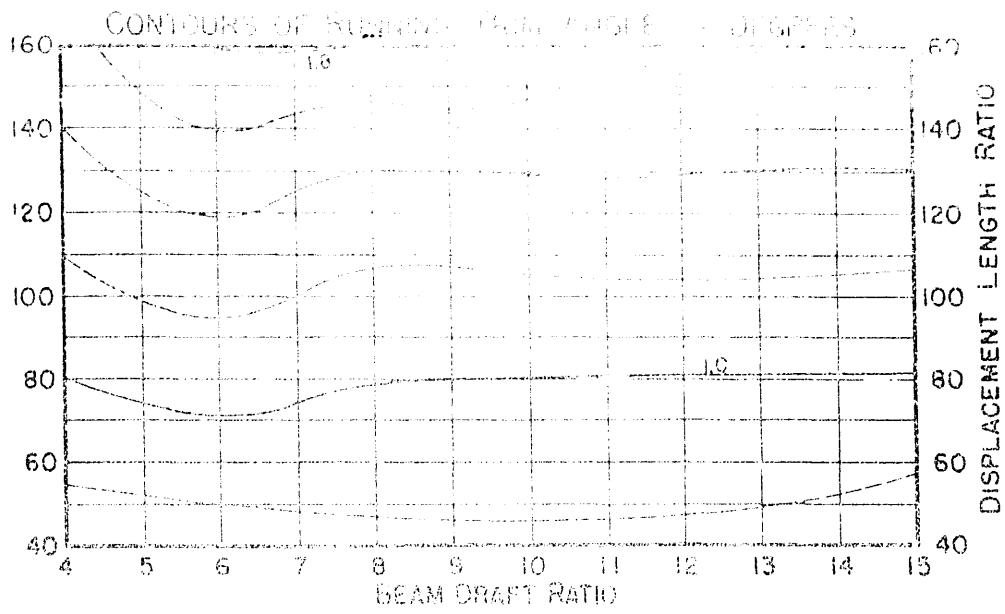


CONTOURS
OF
RUNNING TRIM

71

Speed-Length Ratios 1.5-6.5 in Steps of 0.5

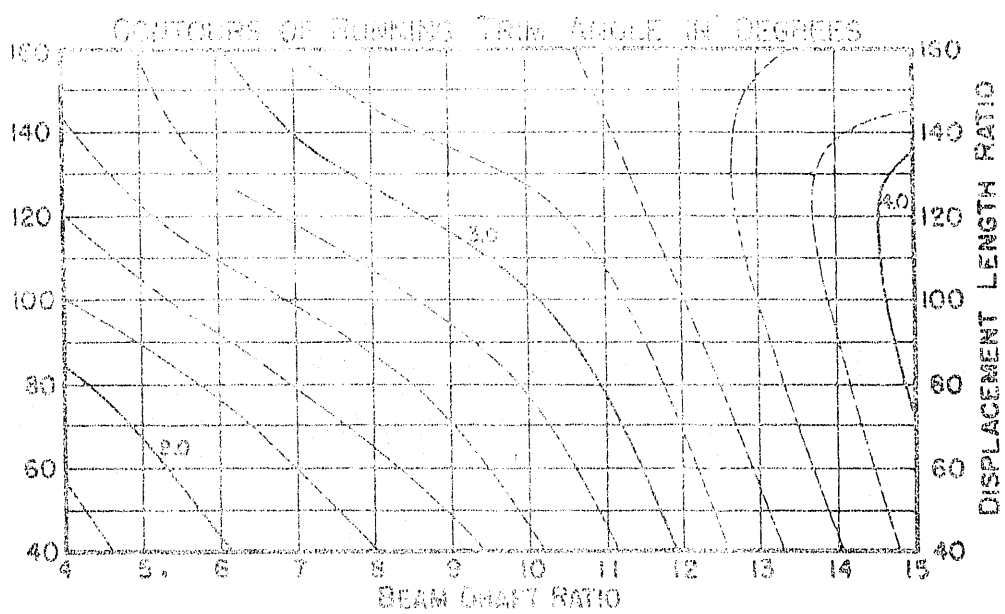
			Pages
100% Displacement (N)			47 to 57
110%	"	(N + 10%)	58 to 68
120%	"	(N + 20%)	69 to 79



$$\frac{v}{\sqrt{\lambda}} = 1.5$$

$$\Delta = N$$

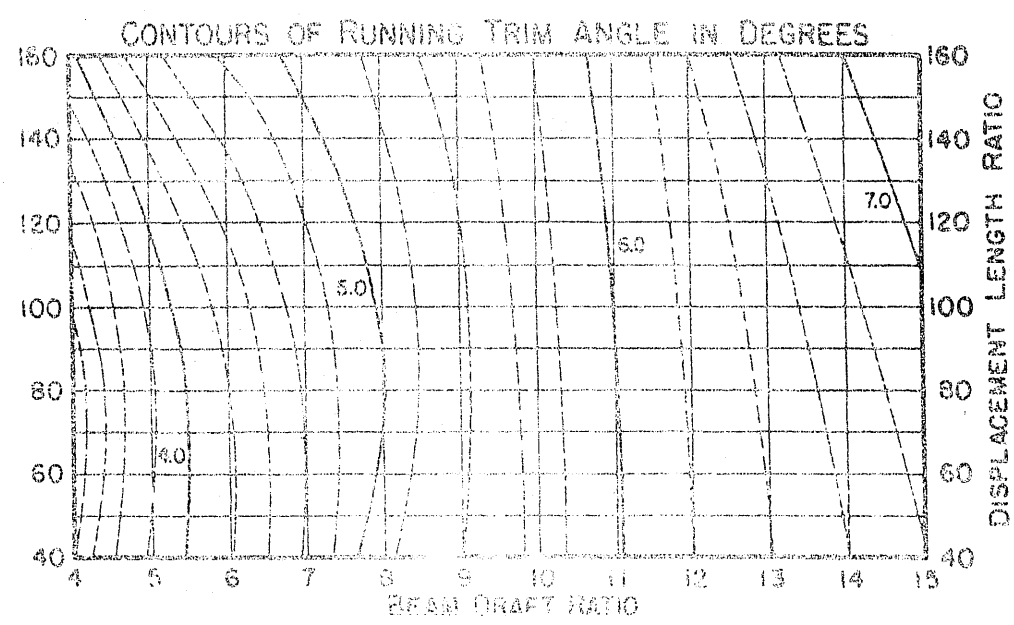
$$\gamma = 0^\circ$$



$$\frac{v}{\sqrt{\lambda}} = 1.5$$

$$\Delta = N$$

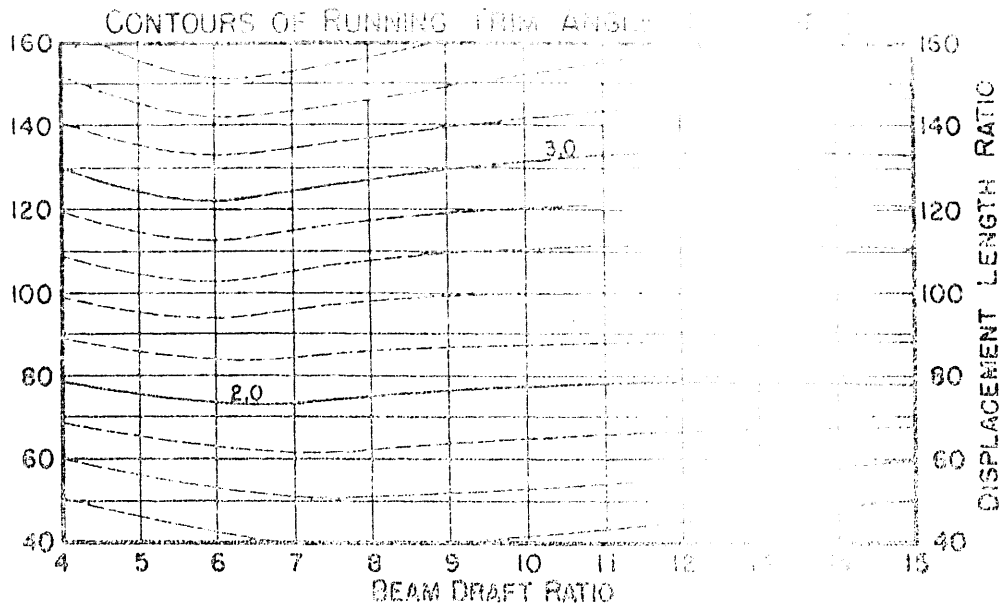
$$\gamma = 2^\circ$$



$$\frac{v}{\sqrt{\lambda}} = 1.5$$

$$\Delta = N$$

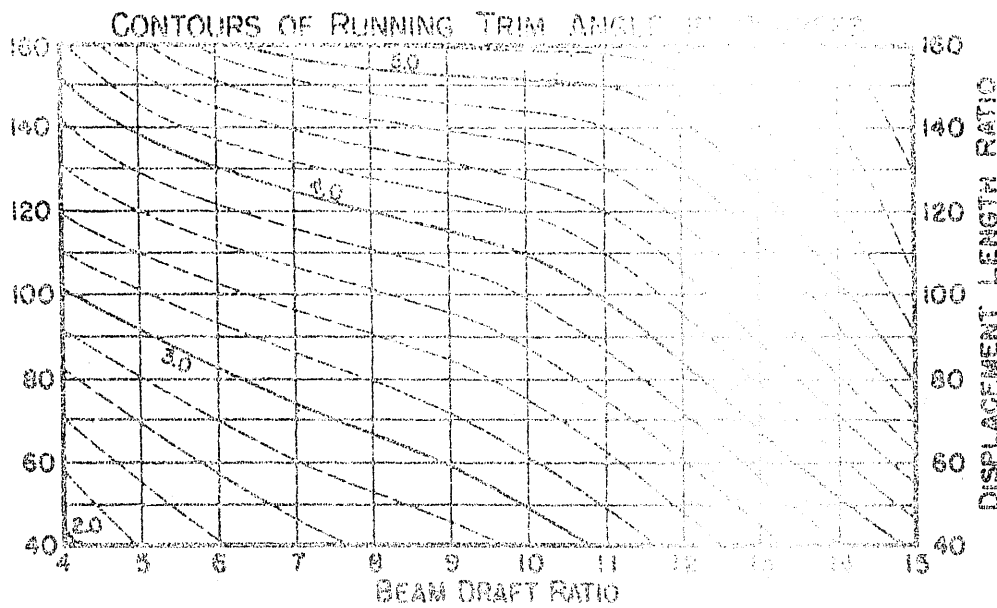
$$\gamma = 4^\circ$$



$$\frac{V}{\sqrt{L}} = 2.0$$

$$\Delta = N$$

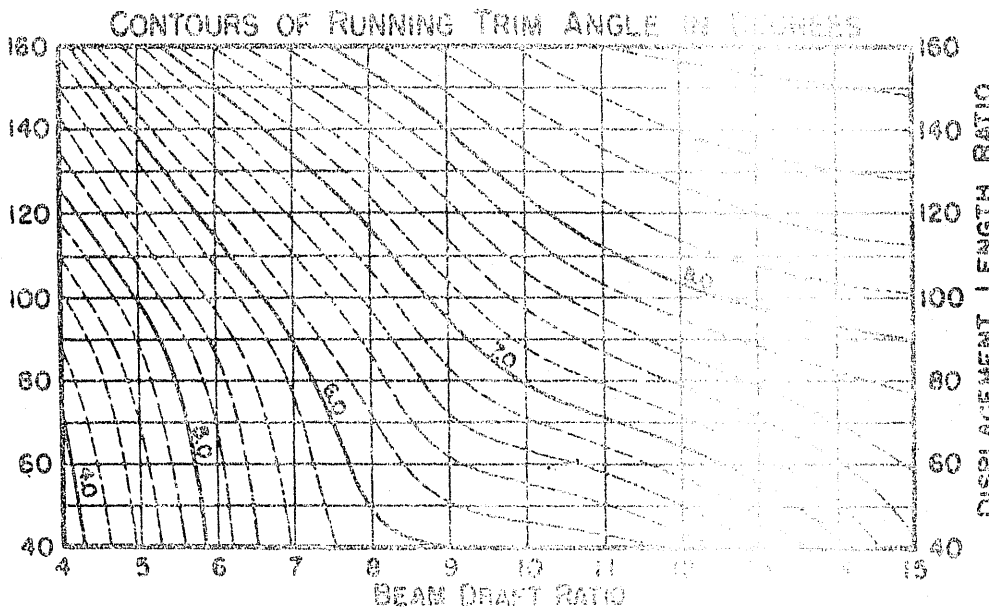
$$\tau = 0^\circ$$



$$\frac{V}{\sqrt{L}} = 2.0$$

$$\Delta = N$$

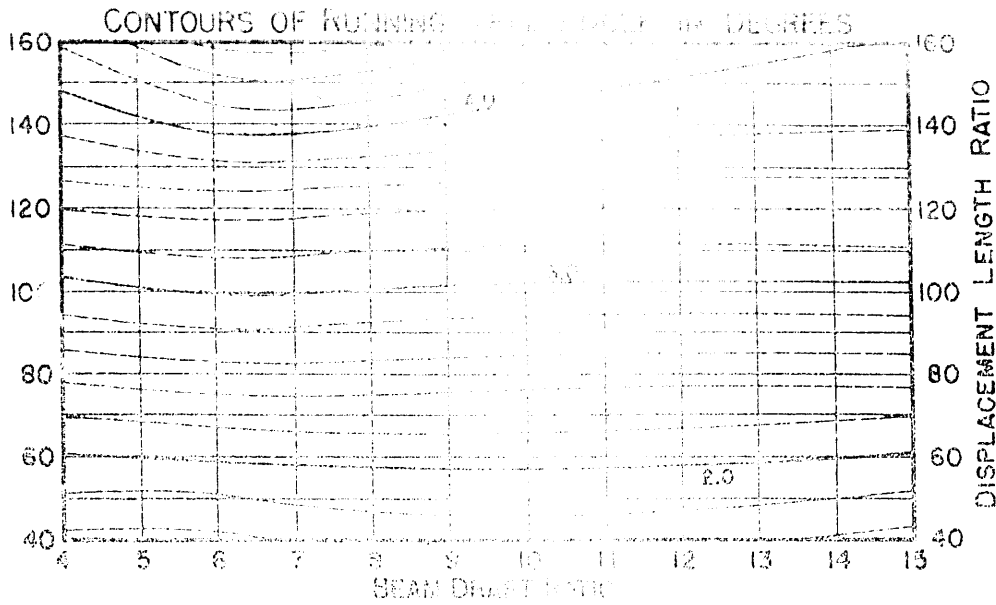
$$\tau = 2^\circ$$



$$\frac{V}{\sqrt{L}} = 2.0$$

$$\Delta = N$$

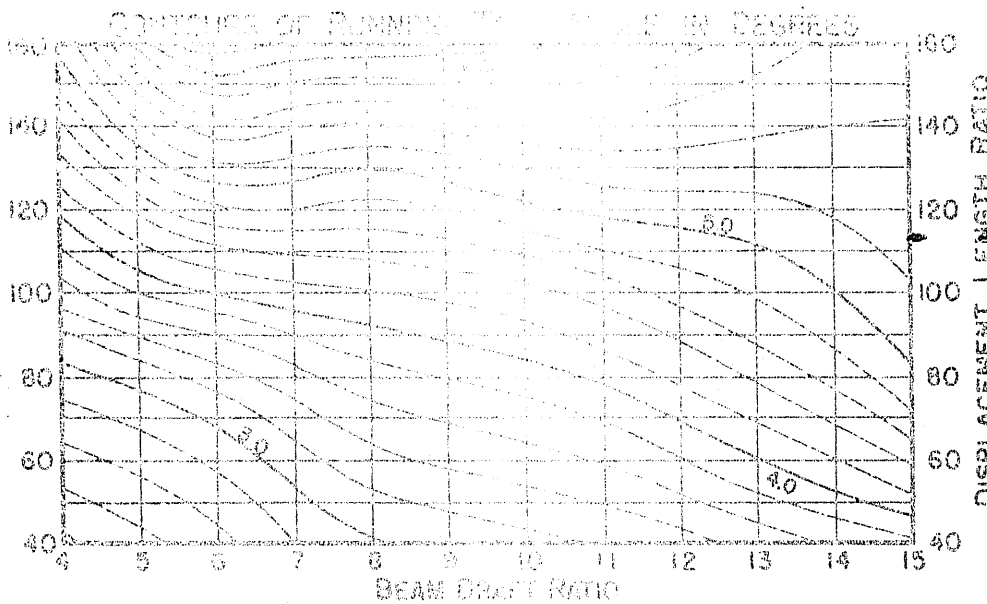
$$\tau = 4^\circ$$



$$\frac{v}{\sqrt{L}} = 2.5$$

$$\Delta = N$$

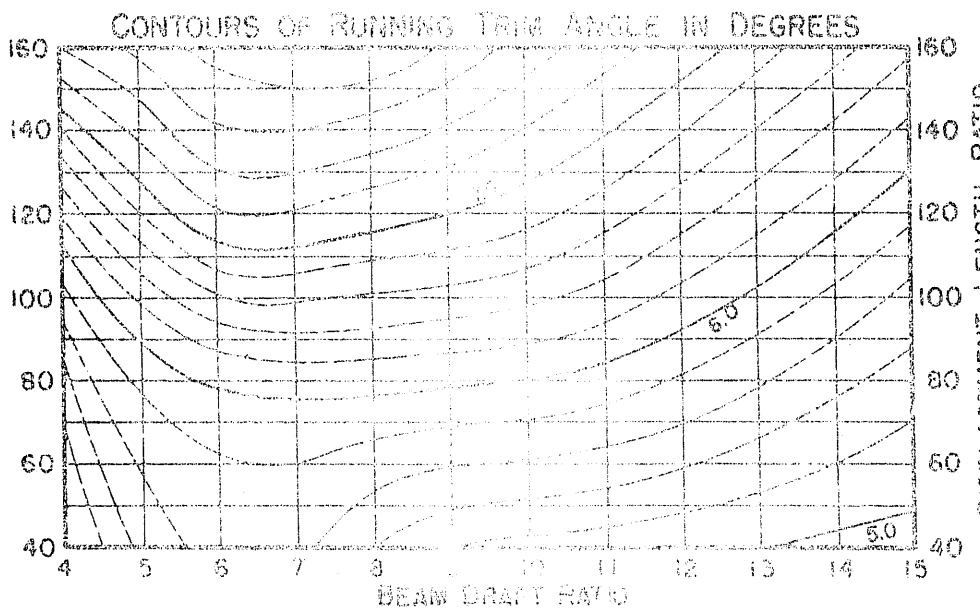
$$\sigma = 0^\circ$$



$$\frac{v}{\sqrt{L}} = 2.5$$

$$\Delta = N$$

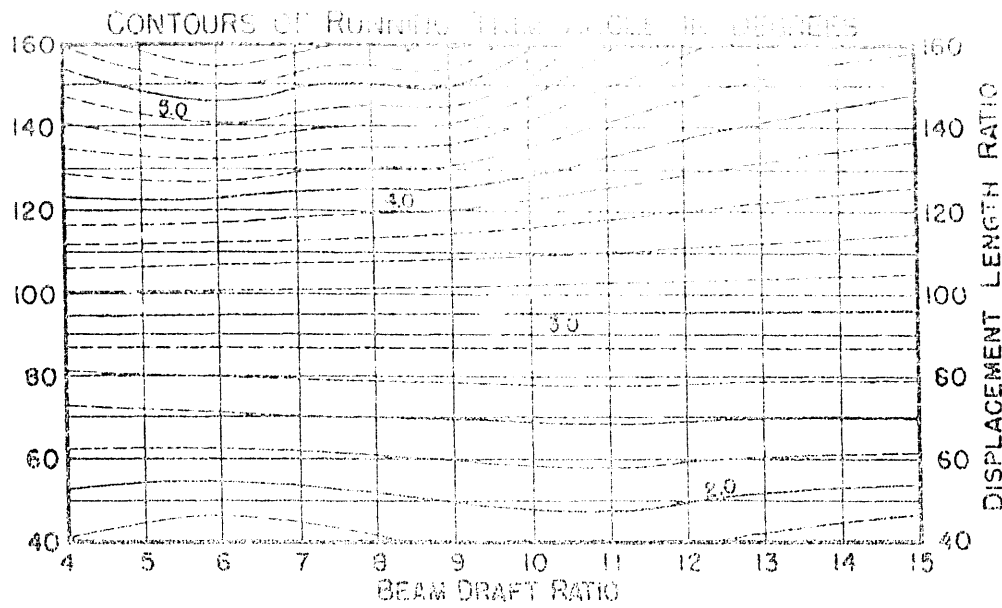
$$\sigma = 2^\circ$$



$$\frac{v}{\sqrt{L}} = 2.5$$

$$\Delta = N$$

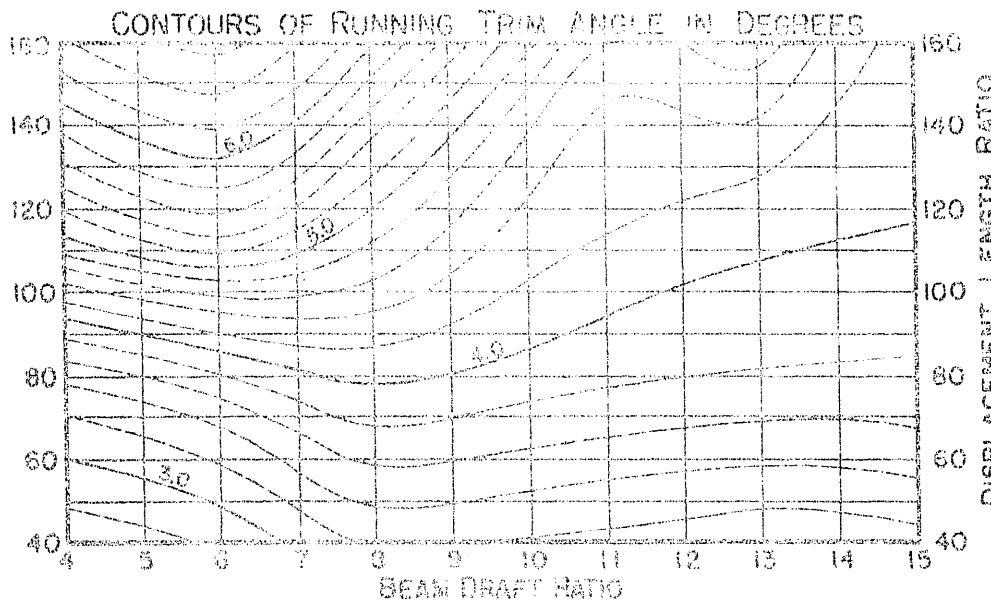
$$\sigma = 4^\circ$$



$$\frac{V}{\sqrt{L}} = 3.0$$

$$\Delta = N$$

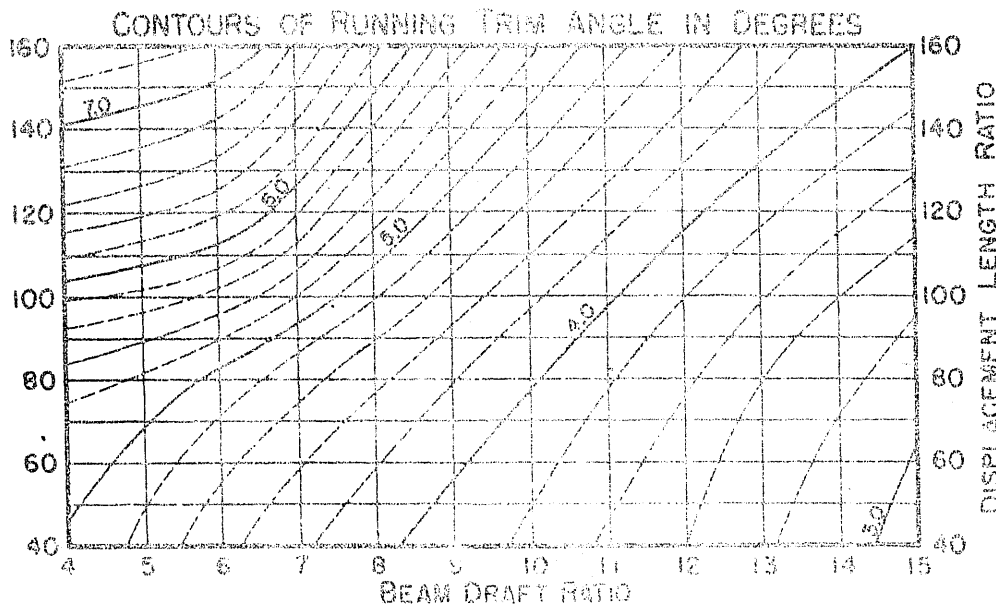
$$\tau = 0^\circ$$



$$\frac{V}{\sqrt{L}} = 3.0$$

$$\Delta = N$$

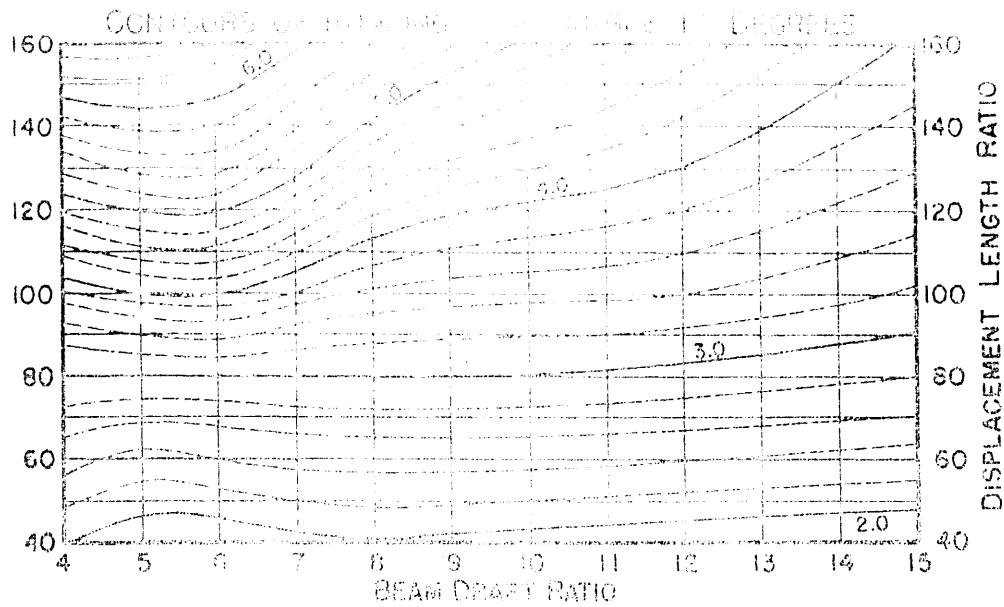
$$\tau = 2^\circ$$



$$\frac{V}{\sqrt{L}} = 3.0$$

$$\Delta = N$$

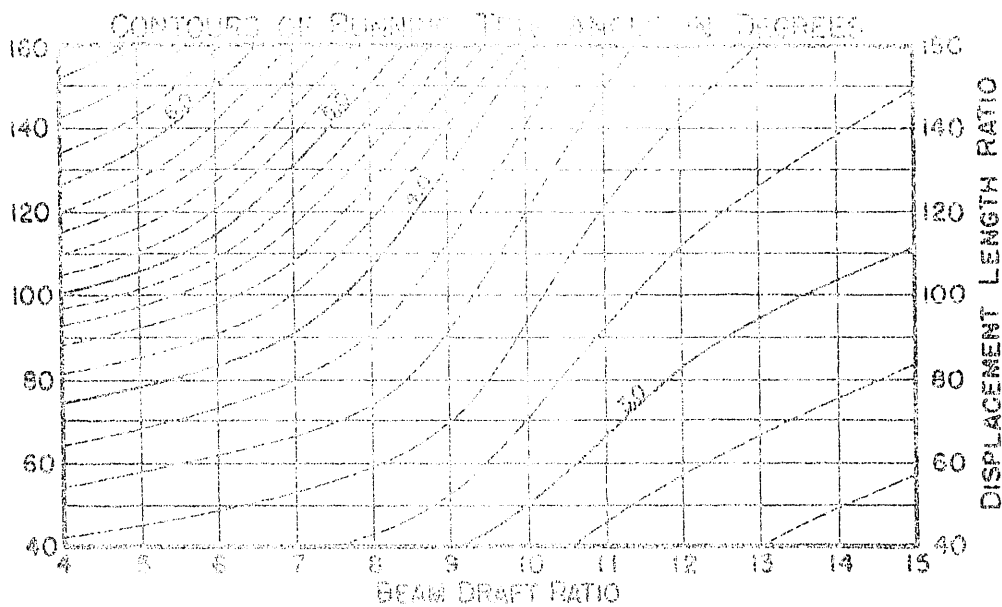
$$\tau = 4^\circ$$



$$\frac{V}{\sqrt{L}} = 3.5$$

$$\Delta = N$$

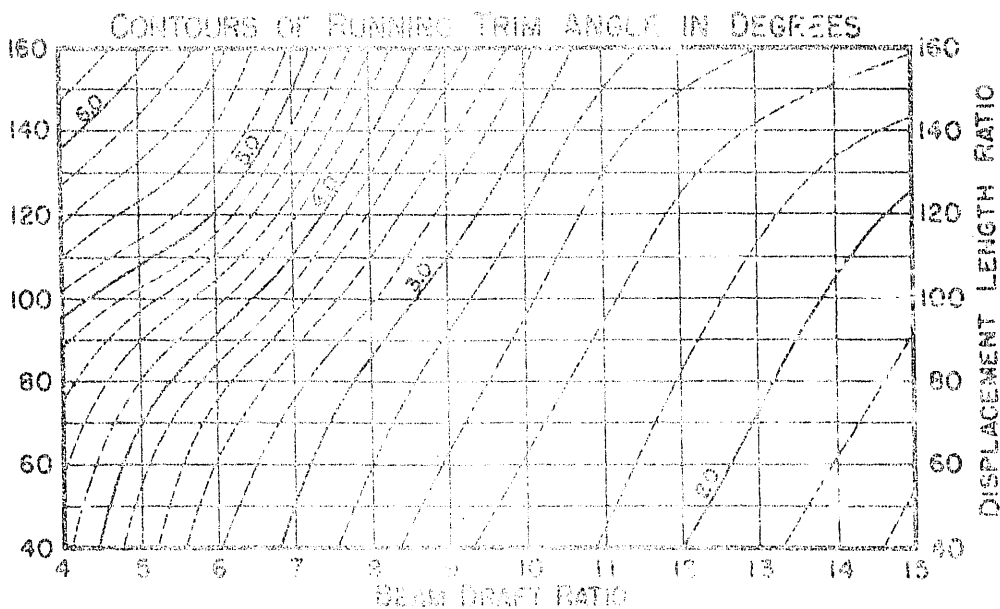
$$\sigma = 0^\circ$$



$$\frac{V}{\sqrt{L}} = 3.5$$

$$\Delta = N$$

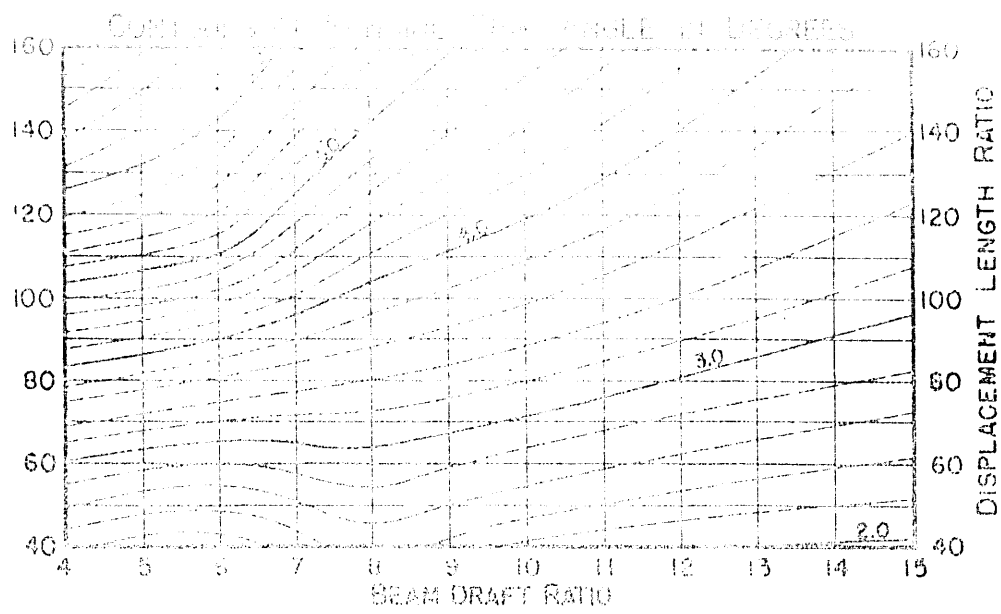
$$\sigma = 2^\circ$$



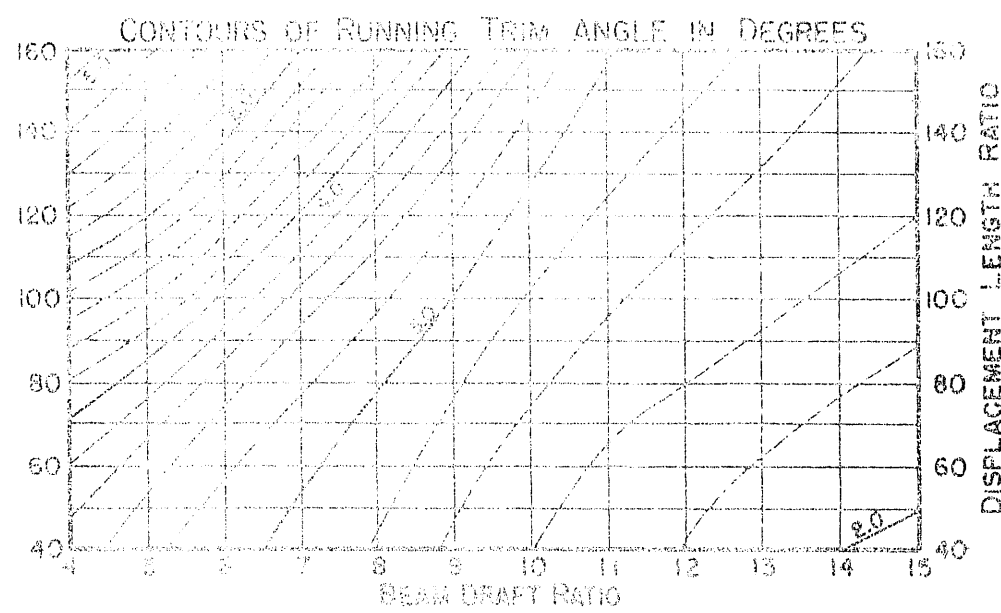
$$\frac{V}{\sqrt{L}} = 3.5$$

$$\Delta = N$$

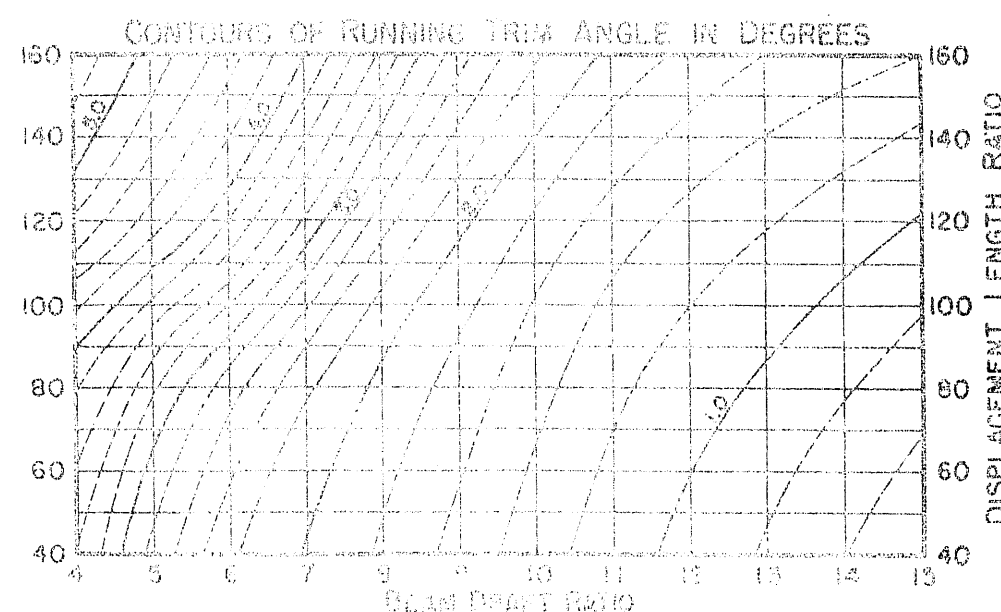
$$\sigma = 4^\circ$$



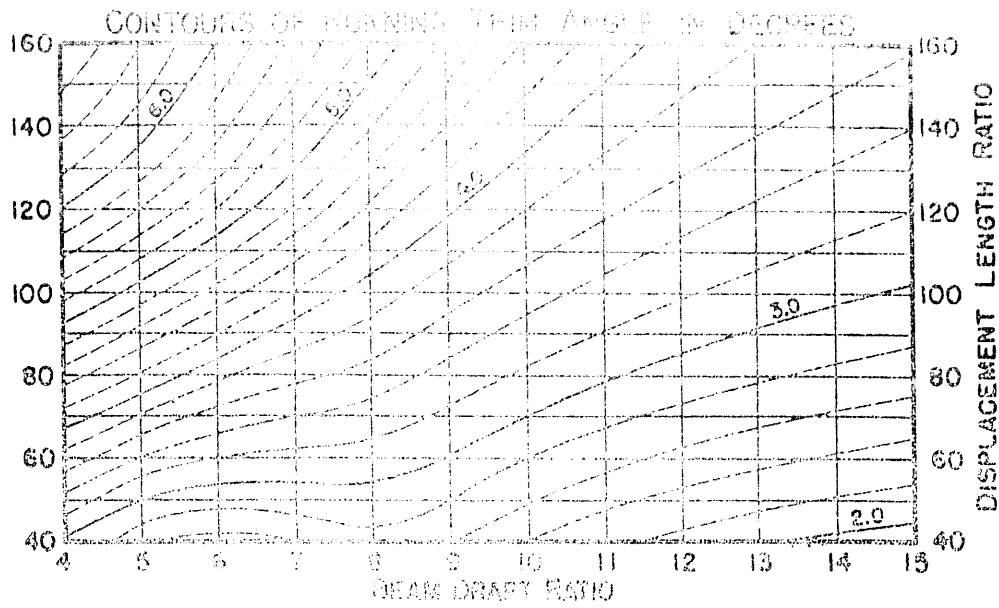
$\frac{V}{\sqrt{L}} = 4.0$
 $\Delta = N$
 $\tau = 0^\circ$



$\frac{V}{\sqrt{L}} = 4.0$
 $\Delta = N$
 $\tau = 2^\circ$



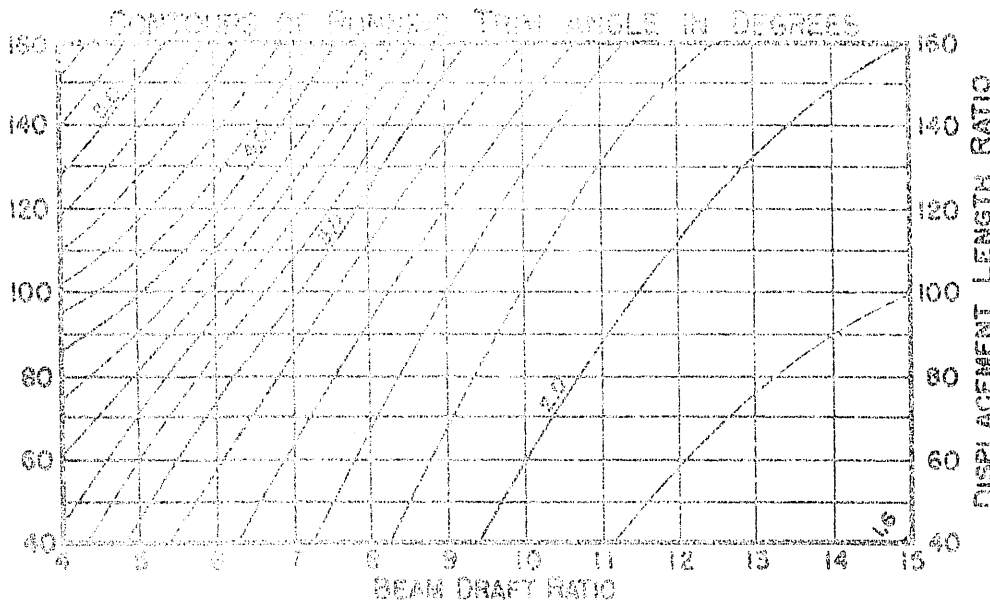
$\frac{V}{\sqrt{L}} = 4.0$
 $\Delta = N$
 $\tau = 4^\circ$



$$\frac{V}{\lambda} = 4.5$$

$$\Delta = N$$

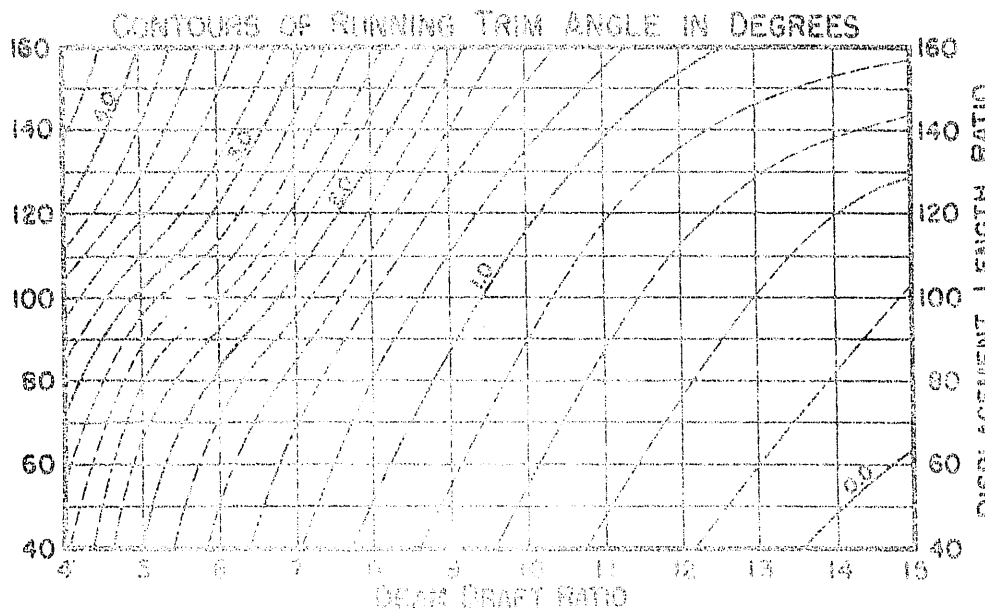
$$\tau = 0^\circ$$



$$\frac{V}{\lambda} = 4.5$$

$$\Delta = N$$

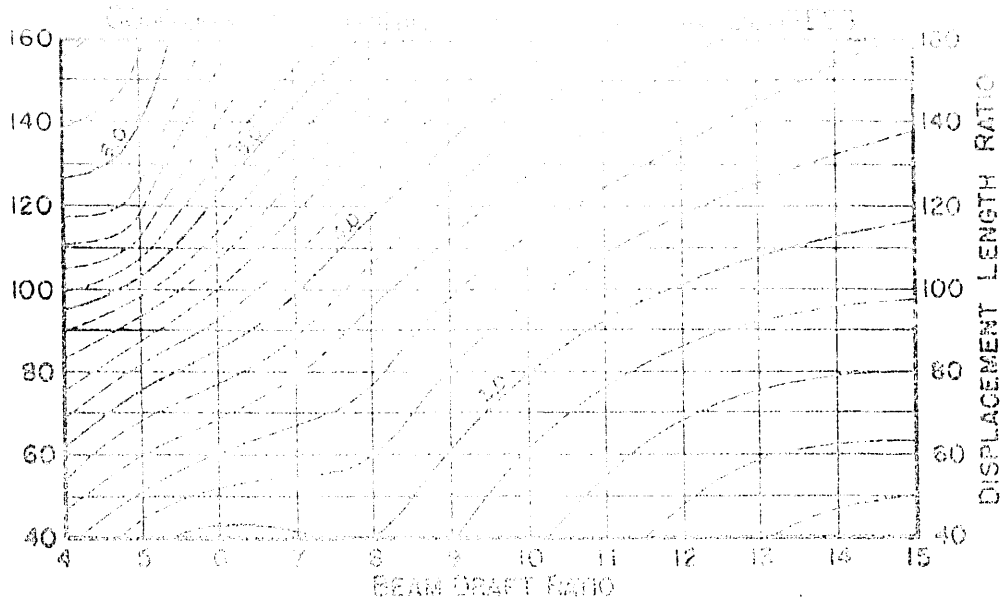
$$\tau = 2^\circ$$



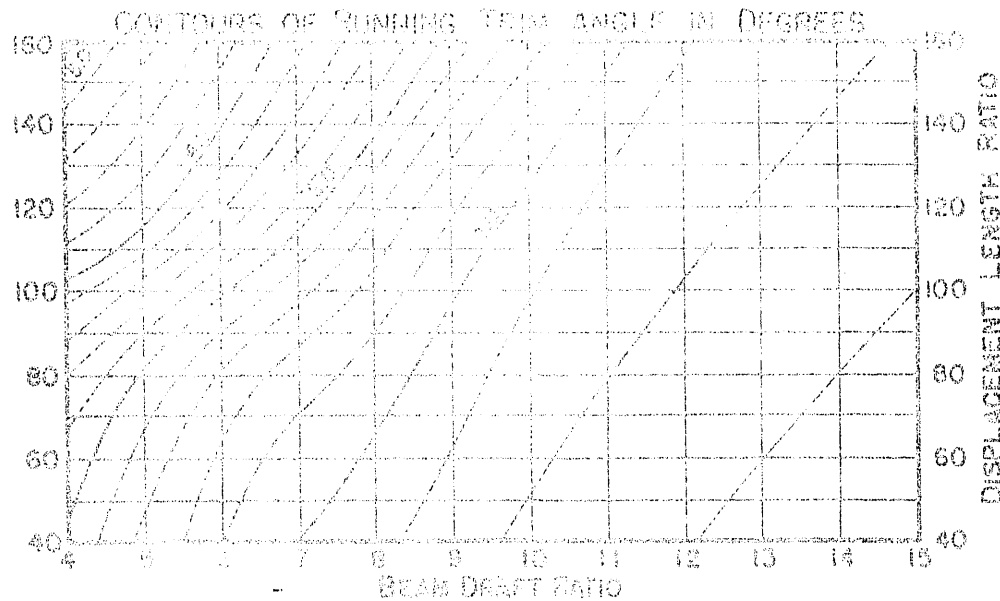
$$\frac{V}{\lambda} = 4.5$$

$$\Delta = N$$

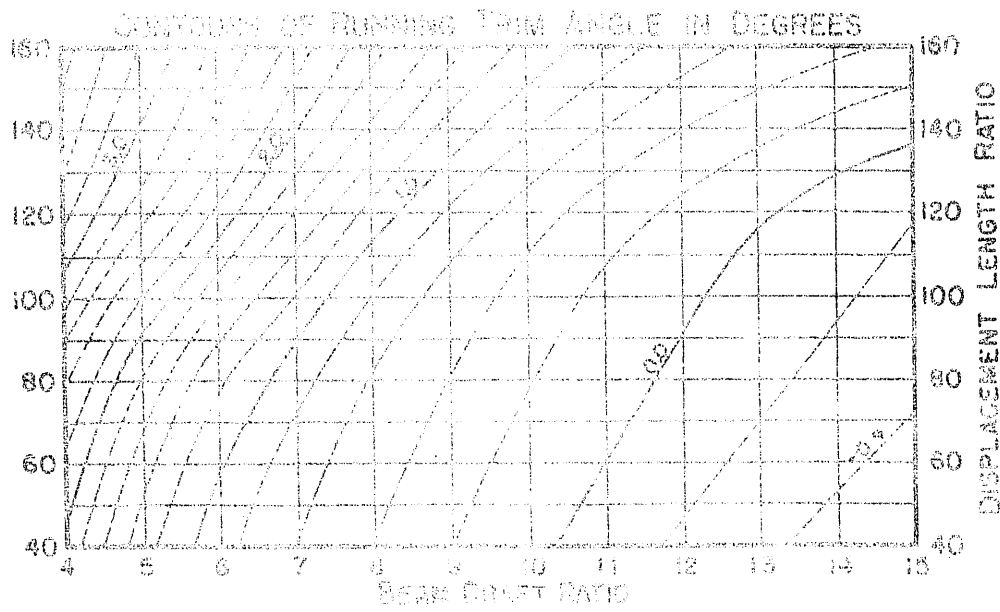
$$\tau = 4^\circ$$



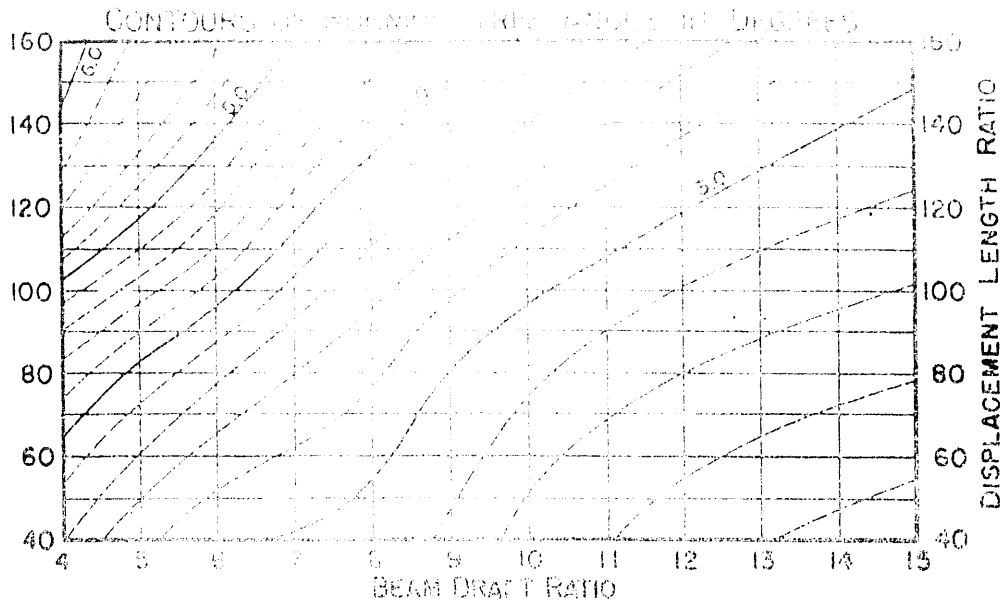
$\frac{v}{\sqrt{L}} = 5.0$
 $\Delta = N$
 $\tau = 0^\circ$



$\frac{v}{\sqrt{L}} = 5.0$
 $\Delta = N$
 $\tau = 2^\circ$



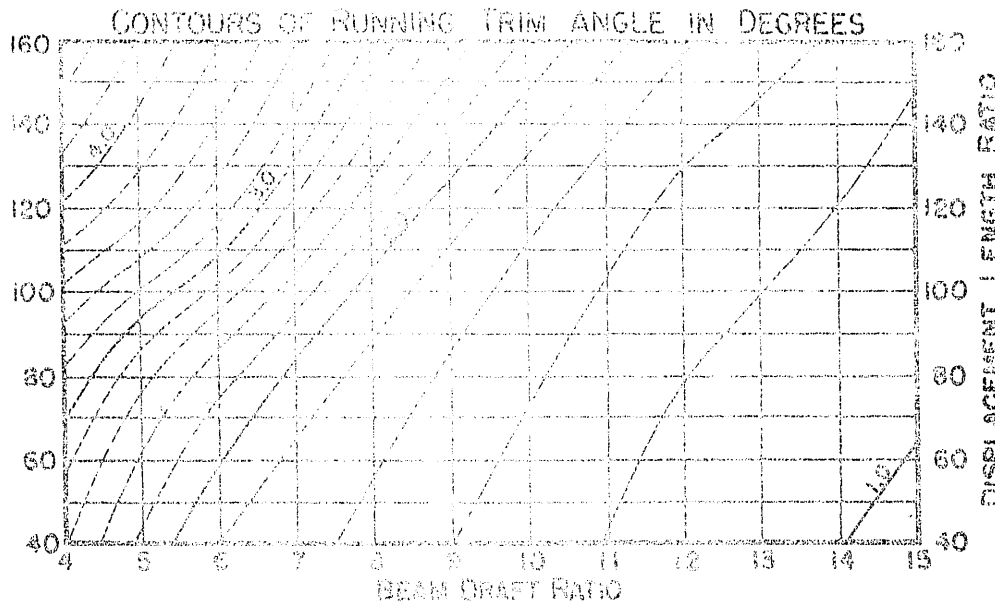
$\frac{v}{\sqrt{L}} = 5.0$
 $\Delta = N$
 $\tau = 4^\circ$



$$\frac{V}{\sqrt{K}} = 5.5$$

$$\Delta = N$$

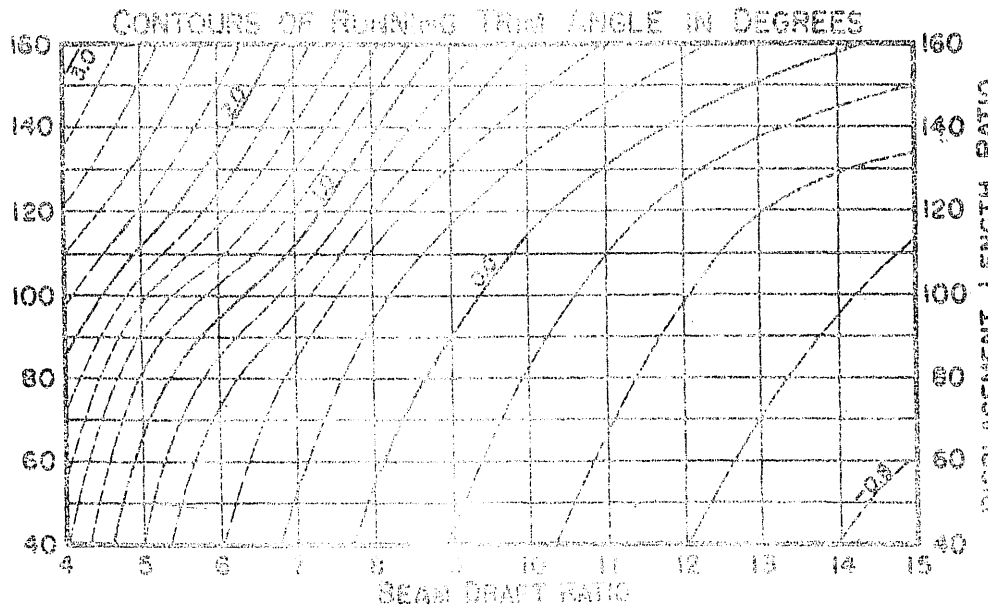
$$\tau = 0^\circ$$



$$\frac{V}{\sqrt{K}} = 5.5$$

$$\Delta = N$$

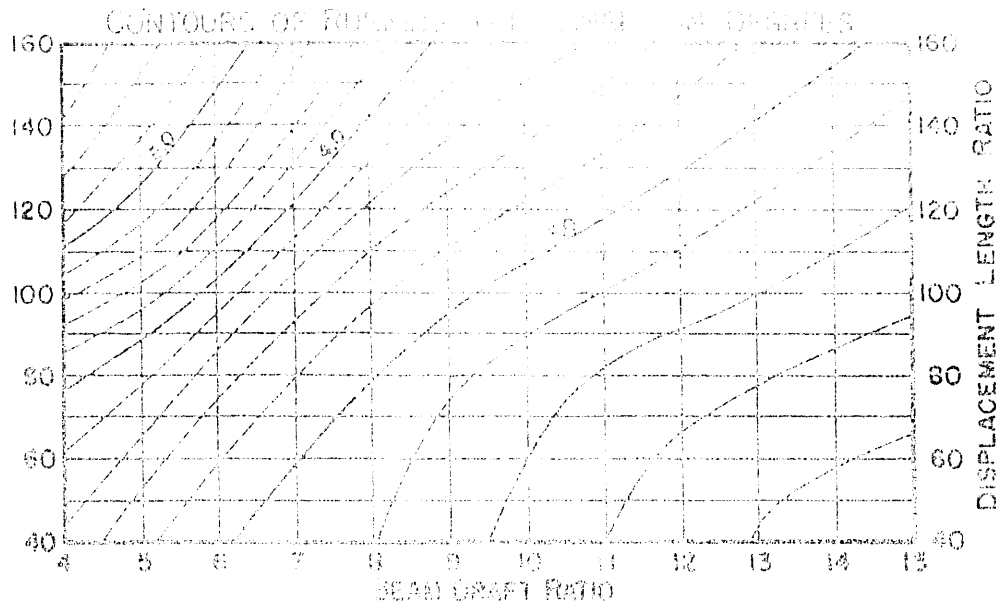
$$\tau = 2^\circ$$



$$\frac{V}{\sqrt{K}} = 5.5$$

$$\Delta = N$$

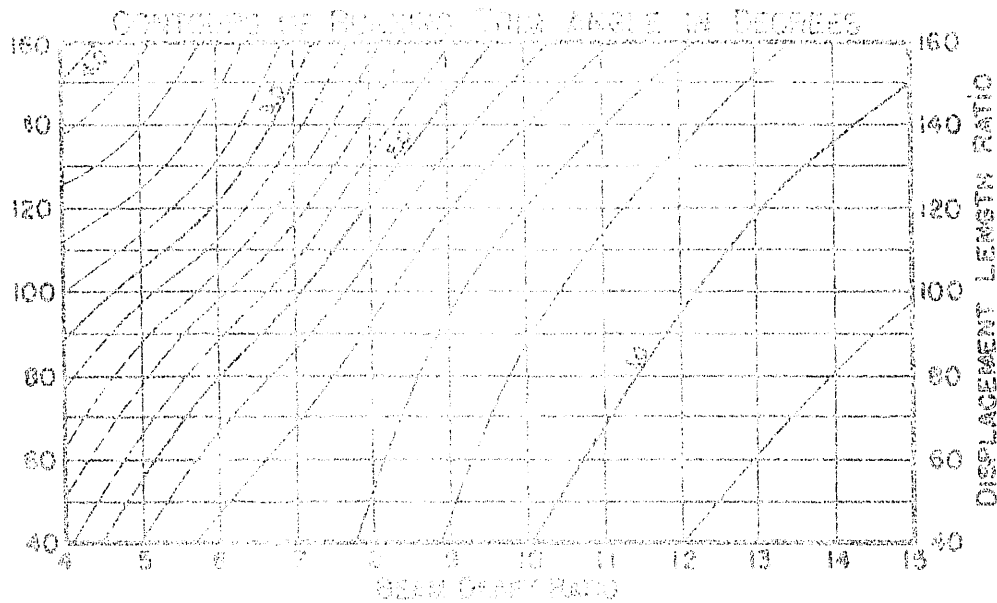
$$\tau = 4^\circ$$



$$\frac{V}{\sqrt{L}} = 6.0$$

$$\Delta = N$$

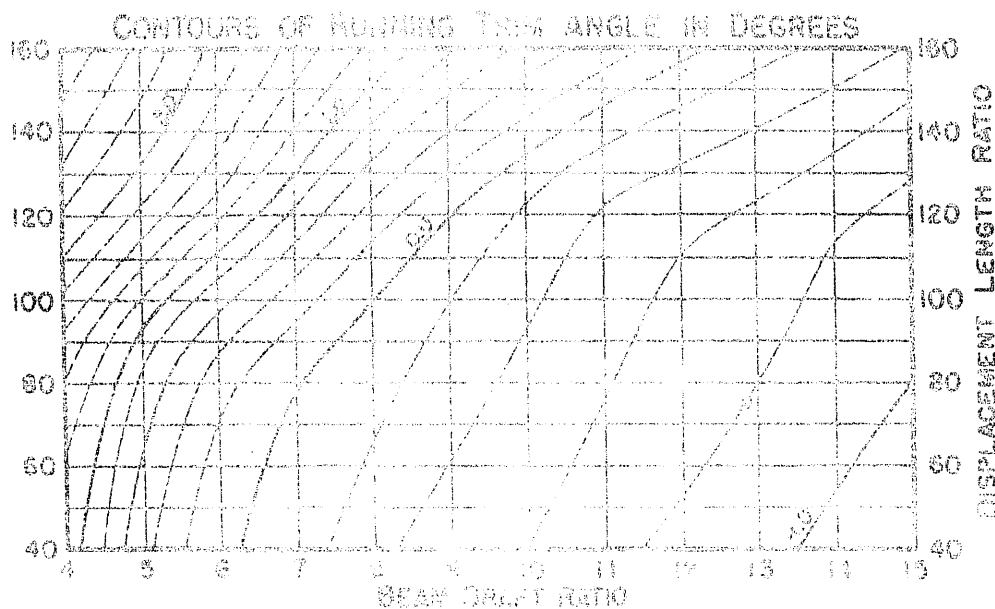
$$\gamma = 0^\circ$$



$$\frac{V}{\sqrt{L}} = 6.0$$

$$\Delta = N$$

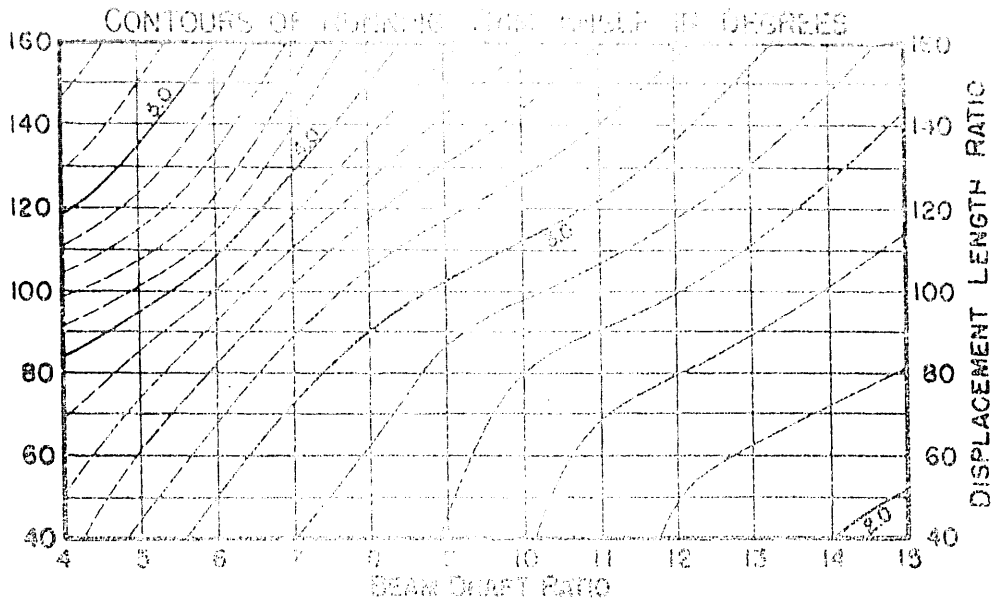
$$\gamma = 2^\circ$$



$$\frac{V}{\sqrt{L}} = 6.0$$

$$\Delta = N$$

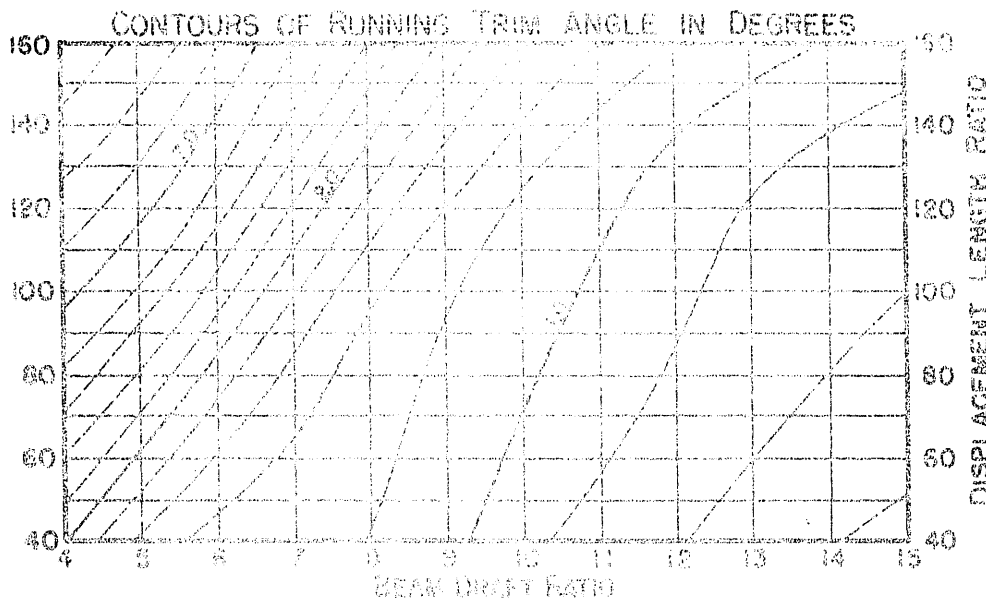
$$\gamma = 4^\circ$$



$$\frac{V}{\Delta} = 6.5$$

$$\Delta = N$$

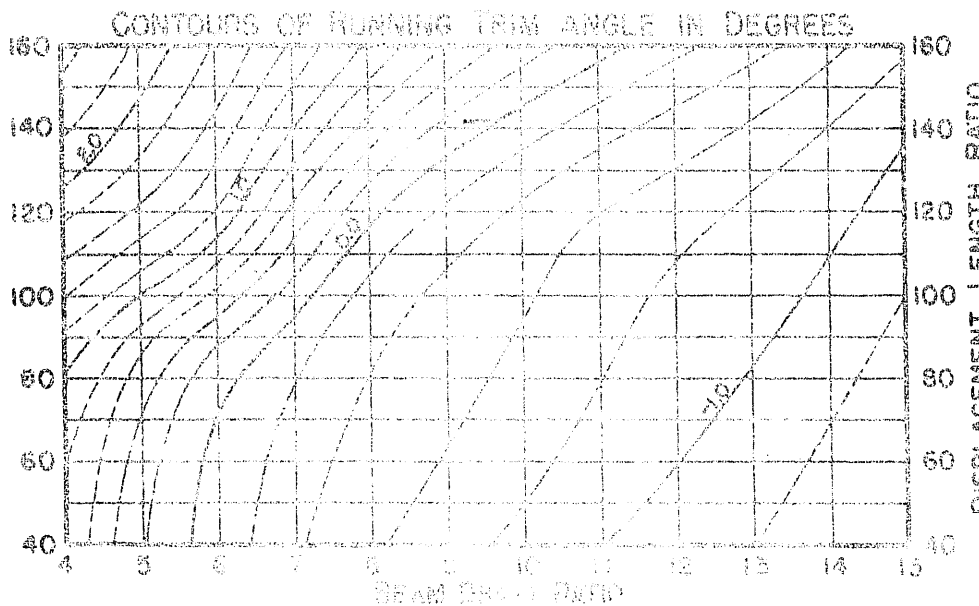
$$\tau = 0^\circ$$



$$\frac{V}{\Delta} = 6.5$$

$$\Delta = N$$

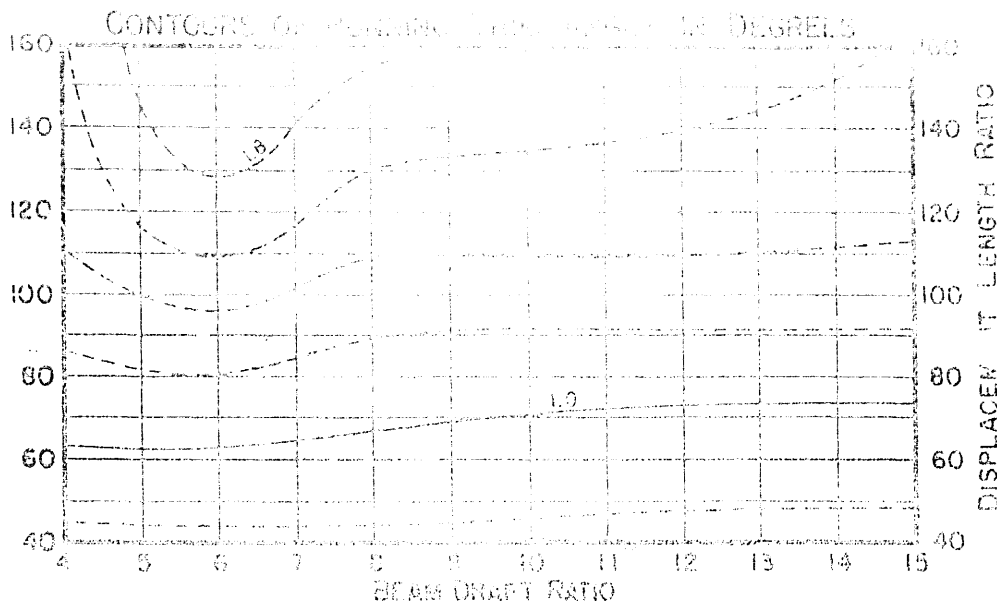
$$\tau = 2^\circ$$



$$\frac{V}{\Delta} = 6.5$$

$$\Delta = N$$

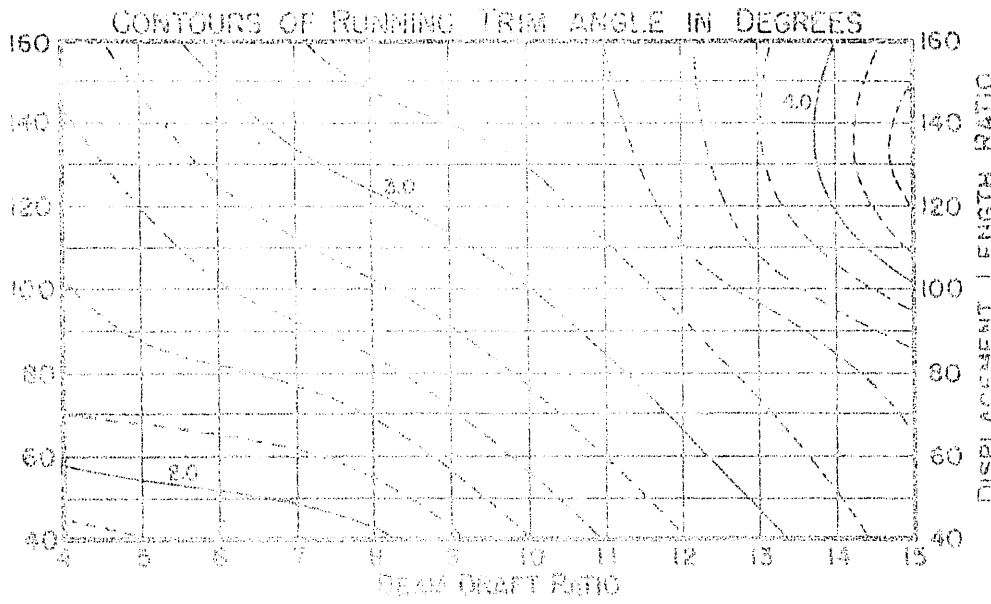
$$\tau = 4^\circ$$



$$\frac{v}{\sqrt{L}} = 1.5$$

$$\Delta = N + 10\%$$

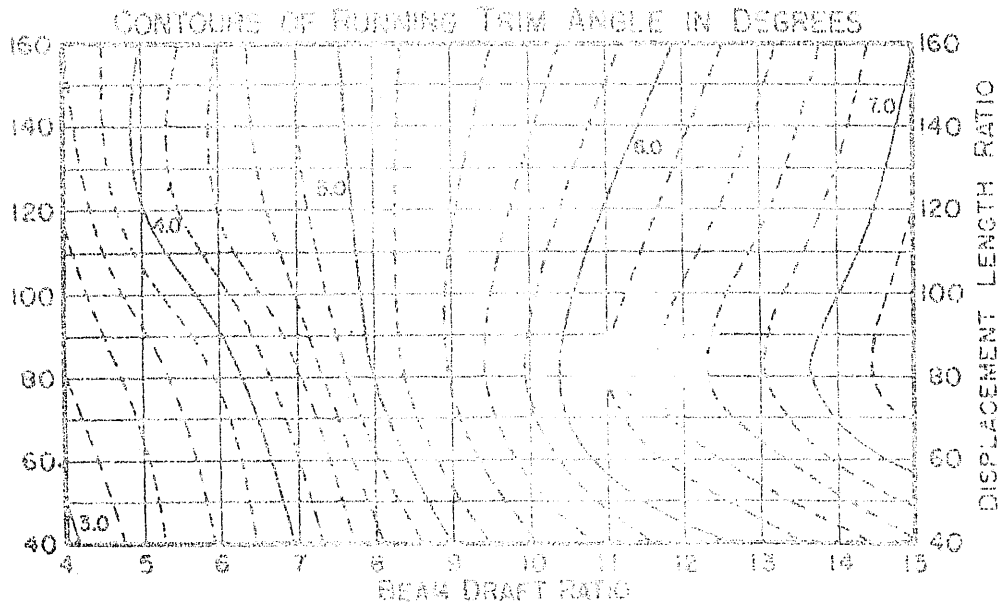
$$\tau = 0^\circ$$



$$\frac{v}{\sqrt{L}} = 1.5$$

$$\Delta = N + 10\%$$

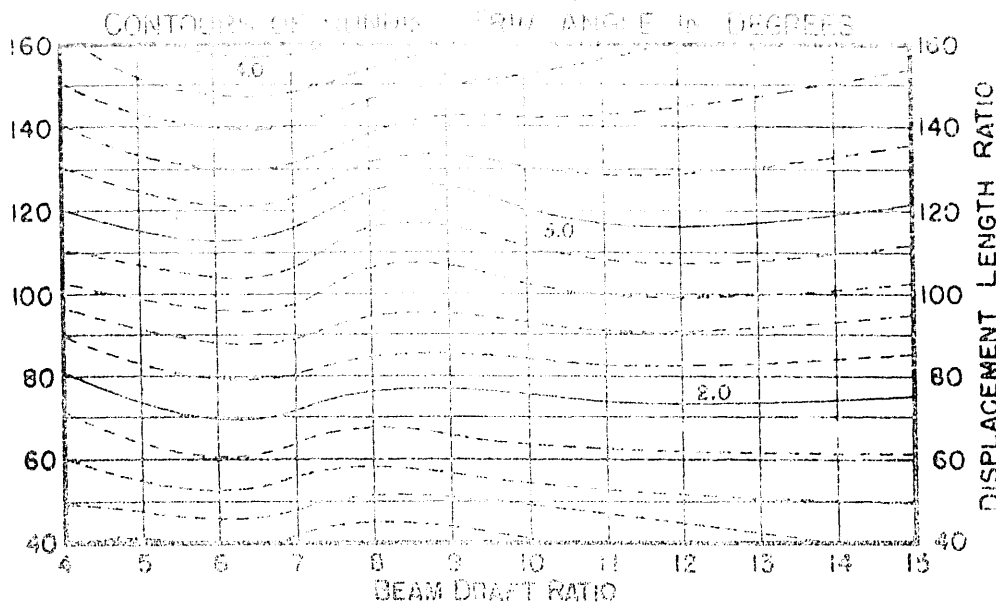
$$\tau = 2^\circ$$



$$\frac{v}{\sqrt{L}} = 1.5$$

$$\Delta = N + 10\%$$

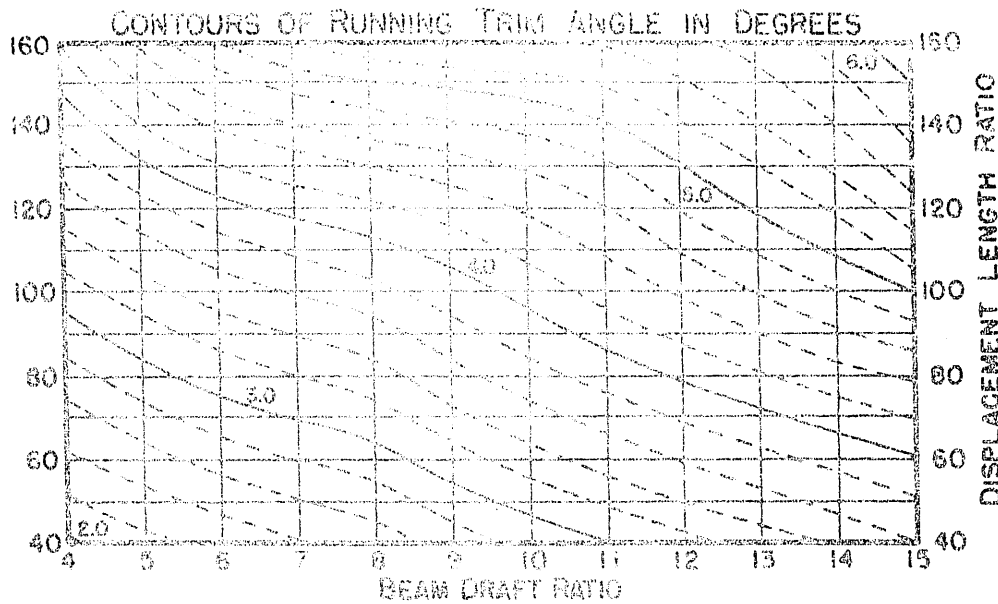
$$\tau = 4^\circ$$



$$\frac{V}{L} = 2.0$$

$$\Delta = N + 10\%$$

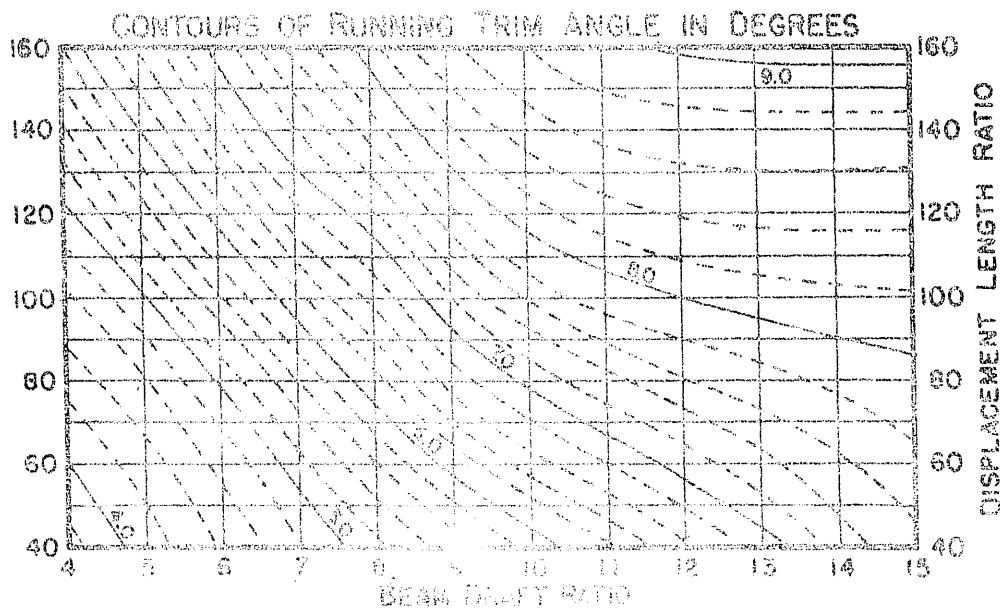
$$\tau = 0^\circ$$



$$\frac{V}{L} = 2.0$$

$$\Delta = N + 10\%$$

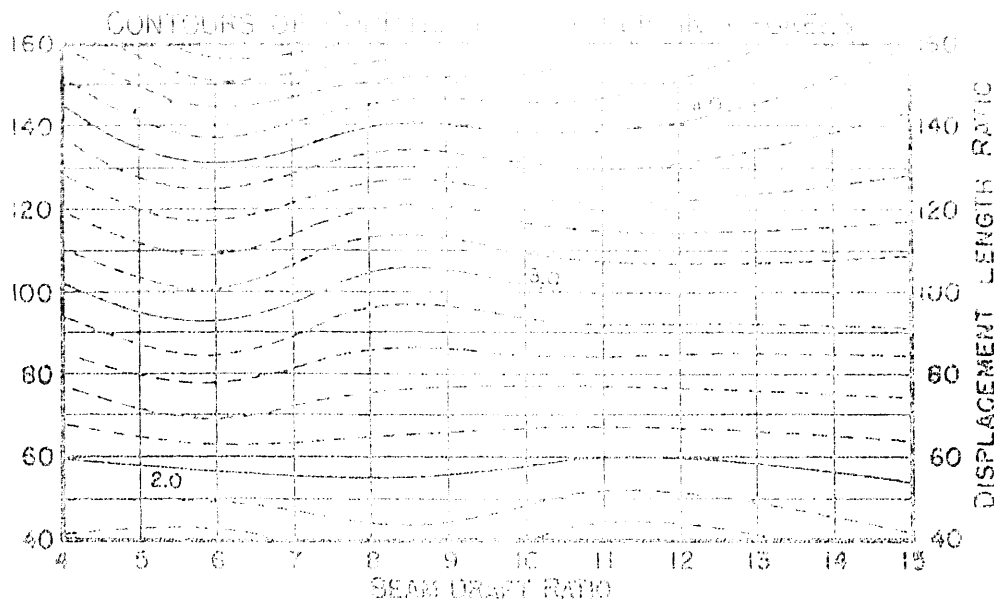
$$\tau = 2^\circ$$



$$\frac{V}{L} = 2.0$$

$$\Delta = N + 10\%$$

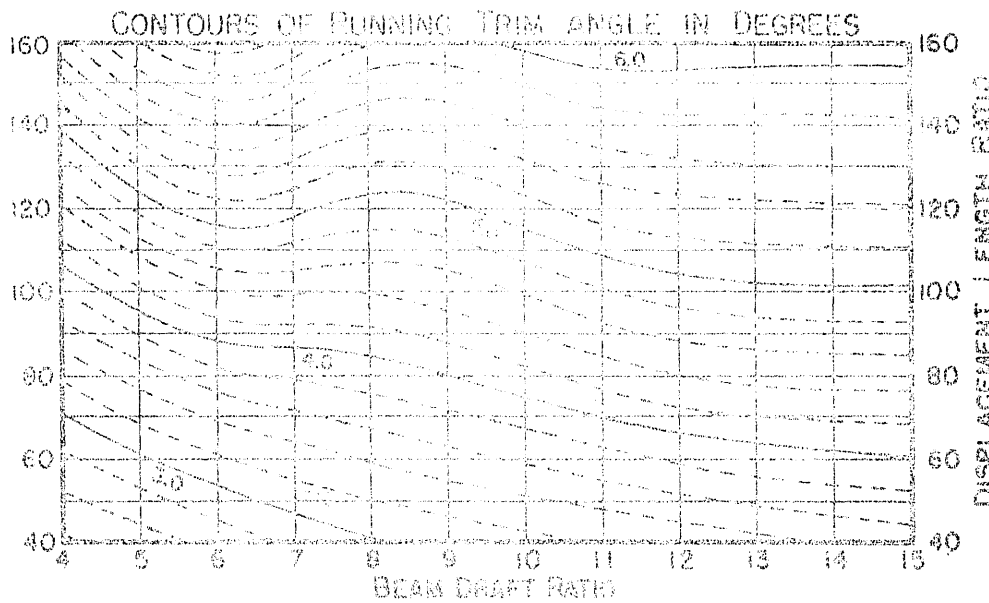
$$\tau = 4^\circ$$



$$\frac{V}{\sqrt{L}} = 2.5$$

$$\Delta = N + 10\%$$

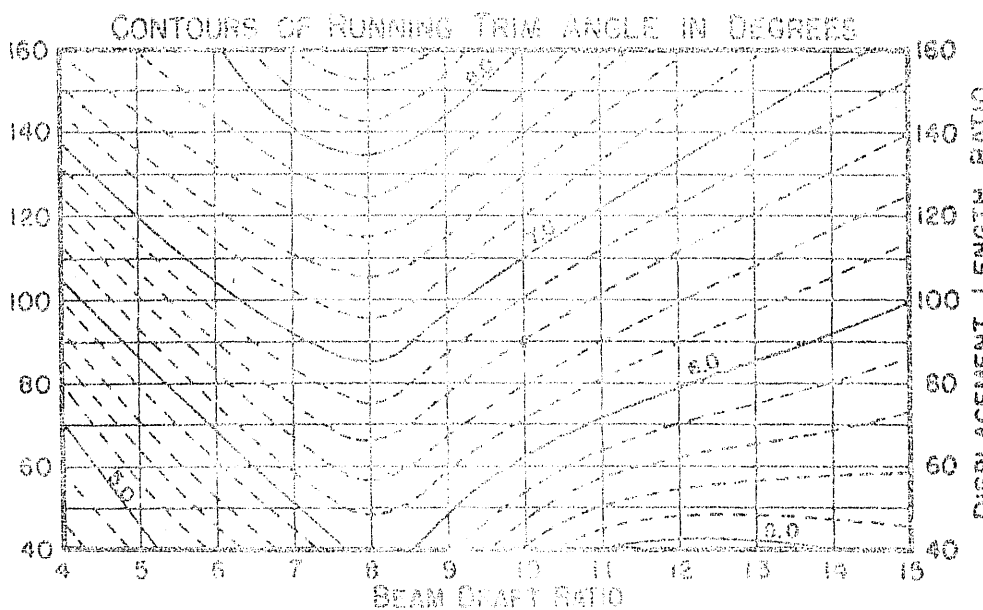
$$\sigma = 0^\circ$$



$$\frac{V}{\sqrt{L}} = 2.5$$

$$\Delta = N + 10\%$$

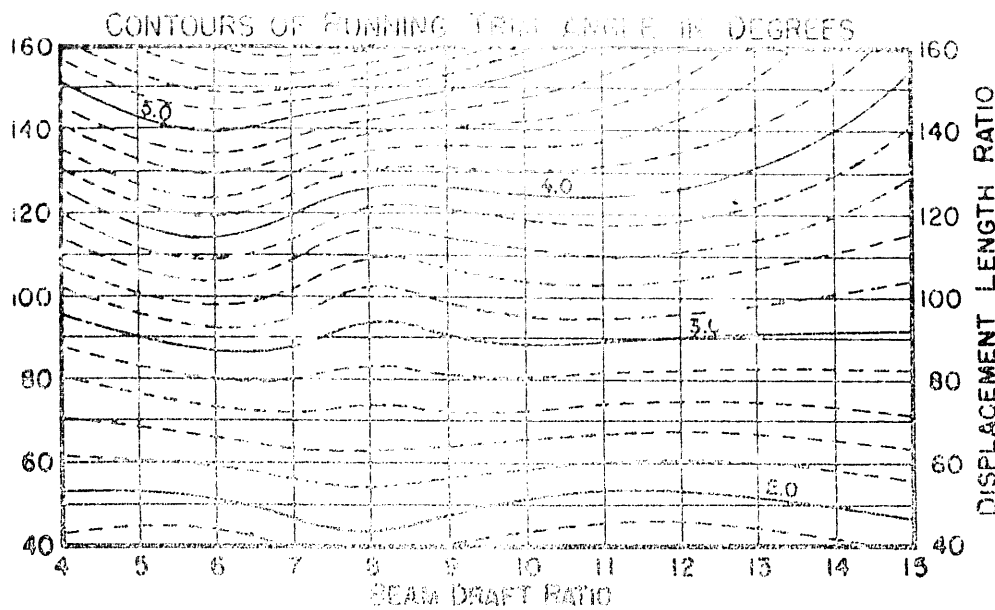
$$\sigma = 2^\circ$$



$$\frac{V}{\sqrt{L}} = 2.5$$

$$\Delta = N + 10\%$$

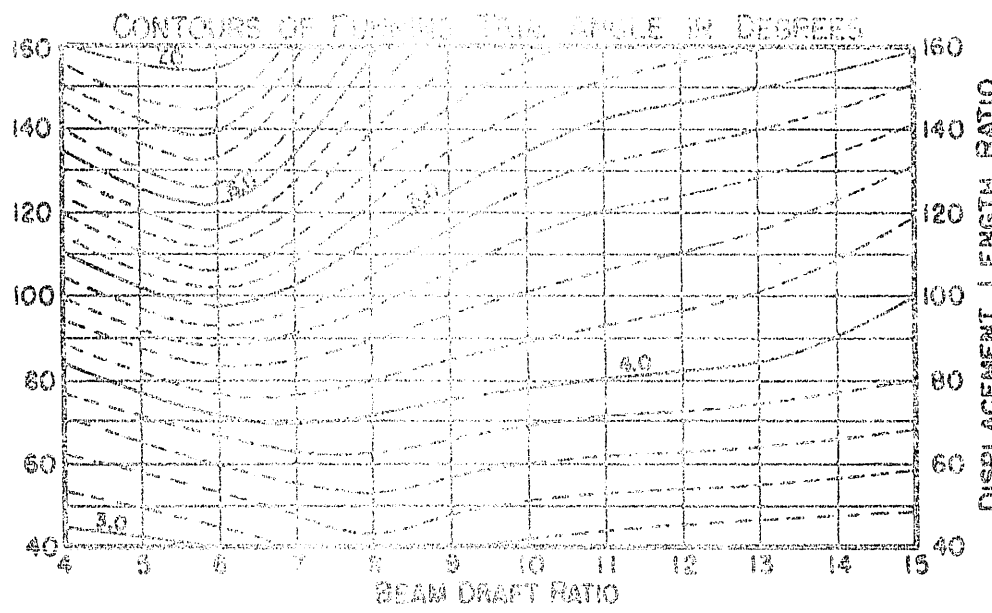
$$\sigma = 4^\circ$$



$$\frac{V}{\sqrt{L}} = 3.0$$

$$\Delta = N + 10\%$$

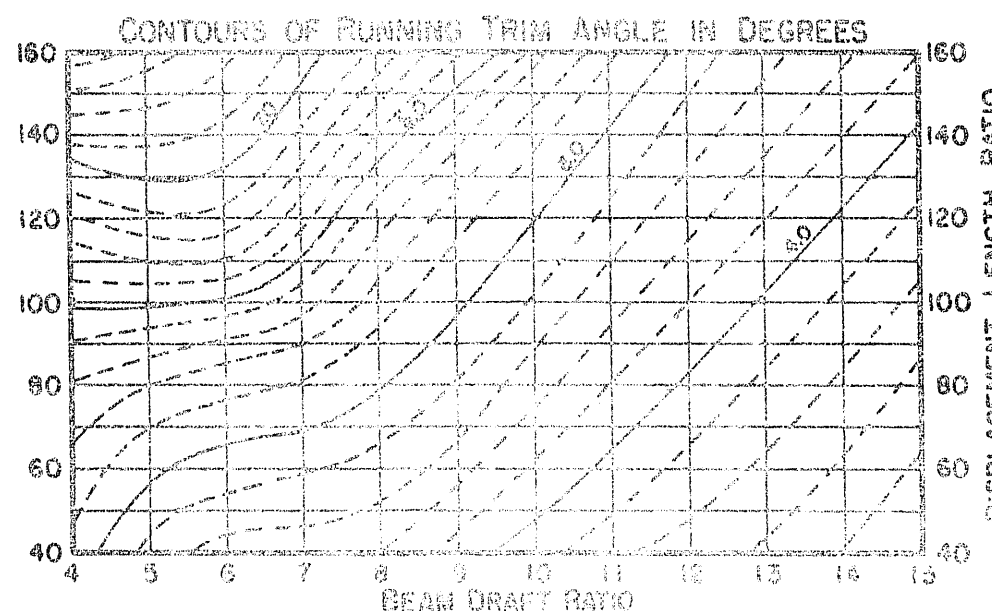
$$T = 0^\circ$$



$$\frac{V}{\sqrt{L}} = 3.0$$

$$\Delta = N + 10\%$$

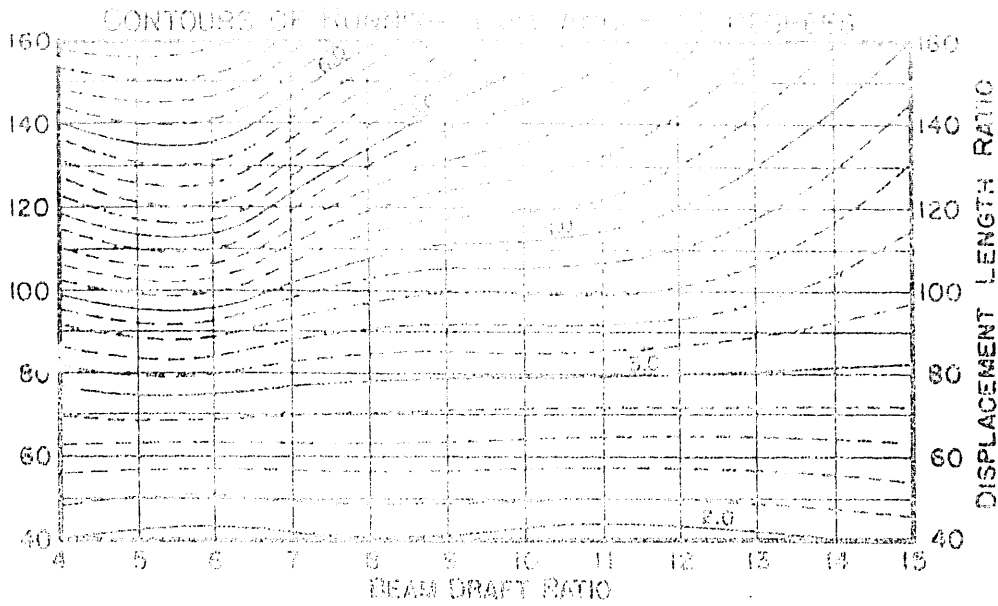
$$T = 2^\circ$$



$$\frac{V}{\sqrt{L}} = 3.0$$

$$\Delta = N + 10\%$$

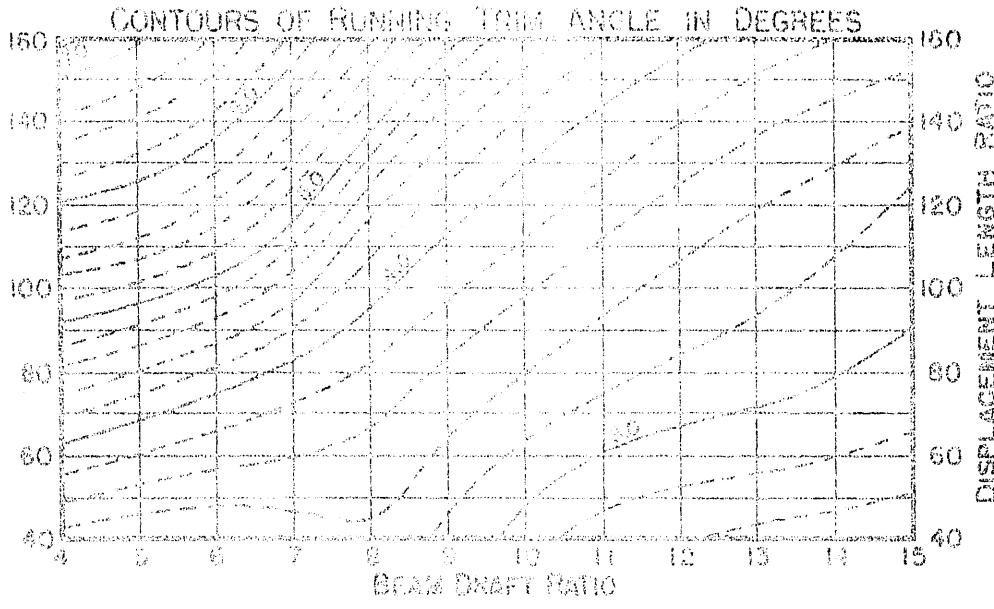
$$T = 4^\circ$$



$$\frac{V}{\sqrt{L}} = 3.5$$

$$\Delta = N + 10\%$$

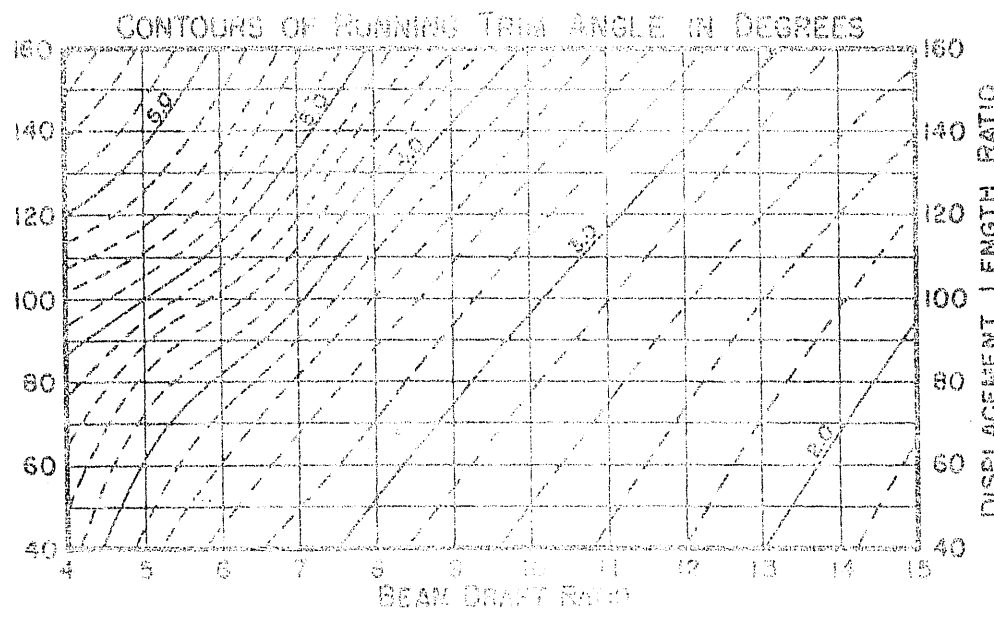
$$\sigma = 0^\circ$$



$$\frac{V}{\sqrt{L}} = 3.5$$

$$\Delta = N + 10\%$$

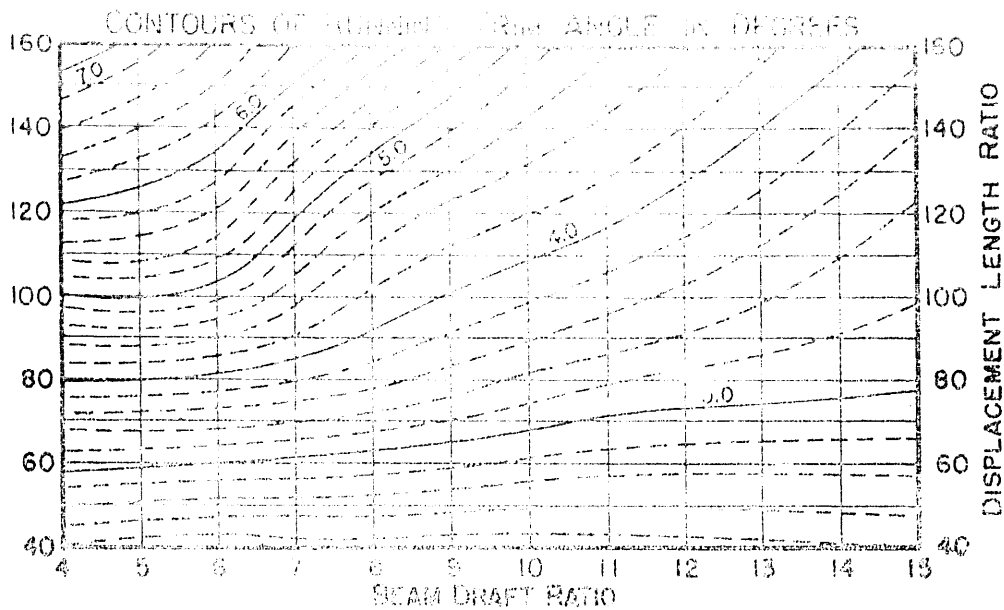
$$\sigma = 2^\circ$$



$$\frac{V}{\sqrt{L}} = 3.5$$

$$\Delta = N + 10\%$$

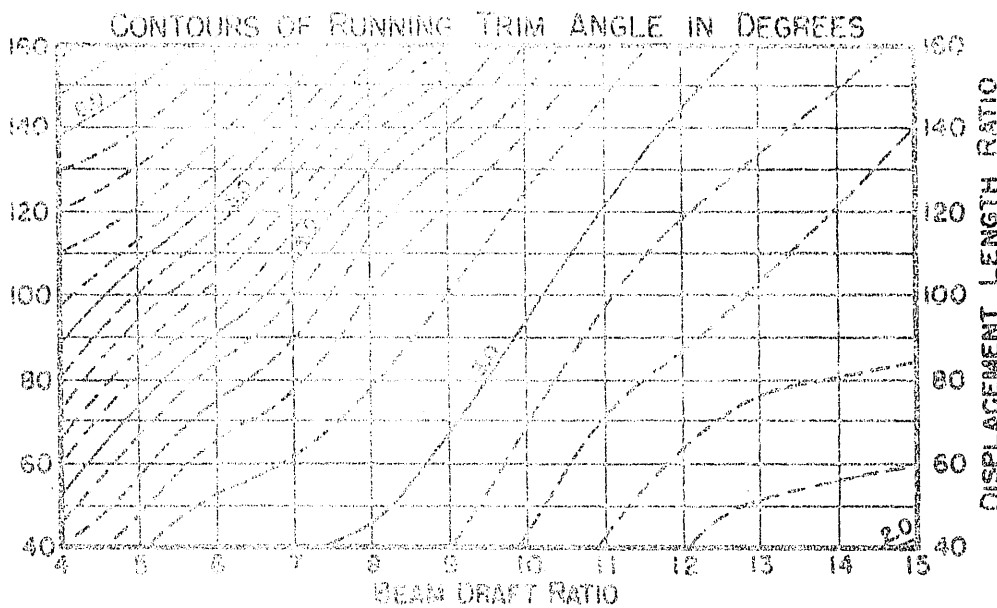
$$\sigma = 4^\circ$$



$$\sqrt{\frac{V}{\Delta}} = 4.0$$

$$\Delta = N + 10\%$$

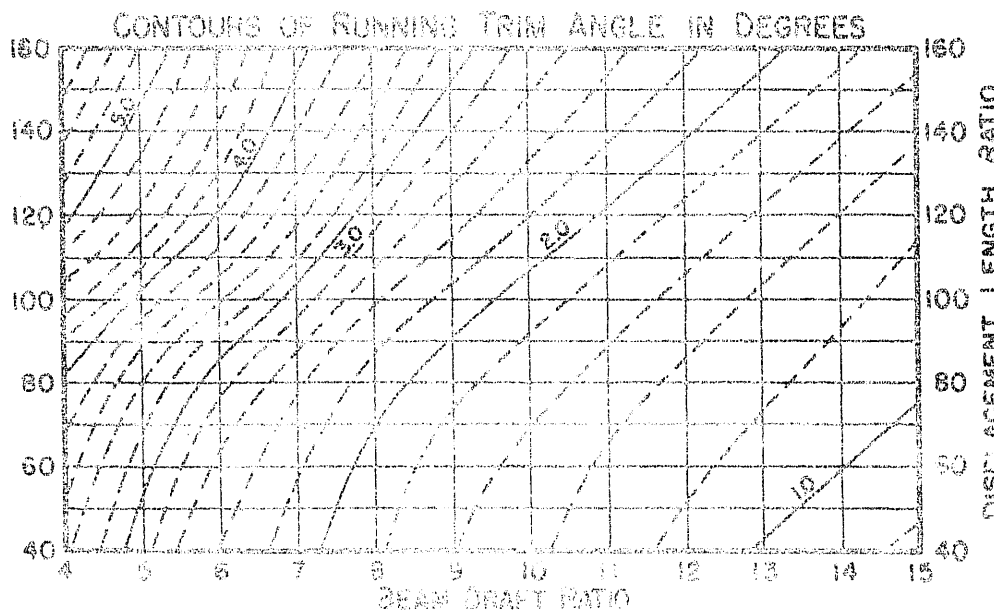
$$\gamma = 0^\circ$$



$$\sqrt{\frac{V}{\Delta}} = 4.0$$

$$\Delta = N + 10\%$$

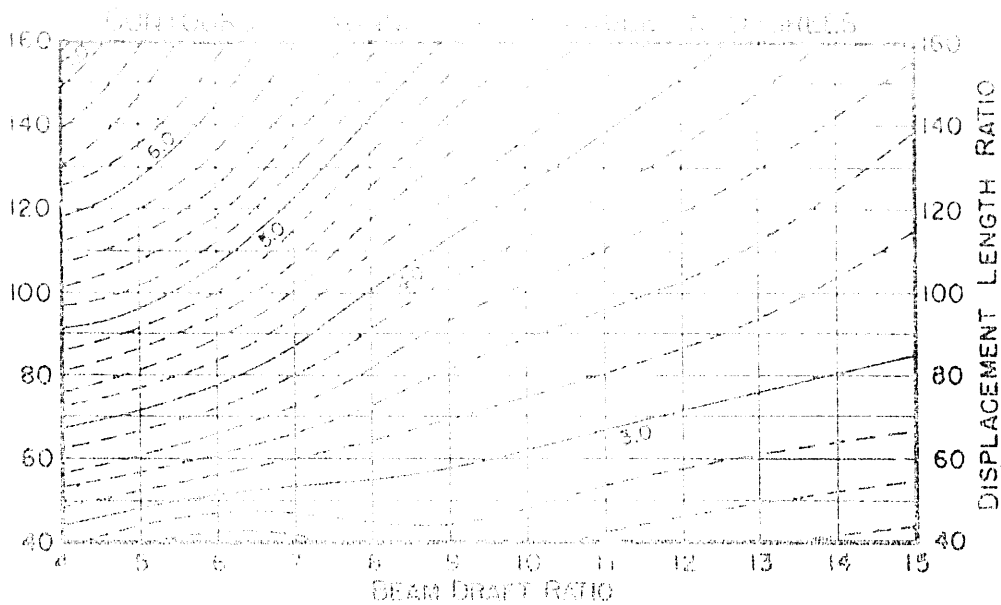
$$\gamma = 2^\circ$$



$$\sqrt{\frac{V}{\Delta}} = 4.0$$

$$\Delta = N + 10\%$$

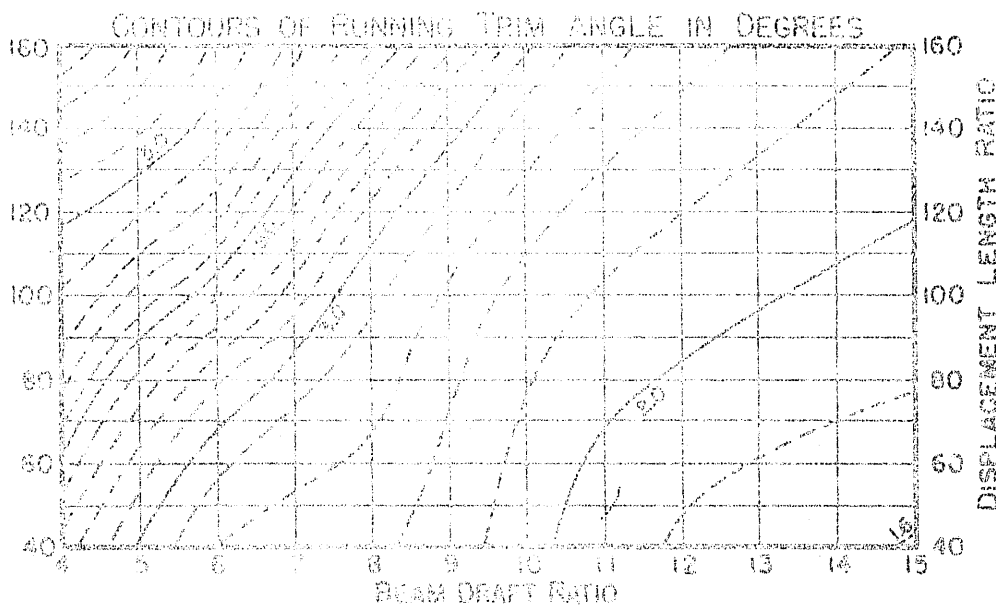
$$\gamma = 4^\circ$$



$$\frac{V}{\sqrt{L}} = 4.5$$

$$\Delta = N + 10\%$$

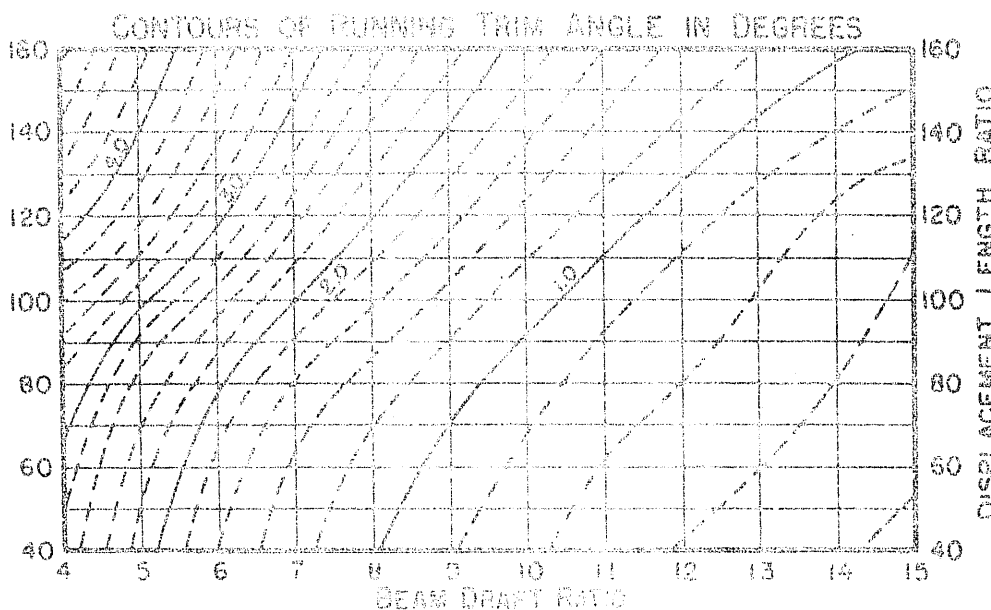
$$\tau = 0^\circ$$



$$\frac{V}{\sqrt{L}} = 4.5$$

$$\Delta = N + 10\%$$

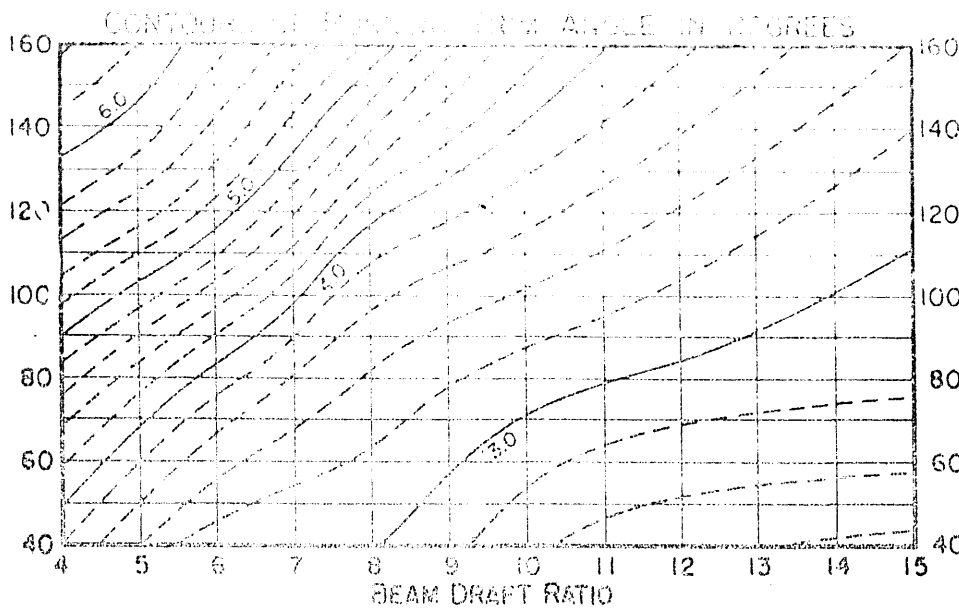
$$\tau = 2^\circ$$



$$\frac{V}{\sqrt{L}} = 4.5$$

$$\Delta = N + 10\%$$

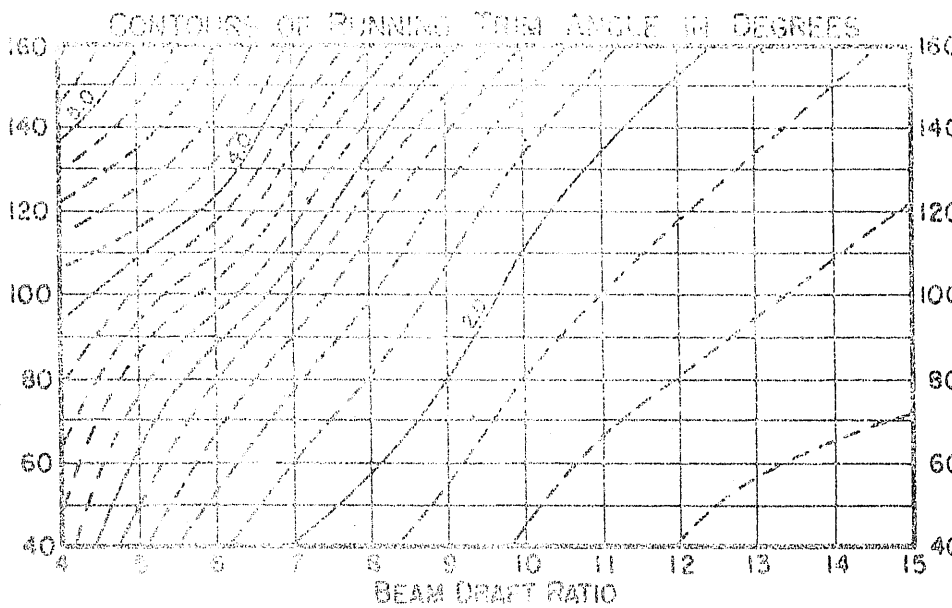
$$\tau = 4^\circ$$



$$\frac{V}{\sqrt{L}} = 5.0$$

$$\Delta = N + 10\%$$

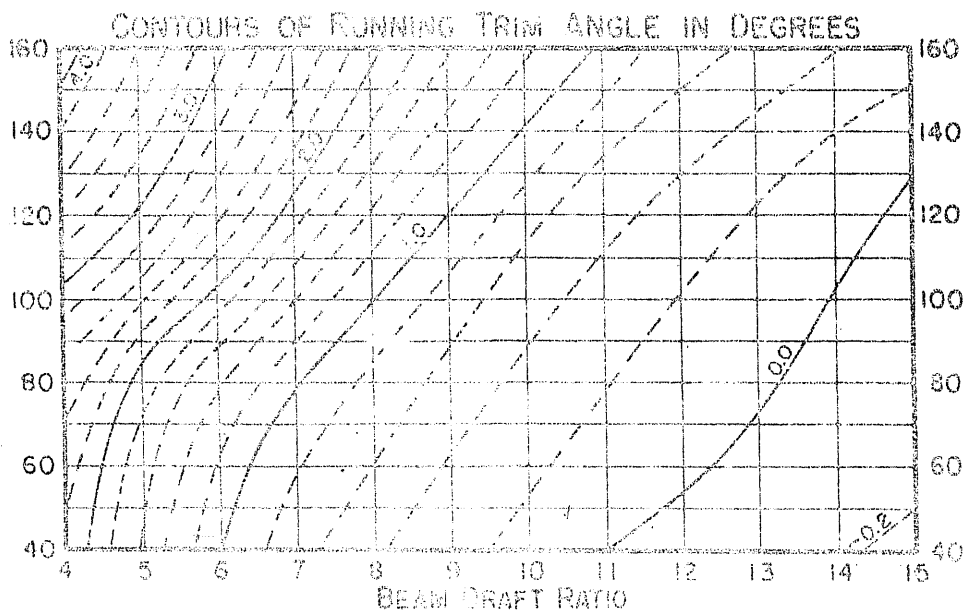
$$\tau = 0^\circ$$



$$\frac{V}{\sqrt{L}} = 5.0$$

$$\Delta = N + 10\%$$

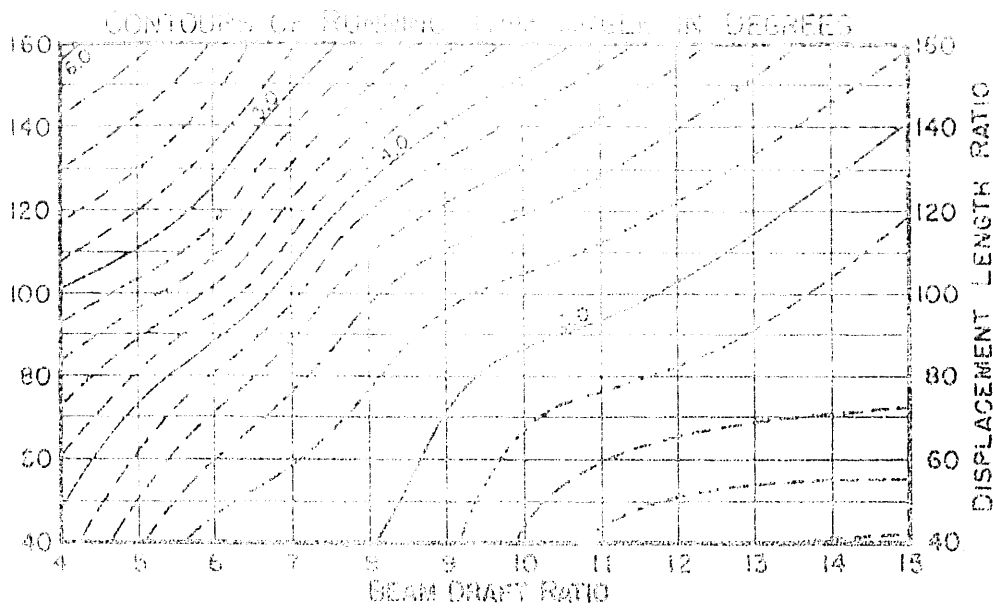
$$\tau = 2^\circ$$



$$\frac{V}{\sqrt{L}} = 5.0$$

$$\Delta = N + 10\%$$

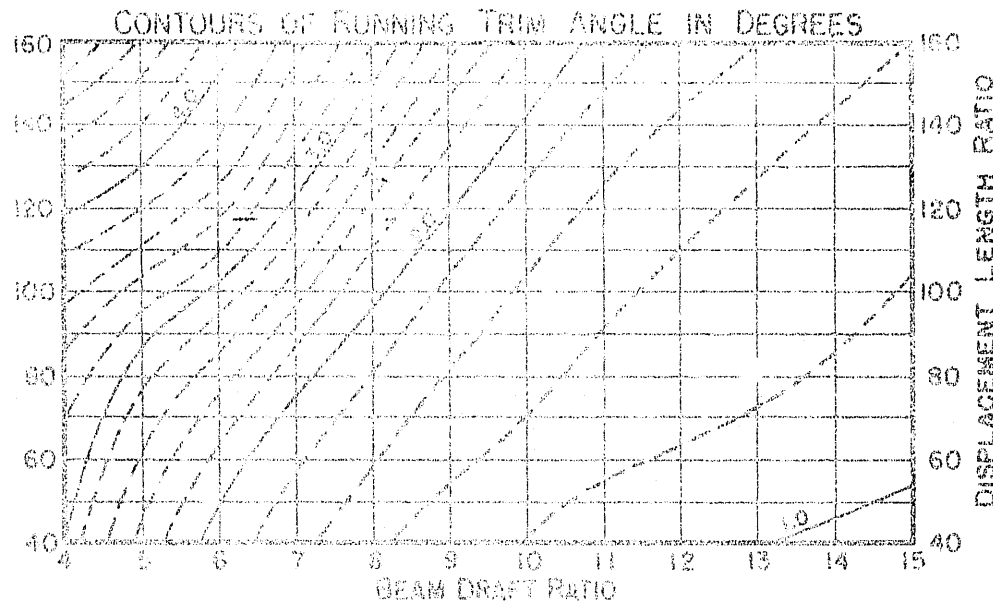
$$\tau = 4^\circ$$



$$\frac{v}{\sqrt{L}} = 5.5$$

$$\Delta = N + 10\%$$

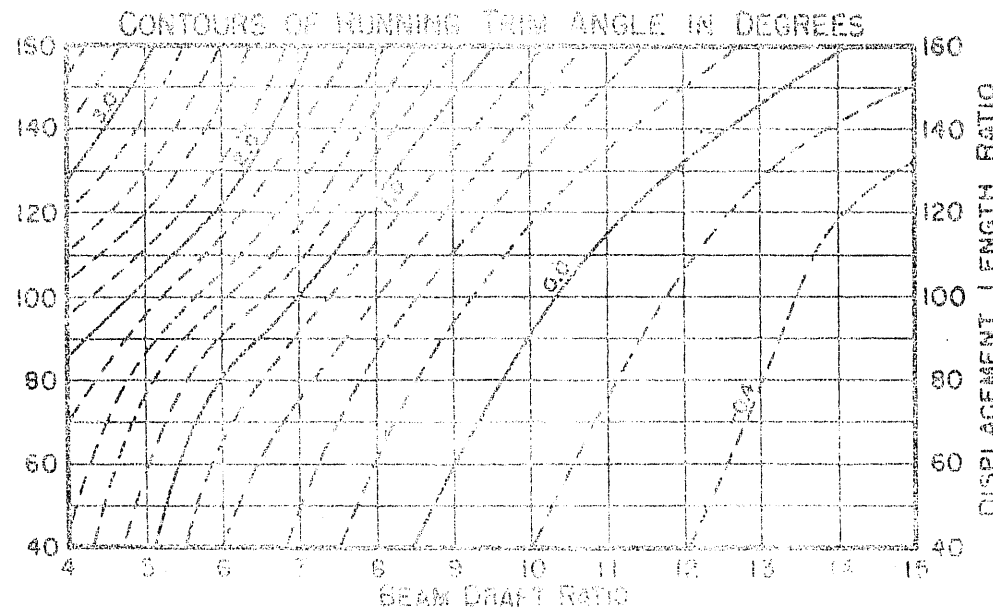
$$\tau = 0^\circ$$



$$\frac{v}{\sqrt{L}} = 5.5$$

$$\Delta = N + 10\%$$

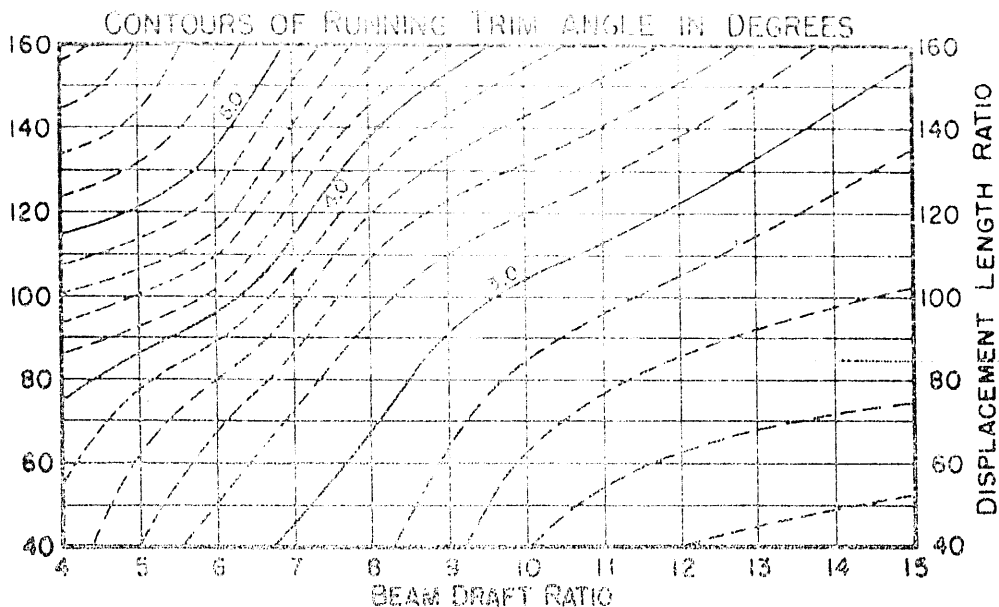
$$\tau = 2^\circ$$



$$\frac{v}{\sqrt{L}} = 5.5$$

$$\Delta = N + 10\%$$

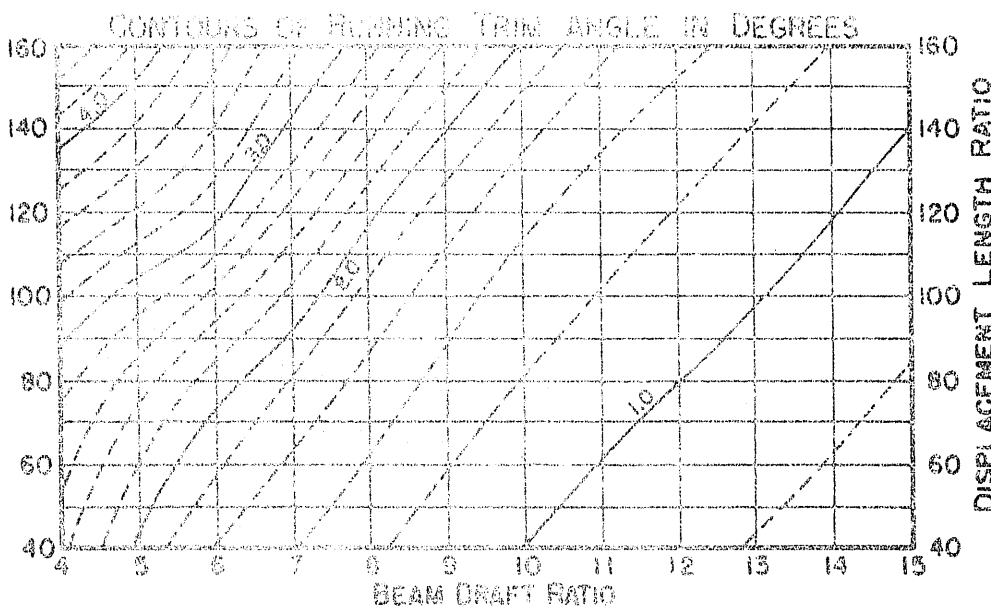
$$\tau = 4^\circ$$



$$\frac{\sqrt{V}}{L} = 6.0$$

$$\Delta = N + 10\%$$

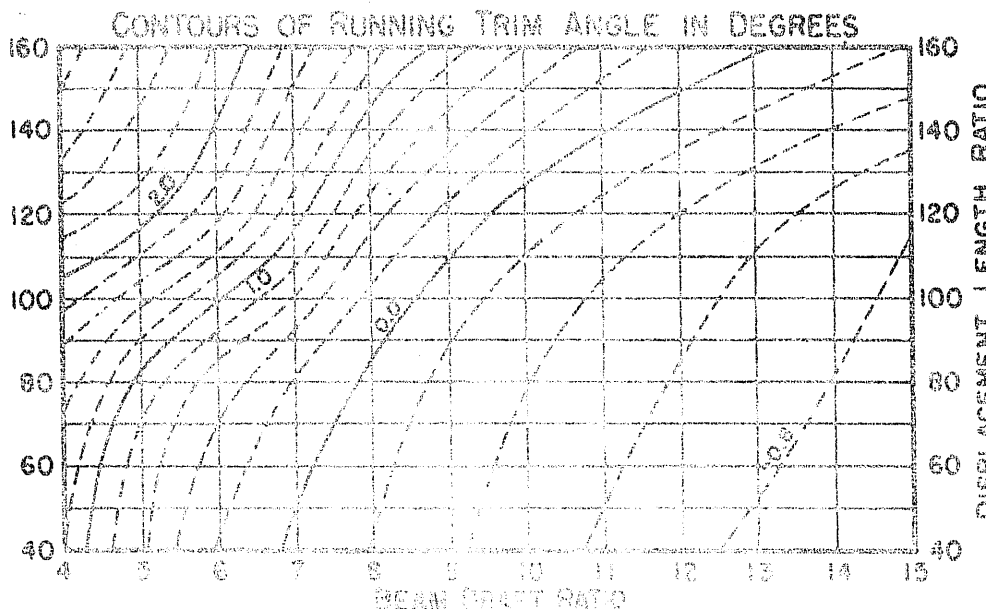
$$\gamma = 0^\circ$$



$$\frac{\sqrt{V}}{L} = 6.0$$

$$\Delta = N + 10\%$$

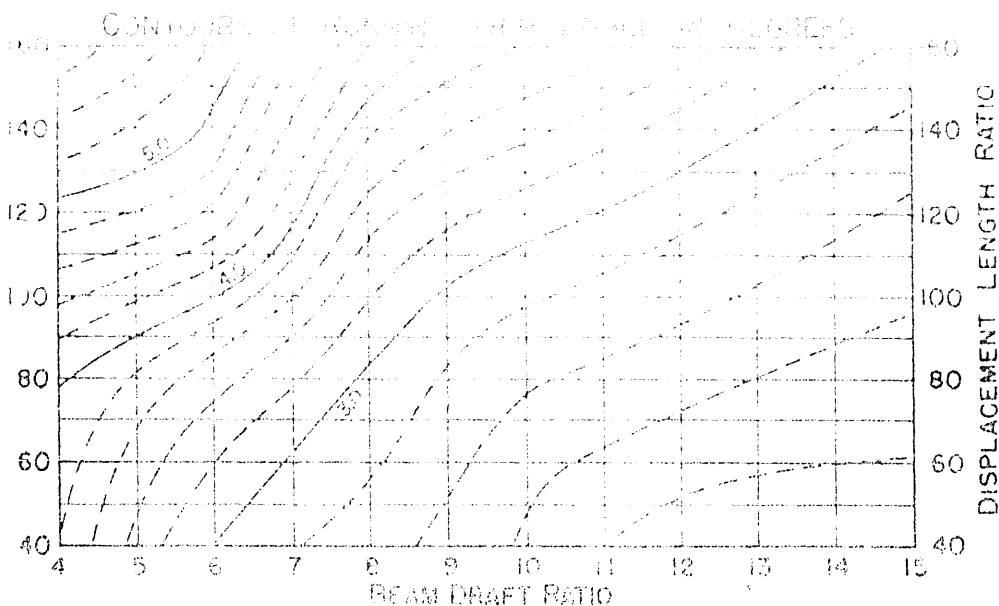
$$\gamma = 2^\circ$$



$$\frac{\sqrt{V}}{L} = 6.0$$

$$\Delta = N + 10\%$$

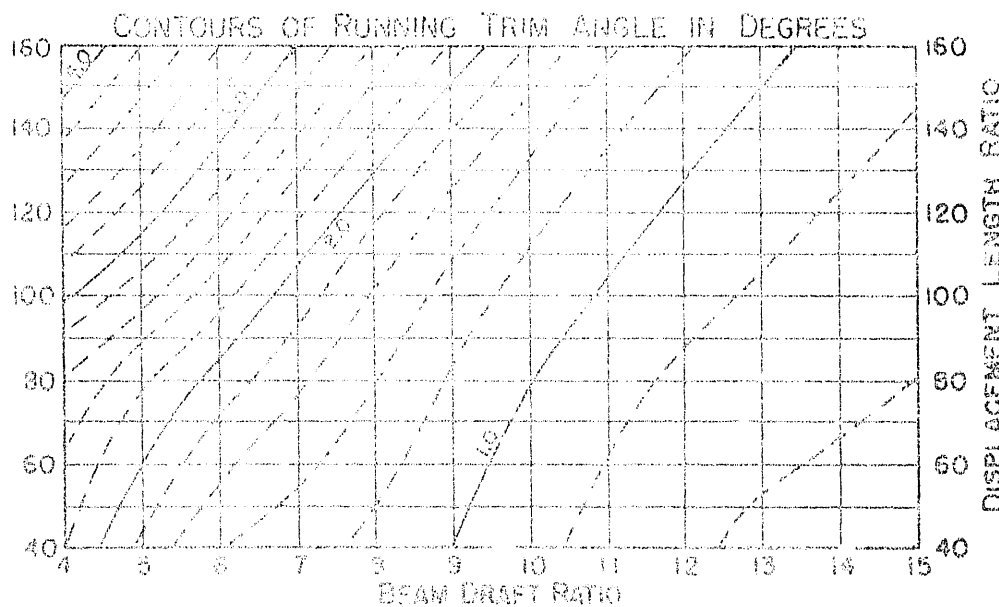
$$\gamma = 4^\circ$$



$$\frac{V}{\sqrt{L}} = 6.5$$

$$\Delta = N + 10\%$$

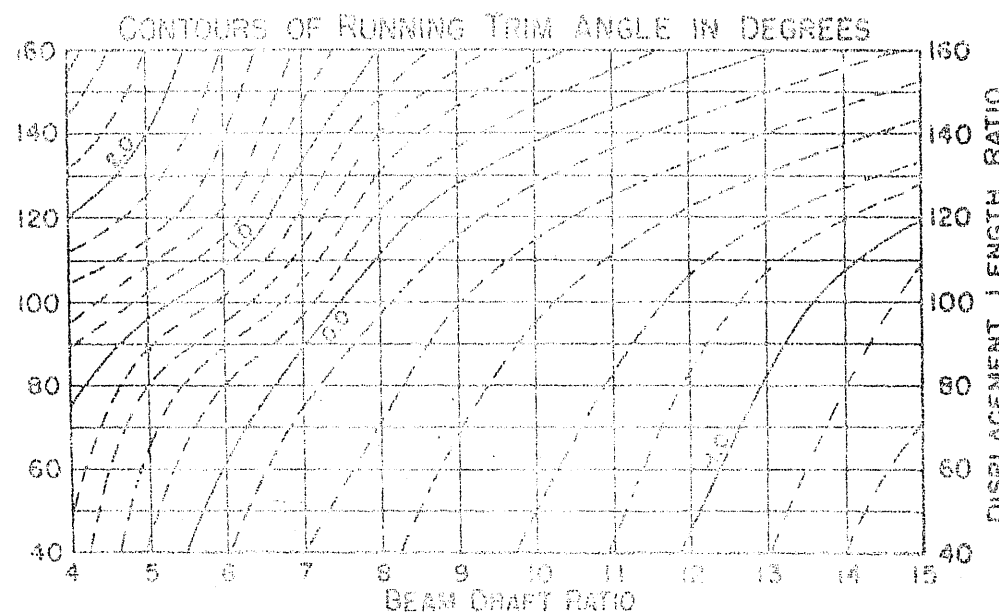
$$\tau = 0^\circ$$



$$\frac{V}{\sqrt{L}} = 6.5$$

$$\Delta = N + 10\%$$

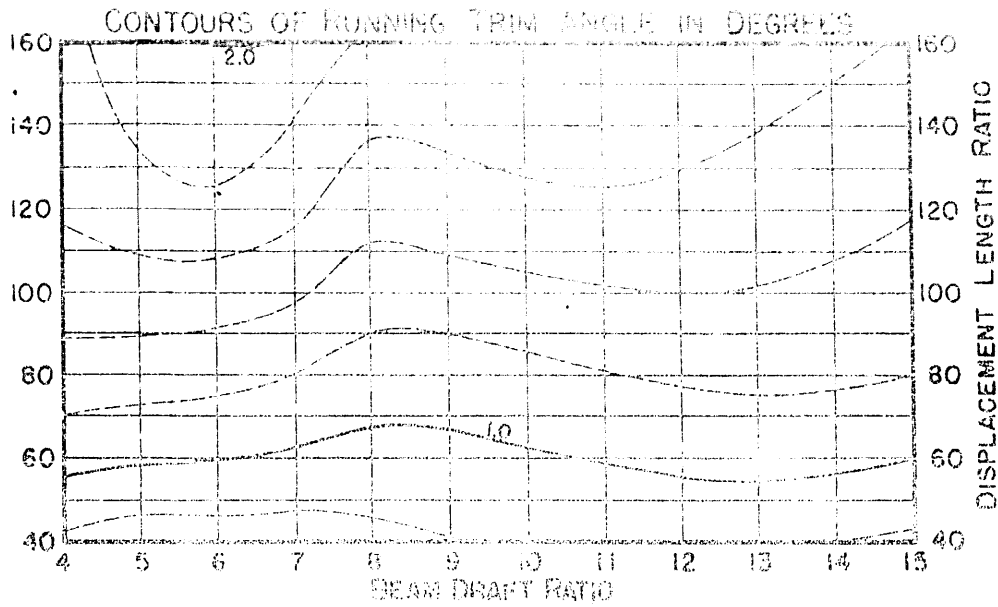
$$\tau = 2^\circ$$



$$\frac{V}{\sqrt{L}} = 6.5$$

$$\Delta = N + 10\%$$

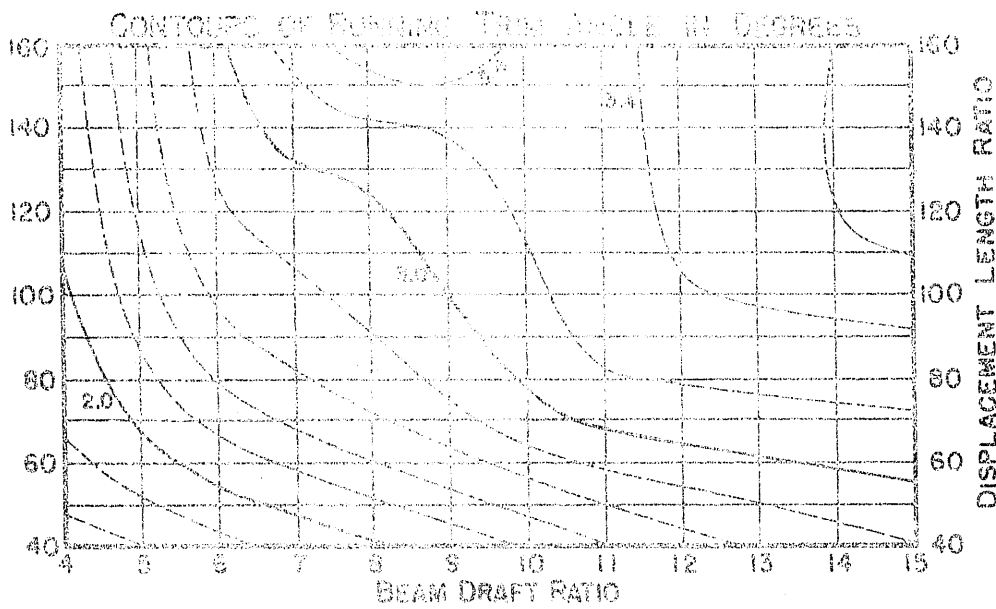
$$\tau = 4^\circ$$



$$\frac{V}{\sqrt{L}} = 1.5$$

$$\Delta = N + 20\%$$

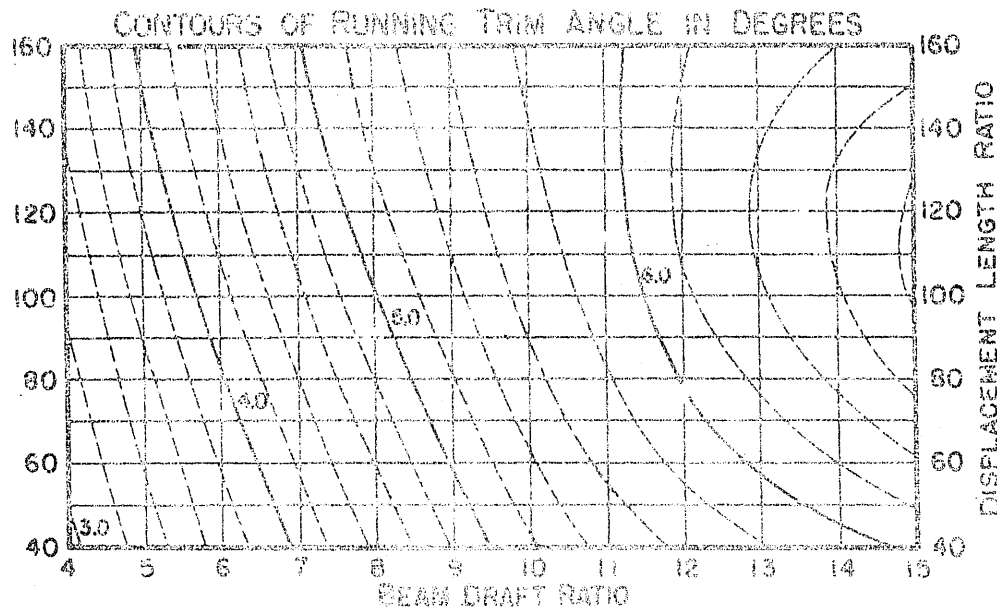
$$\gamma = 0^\circ$$



$$\frac{V}{\sqrt{L}} = 1.5$$

$$\Delta = N + 20\%$$

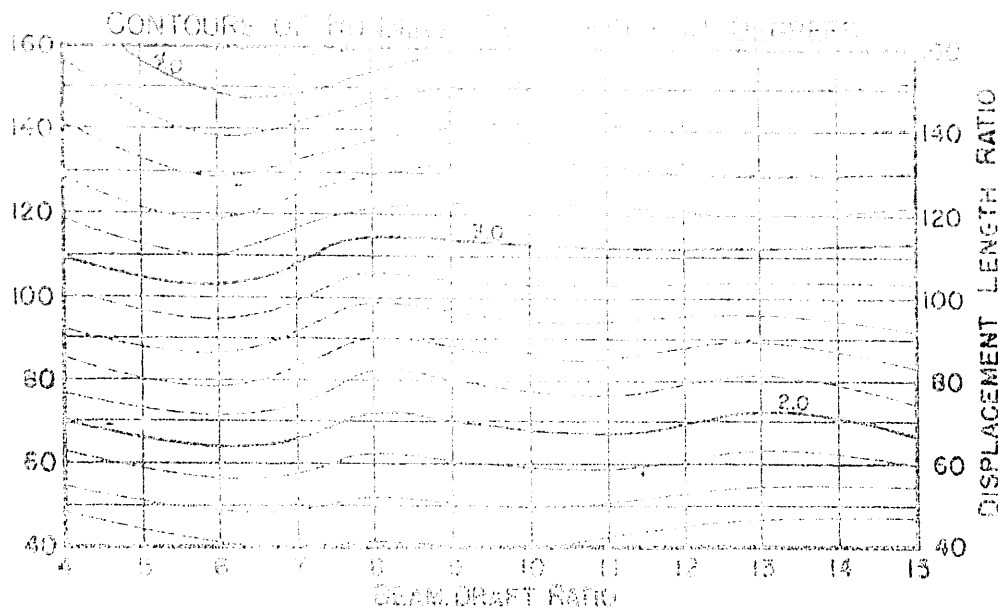
$$\gamma = 2^\circ$$



$$\frac{V}{\sqrt{L}} = 1.5$$

$$\Delta = N + 20\%$$

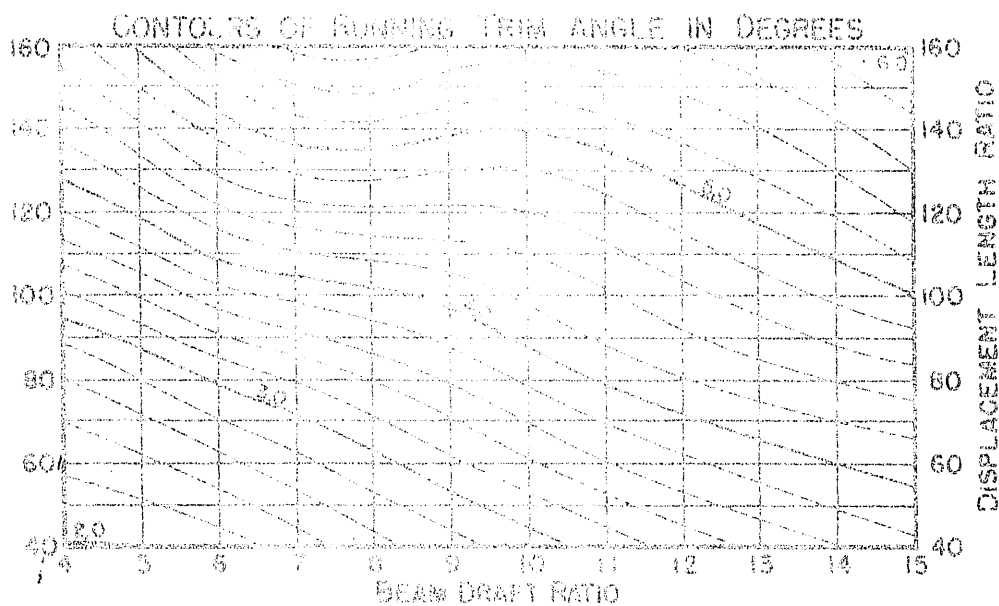
$$\gamma = 4^\circ$$



$$\frac{v}{\sqrt{L}} = 2.0$$

$$\Delta = N + 20\%$$

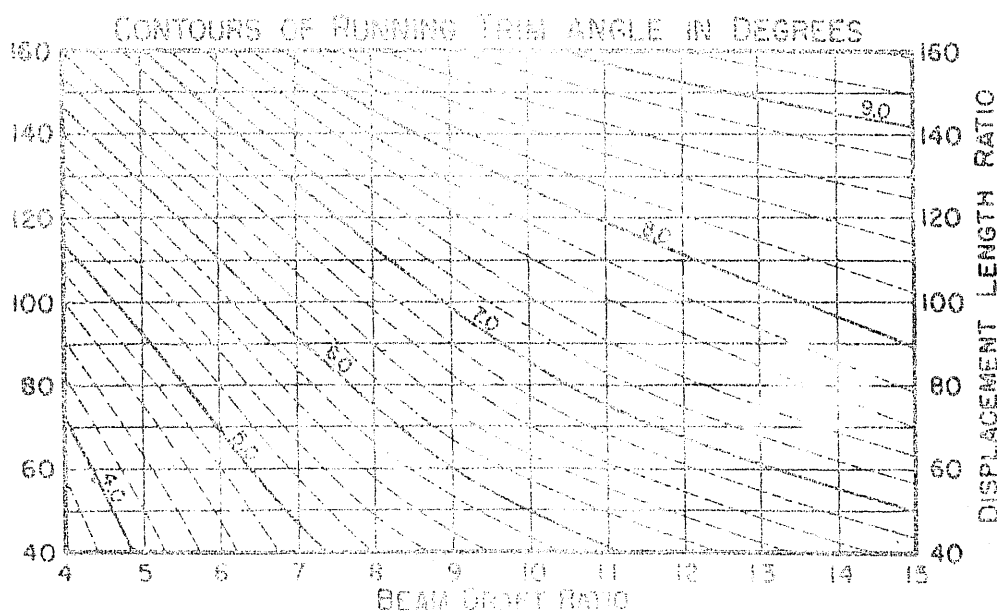
$$\tau = \dots$$



$$\frac{v}{\sqrt{L}} = 2.0$$

$$\Delta = N + 20\%$$

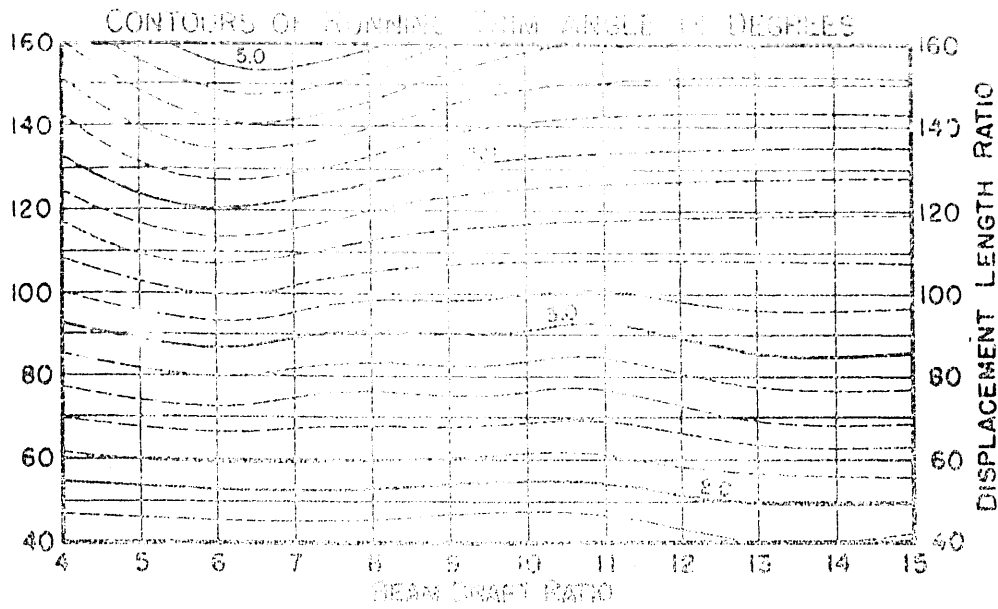
$$\tau = 2^\circ$$



$$\frac{v}{\sqrt{L}} = 2.0$$

$$\Delta = N + 20\%$$

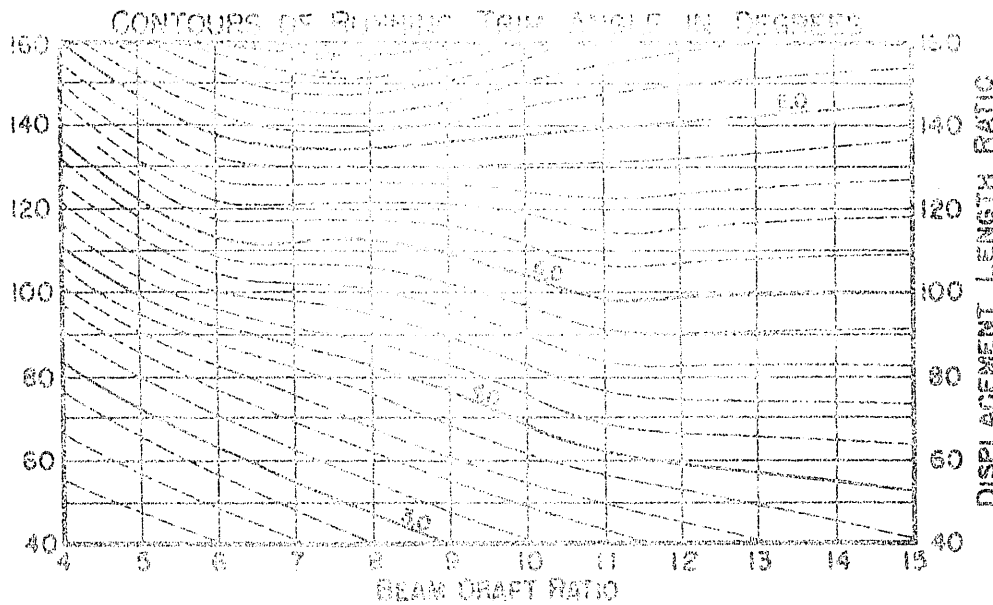
$$\tau = 4^\circ$$



$$\frac{V}{\sqrt{L}} = 2.5$$

$$\Delta = N + 20\%$$

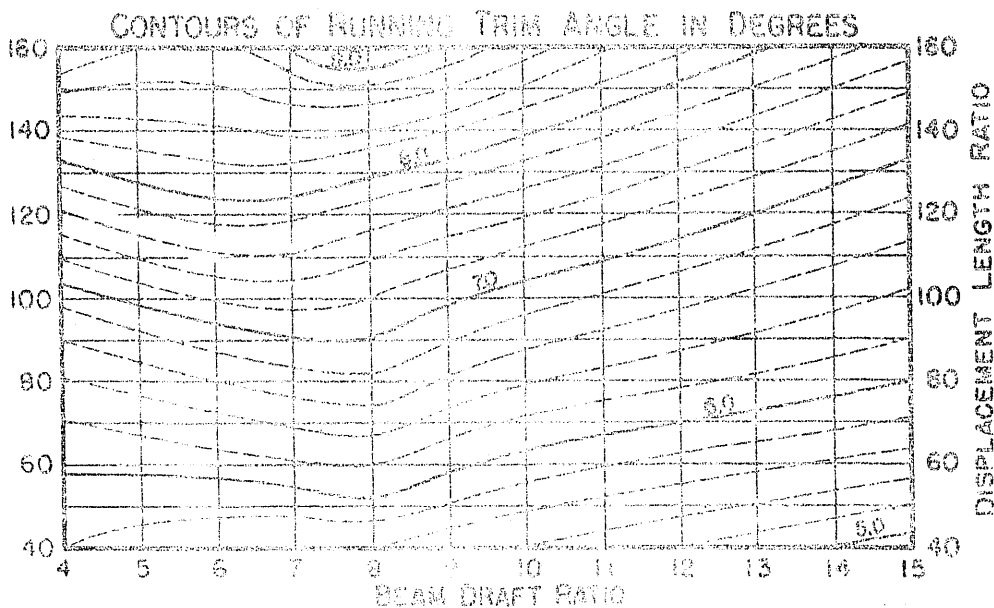
$$J = 0^\circ$$



$$\frac{V}{\sqrt{L}} = 2.5$$

$$\Delta = N + 20\%$$

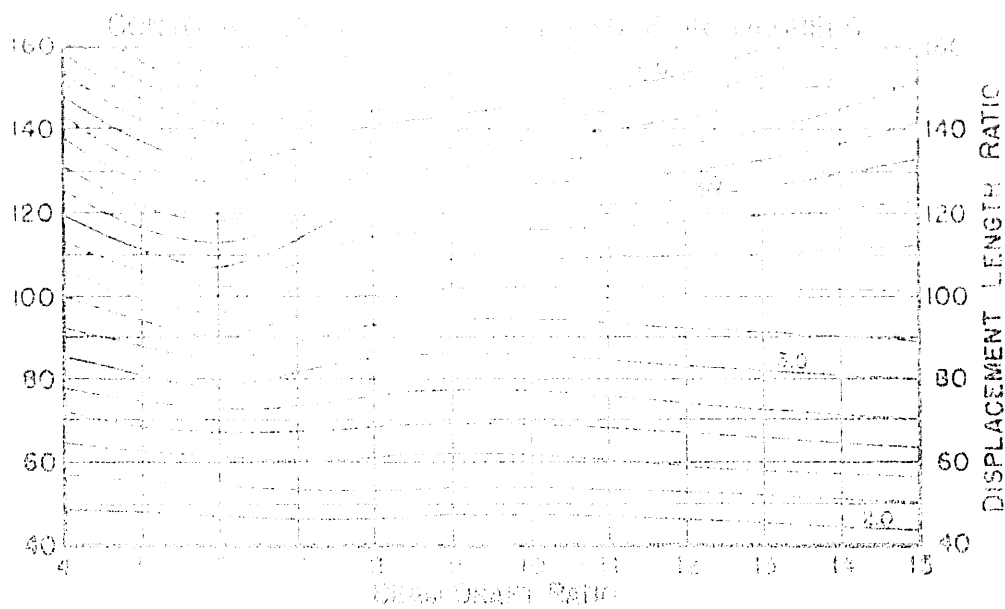
$$J = 2^\circ$$



$$\frac{V}{\sqrt{L}} = 2.5$$

$$\Delta = N + 20\%$$

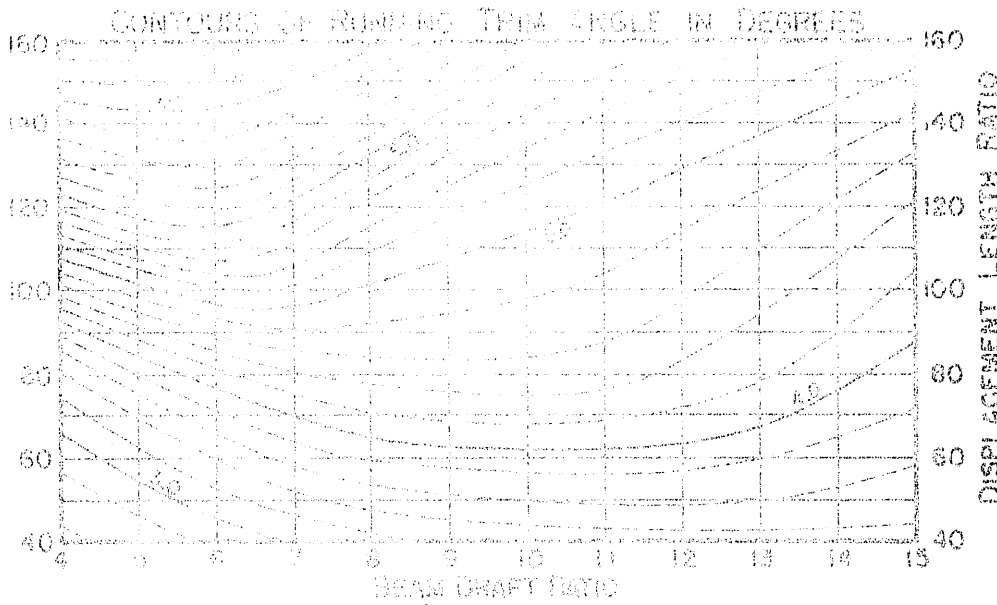
$$J = 4^\circ$$



$$\frac{V}{\sqrt{L}} = 3.0$$

$$\Delta = N + 20\%$$

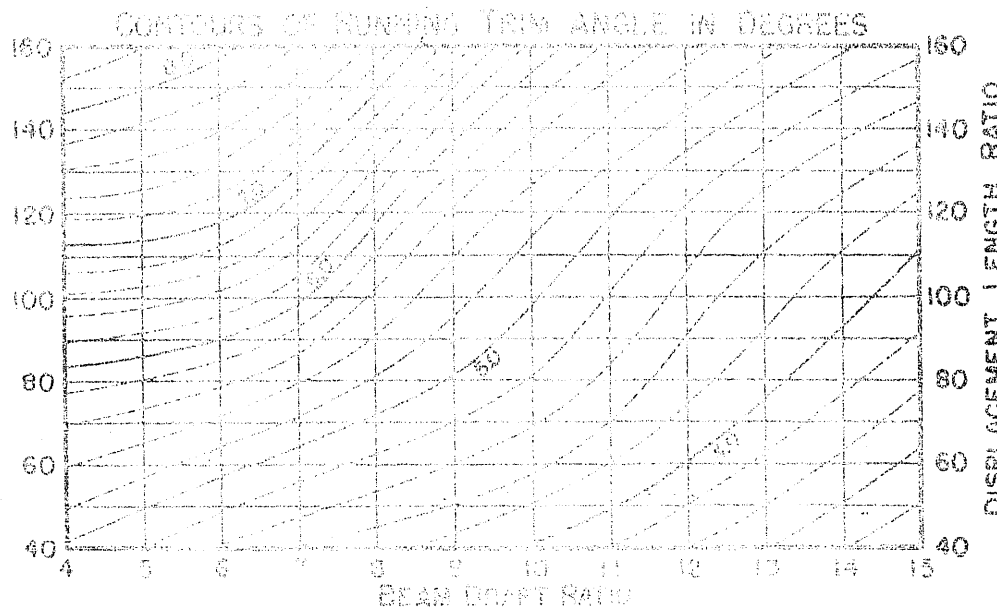
$$\tau = 0^\circ$$



$$\frac{V}{\sqrt{L}} = 3.0$$

$$\Delta = N + 20\%$$

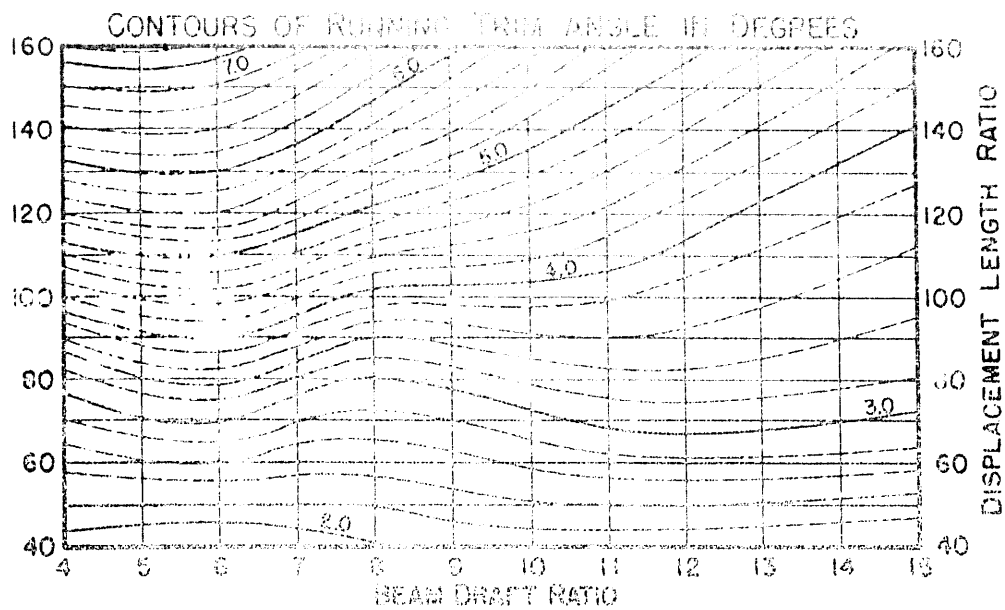
$$\tau = 2^\circ$$



$$\frac{V}{\sqrt{L}} = 3.0$$

$$\Delta = N + 20\%$$

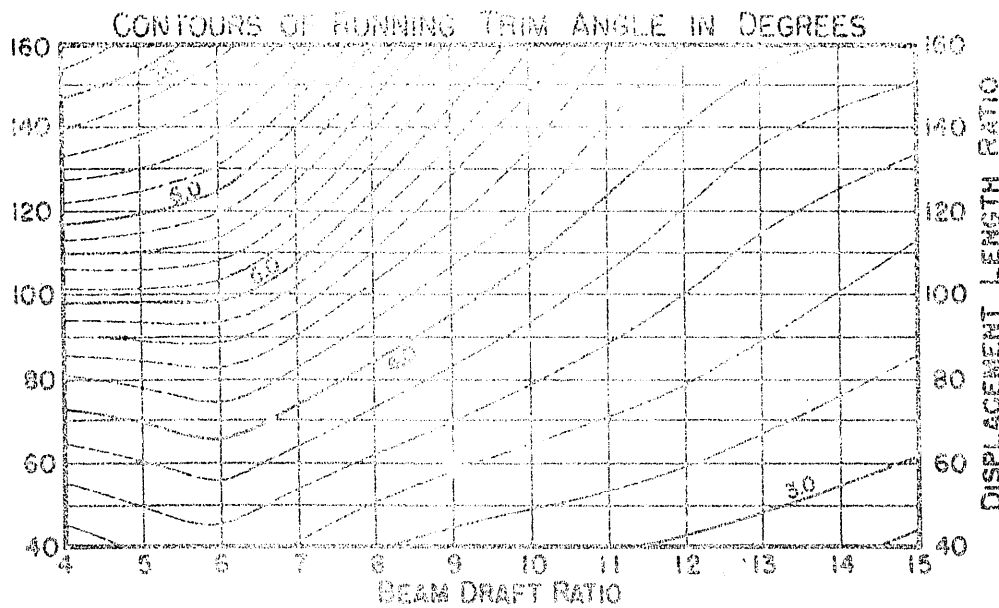
$$\tau = 4^\circ$$



$$\frac{V}{\sqrt{L}} = 3.5$$

$$\Delta = N + 20\%$$

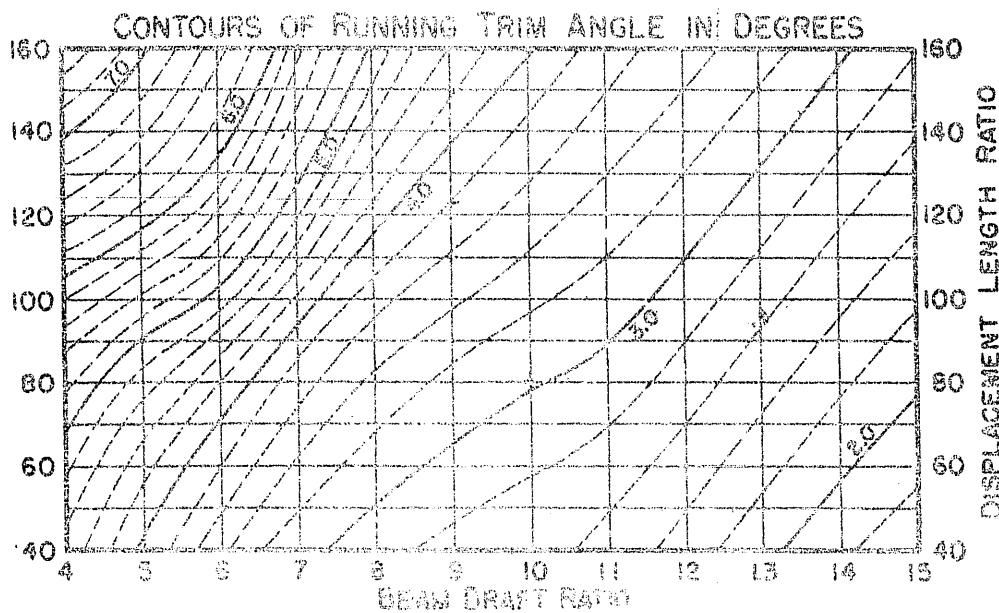
$$T = 0^\circ$$



$$\frac{V}{\sqrt{L}} = 3.5$$

$$\Delta = N + 20\%$$

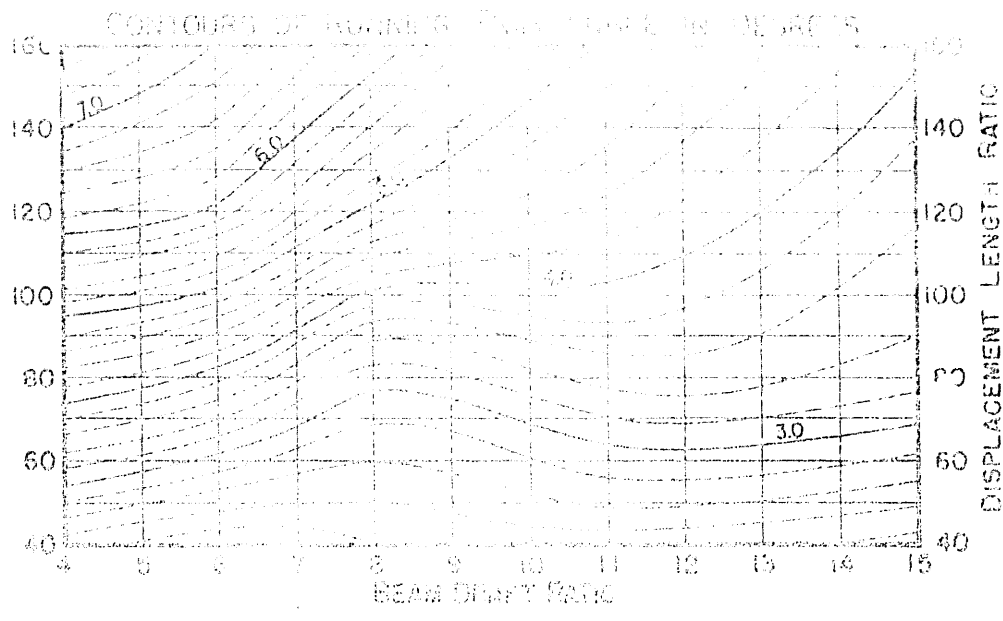
$$T = 2^\circ$$



$$\frac{V}{\sqrt{L}} = 3.5$$

$$\Delta = N + 20\%$$

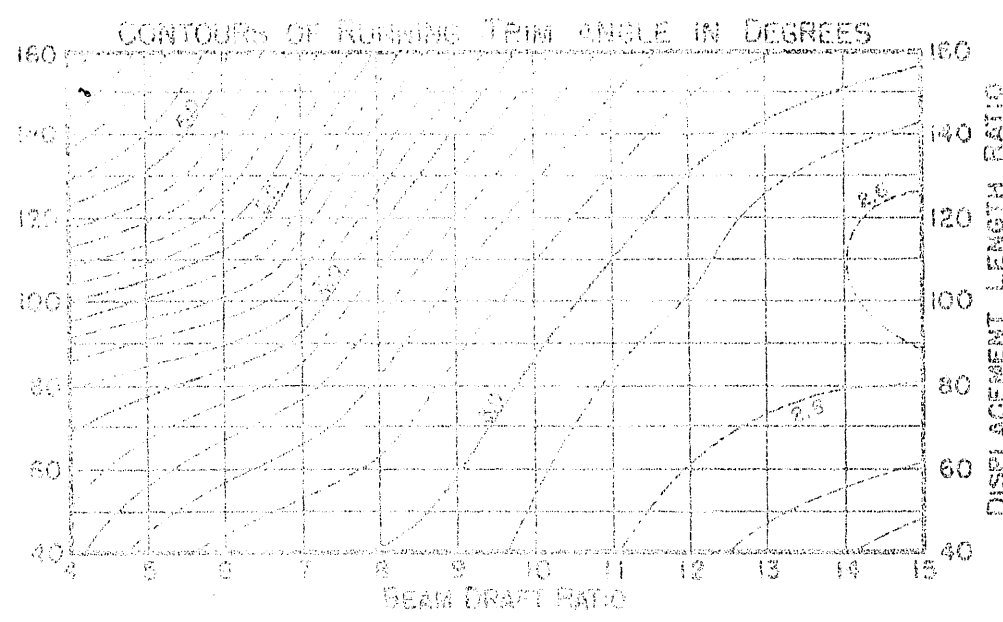
$$T = 4^\circ$$



$$\frac{v}{\sqrt{L}} = 4.0$$

$$\Delta = N + 20\%$$

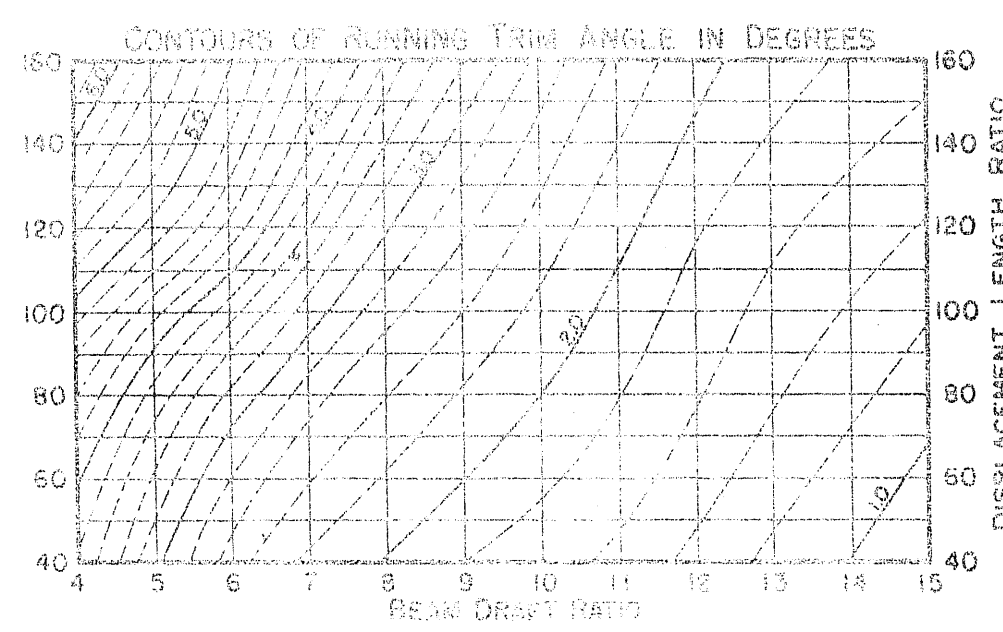
$$\tau = 0^\circ$$



$$\frac{v}{\sqrt{L}} = 4.0$$

$$\Delta = N + 20\%$$

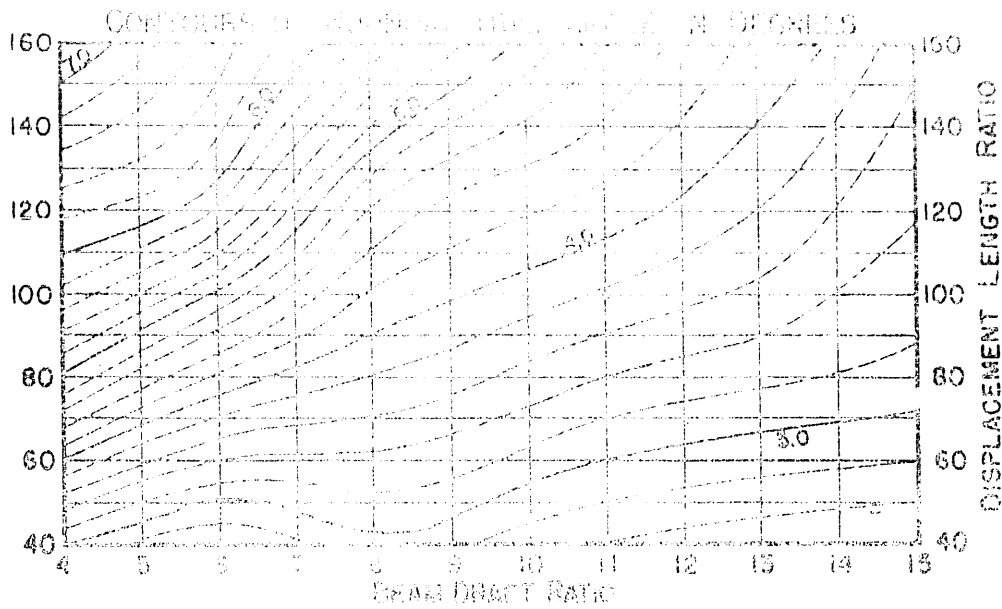
$$\tau = 2^\circ$$



$$\frac{v}{\sqrt{L}} = 4.0$$

$$\Delta = N + 20\%$$

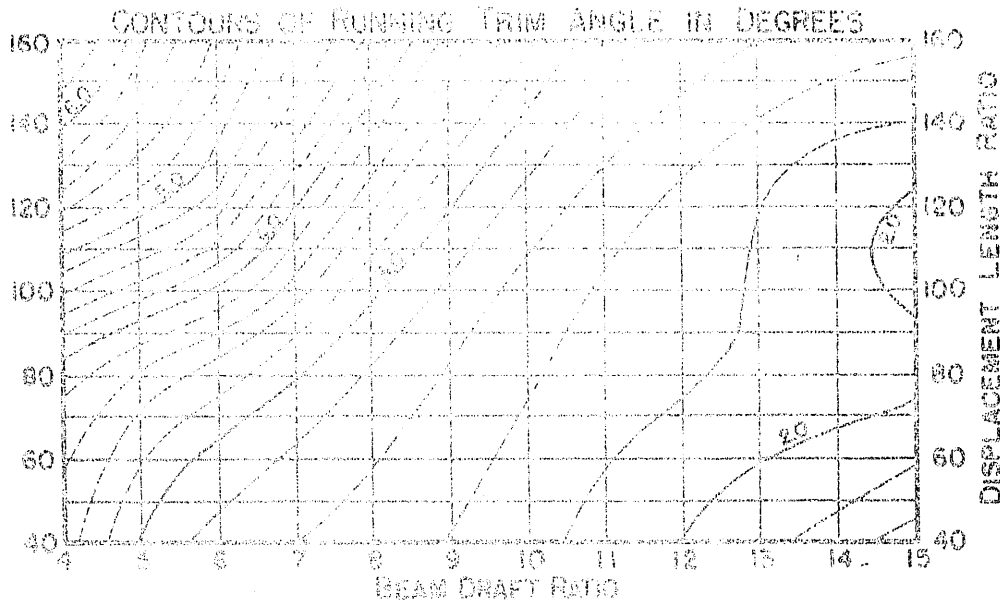
$$\tau = 4^\circ$$



$$\frac{V}{\sqrt{L}} = 4.5$$

$$\Delta = N + 20\%$$

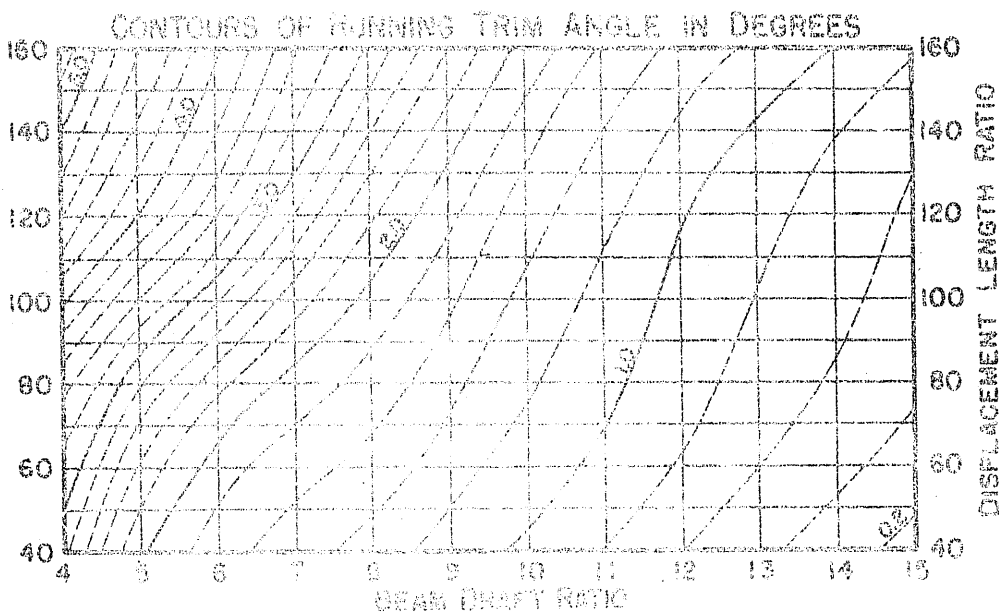
$$\gamma = 0^\circ$$



$$\frac{V}{\sqrt{L}} = 4.5$$

$$\Delta = N + 20\%$$

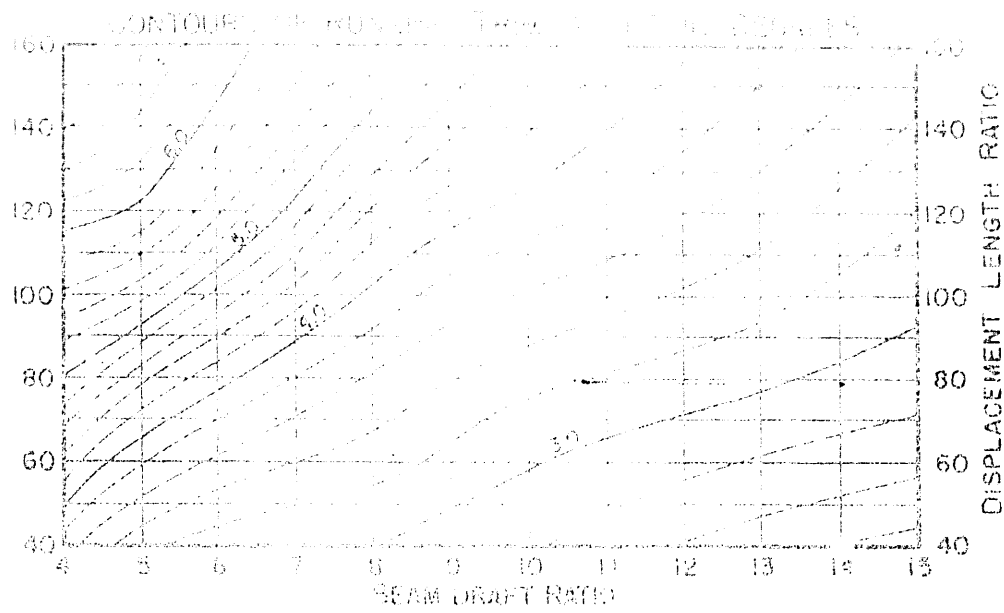
$$\gamma = 2^\circ$$



$$\frac{V}{\sqrt{L}} = 4.5$$

$$\Delta = N + 20\%$$

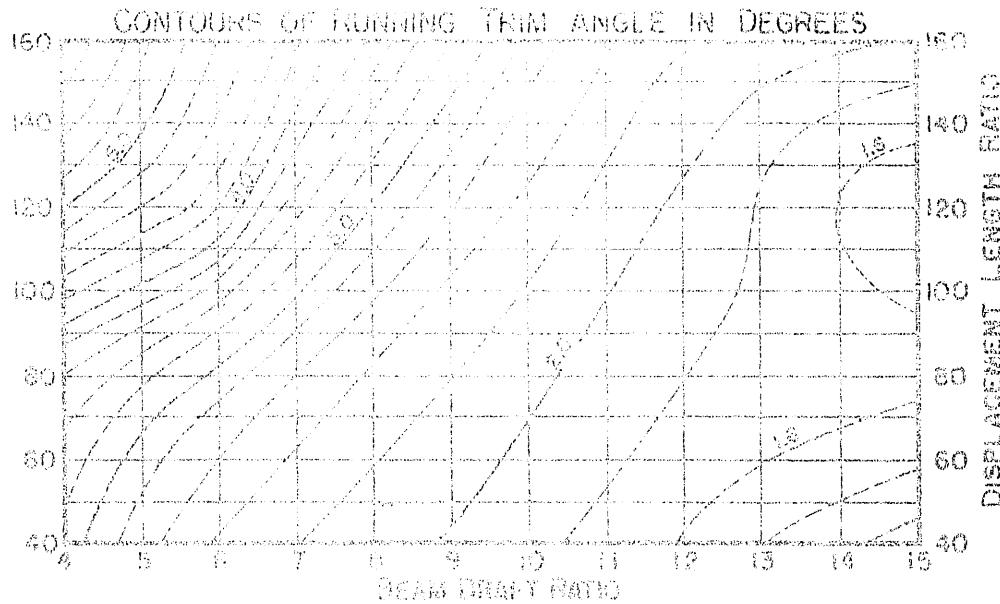
$$\gamma = 4^\circ$$



$$\frac{v}{\sqrt{L}} = 5.0$$

$$\Delta = N + 20\%$$

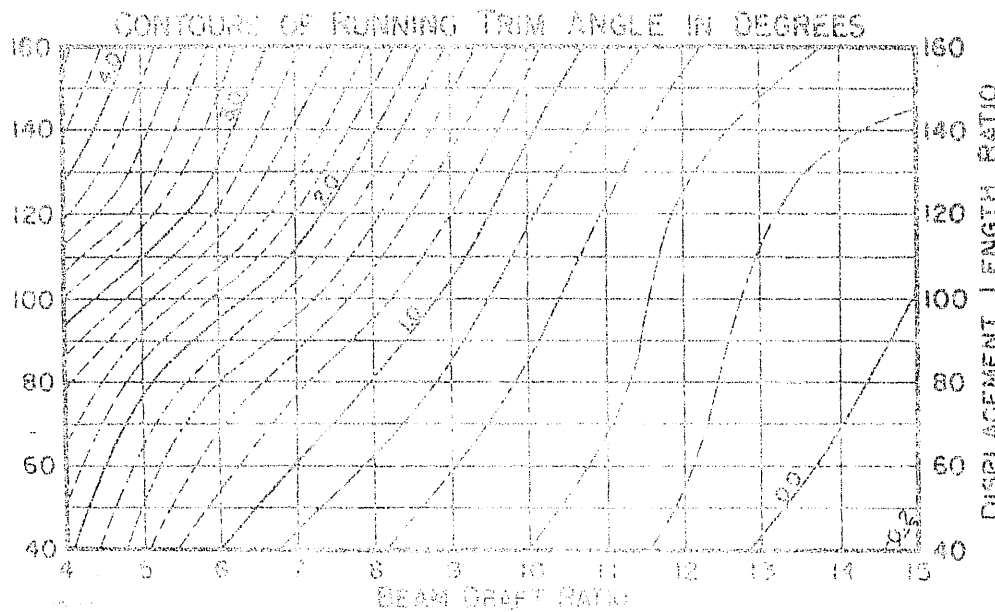
$$\tau = 0^\circ$$



$$\frac{v}{\sqrt{L}} = 5.0$$

$$\Delta = N + 20\%$$

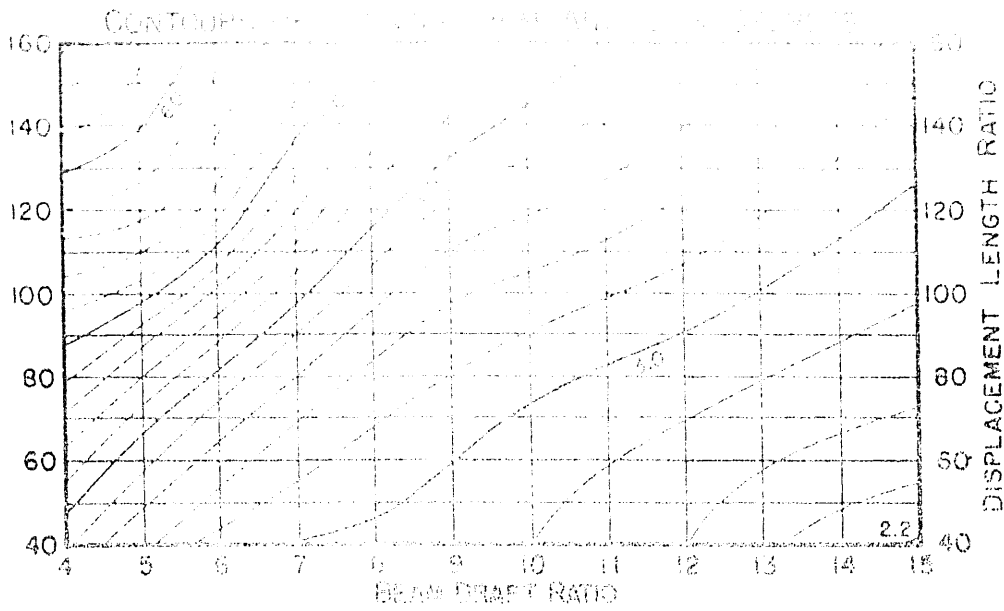
$$\tau = 2^\circ$$



$$\frac{v}{\sqrt{L}} = 5.0$$

$$\Delta = N + 20\%$$

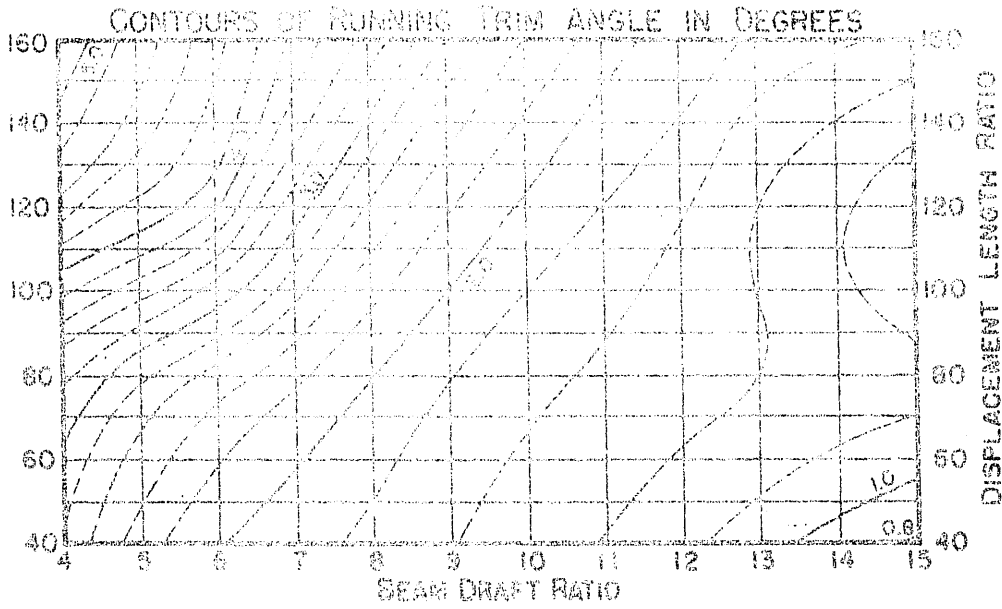
$$\tau = 4^\circ$$



$$\frac{V}{\sqrt{L}} = 5.5$$

$$\Delta = N + 20\%$$

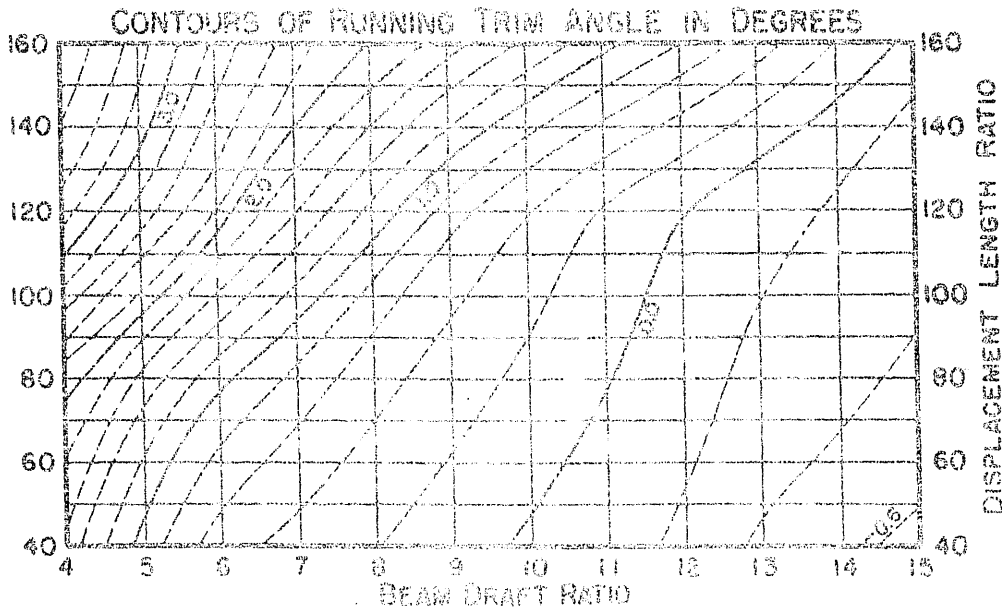
$$\gamma = 0^\circ$$



$$\frac{V}{\sqrt{L}} = 5.5$$

$$\Delta = N + 20\%$$

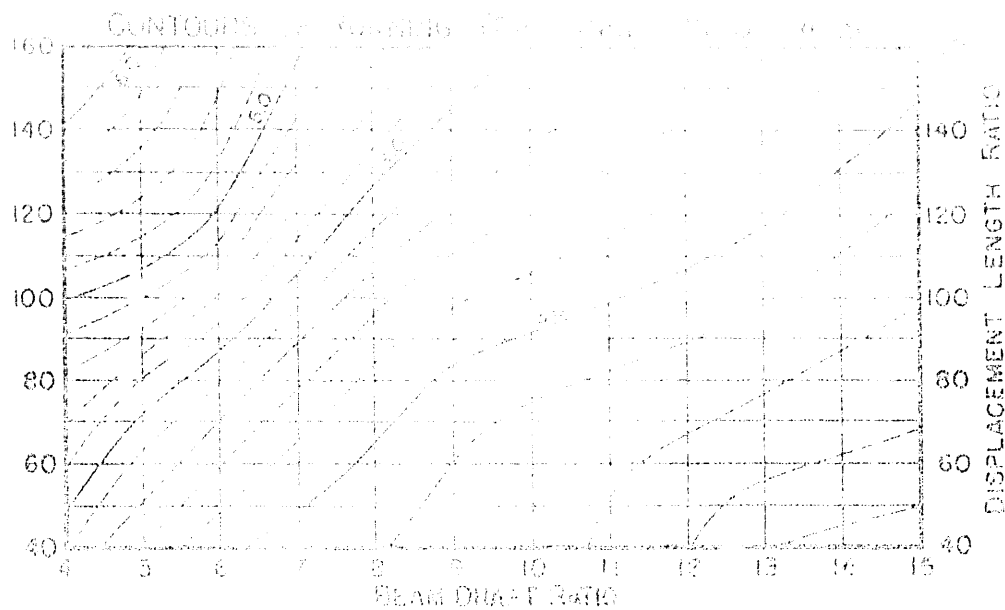
$$\gamma = 2^\circ$$



$$\frac{V}{\sqrt{L}} = 5.5$$

$$\Delta = N + 20\%$$

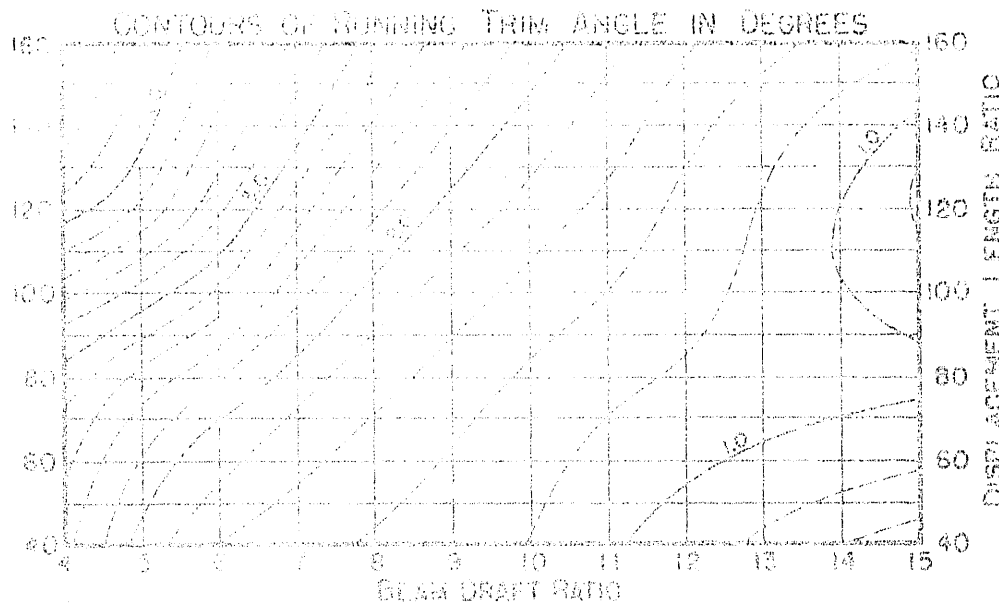
$$\gamma = 4^\circ$$



$$\frac{v}{L} = 6.0$$

$$\Delta = N + 20\%$$

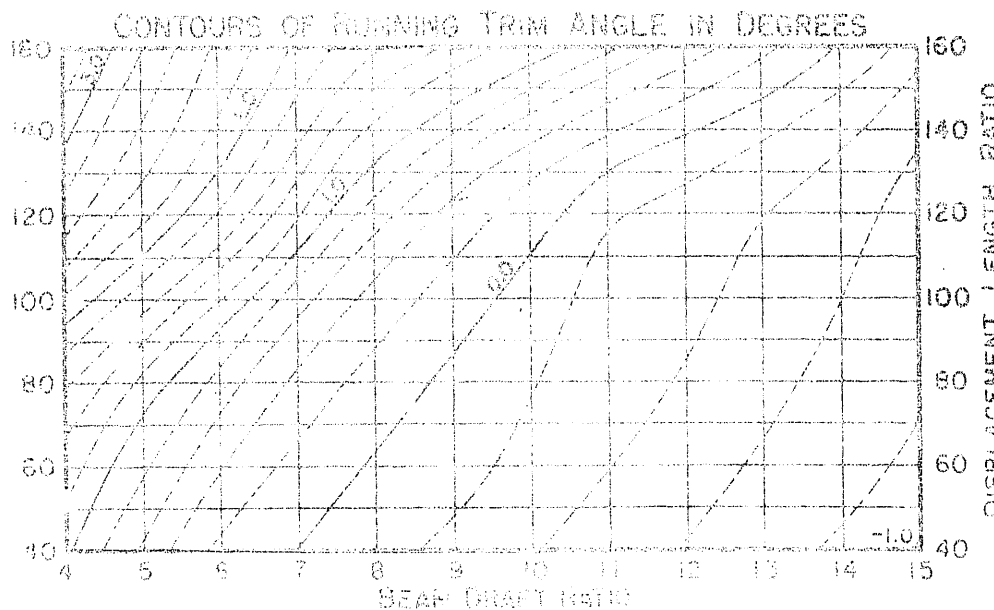
$$T = 0^\circ$$



$$\frac{v}{L} = 6.0$$

$$\Delta = N + 20\%$$

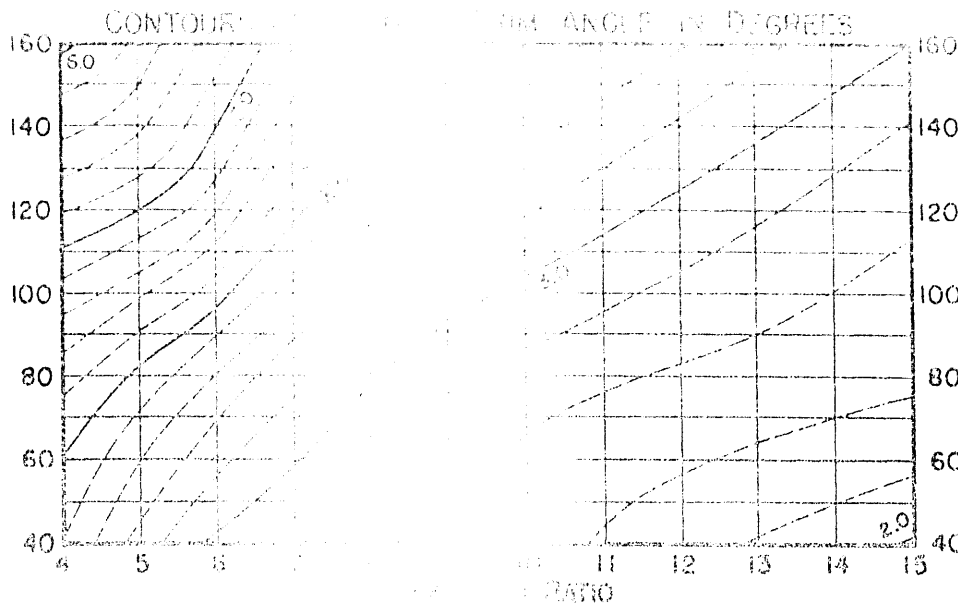
$$T = 2^\circ$$



$$\frac{v}{L} = 6.0$$

$$\Delta = N + 20\%$$

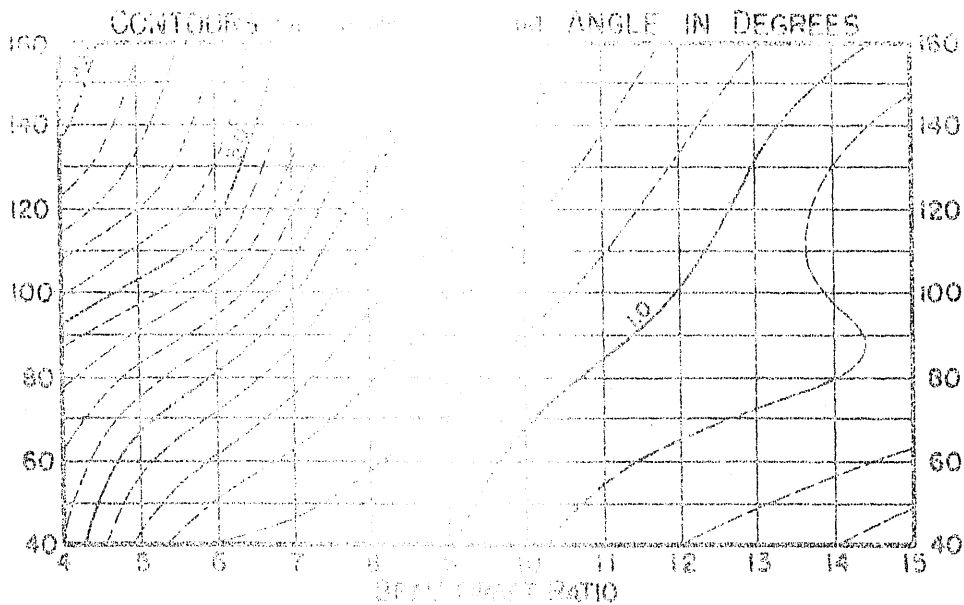
$$T = 4^\circ$$



$$\frac{V}{\sqrt{L}} = 6.5$$

$$\Delta = N + 20\%$$

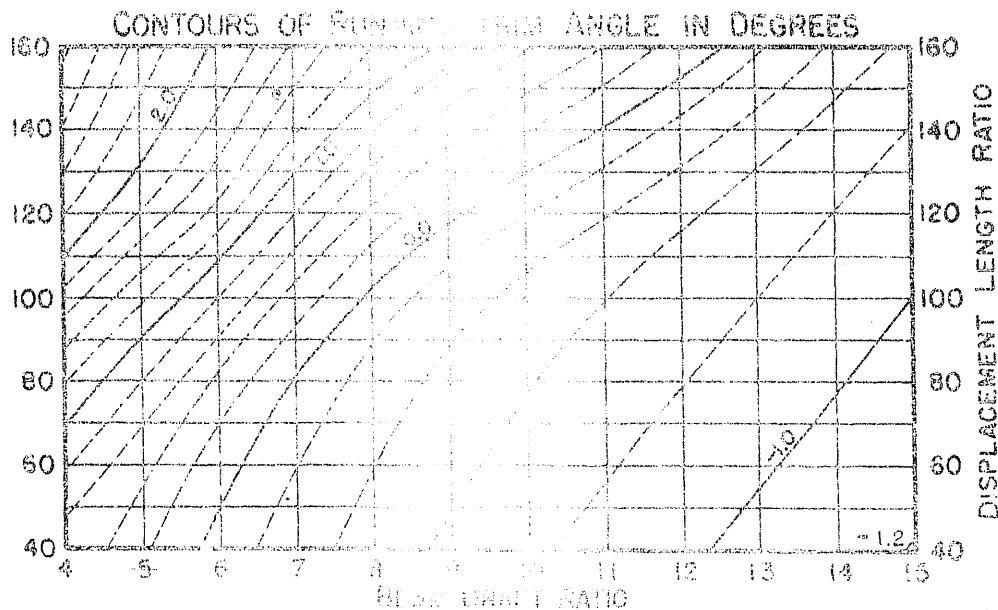
$$\gamma = 0^\circ$$



$$\frac{V}{\sqrt{L}} = 6.5$$

$$\Delta = N + 20\%$$

$$\gamma = 2^\circ$$



$$\frac{V}{\sqrt{L}} = 6.5$$

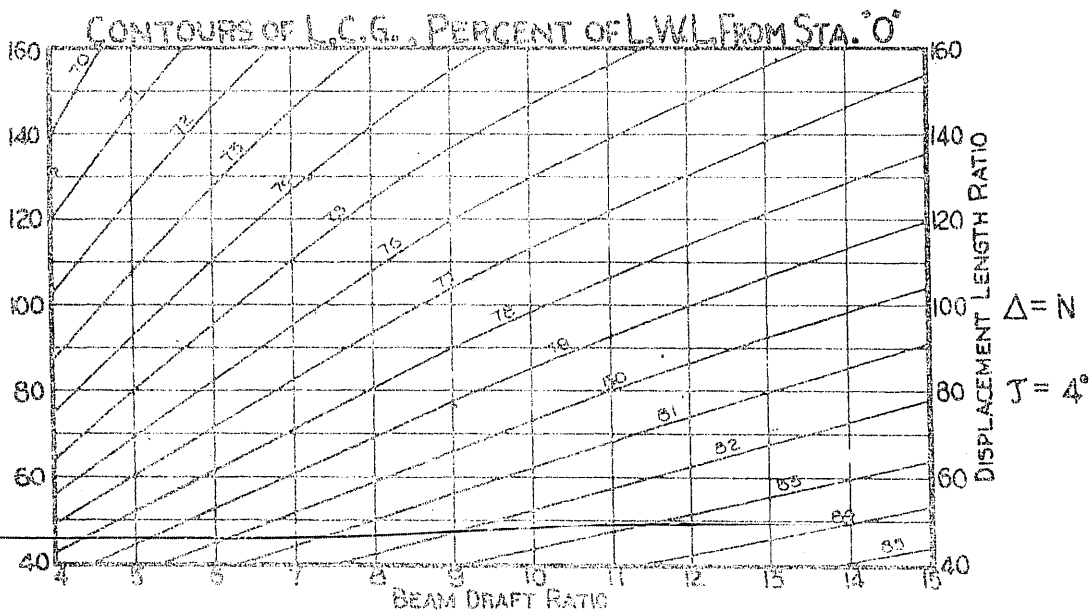
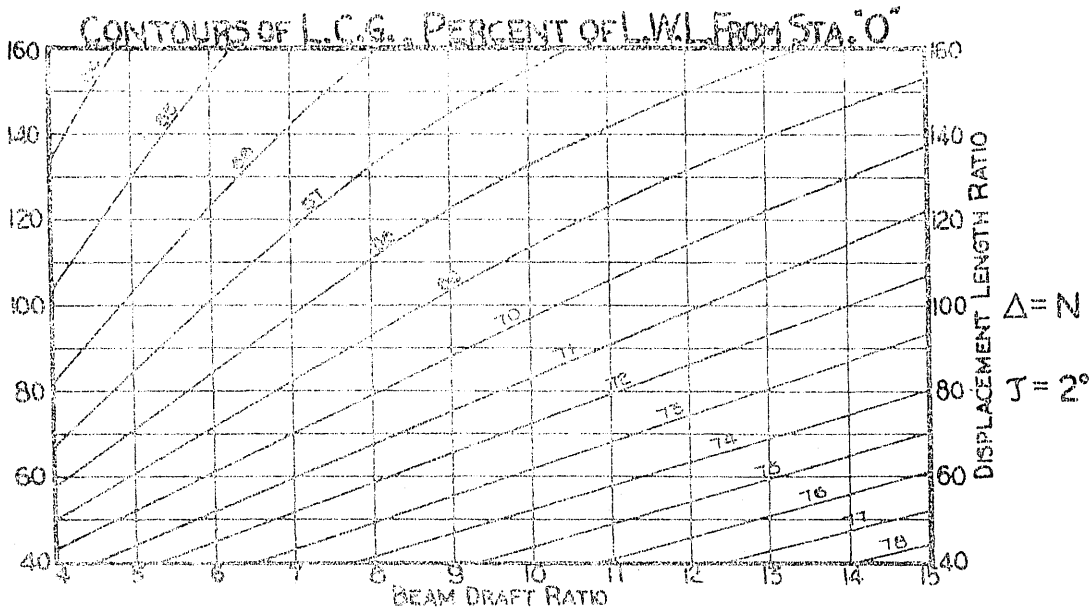
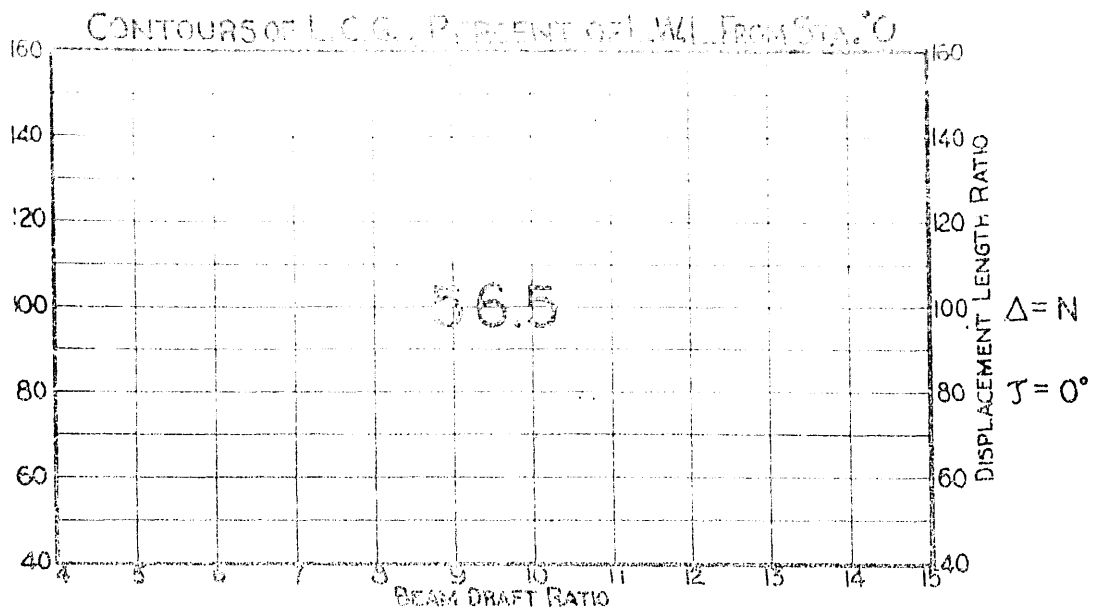
$$\Delta = N + 20\%$$

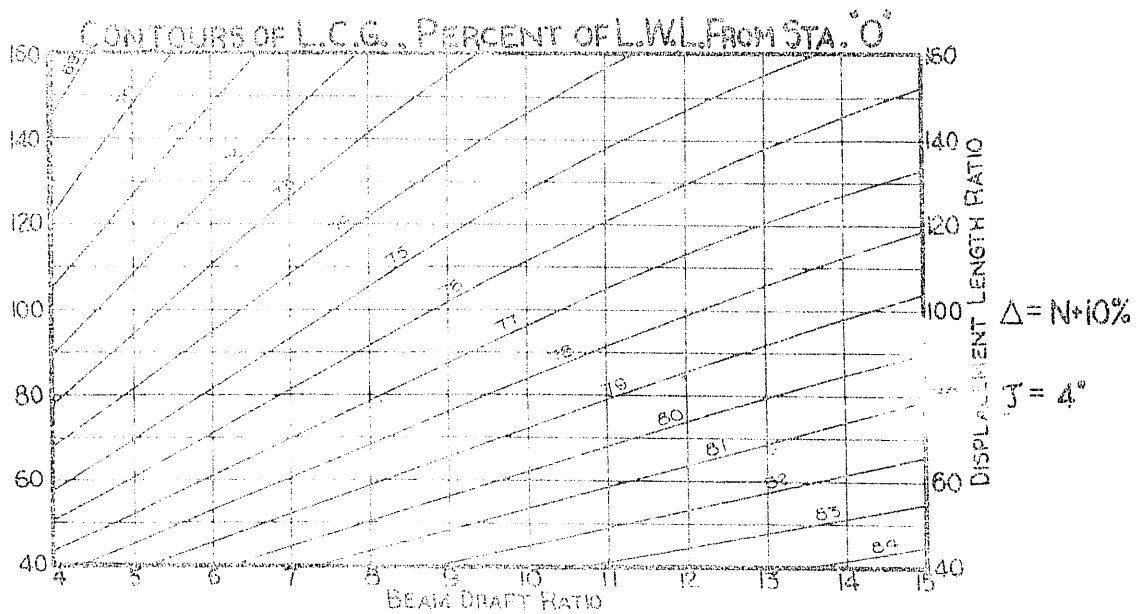
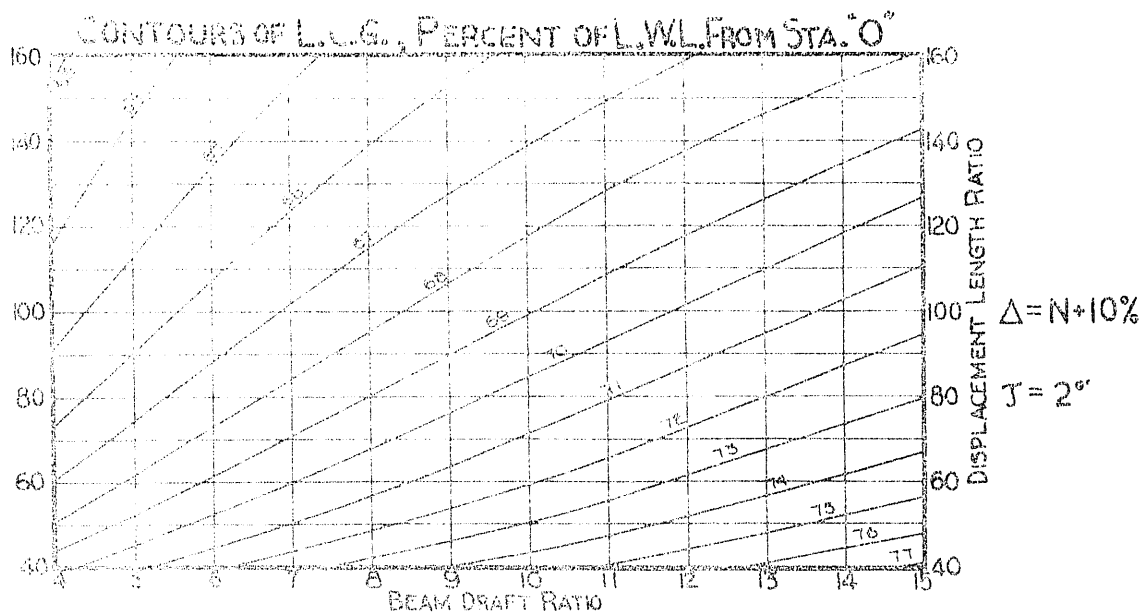
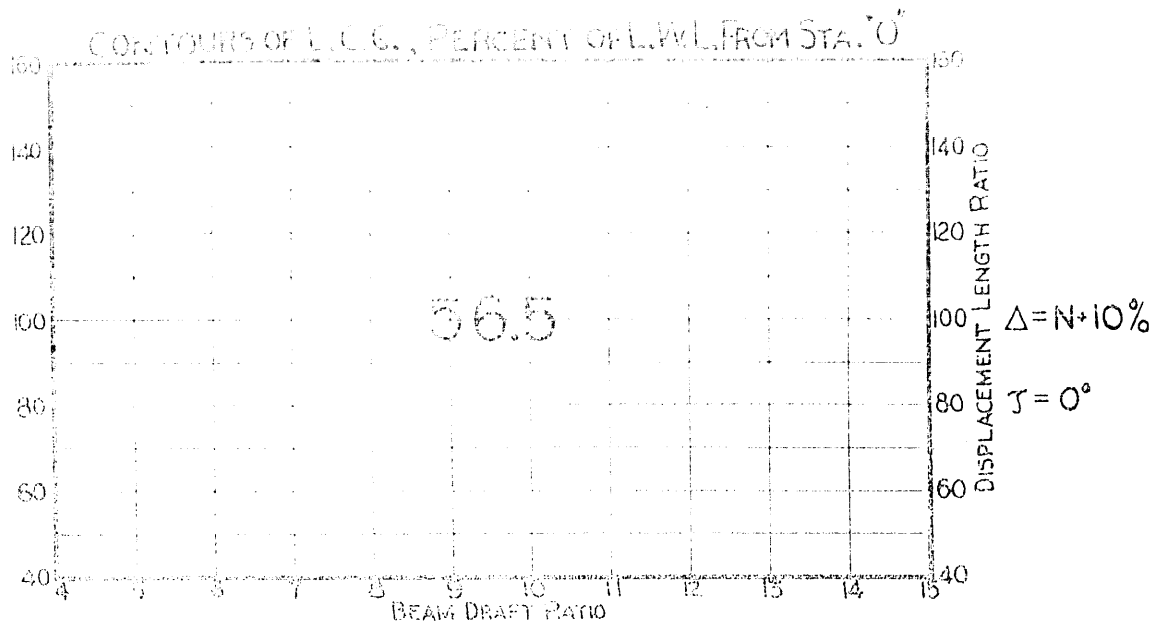
$$\gamma = 4^\circ$$

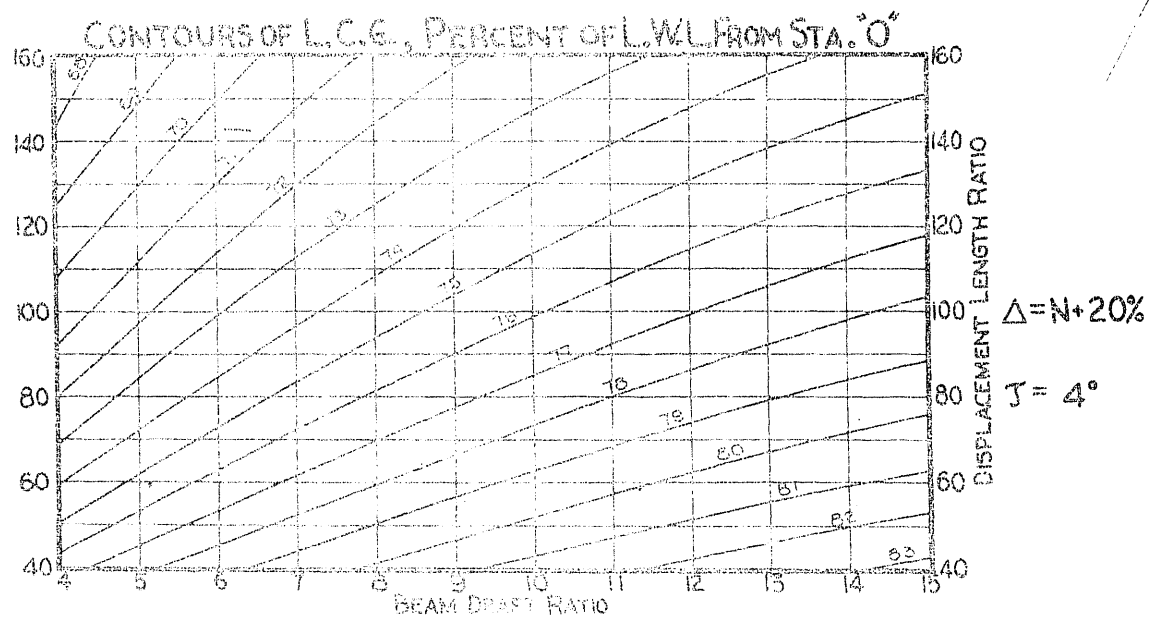
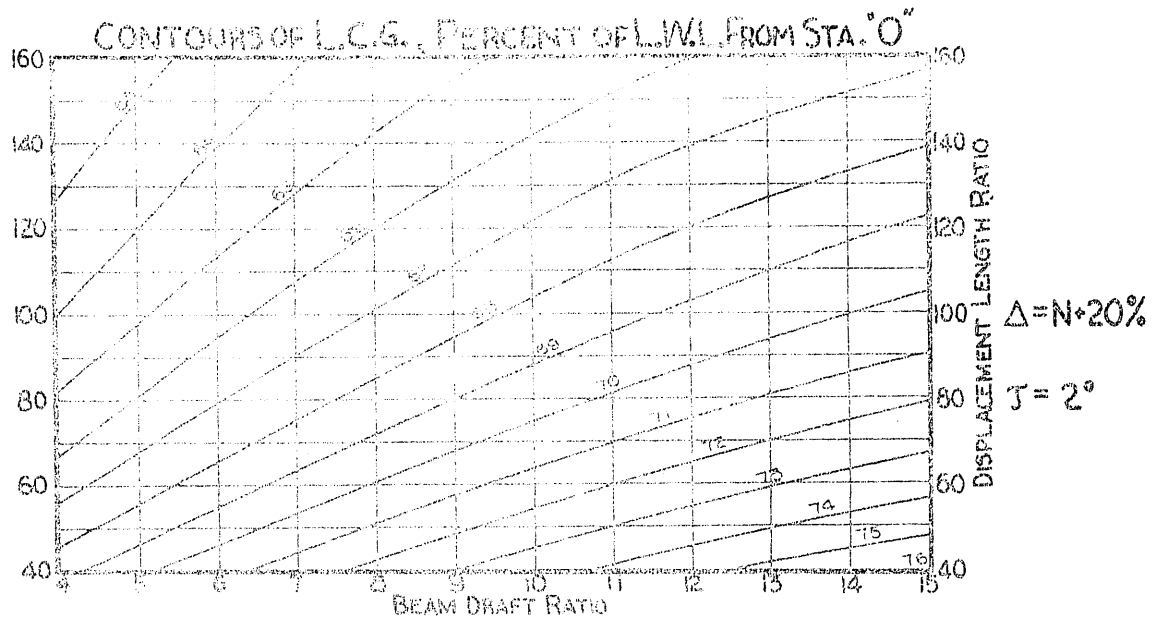
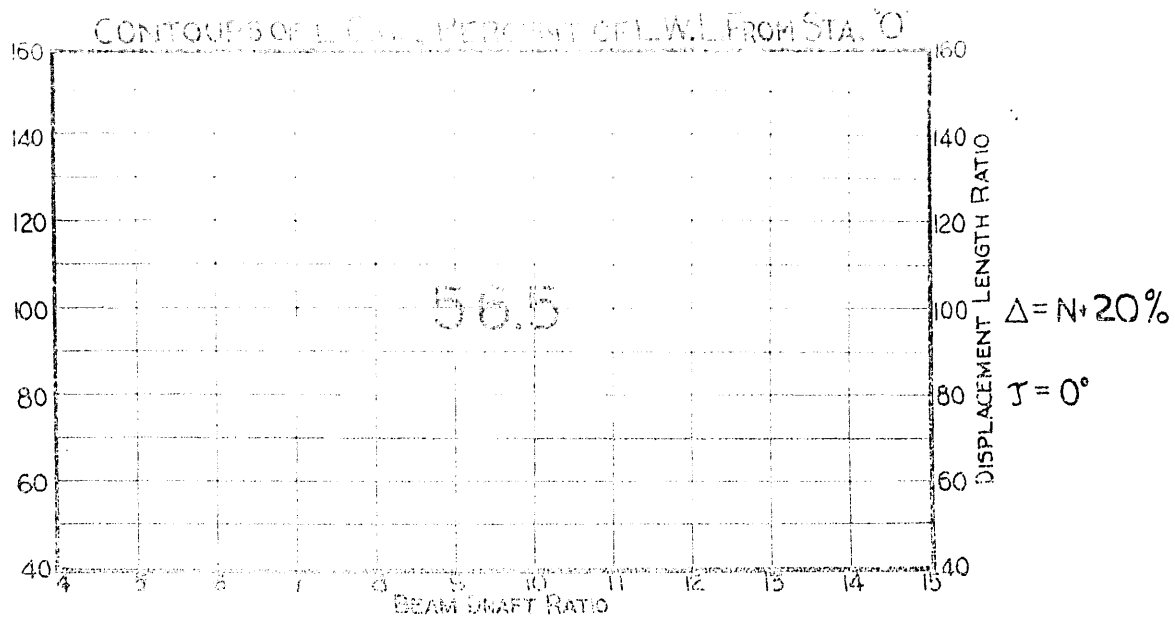
CONTENTS
OF
DISPLACEMENT CENTERS OF GRAVITY

Experimental Conditions at which Tests were Made

	Page
100% Displacement (N)	81
110% " " (N + 10%)	82
120% " " (N + 20%)	83



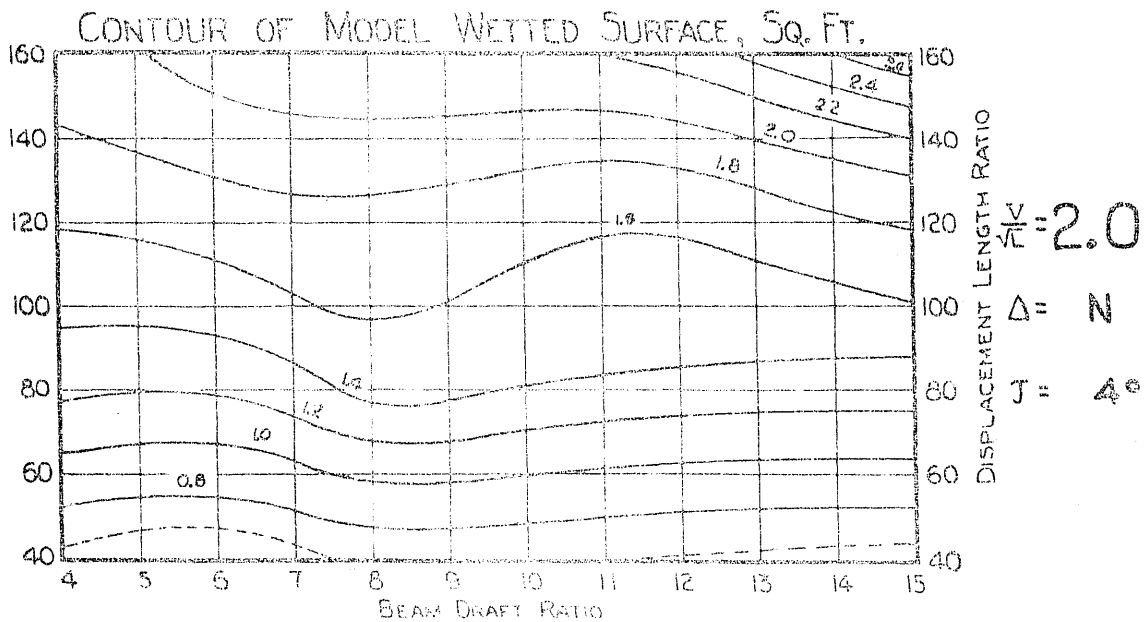
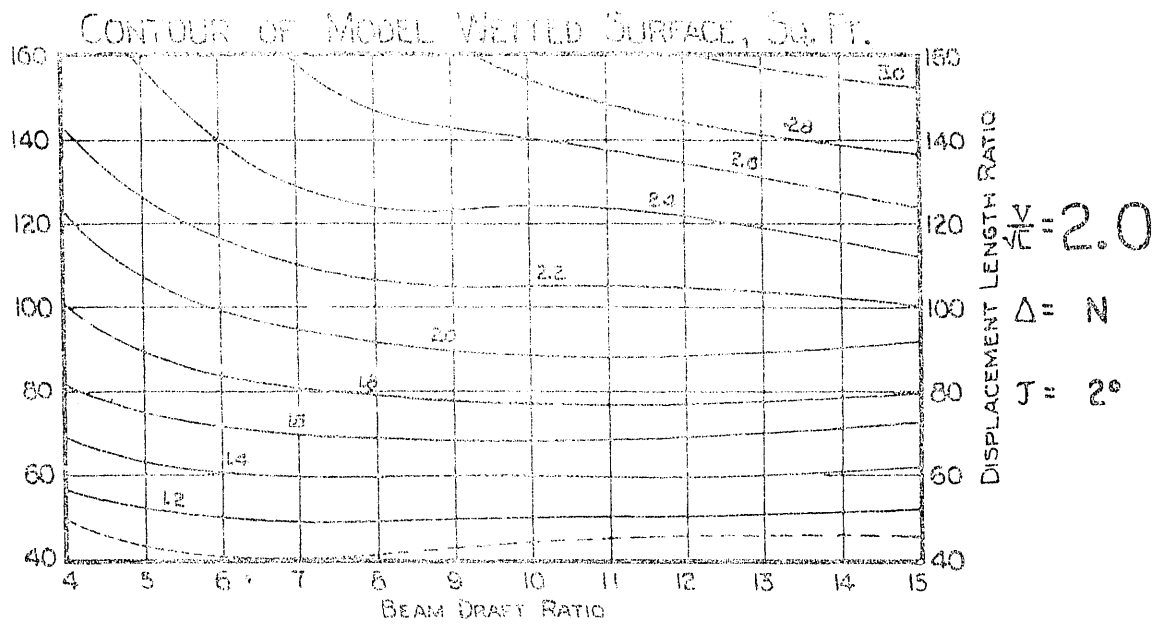
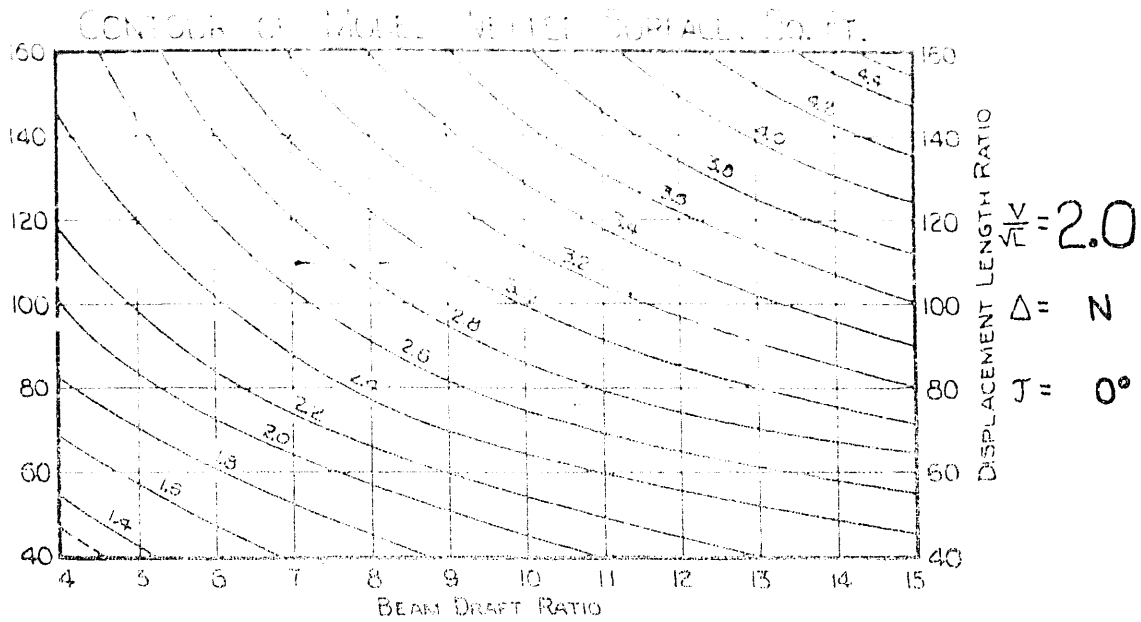


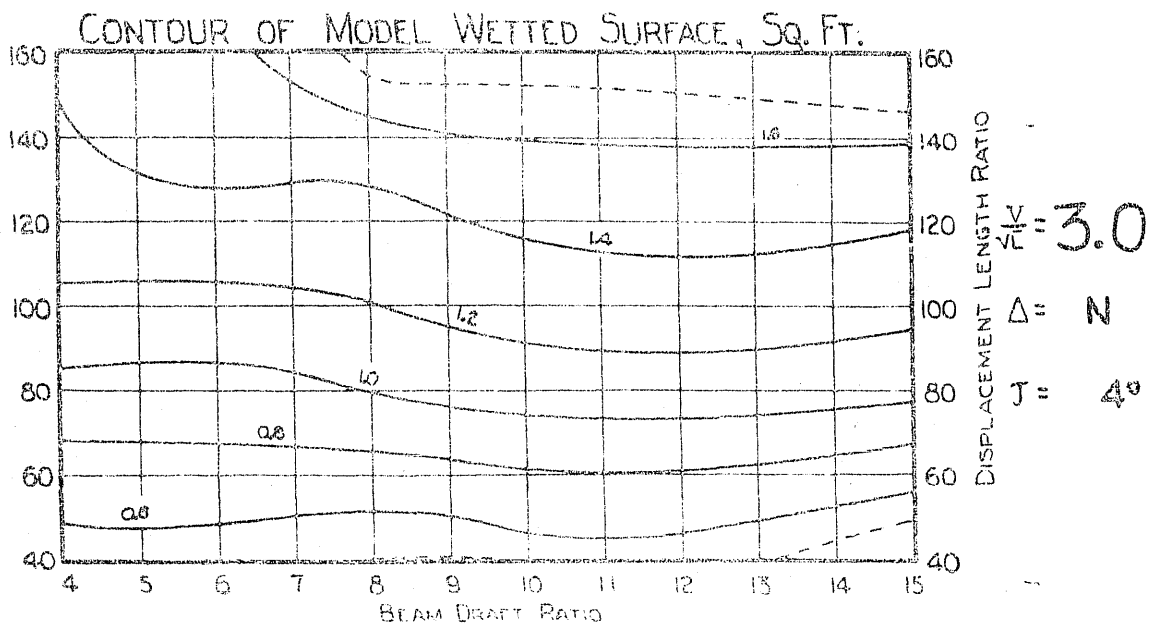
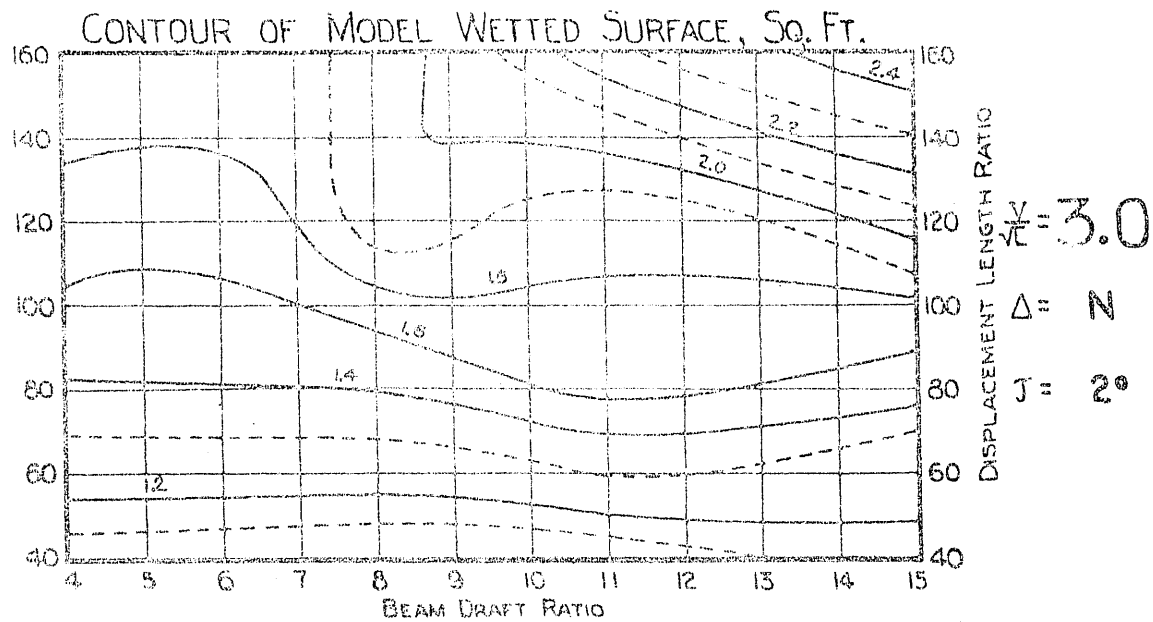
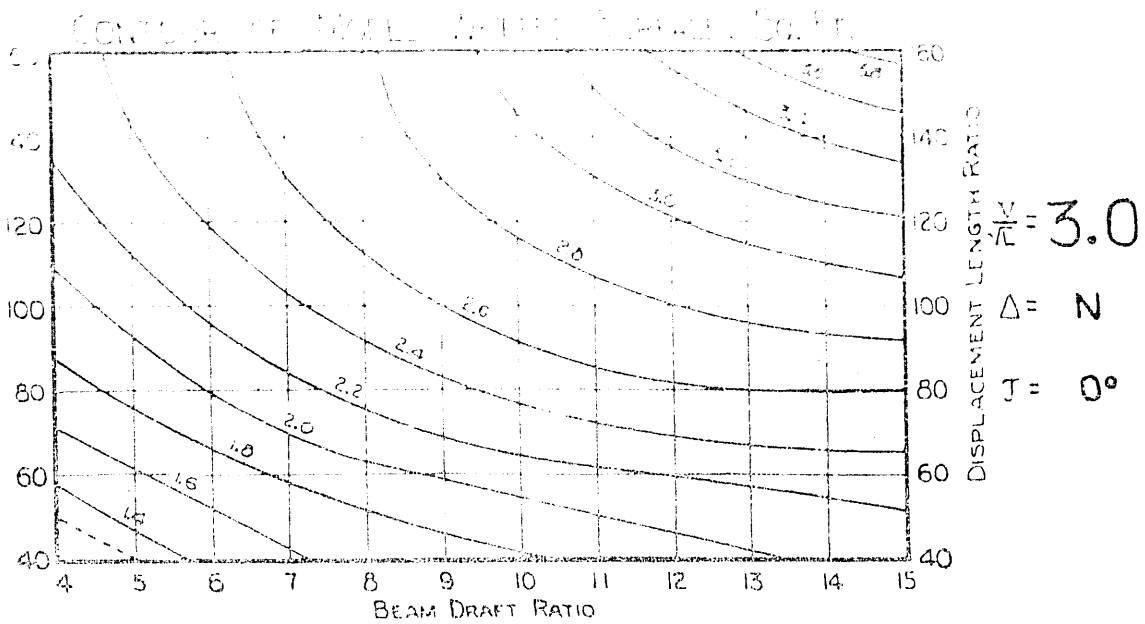


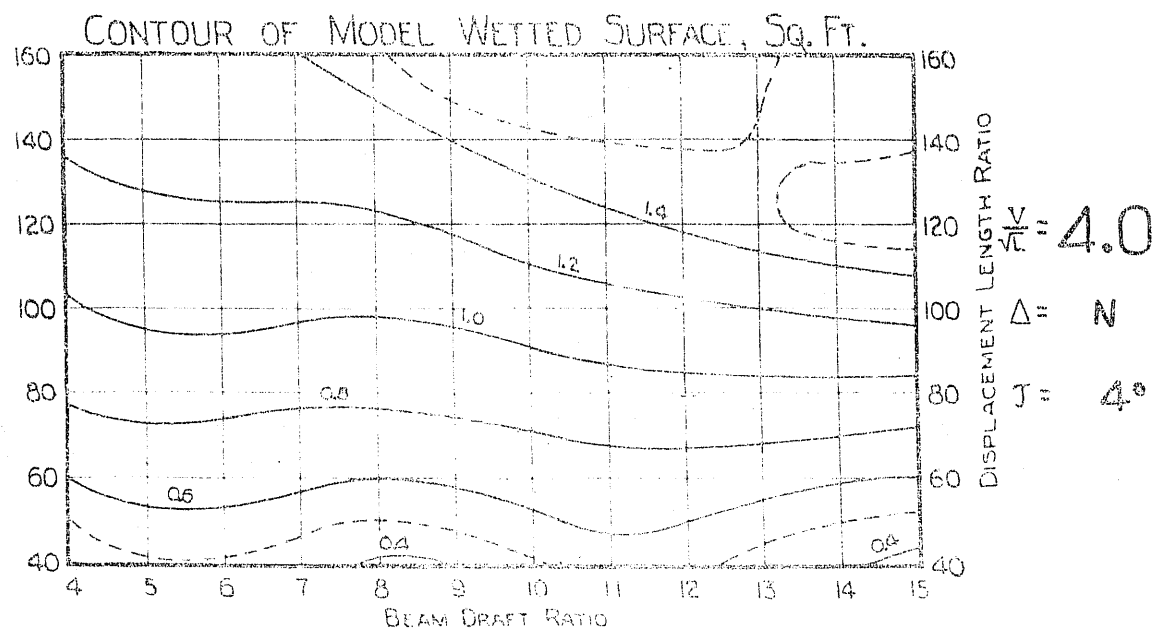
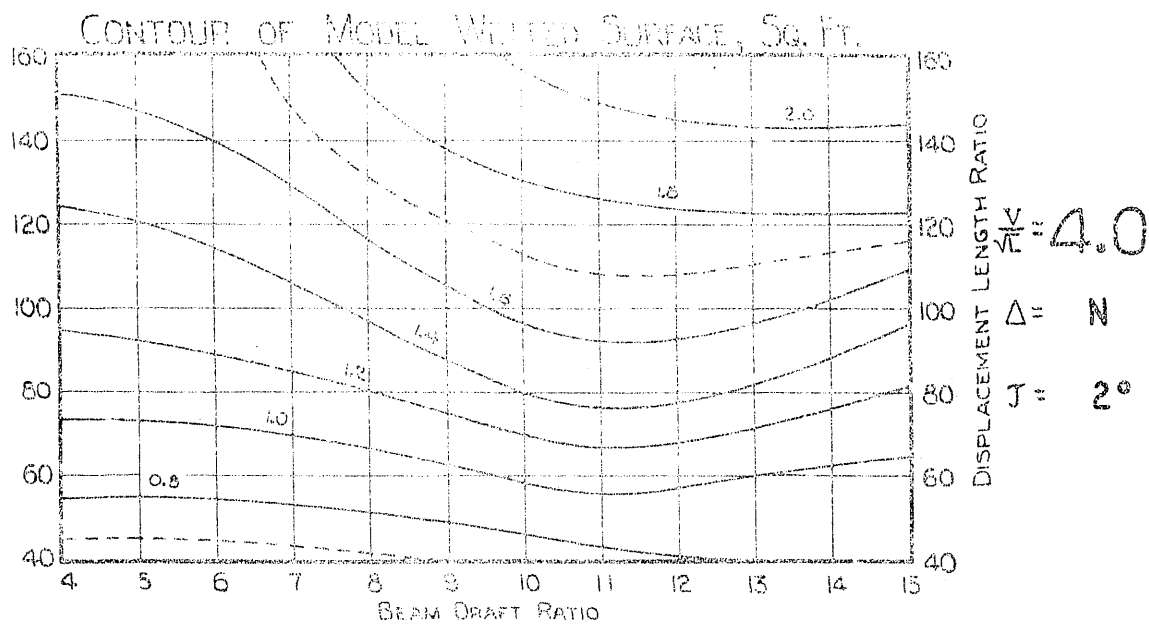
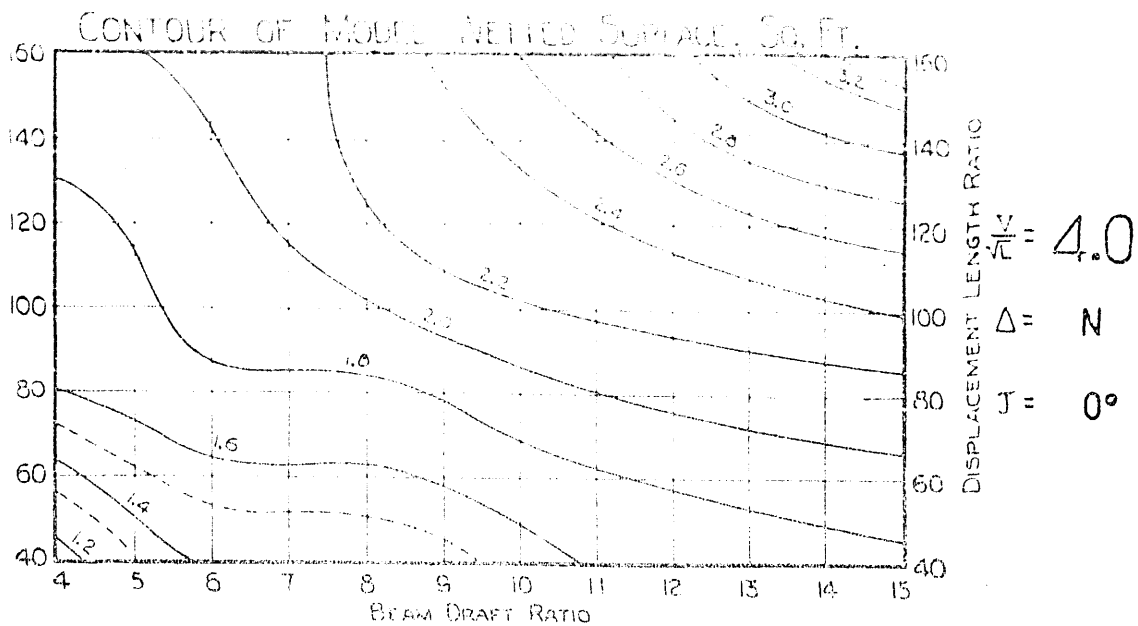
CONTOURS
OF
JETTED AREAS

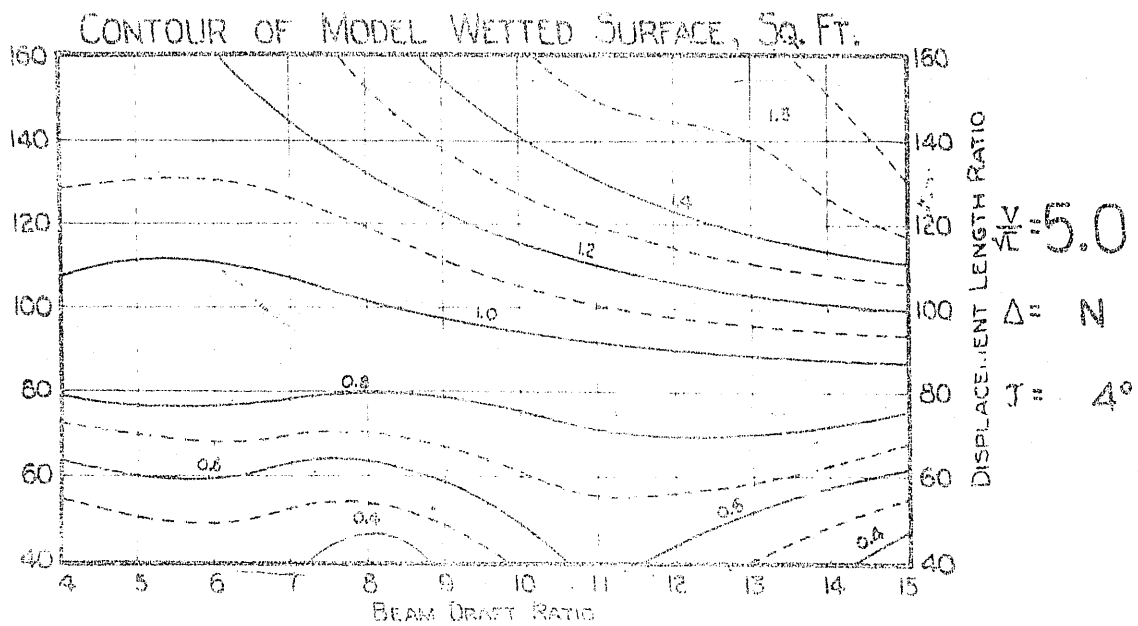
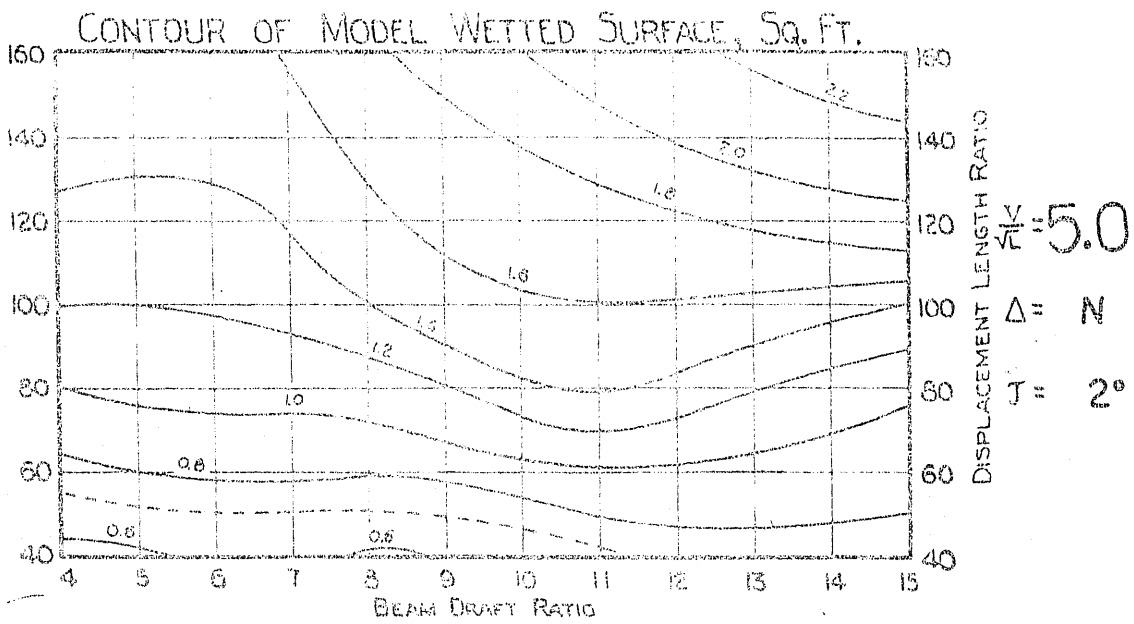
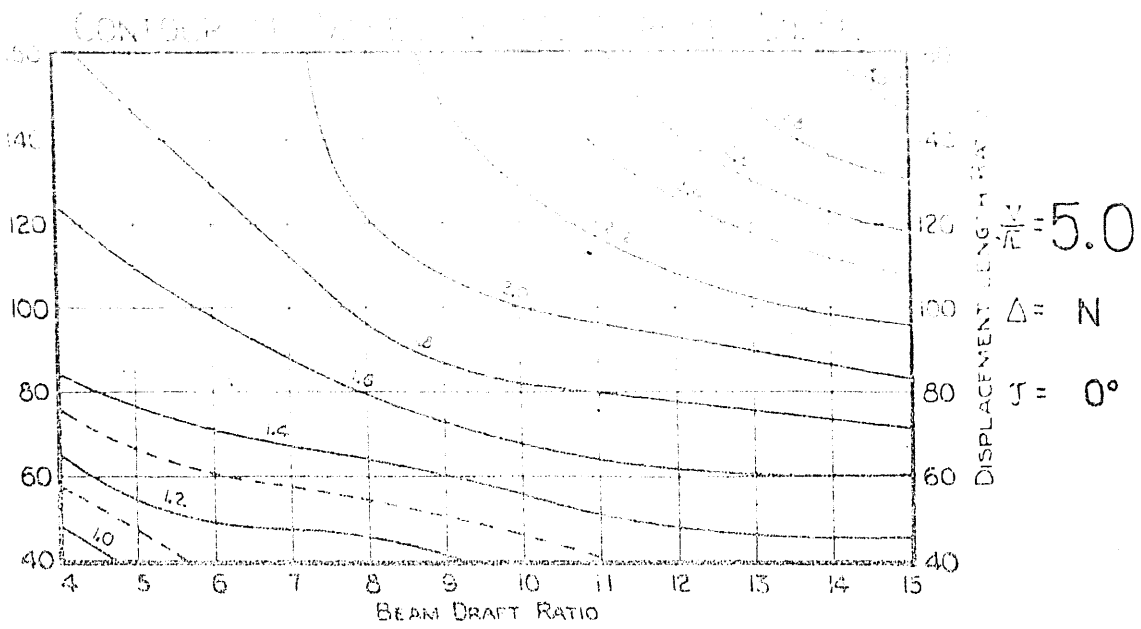
Speed-Length Ratios 2.0-6.0 in Steps of 1.0

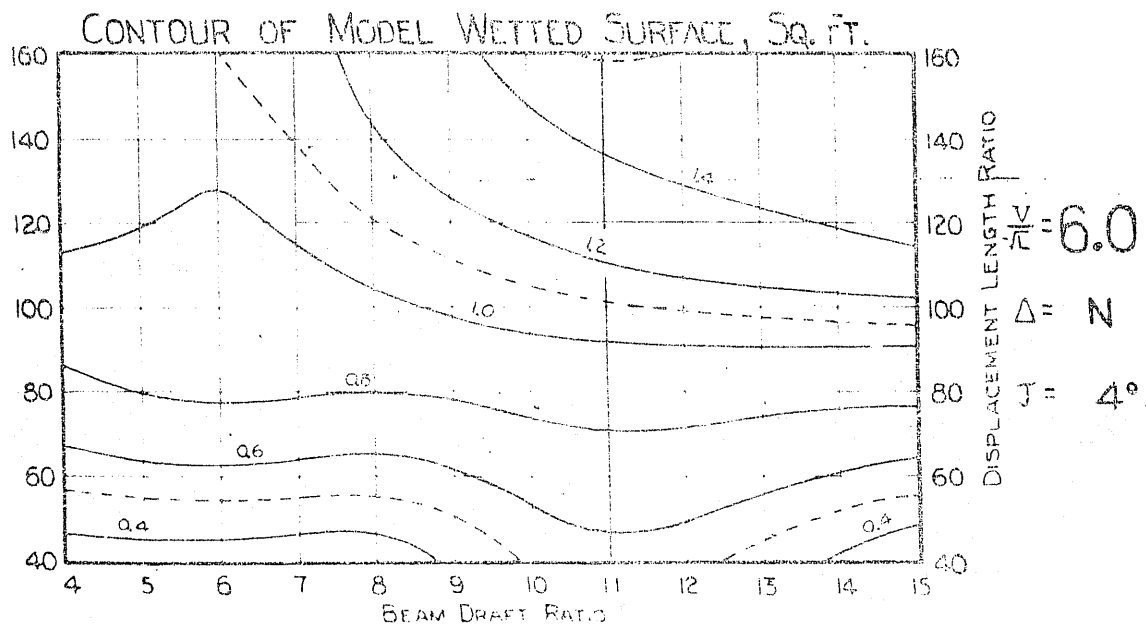
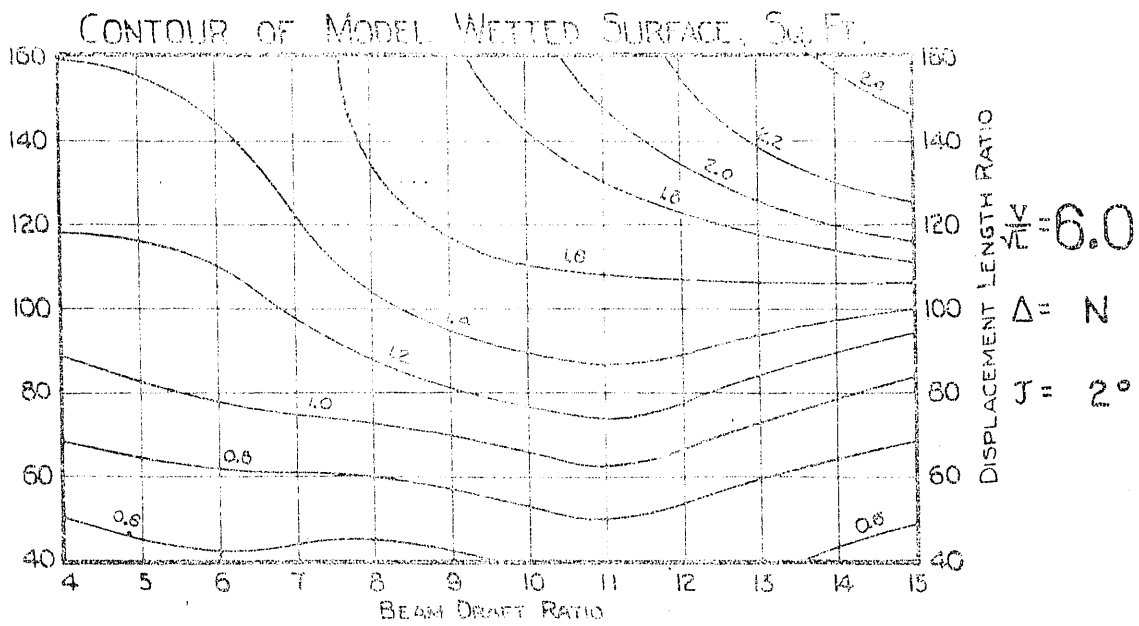
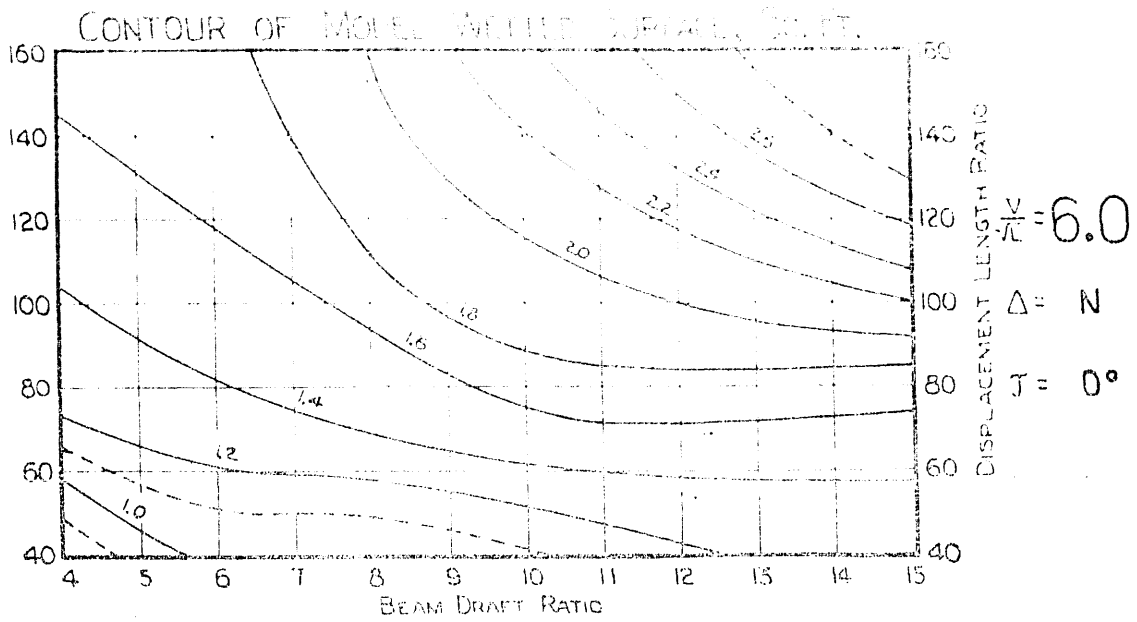
	Pages
100% Displacement (N)	85 to 89
120% " (N + 20%)	90 to 94

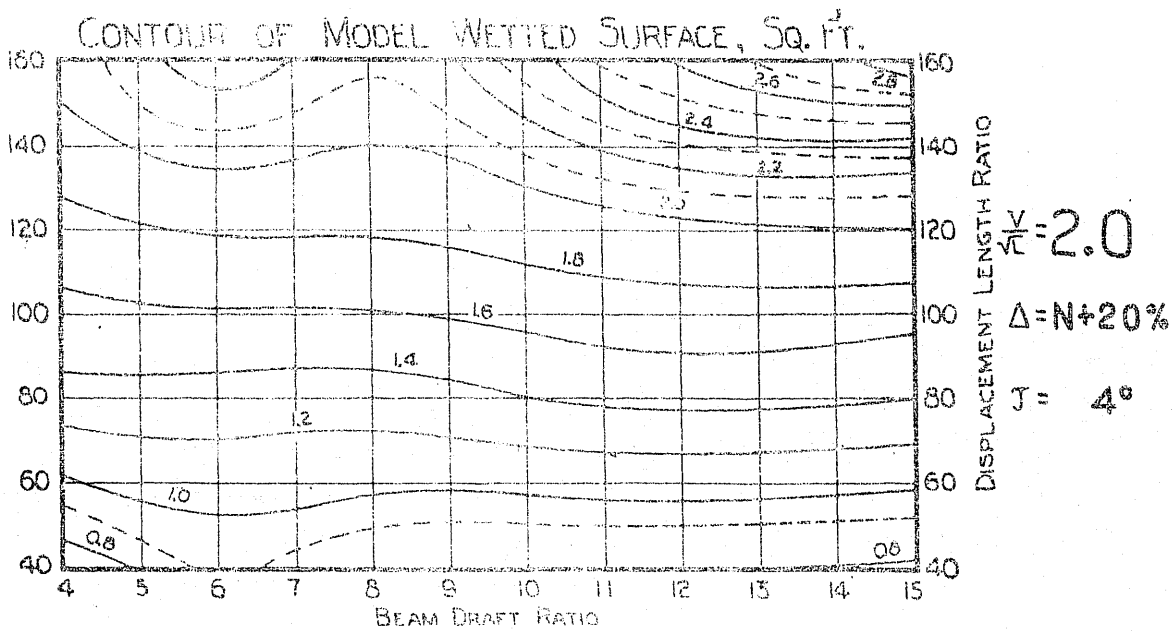
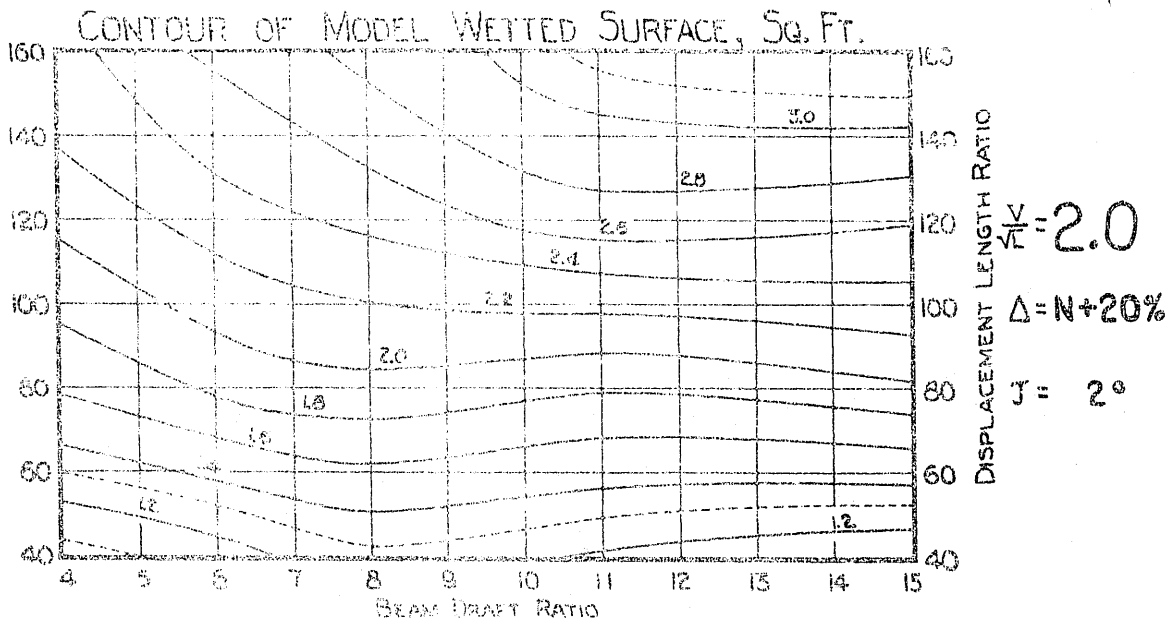
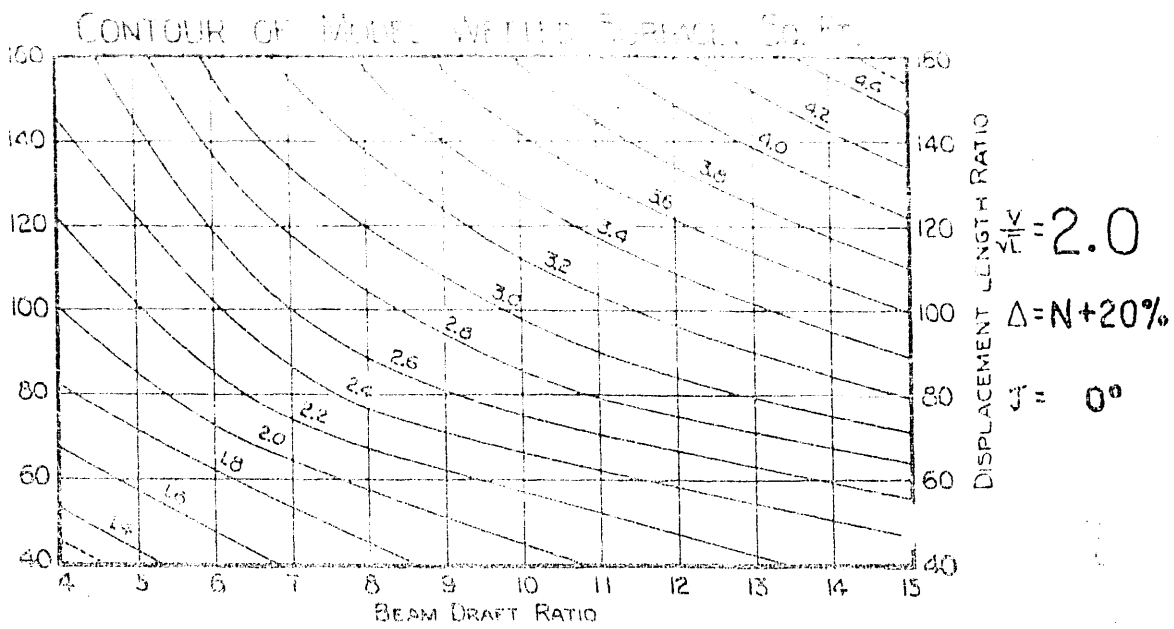


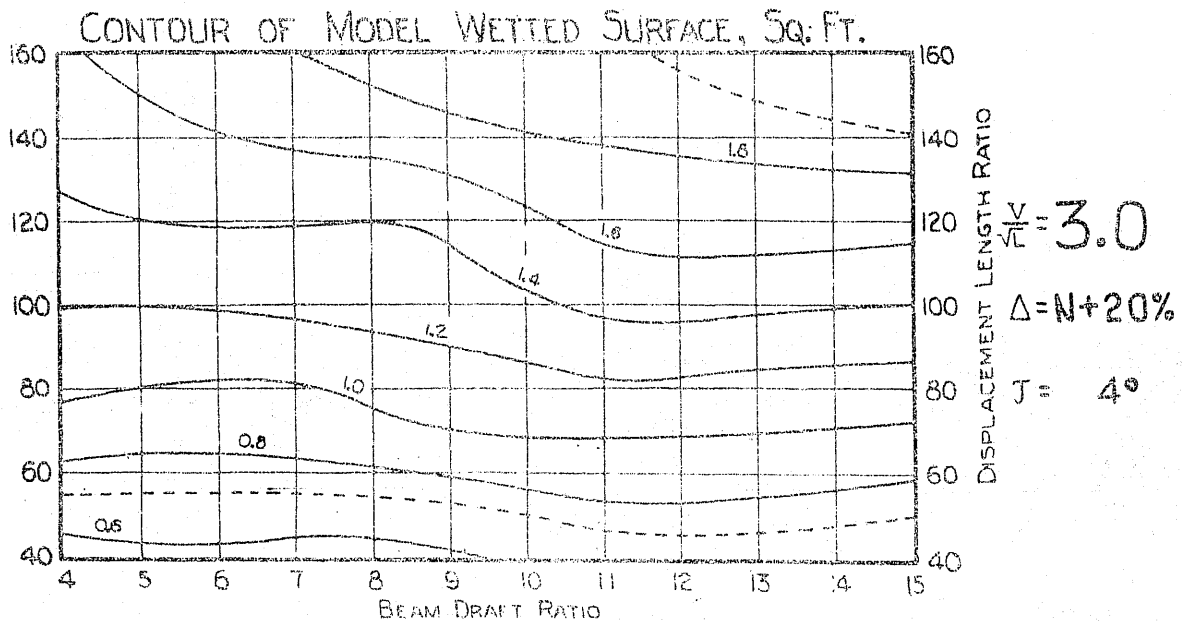
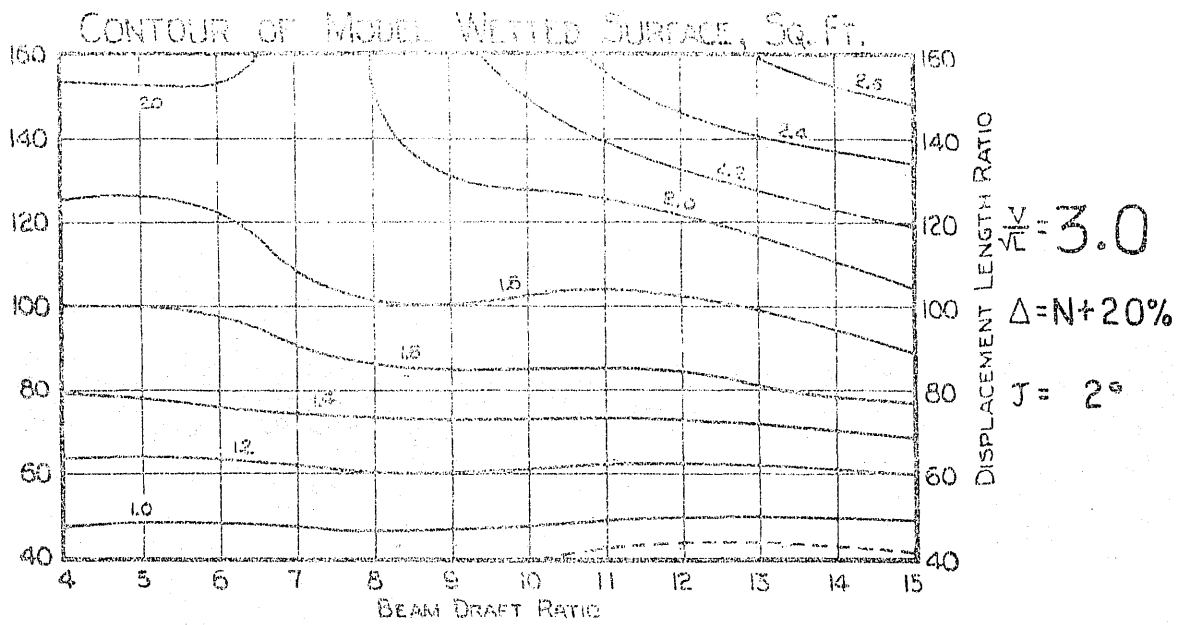
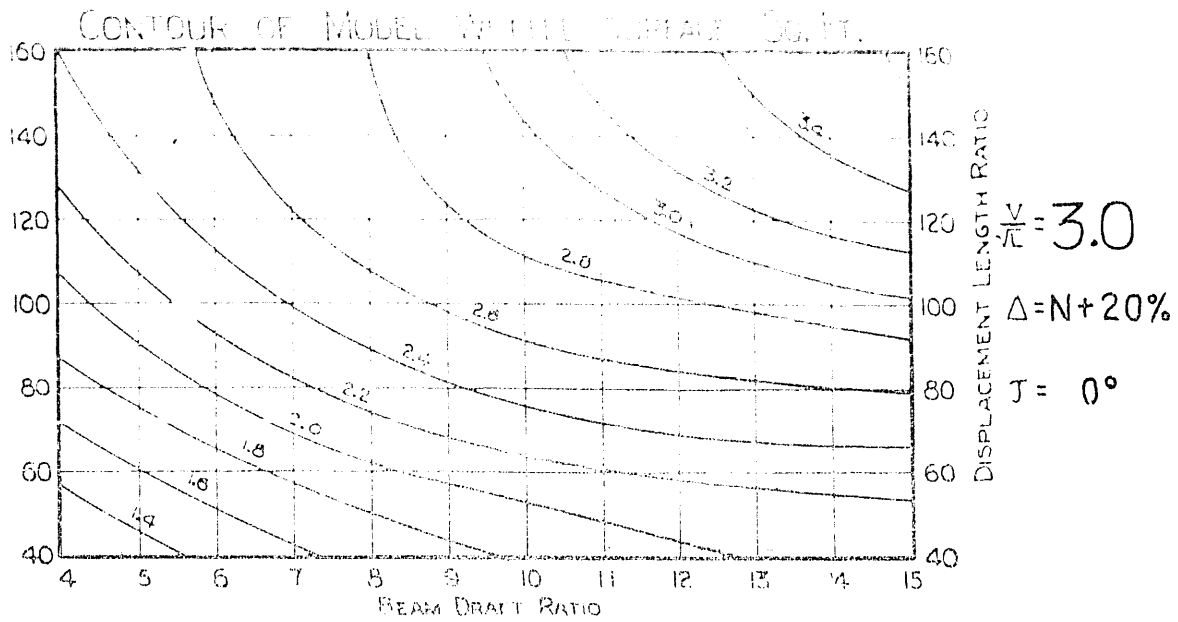


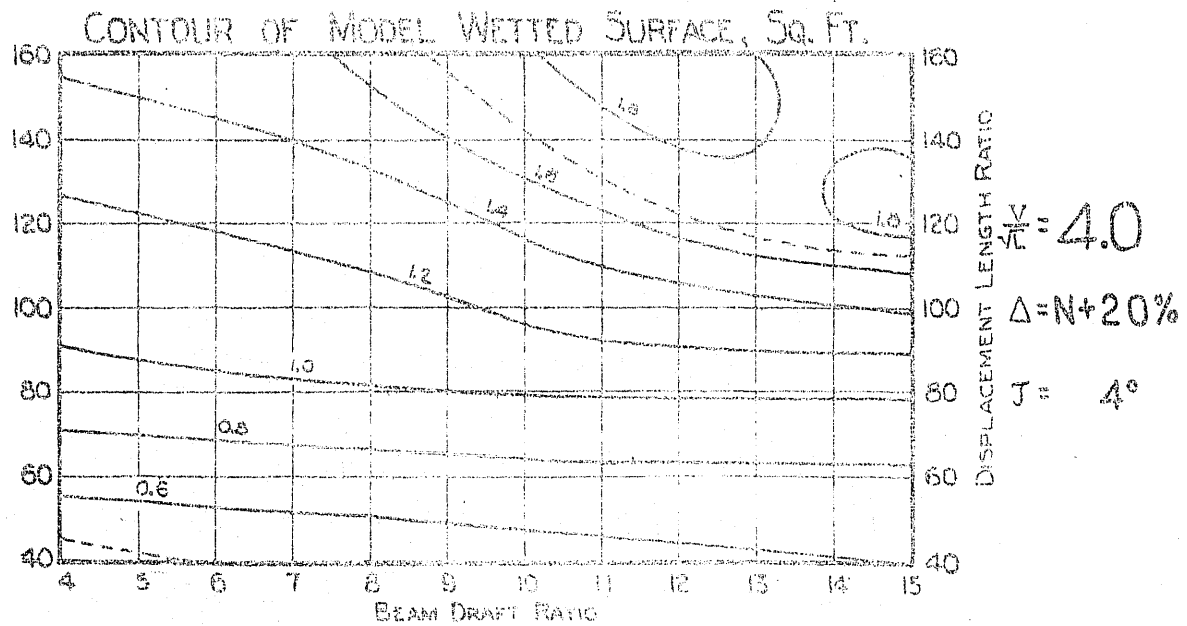
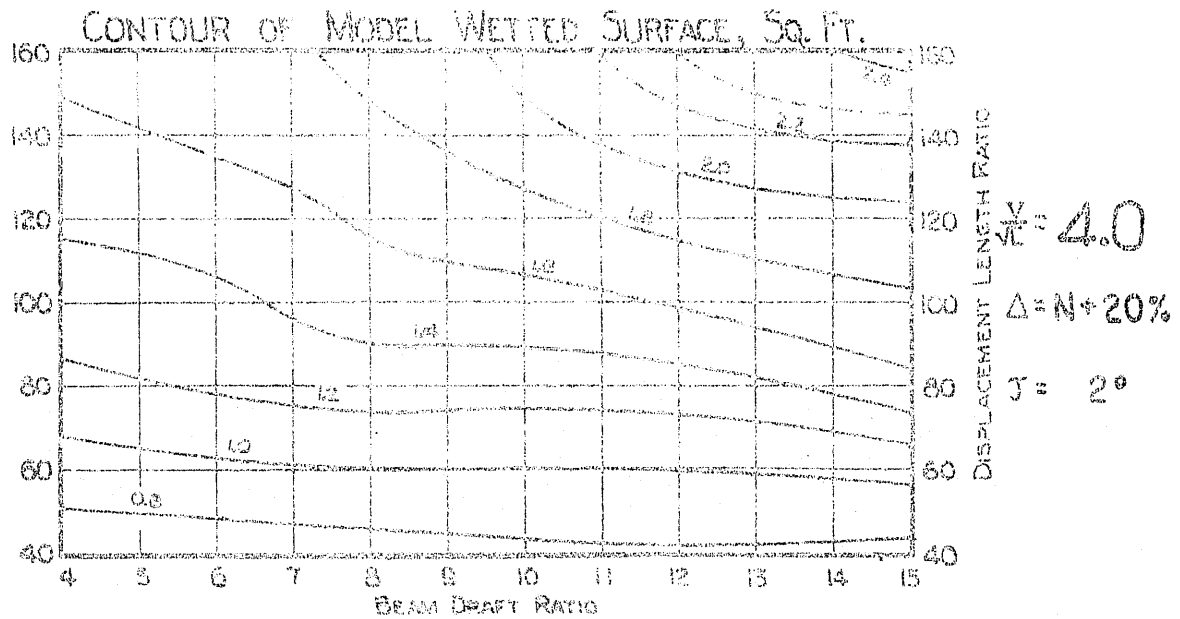
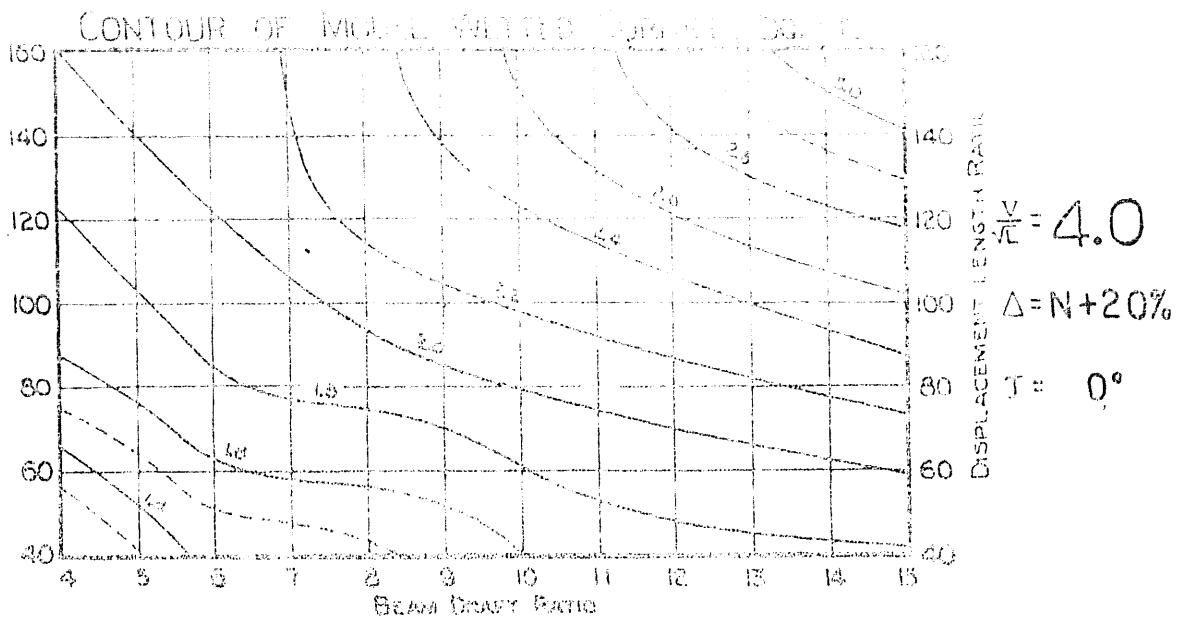


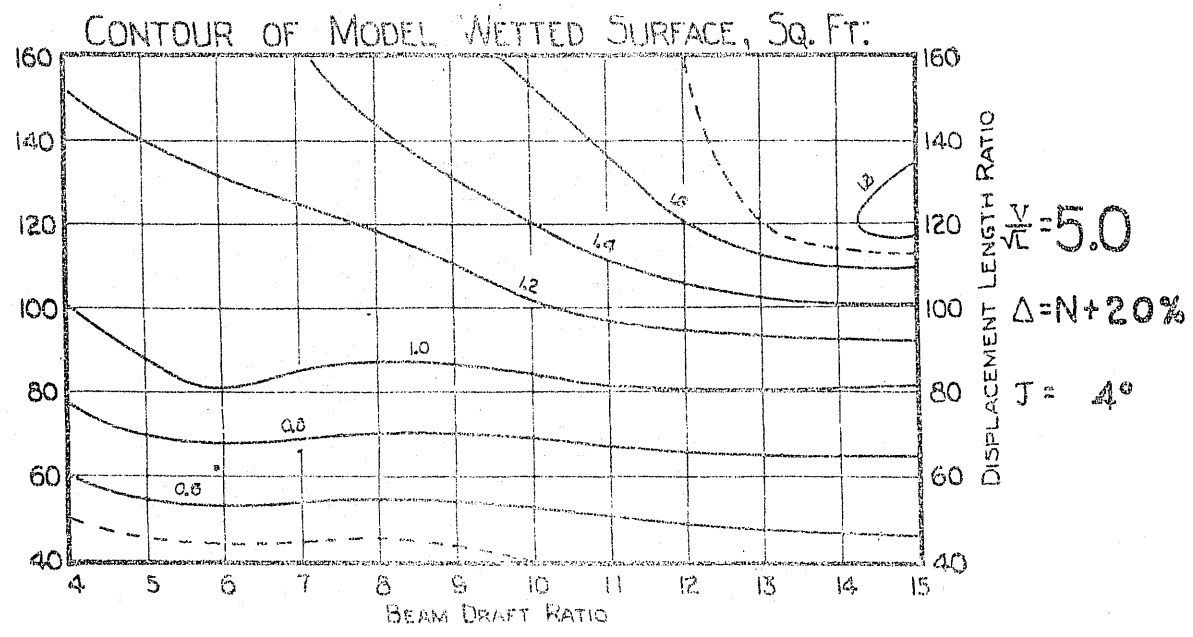
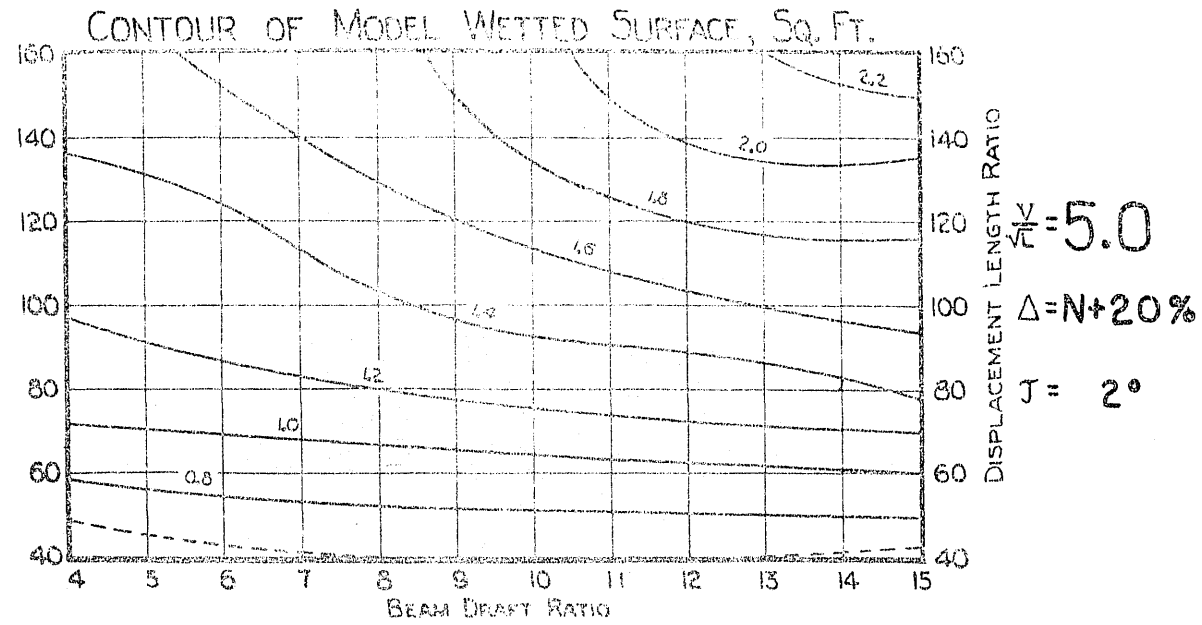
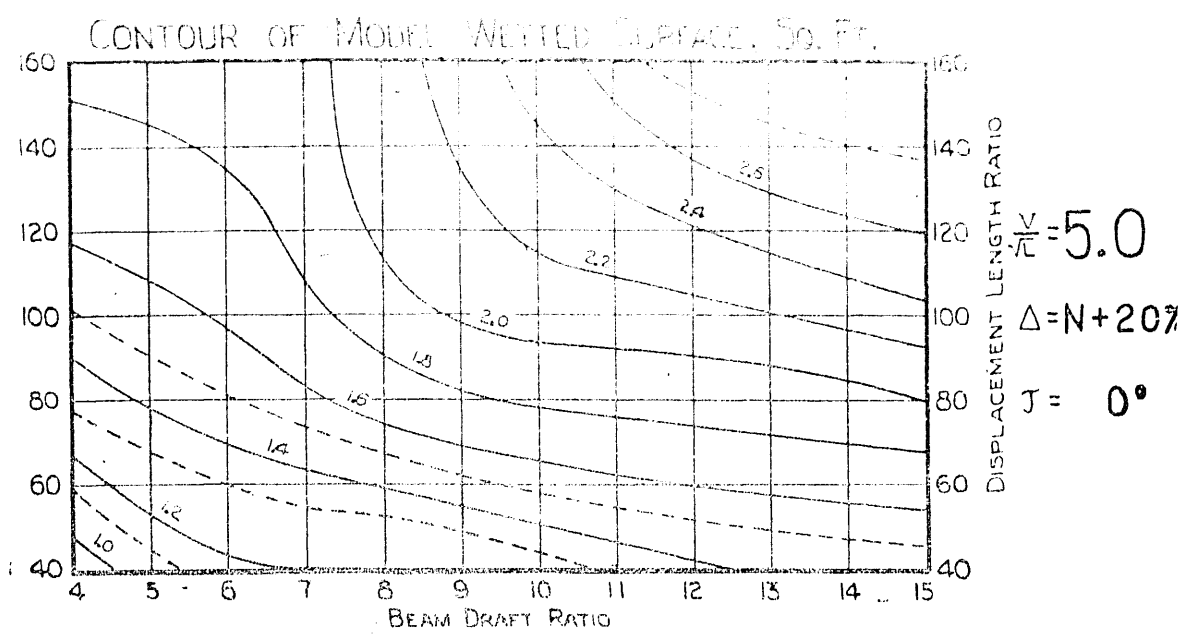


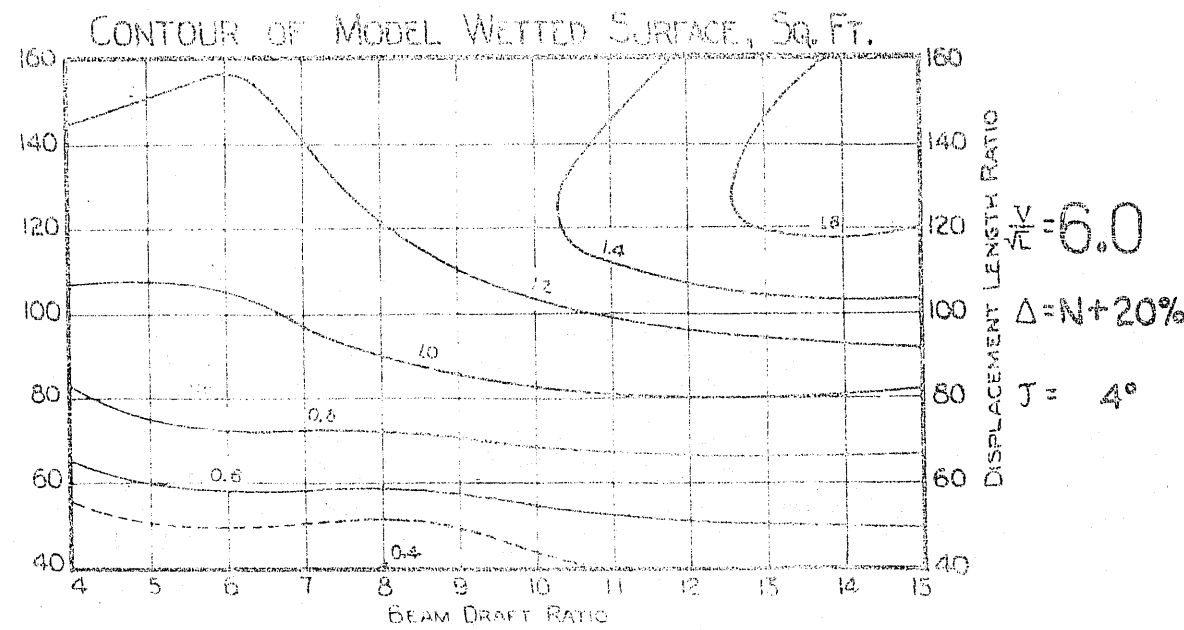
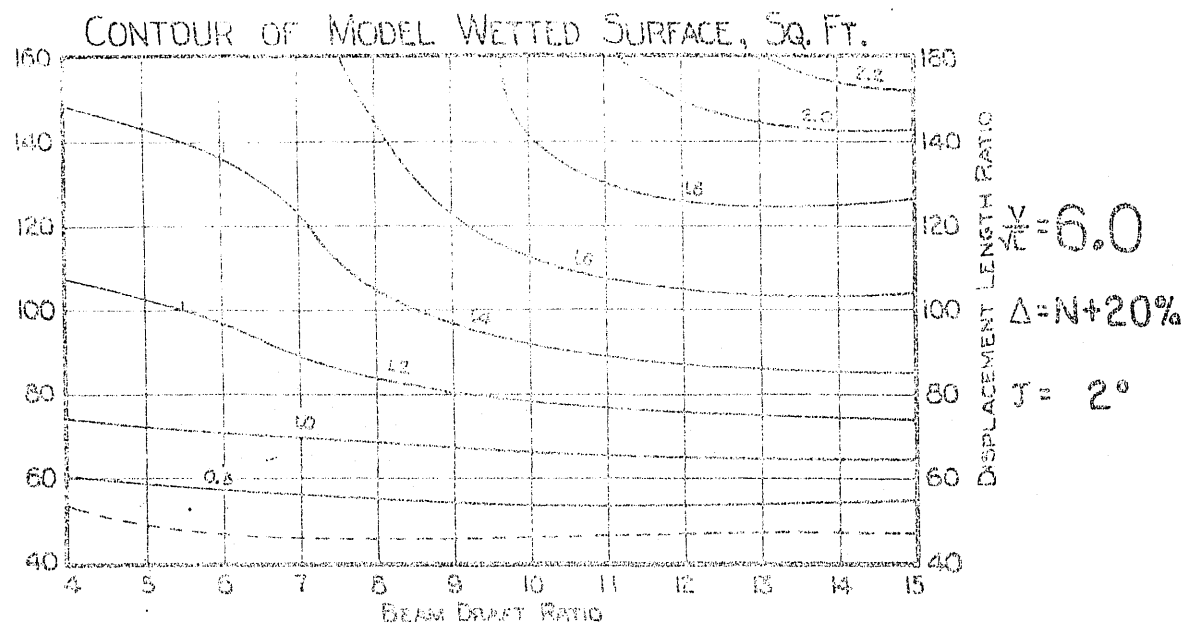
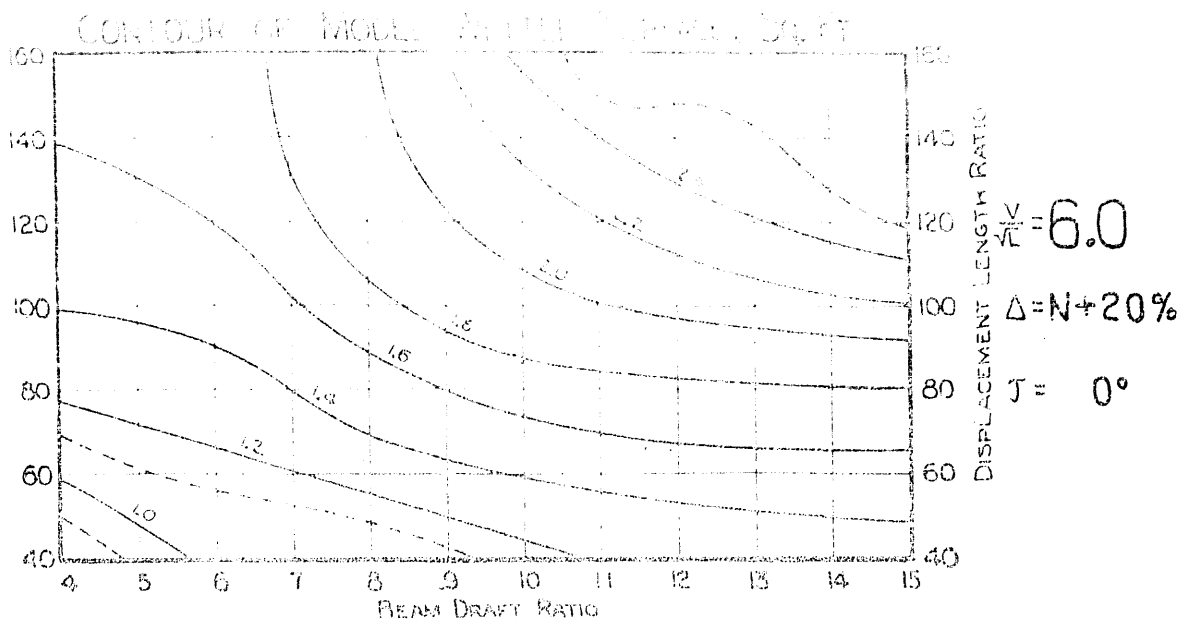






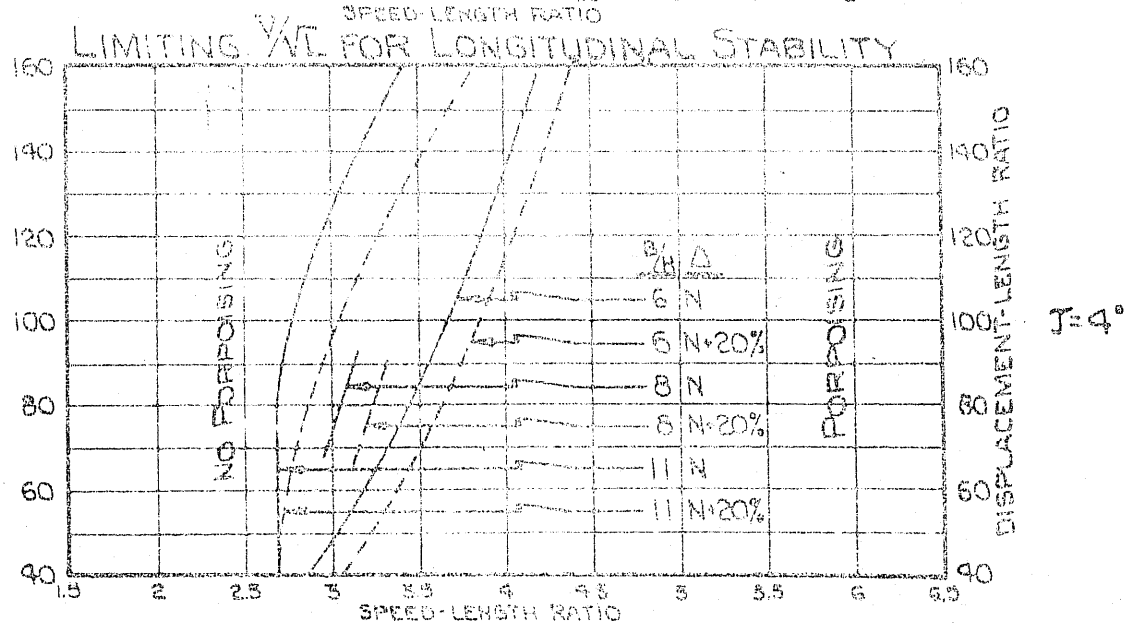
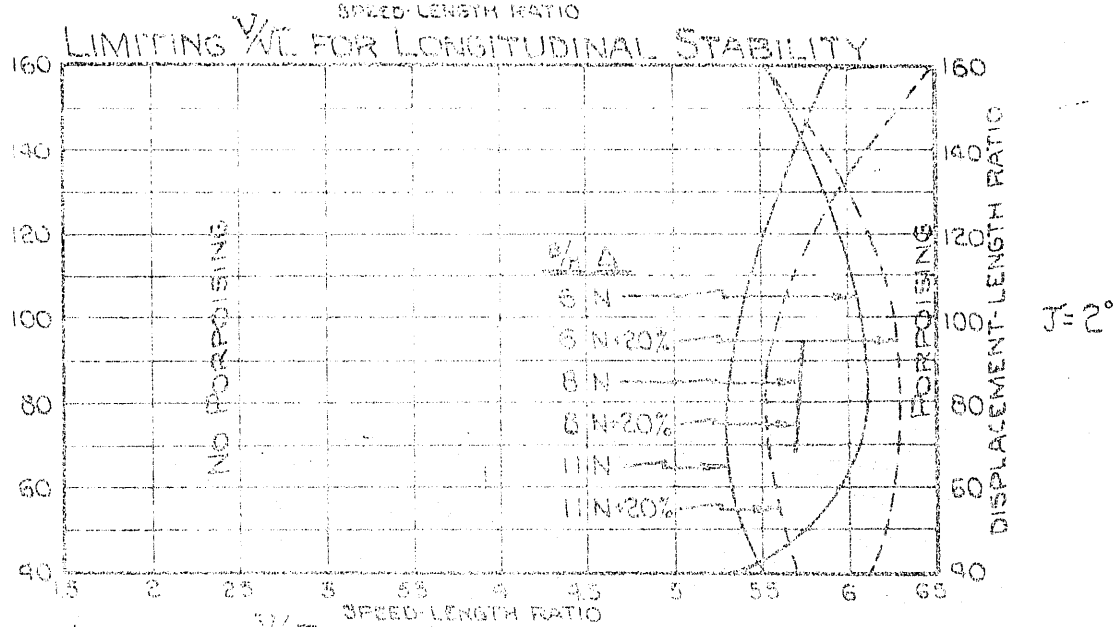
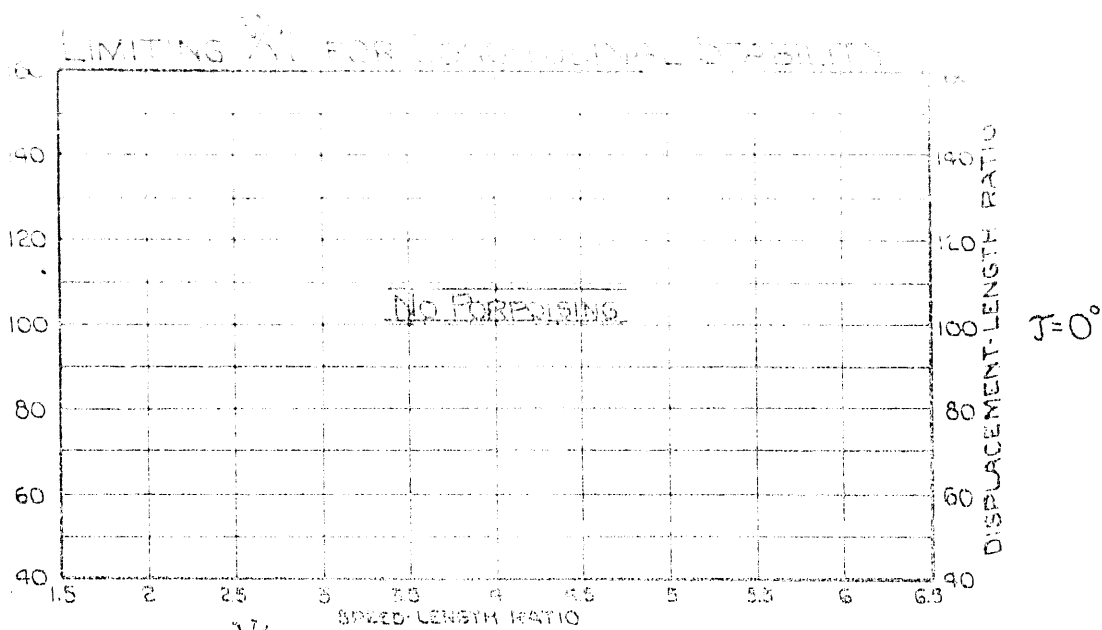






CHARTS
OF
LIMITING SPEED-LENGTH RATIO
FOR
LONGITUDINAL STABILITY
AND
CHARTS OF GRAPHICAL RECORDS
OF
PORPOISING CYCLES

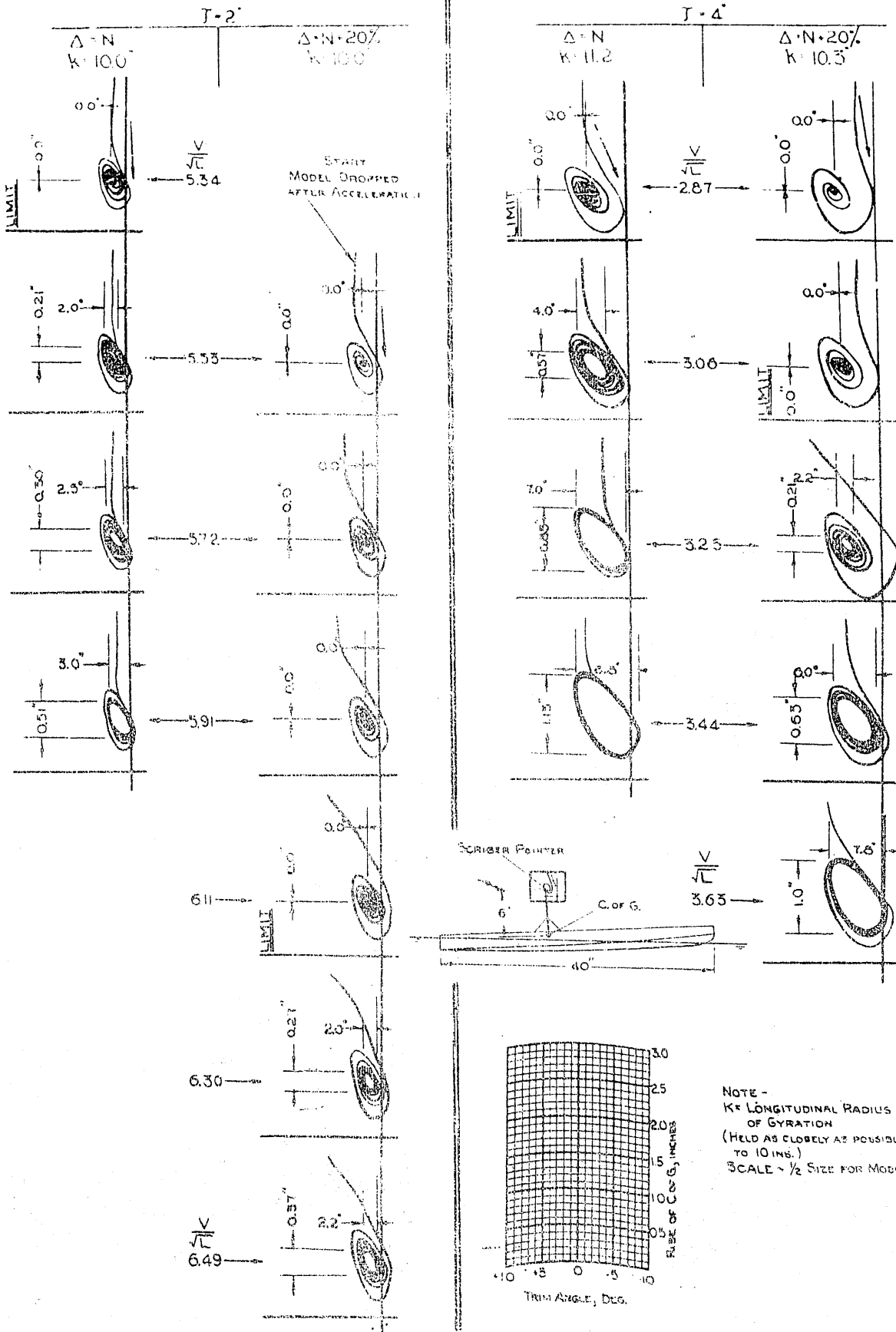
Pages
96 to 103



WORKING CHARACTERISTICS

$\frac{\Delta}{(100)} = 40$

$\frac{B}{H} = 6$

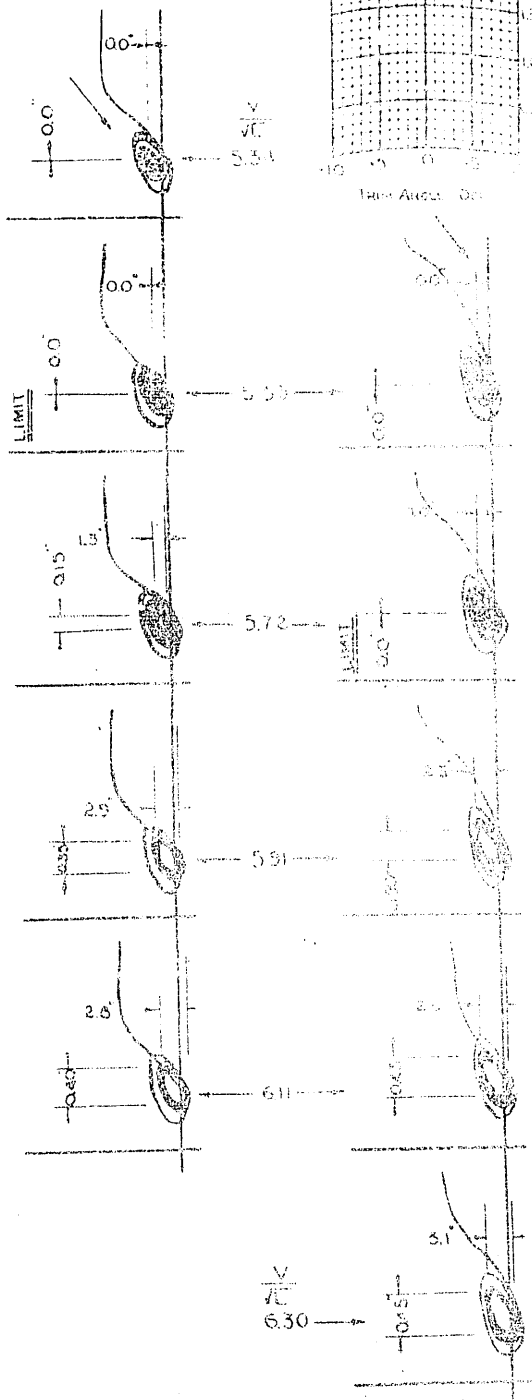
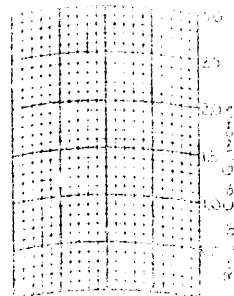


3-11
K-103

T-2

Δ·N·20%
K-103

NOTE:
LONGITUDINAL RADIUS
OF GYRATION
(HELD AS CLOSELY AS
POSSIBLE TO 0 INK)
SCALE = 1/2 SIZE FOR MODEL

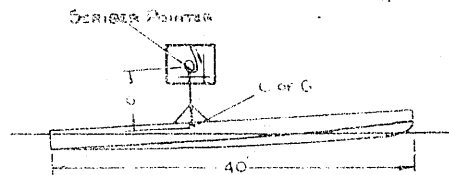
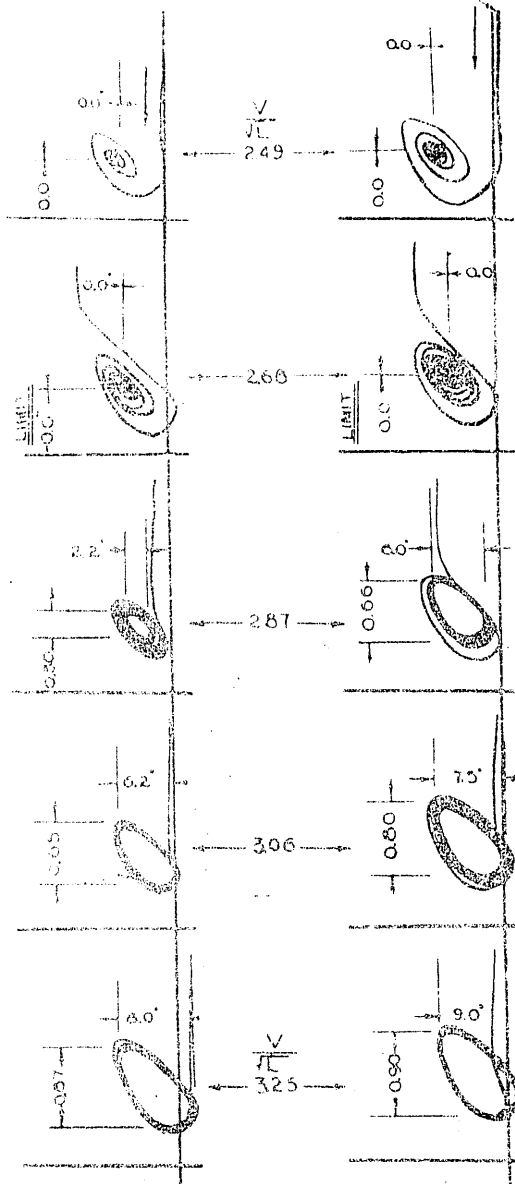


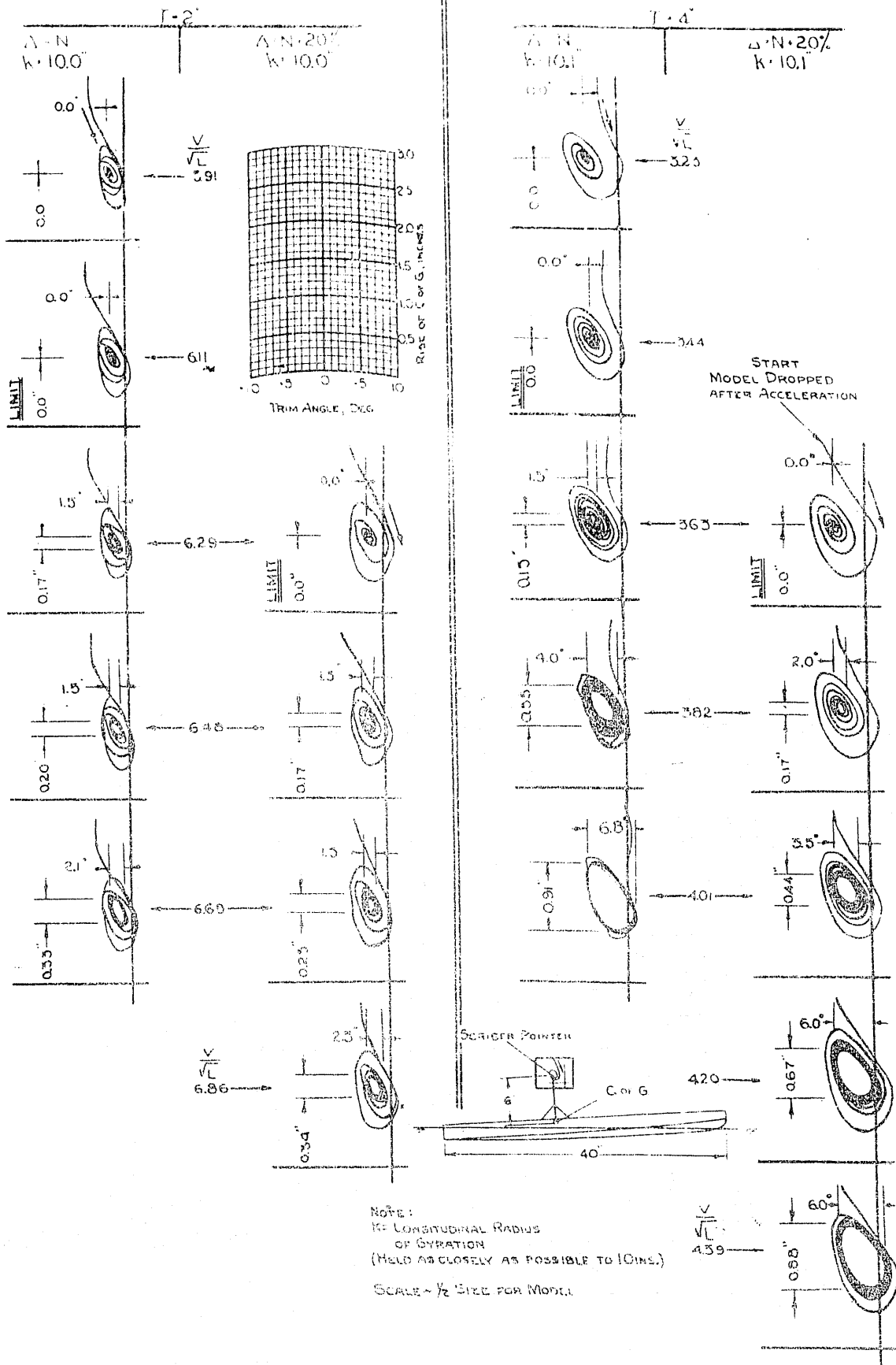
3-11
K-122

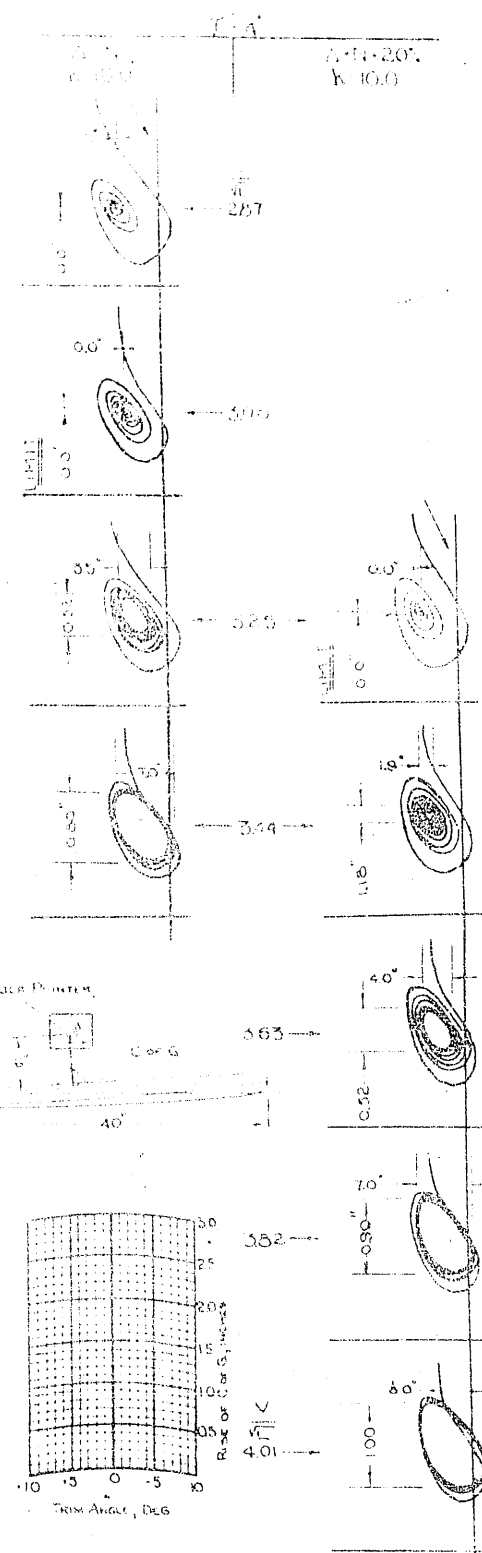
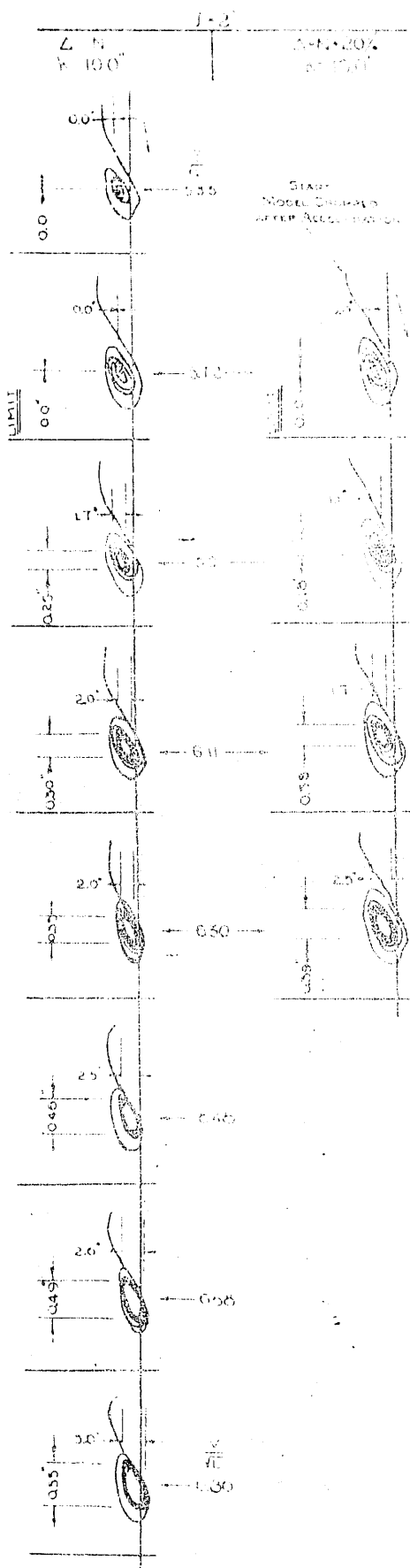
T-4

Δ·N·20%
K-101

START
MODEL DROPLET
AFTER ACCELERATION





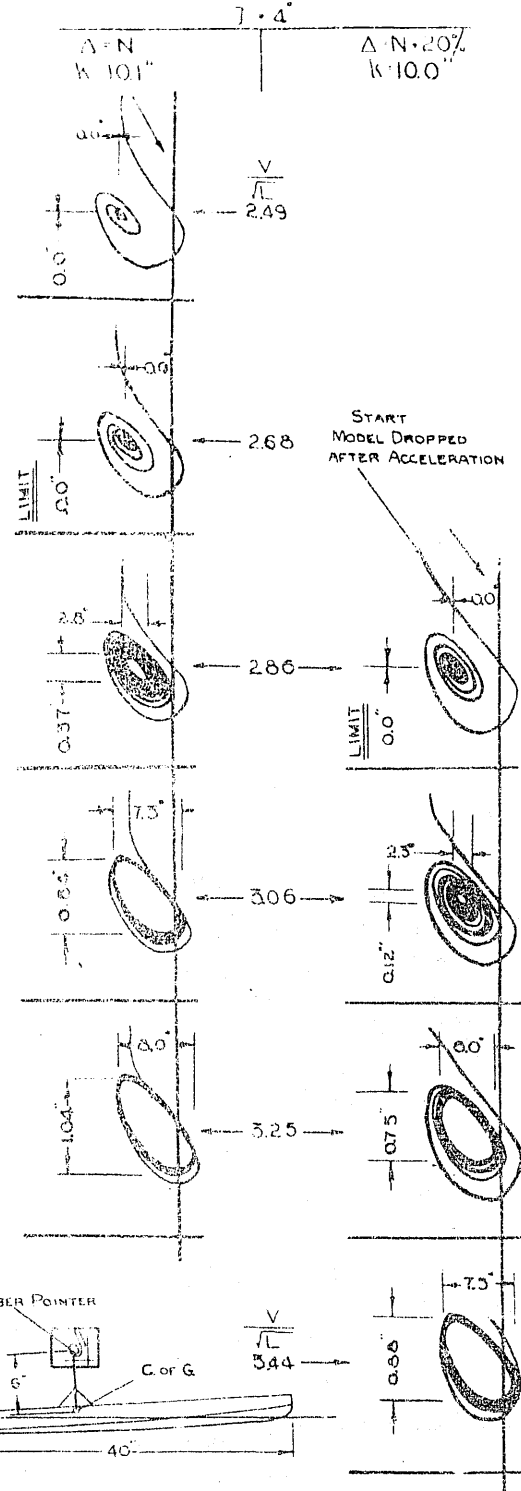
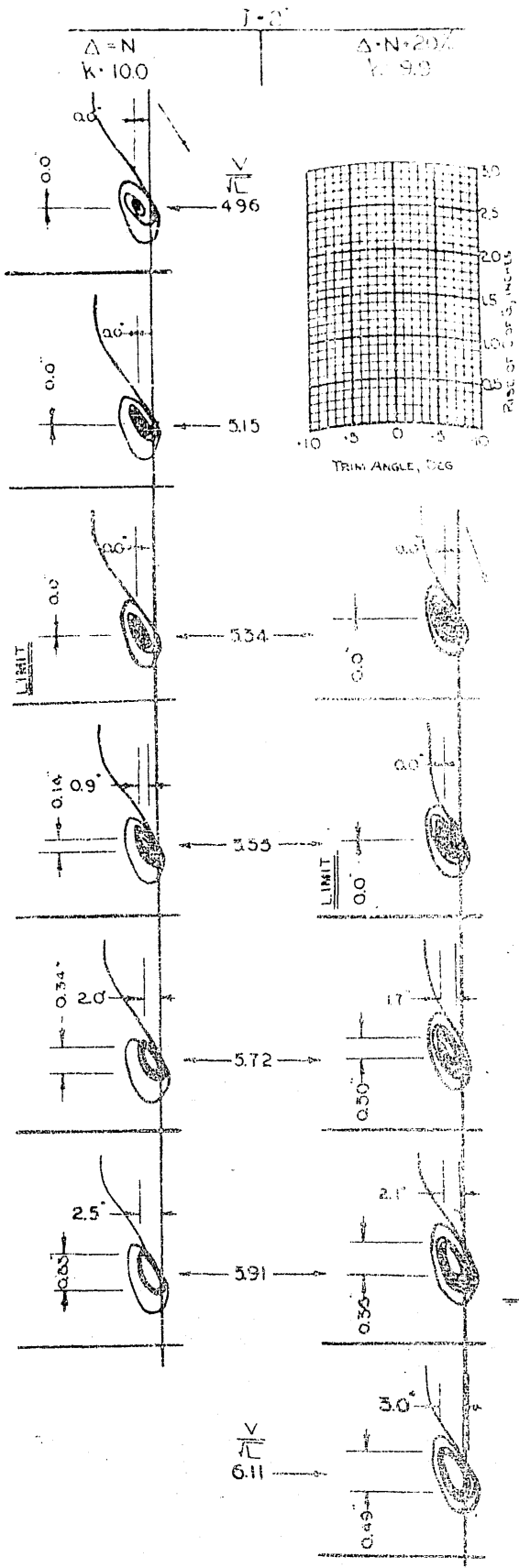


NOTE:
K = LONGITUDINAL RADIUS
OF GYRATION
(HELD AS CLOSELY AS POSSIBLE TO 10 IN.)

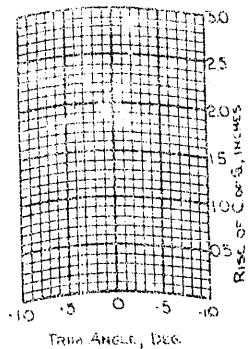
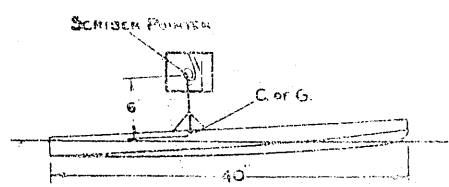
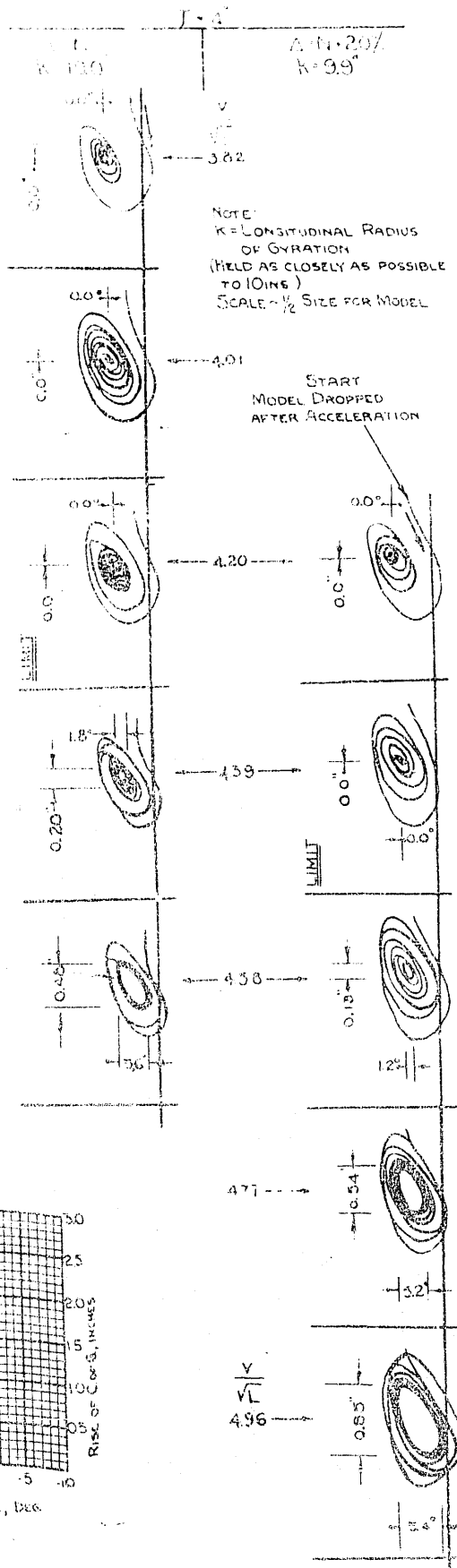
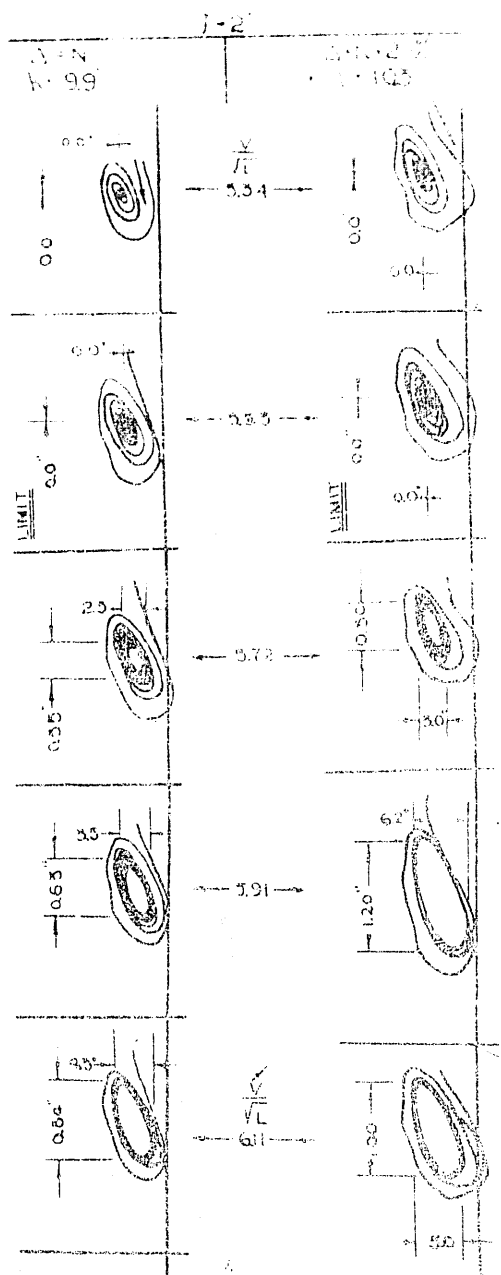
SCALE - 1/2 SIZE FOR MODEL

PORTLAND CEMENT

$\frac{9}{100} = 0.09$ $\frac{11}{100} = 0.11$



NOTE:
 K: LONGITUDINAL RADIUS
 OF GYRATION
 (HELD AS CLOSELY AS POSSIBLE TO 10 IN.)
 SCALE - 1/2 SIZE FOR MODEL



Initial Distribution for Revised Edition
of TMB Report R-47

Copies

- 8 Chief of the Bureau of Ships, Project Records (Code 362) for distribution:
 - 1 Special Assistant to Chief of the Bureau (Code 106)
 - 3 Project Records (Code 362)
 - 2 Ship Design (Code 400)
 - 2 Preliminary Design (Code 420)
- 2 Chief of Naval Research, c/o Science Technology Project, Library of Congress
- 2 Commandant, U.S. Coast Guard
- 4 Director, Experimental Towing Tank, Stevens Institute of Technology, 711 Hudson St., Hoboken, N.J.

Re-analysis of Series 50 Tests of V-Bottom Motor Boats

Michael G. Morabito¹ (M)

1. United States Naval Academy, Department of Naval Architecture and Ocean Engineering



Series 50 is the largest U.S. planing hull series. Originally developed for semi-planing PT boat type hulls, the tests were conducted in 1940-1941 and consisted of twenty 1m long models tested at nine loading conditions each and a range of speeds for a total of over 2000 test runs. The volumetric Froude numbers tested ranged from 1 to 6. The parent hull of the series has warp, rocker in the buttock lines and a tapered stern, features that are undesirable in very high speed craft, but are often necessary in the design of semi-planing hulls such as motor yachts. Analysis of all of the series data showed that the flow was not fully turbulent on all of the runs, especially conditions with wide beam and short wetted lengths. A thorough re-analysis of the data was undertaken and for runs with suspected transitional flow, the lift, wetted length and trim angle were used to determine resistance, using a modification of methods employed for prismatic planing hulls. Plots are developed showing mean wetted length and residuary resistance to weight ratio as a function of Froude number, allowing the data to be rapidly expanded to any scale ratio. Corrections for aerodynamic resistance, trim flaps and appendages are discussed, and example calculations are provided.

KEY WORDS: model testing, small craft, powering estimation, hull form, high-speed craft

NOMENCLATURE

A_P projected horizontal bottom area of chines (m²)
 $\frac{A_P}{L_P \cdot B_{PX}}$ planing area coefficient
 $\frac{A_P}{\nabla^{2/3}}$ bottom loading coefficient
 A_T section area of transom (m²)
 A_T/A_X transom area ratio
 A_X maximum section area (m²)
 A_A vertical projected frontal area for aerodynamic resistance (m²)
 B_{PA} average chine beam of planing surface (m) = $\frac{A_P}{L_P}$
 B_{PA}/B_{PX} ratio of average chine beam to maximum chine beam
 B_{PT} chine beam at transom (m)
 B_{PT}/B_{PX} ratio of transom chine beam to maximum chine beam
 B_{PX} maximum chine beam (m)
 B_{PX}/T beam-draft ratio of planing bottom
 C_{AP} centroid of planing bottom area, measured forward of the transom (m)
 $\frac{C_{AP}}{L_P}$ centroid of planing area to length ratio
 C_B block coefficient = $\frac{\nabla}{LWL \cdot B_{PX} \cdot T}$
 C_{DA} aerodynamic drag coefficient
 C_F friction coefficient
 $C_{F,EXP}$ friction coefficient derived experimentally

c_F fore-aft chord length of trim flap (m)
 C_P prismatic coefficient = $\frac{\nabla}{LWL \cdot A_X}$
 C_X max section coefficient = $\frac{A_X}{B_{PX} \cdot T}$
 C_Δ load coefficient = $\frac{\nabla}{B_{PX}^3}$
 D propeller diameter (m)
 F_∇ volumetric Froude number = $\frac{v}{\sqrt{g \nabla^{1/3}}}$
 g acceleration due to gravity (m/s²)
 $H_{1/3}$ significant wave height of the sea state (m)
 L lift component (N)
 L_C chine wetted length (m)
 L_K keel wetted length (m)
 L_M mean wetted length = $\frac{L_K - L_C}{2}$ (m)
 L_P length of planing surface (m)
 L_P/B_{PX} length-beam ratio of planing bottom area
 $\frac{L_P}{\nabla^{1/3}}$ volumetric coefficient of planing surface
 LCG longitudinal center of gravity, measured forward of the transom (m)
 $\frac{LCG}{\nabla^{1/3}}$ LCG volumetric coefficient
 LWL waterline length (m)
 P Planing hull bottom pressure (N/m²)
 R resistance component (N)
 R_F frictional resistance (N)
 $R_{F,EXP}$ frictional resistance derived experimentally (N)
 R_P pressure resistance (N)
 R_R residuary resistance (N)

R_{THULL}	total hull resistance (N)
R_{TALL}	total resistance including wind, appendages, etc (N)
S	wetted surface area - varies with speed (m^2)
S_F	athwartships span of trim flap (m)
T	draft (m)
T_P	propeller thrust(N)
T_Y	vertical component of propeller thrust (N)
T_X	horizontal component of propeller thrust (N)
V	the free stream velocity (m/s)
V_1	mean bottom velocity (m/s)
W	weight, force (N)
W_E	effective weight supported by hull (N)
$\frac{1}{2}\alpha_E$	half-entrance angle of design waterline (deg.)
β_5	midships deadrise angle (deg.)
β_{10}	transom deadrise angle (deg.)
δ	trim flap deflection (deg)
$\delta\tau$	change in trim from static(deg.)
Δ	displacement, mass (kg)
ρ	mass density of water (kg/m^3)
ρ_A	mass density of air (kg/m^3)
τ_{BL}	baseline trim angle = $\tau_O + \delta\tau$ (deg)
τ_C	average chine trim angle aft of amidships (deg.)
τ_H	equivalent hydrodynamic trim of planing surface = $\tau_{BL} + \tau_{0.25}$
τ_K	average keel trim angle aft of amidships (deg.)
τ_O	initial static baseline trim (deg.)
$\tau_{0.25}$	average quarter-buttock (hydrodynamic) trim angle aft of amidships (deg.)

INTRODUCTION

Series 50 (Davidson and Suarez, 1941) was one of the earliest and largest systematic series of planing hulls. Originally developed by the United States Experimental Model Basin and tested at Stevens Institute of Technology in 1941, the hulls were intended to explore the design space for PT boats and other small craft. With 20 models and over 180 loading conditions, Series 50 is still the most extensive planing hull standard series tested in the U.S. Having been tested at a time before most modern planing hull notation was developed, the Series 50 was presented using contour plots, similar to the original Taylor Standard Series, (Taylor, 1933) using beam-to-draft ratio, displacement-length ratio, and static trim as variables. Because of this unconventional presentation, the series is very difficult for modern planing boat designers to use. The purpose of this study is to update the original Series 50 into a format that is useful to today's designers. Using the original tabulated data (Wong and Suarez, 1941), new standard series charts are

developed and tables of faired resistance, trim and surface area data are provided for interpolation.

The hull design of Series 50 includes warp, beam taper, concave sections and buttock line rocker. These features are known to increase resistance on high speed planing craft, but are often necessary on semi-planing hulls such as sport fishing boats and motor yachts. It is difficult for designers to estimate how much of a resistance penalty will be incurred by adding these hull features. Warp, an increase in deadrise toward the bow, reduces slamming accelerations in a seaway. Rocker and beam taper reduce transom area, minimizing transom base drag at pre-planing speeds. Additionally, rocker (or alternately propeller pockets) is sometimes necessary to increase propeller tip clearance when the draft or shaft angle is limited. Chine flats, which are producible versions of concave sections, are used to deflect spray. All of these features have positive attributes but can potentially increase resistance.

MODELS AND TEST MATRIX

Series 50 consisted of twenty models of 1.02 m length derived from a single parent. The models were designed by the United States Experimental Model Basin, Washington, D.C. Variations included five beam-to-draft ratios and four displacement-length ratios. Figure 1 shows the linesplan of the parent hull.

All models had a block coefficient $C_B = 0.407$. Hulls with greater bottom loading had smaller beam to draft ratios and consequently higher deadrise. The draft can be determined as follows:

$$T = \frac{\nabla}{C_B L_P B_{PX}}$$

If non-dimensional coefficients are used, this is equal to:

$$\frac{B}{T} = C_B \frac{\left(L_P / \nabla^{1/3}\right)^3}{(L/B)^2}$$

Figure 2 shows the effect of varying beam-draft ratio on the body plans. B/T of 4, 6 and 8 represent typical patrol boat hulls. B/T of 11 and 15 are more representative of low deadrise outboard motor boats for inland lakes. Although these flatter models have unusually low freeboard, the hulls are dry above the chine during resistance tests so the lack of freeboard has no effect on resistance. The important feature of these planing hulls is the shape of the bottom below the chines, not the freeboard or flare. Figure 3, taken from Davidson and Suarez (1941) shows a photograph of all of the models in the series.

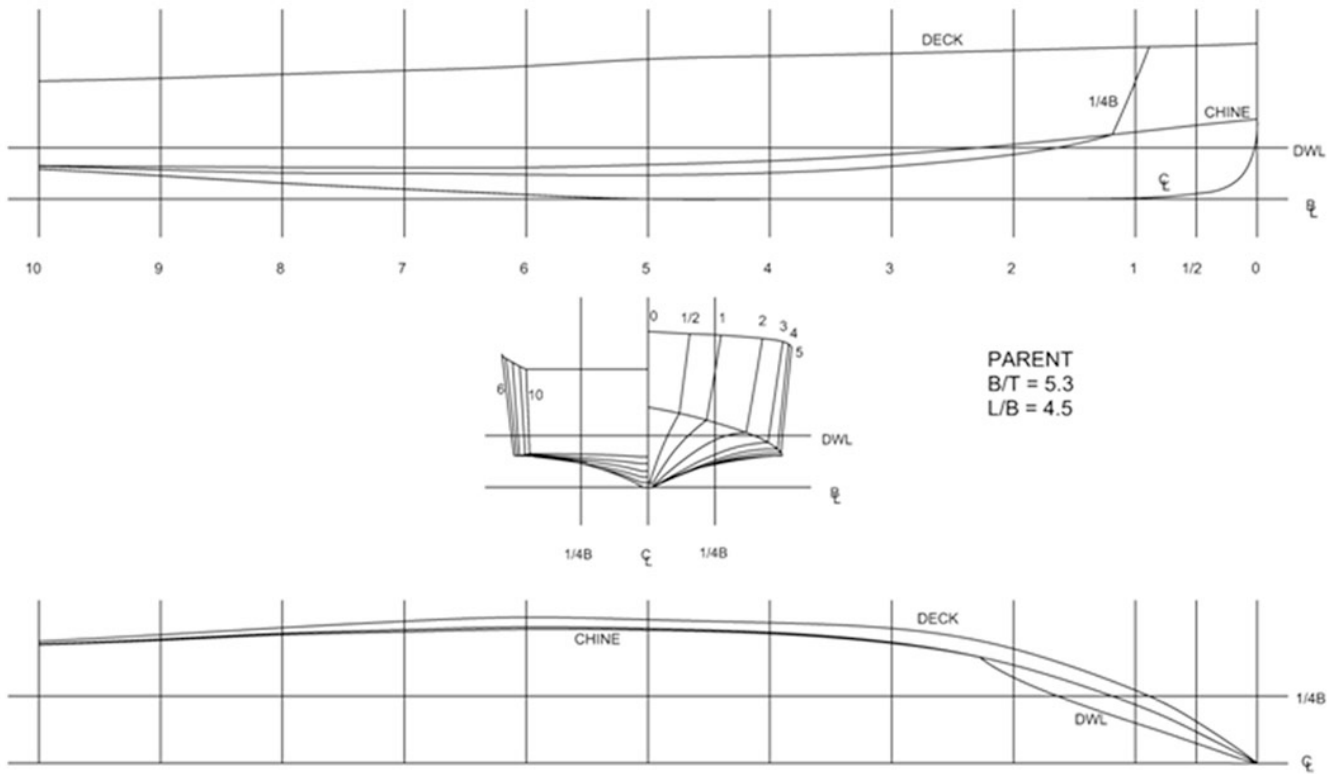


Figure 1: Linesplan of United States Experimental Model Basin Series 50 Parent Hull

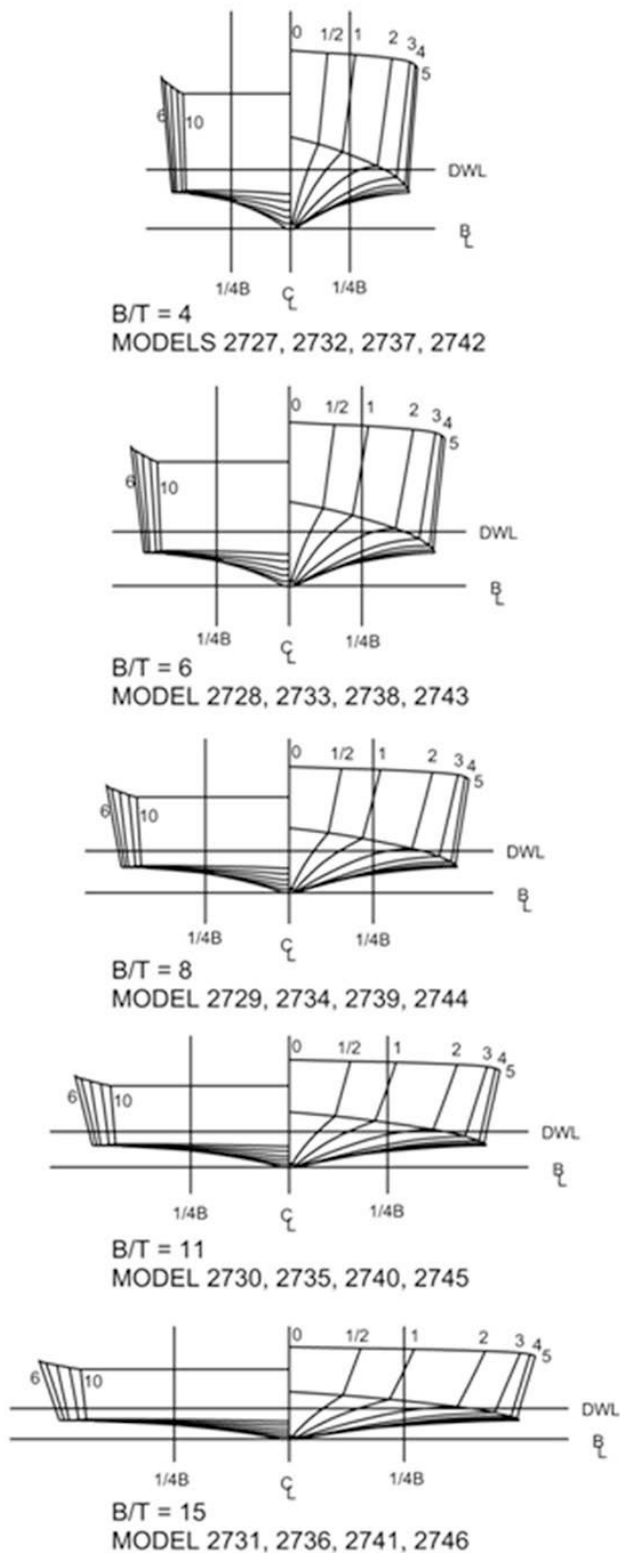


Figure 2: Body Plans of Series 50 Variants

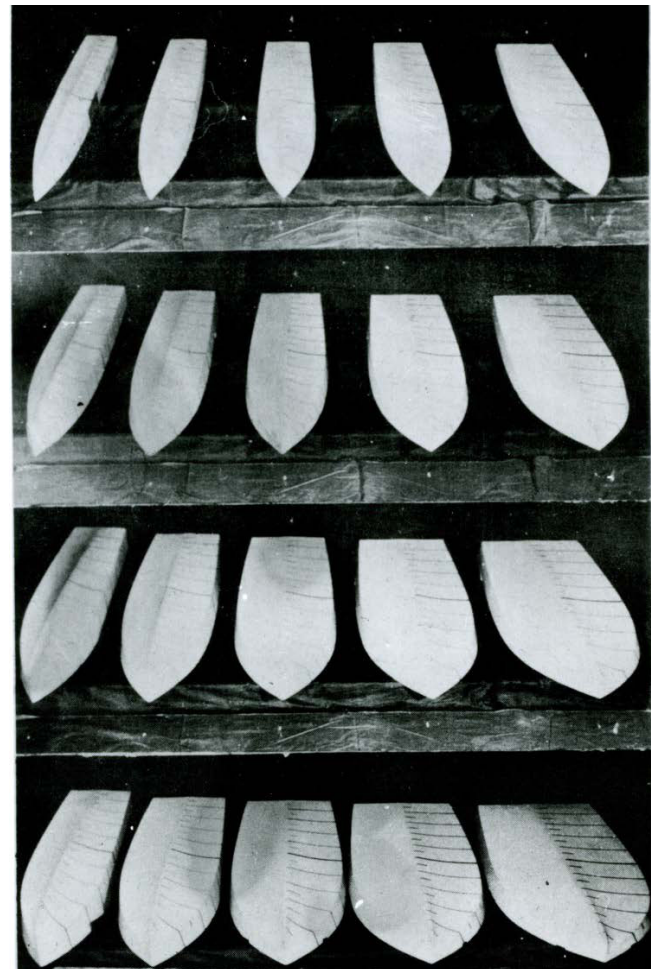


Figure 3: Photograph of U.S. Experimental Model Basin Series 50 (Davidson and Suarez, 1941)

Many of the design variables familiar to today's planing boat designers was not fully developed until the 1960's. To make this series useful to today's designers, the lines have been reanalyzed and modern planing coefficients utilized. Table 1 shows the characteristics common to all models in the series, which do not change with variations in beam-draft ratio or displacement-length ratio. Table 2 shows the table of offsets of the hull, normalized on beam and draft. Table 3 shows the characteristics of each particular hull, demonstrating the broad range of parameters tested in this series. Of particular interest is the deadrise variation. The $B/T = 4$ hulls have 20-degree deadrise at amidships, flattening aft: very typical of modern hulls. Volumetric coefficient and bottom loading have been calculated for the design load as well as 20% overload, which correspond to the extreme load cases tested.

Table 4 shows the test matrix. For each model, nine loading conditions were tested, with three initial static trim angles (0, 2, 4 degrees) and three displacements (100%, 110% and 120%). Figure 4 shows scatter plots of the range of applicability of the series, in terms of typical planing parameters: bottom loading, displacement-length ratio, displacement LCG ratio, LCG-length ratio.

Table 1: Characteristics of all Models in Series

C_B = Block Coefficient	0.407
$\frac{A_P}{L_P \cdot B_{PX}}$ = Planing Area Coefficient	0.84
$\frac{C_{AP}}{L_P}$ = Centroid of planing area to length % forward of transom	44%
B_{PT}/B_{PX} = Ratio of transom chine beam to maximum chine beam	0.88
B_{PA}/B_{PX} = Ratio of average chine beam to maximum chine beam	0.84
Location of Max Beam as a percentage of L_P from transom	42%
C_X = Max Section Coefficient = $\frac{A_X}{B_{PX}T}$	0.60
A_T/A_X = Transom Area Ratio	0.55
τ_{BL} = Baseline trim angle at design load (deg)	0
Design LCG as a percentage of L_P from transom	43.5%

Table 2: Table of Offsets and Enlargements from Parent Form

STA.	HALF-BREADTHS							DIAGONALS				HEIGHTS				
	KEEL	WATER-LINES			CHINE	DECK	1	2	KEEL	CHINE			DECK			
		1	2	3						A	B	C				
1/2	0.15	0.24	0.63	1.55	1.285	1.72	0.595	1.01	0.89	2.99				3.46	6.65	
1	0.175	0.57	1.36	2.77	2.34	2.99	1.015	1.73	0.71	1.98				3.14	6.58	
2	0.195	1.23	3.22	4.44	3.915	4.64	1.54	2.7	0.53	1.23	2.12	2.57	2.58	6.43		
3	0.22	1.77	4.83	5.28	4.8	5.415	1.8	3.235	0.46	0.985	1.705	2.095	2.22	6.29		
4	0.23	2.21	5.225	5.59	5.175	5.685	1.93	3.575	0.485	0.92	1.5	1.835	1.99	6.14		
5	0.235	2.54	5.345	5.71	5.28	5.78	1.98	3.77	0.57	0.9	1.405	1.7	1.83	6		
6	0.24	2.61		5.67	5.24	5.73	1.95	3.84	0.73	0.975	1.39	1.645	1.765	5.86		
7	0.24	2.32		5.54	5.13	5.57	1.81	3.785	0.94	1.125	1.46	1.665	1.745	5.71		
8	0.24	1.68		5.34	4.995	5.35	1.61	3.7	1.17	1.31	1.55	1.705	1.765	5.57		
9	0.24	0.24		5.08	4.82	5.075	1.325	3.525	1.44	1.535	1.68	1.775	1.81	5.42		
10	0.24			4.81	4.63	4.81	0.985	3.28	1.73	1.775	1.835	1.865	1.865	5.28		

Model	Enlargement	
	Beam	Draft
2727	0.4444	0.5765
2728	0.5441	0.4705
2729	0.6280	0.4075
2730	0.7365	0.3475
2731	0.8600	0.2976
2732	0.6282	0.816
2733	0.7695	0.6655
2734	0.8887	0.577
2735	1.0420	0.4916
2736	1.2177	0.4213
2737	0.7694	0.9989
2738	0.9431	0.816
2739	1.088	0.7063
2740	1.276	0.6022
2741	1.49	0.5158
2742	0.8884	1.1535
2743	1.0884	0.942
2744	1.257	0.8159
2745	1.474	0.6958
2746	1.722	0.5958

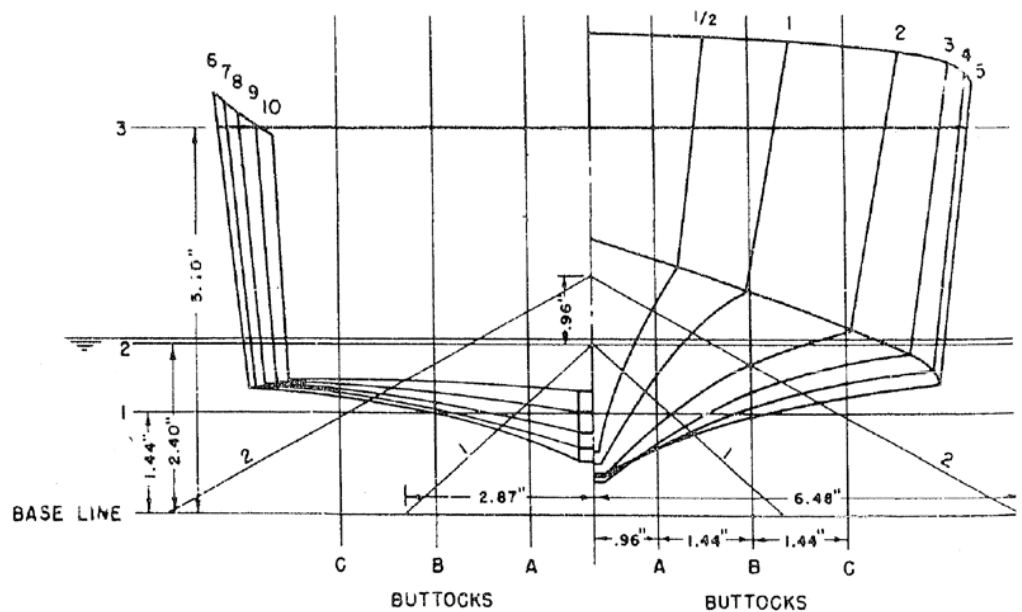


Table 3: Principal Characteristics of Specific Test Models

Model:	2727	2728	2729	2730	2731	2732	2733	2734	2735	2736
$\frac{L_P}{\nabla^{1/3}}$	8.41-8.94	8.41-8.94	8.41-8.94	8.41-8.94	8.41-8.94	6.68-7.09	6.68-7.09	6.68-7.09	6.68-7.09	6.68-7.09
L_P/B_{PX}	8.51	6.95	6.02	5.13	4.40	6.02	4.92	4.26	3.63	3.11
B_{PX}/T	4	6	8	11	15	4	6	8	11	15
$\frac{A_P}{\nabla^{2/3}}$	7.0-7.9	8.5-9.6	9.8-11.1	11.5-13.0	13.5-15.1	6.2-7.0	7.6-8.6	8.8-9.9	10.3-11.6	12.0-13.5
C_Δ	0.86-1.03	0.47-0.56	0.30-0.36	0.19-0.23	0.12-0.14	0.61-0.73	0.33-0.40	0.22-0.26	0.13-0.16	0.084-0.10
β_5	20	13	10	7.1	5.2	20	13	10	7.1	5.2
β_{10}	2.0	1.4	1.0	0.75	0.55	2.0	1.4	1.0	0.75	0.55
$\frac{1}{2}\alpha_E$	11	14	16	19	21	16	19	22	26	29
τ_K	-2.0	-1.6	-1.4	-1.2	-1.0	-2.8	-2.3	-2.0	-1.7	-1.4
$\tau_{0.25}$	-0.59	-0.48	-0.42	-0.35	-0.30	-0.83	-0.68	-0.59	-0.50	-0.43
τ_C	0.06	0.05	0.04	0.04	0.03	0.09	0.07	0.06	0.05	0.04

Table 3: (continued) Principal Characteristics of Specific Test Models

Model:	2737	2738	2739	2740	2741	2742	2743	2744	2745	2746
$\frac{L_P}{\nabla^{1/3}}$	5.83-6.20	5.83-6.20	5.83-6.20	5.83-6.20	5.83-6.20	5.30-5.63	5.30-5.63	5.30-5.63	5.30-5.63	5.30-5.63
L_P/B_{PX}	4.92	4.01	3.48	2.96	2.54	4.26	3.48	3.01	2.57	2.20
B_{PX}/T	4	6	8	11	15	4	6	8	11	15
$\frac{A_P}{\nabla^{2/3}}$	5.8-6.5	7.1-8.0	8.2-9.2	9.6-10.8	11.2-12.7	5.5-6.2	6.8-7.6	7.8-8.8	9.1-10.3	10.7-12.1
C_Δ	0.50-0.60	0.27-0.33	0.18-0.21	0.11-0.13	0.069-0.082	0.43-0.52	0.24-0.28	0.15-0.18	0.095-0.11	0.060-0.071
β_5	20	13	10	7.1	5.2	20	13	10	7.1	5.2
β_{10}	2.0	1.4	1.0	0.75	0.55	2.0	1.4	1.0	0.75	0.55
$\frac{1}{2}\alpha_E$	19	23	26	30	34	22	26	30	34	38
τ_K	-3.4	-2.8	-2.4	-2.0	-1.7	-3.9	-3.2	-2.8	-2.4	-2.0
$\tau_{0.25}$	-1.0	-0.83	-0.72	-0.61	-0.53	-1.2	-0.96	-0.83	-0.71	-0.61
τ_C	0.10	0.09	0.07	0.06	0.05	0.12	0.10	0.09	0.07	0.06

Table 4: Series 50 Test Matrix

Variable	Test Conditions			
Beam-Draft Ratio	4	6	8	11 15
Design $\frac{L_P}{\nabla^{1/3}}$	8.94	7.09	6.20	5.63
Displacement	100%	110%	120%	
Static Trim (deg.)	0	2	4	
Froude Number $\frac{V}{\sqrt{gL_P}}$	0.13	to	2.05	

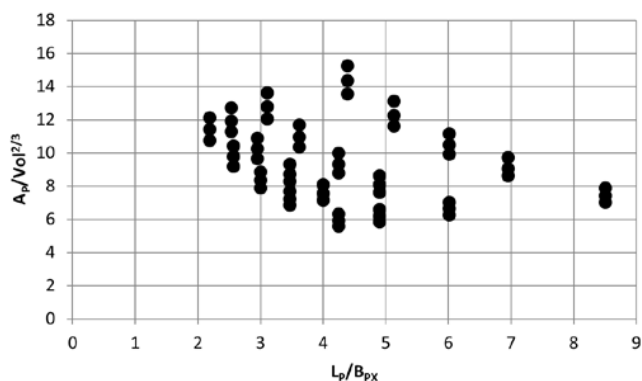


Figure 4a: Range of Applicability of Series 50 – Bottom Loading

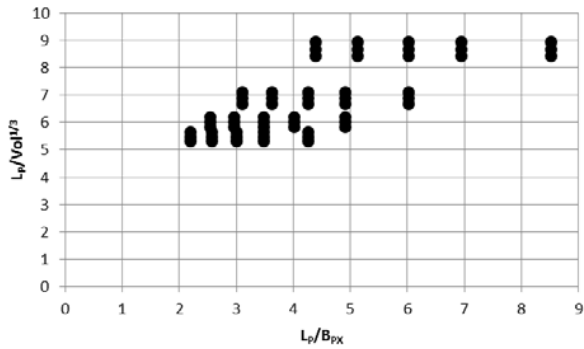


Figure 4b: Range of Applicability of Series 50 – Displacement Length Ratio

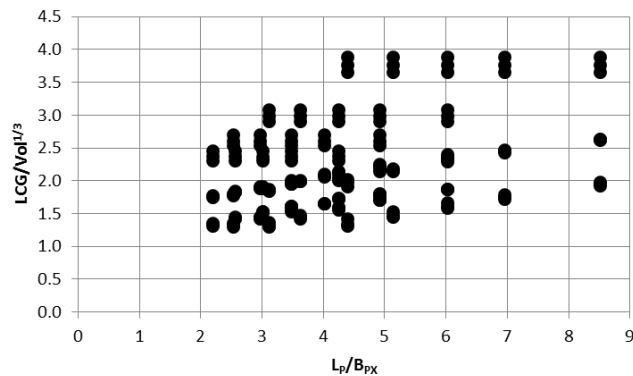


Figure 4c: Range of Applicability of Series 50 – Displacement LCG Ratio

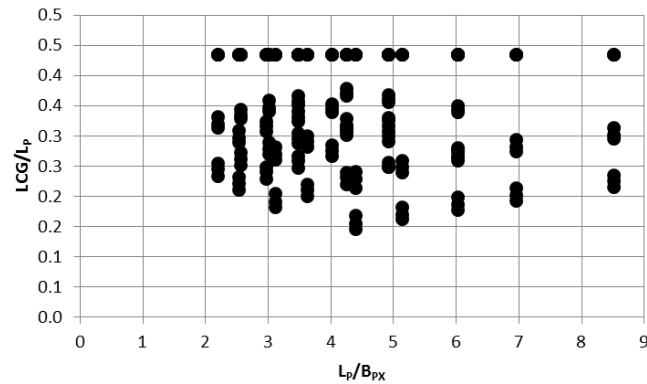


Figure 4d: Range of Applicability of Series 50 – LCG to Length Ratio

TEST PROCEDURE AND DATA COLLECTION

All tests were conducted in the Experimental Towing Tank at Stevens Institute of Technology. The tank (Figure 5) measured 30 m in length, 2.75 m wide and 1.37 m deep, and had a semi-circular cross section. Figure 6 shows a typical photograph of the test apparatus. Resistance was measured with a drag balance consisting of a counterweight, to take up the majority of the model resistance, a soft auxiliary spring to measure the difference between the model resistance and the initial counterweight, as well as a damper to steady the resistance dial

(Davidson , 1941). This system provided for accurate resistance measurements, because the dial, which was manually read as the model moved, only measured a small percentage of the total resistance of the model, the remainder being carried by the precision pan weights. For runs with very light displacements, the model was “unloaded” meaning that a vertical lift force was applied at the center of gravity because the weight of the model and apparatus exceeded the displacement. Separate gages were provided for trim and heave.

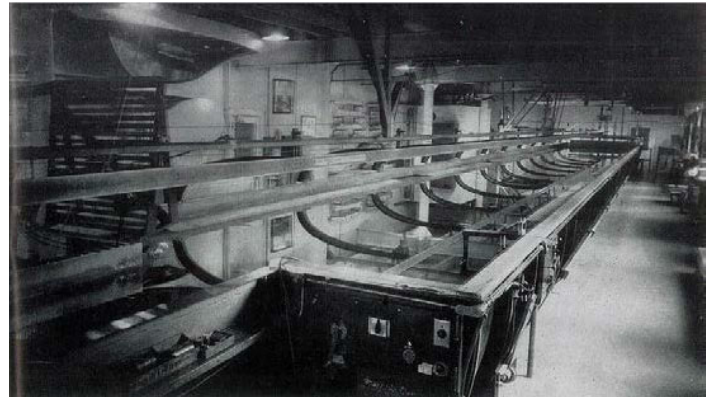


Figure 5: Photograph of Experimental towing tank

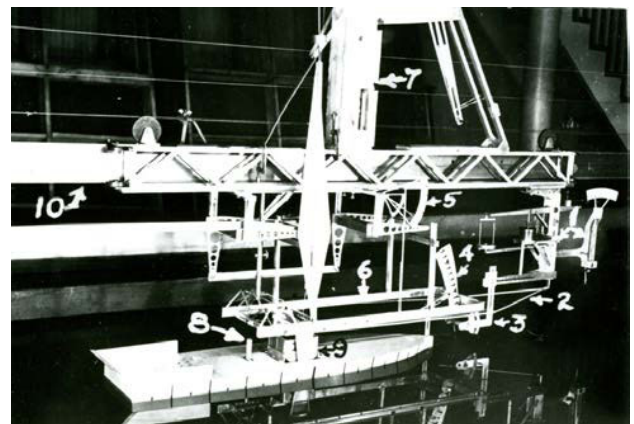


Figure 6: Photograph of test apparatus (Davidson, 1941)
Key: (1) Resistance Dynamometer (2) Towbar (3) Strut Holder and Strut (4) Trim Scale (5) Towpoint Heave Scale (6) Counterbalanced Frame (7) Support for Unloading Pulley (8) Pitch Damping Dashpot (9) Towing Axle Jig and Bearing Supports (10) Carriage Rail

The model was towed horizontally with a shaft line height corresponding to an average shaft position, equal to 0.5 inches (12.7mm), or $L_p/80$ above the design waterline at station 5 for all models. The effect of shaft line angle on the running trim is discussed in the section on corrections for wind, thrust line and appendages, including a diagram of the tow point. The model was striped at 2-inch (50mm) increments, and keel and chine wetted lengths were recorded based on visual observation to a resolution of 0.2 inches (5mm).

Turbulence stimulation is necessary on planing models of this size. It is not practical to install turbulence stimulation, such as sand strips or studs, on planing models because of the variation in wetted length with speed. A 1mm diameter strut was towed 0.1m ahead of the model to increase the ambient turbulence level in the water ahead of the model. Using struts ahead of the model is less effective than turbulence stimulators that are located on the hull surface, because surface stimulation introduces a momentum deficit into the flow, increasing the momentum thickness Reynolds number and making transition to turbulence more likely.

Savitsky and Ross (1952) presented a study of the effectiveness of stimulation using struts ahead of the model and found that for certain cases it can induce turbulent flow; however the method is unreliable and they recommended to test planing hull models at Reynolds numbers greater than 2 million to avoid the need for stimulation. Of the configurations tested, the single strut located just ahead the bow (the same configuration tested in Series 50) was the most effective. The Reynolds numbers tested in Series 50 range from 100,000 to 4 million. Lower Reynolds numbers occurred in runs with aft LCG, where the mean wetted length was shorter.

To further facilitate transition, the water in the towing tank was heated to 20 degrees Celsius, even during the winter, slightly reducing the kinematic viscosity and increasing the Reynolds number.

RESISTANCE OF SERIES 50

In this section, the method used to derive the residuary-resistance to weight ratio for Series 50 is discussed. Following Froude's hypothesis, the total resistance can be taken as the sum of two components (1) the frictional resistance, consisting of all shear forces on the wetted portions of the hull due to fluid viscosity, and (2) residuary resistance, which is the result of normal forces acting on the hull. The residuary resistance includes wavemaking, wave breaking, base drag and all other forces that are not caused by shear. Form factor is not ordinarily used in planing craft because the viscous pressure component of resistance is negligible, and it is not possible to accurately determine the form factor because of transom immersion (ITTC, 2002).

$$R_T = R_R + R_F = R_R + C_F \frac{1}{2} \rho V_1^2 S$$

Where,

- C_F = friction coefficient
- S = wetted surface area - varies with speed (m^2)
- R_T = total resistance (N)
- R_F = frictional resistance (N)
- R_R = residuary resistance (N)
- V = the free stream velocity (m/s)
- V_1 = the mean bottom velocity (m/s)
- ρ = mass density of water (kg/m^3)

Planing hulls have a significant component of dynamic lift, evidenced by their tendency to rise out of the water at high speeds. Bernoulli's principle indicates that $P + \frac{1}{2} \rho V^2 = constant$. To generate lift, P increases and there must be a reduction in the velocity of the flow. The mean bottom velocity, V_1 will be less than the free stream velocity, V for a planing hull. Savitsky (1964) developed a method to estimate this reduction in velocity; however, it is not ordinarily used in the expansion of model test data because of the complexity of evaluating it and the small effect on total resistance. At low trim angles, where the dominant component of resistance is frictional, V_1 approaches V so only a small error is introduced by assuming the following:

$$R_{THULL} = R_R + C_F \frac{1}{2} \rho V^2 S$$

The residuary resistance to weight ratio was computed using the following calculation, where subscript M refers to model:

$$\frac{R_R}{W} = \frac{R_{T,M} - C_{F,M} \frac{1}{2} \rho_M V_M^2 S_M}{W_M}$$

$C_{F,M}$ is ordinarily calculated using either the International Towing Tank Conference 1957 model ship correlation line, or the Schoenherr flat plate turbulent friction formula, seen below:

$$C_{F_{Schoenherr}} = \left[\frac{0.242}{\text{LOG}_{10}(Re C_{F_{Schoenherr}})} \right]^2$$

$$C_{F_{ITTC}} = \frac{0.075}{(\text{LOG}_{10} Re - 2)^2}$$

The Schoenherr and ITTC formulations are nearly identical at full scale, but the ITTC line was increased at low Reynolds numbers to improve correlation between small and large models of ships. This built in form factor introduces a small error in planing hull models, which have bottoms more similar to flat plates. Savitsky and Ross (1952) showed that the turbulent friction coefficients measured from small planing models agreed well with the Schoenherr line. Following the recommendations of Clement and Blount (1963), Savitsky (1964), Hadler (1966), Blount and Fox (1976) and Savitsky and Brown (1976), the Schoenherr friction line is used for the determination of $\frac{R_R}{W}$.

The Reynolds number for friction calculation must be based on measured wetted lengths, which vary with speed. It is customary in the previously mentioned references to use the mean wetted length, L_M for determination of the friction coefficient, because it represents an average value over the bottom of the hull.

$$Re = \frac{V L_M}{\nu}$$

Wetted Length and Area

In the original tabulation of the Series 50 tests, wetted length at the chine and keel, which vary with speed, were recorded (Wong and Suarez, 1941). It is necessary to determine wetted area as a function of these wetted lengths. At planing speeds, it is assumed that there is no side wetting or transom wetting, so the girth, measured between chines can be integrated over its wetted length to determine wetted surface area. This calculation included the effects of stern taper, curved cross sections and deadrise for a model with $\frac{B}{T} = 8$, near the middle of the series.

The variation in wetted surface area with changes in $\frac{B}{T}$, is small. The following is an approximation for the wetted surface area of Series 50 hulls:

$$S = 0.962L_M B_{PX}$$

Where,

B_{PX} = the maximum chine beam of the planing surface (m)

L_C = Chine wetted length (m)

L_K = keel wetted length (m)

L_M = the mean wetted length = $\frac{L_K + L_C}{2}$ (m)

In addition to the area wetted by solid water, there is a portion of the hull wetted by whisker spray, a thin spray sheet originating at the spray root line. Savitsky, Datla and Delorme (2006) studied this in detail, developing a method to estimate the magnitude of the whisker spray resistance. In the present study, the resistance due to whisker spray is included in the residuary resistance – a typical simplification applied to most planing boat model tests. Inclusion of whisker spray drag in the residuary resistance will result in a small over-prediction of total resistance at full scale.

Transitional Friction Resistance

Clement and Blount (1963) pointed out that for some of the Series 50 data points in the planing range, the values of total resistance coefficient are less than the values of frictional resistance coefficient for fully turbulent flow, indicating transitional flow. During the present analysis of all of the data in the series, it was found that transitional flow occurred primarily on hulls with large beam and aft LCG, even at the highest speeds tested. This is likely because in these conditions (1) the strut was not effective at inducing turbulence far from the centerline, (2) the short wetted lengths caused by aft LCG resulted in lower Reynolds numbers, (3) the strut was a longer distance in front of the stagnation line, (4) there was a strong favorable pressure gradient, which tends to cause re-laminarization, and (5) frictional resistance is the dominant resistance component at high speeds, making small errors in friction obscure the measurement of residuary resistance.

Figure 7 shows the contribution of frictional and residuary resistance to total resistance as a function of volumetric Froude number for a typical Series 50 hull. At high speeds, friction becomes the dominant component, and transitional flow can have a significant effect on total resistance. The easiest method

to account for transitional friction coefficient is to use a transitional friction line, like the Prandtl-Schlichting line. This was not possible for Series 50 because the transition point was not solely a function of Reynolds number, but depended on model geometry and loading.

Because of the uncertainty of estimating transitional friction coefficient, another approach was taken, in which the residuary resistance was compared with a commonly used approximation for planing hulls: pressure resistance.

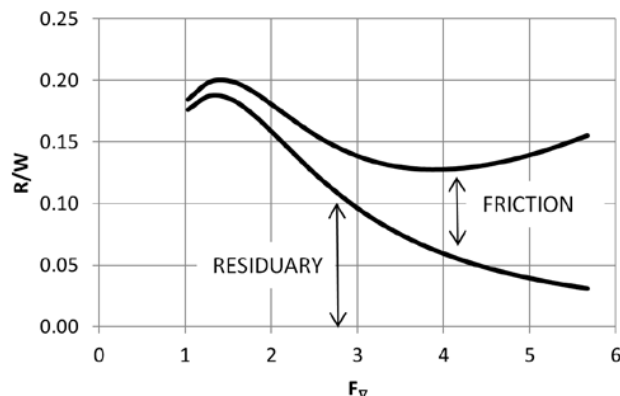


Figure 7: Relative contributions of residuary and frictional resistance to total resistance of a planing hull.

Pressure Resistance

Although it is not possible to predict the transitional behavior of the frictional resistance, it is possible to establish an approximate value for residuary resistance at high speeds. This value may be used to identify test conditions with transitional flow and to correct the residuary resistance for these conditions.

The normal force (the integral of the pressure acting on the hull) is resolved into vertical lift and horizontal drag components for hulls with parallel buttock lines (i.e. prismatic hulls), because pressure always acts normal to the bottom. Figure 8 shows that from this relation, the pressure resistance can be determined using only the lift and the trim angle. This takes into consideration all forces acting normal to the hull, which includes any wavemaking resistance components. Not seen in the figure is the vertical component of lift due to friction resistance, which is small and neglected here. William Froude (1875) was the first to point out this relation for planing surfaces:

$$\frac{R_P}{W} = \tan \tau_H$$

Where,

R_P = pressure resistance (N)

W = total weight lifted, or displacement (N)

τ_H = hydrodynamic angle of attack (deg)

N = normal force (N)

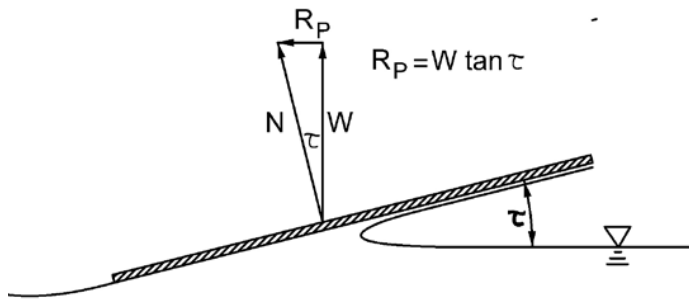


Figure 8: Pressure component of flat plate resistance (vertical component due to friction neglected)

This relation holds for all prismatic hulls planing at speeds in which the transom is dry, regardless of deadrise angle, and forms the basis for Savitsky’s (1964) resistance prediction method. For non-prismatic hulls, such as Series 50, the relation only applies when the curved portions of the bow are carried clear of the water, and the trim angle is taken as the average angle of attack of the wetted portion of the bottom, which can be approximated as the mean quarter-buttock line trim angle (Savitsky, 2012). In the original tabulation of the Series 50, (Wong and Suarez, 1941) the static baseline trim τ_o and the change in trim $\delta\tau$ for each speed is given. The effective hydrodynamic trim angle can then be estimated as follows:

$$\tau_H = \tau_o + \delta\tau + \tau_{0.25} = \tau_{BL} + \tau_{0.25}$$

Where, $\tau_{0.25}$ is the difference between the baseline and the quarter-buttock line trim in the region of the hull where planing is occurring.

The well-established principle that $\frac{R_P}{W} = \tan\tau_H$ can be used to check for runs with possible transitional flow. If the residuary resistance to weight ratio calculated from the resistance measurements is significantly less than $\tan\tau_H$ at speeds above hump, it is likely that there was transitional flow. If this is the case, the accuracy of the predicted total resistance can be significantly improved by substituting the calculated pressure resistance for the measured residuary resistance at conditions with known transitional flow.

To check the validity of the approximation $\frac{R_P}{W} = \tan\tau_H$, it was compared with some of the data from Metcalf’s (2005) Coast Guard 47’ Motor Lifeboat Series. These model tests, conducted at David Taylor Model Basin, were made on a 10-foot model -- large enough to expect turbulent flow at planing speeds. Each hull had a small amount of warp, resulting in a quarter-beam trim angle $\tau_{0.25} \approx 1$ degree. The effective hydrodynamic trim was computed using: $\tau_H = \tau_o + \delta\tau + \tau_{0.25}$. The residuary resistance-to-weight ratio was calculated using the ITTC 1957 model-ship correlation line and the wetted length and surface area reported in the paper. This analysis procedure followed the methods presented by the authors of the series.

The approximate method, $\frac{R_P}{W} = \tan\tau_H$, is invalid when the curved portions of the bow are immersed. Therefore, comparisons were made for conditions where the wetted length was less than 90% of the length of the planing surface. Figure 9 shows a comparison between residuary resistance-to-weight ratio and the approximation, $\frac{R_P}{W} = \tan\tau_H$ for the parent hull of the series at its mid loading condition.

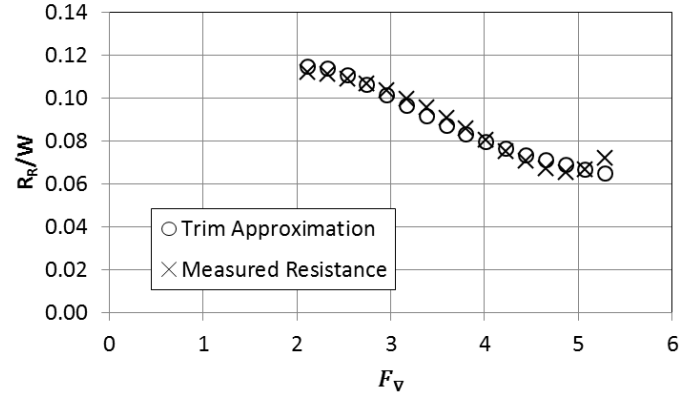


Figure 9: Comparison between measured residuary resistance to weight ratio and approximation, $\frac{R_P}{W} = \tan\tau_H$, for the parent hull of the Coast Guard 47’ Motor Lifeboat Series.

To ensure that the positive correlation seen in the parent model was typical of the entire series, the approximate method was applied to all the data in the series in which the wetted length was less than 90% of the length of the planing surface. This corresponded to about 60% of the data points. Table 5 summarizes the statistics of the approximation. A correlation coefficient of 1.0 represents a perfect fit. On average, the correlation coefficient for the entire series was 0.881, compared to the correlation coefficient of the parent hull, seen in Figure 9 of 0.983. This indicates that the fit for the whole series is not as good as seen in the parent model, but is still statistically significant. The average residual error is about 10% of the mean value of residuary resistance to weight ratio.

Table 5: Statistics of measured versus predicted residuary resistance to weight ratio of Coast Guard 47’ Motor Lifeboat Series.

Statistic	Value
Mean Squared Error	0.000112
Correlation Coefficient	0.881
Average Absolute Value of Residual	0.00841
Average $\frac{R_R}{W}$	0.0804

The pressure resistance approximation may be used to determine a value of experimental friction coefficient on the bottom of a prismatic planing hull. This experimental friction coefficient should match the ATTC line for conditions with known turbulent flow. Savitsky and Ross (1952) used this

technique to develop guidelines on minimum Reynolds number for planing hull towing tests. The calculations are as follows:

$$R_{F,EXP} = R_{T,M} - \Delta \tan \tau_H$$

$$C_{F,EXP} = \frac{R_F}{\frac{1}{2} \rho V_1^2 S}$$

Where, V_1 is slightly less than the free stream velocity because Bernoulli's principle requires a reduction in velocity with increase in dynamic pressure. The ratio V_1/V may be estimated from Figure 14 in Savitsky's (1964) paper.

Model 2738 was chosen for analysis because of its similarity to modern planing hull forms, and because the Reynolds numbers attained at the forward LCG are high enough to expect turbulent flow, whereas the Reynolds numbers during aft LCG runs are likely transitional. Figure 10 shows a plot of experimental friction coefficient versus Reynolds number for Model 2738 at the mid displacement and the three LCGs tested. Runs at volumetric Froude numbers below 1.5 were omitted because these speeds are not fully planing. The figure clearly shows that at the forward LCG, the experimental friction coefficient for this model closely matches the ATTC friction line. This agreement supports the pressure resistance approximation. Transitional flow occurs at the aft LCG, which has much lower Reynolds numbers due to the short wetted length.

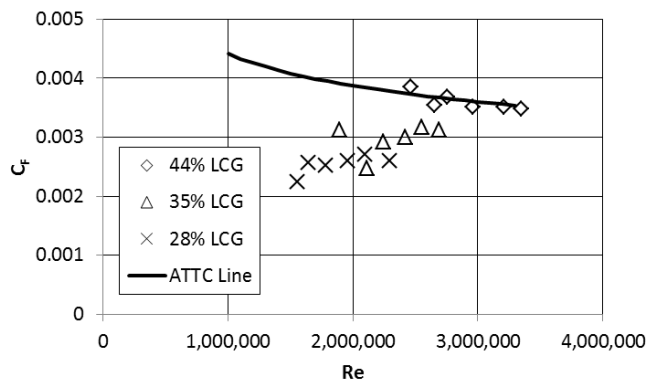


Figure 10: Comparison of Experimentally Derived Friction Coefficient for Model 2738 and the ATTC Friction Line

PRESENTATION OF SERIES DATA

To make the series convenient for today's designers, it is presented in two formats, faired plots as well as data tables that may be utilized in a computerized lookup and interpolation procedure.

To simplify the presentation of the data, only the most important results are tabulated and plotted. Residuary resistance to weight ratio and mean wetted length are necessary for calculation of total resistance. Trim angle, although not necessary for resistance prediction, is an important indicator of performance.

Although nine combinations of LCG and displacement were tested, for a given LCG, the residuary resistance to weight ratio, mean wetted length and trim for each of the three displacements collapsed onto the same curves as a function of volumetric Froude number, reducing the required number of plots and tables by a factor of three.

To arrive at the faired data, the results from each of the three displacements were averaged, smoothed and interpolated to regular increments of volumetric Froude number, using a 3-segment spline interpolation. Generally, the 120% displacement had slightly higher baseline trim and residuary resistance to weight ratio than the faired curve and the 100% displacement had less trim and resistance than the faired curve. The variation about the mean curve fit for each of the three variables was:

$$\tau_{BL} \pm 0.5 \text{ deg}$$

$$\frac{R_R}{W} \pm 0.01$$

$$L_M/L_P \pm 0.03$$

Residuary Resistance, Trim and mean wetted length increased with increases in displacement.

Faired Data Tables

Appendix A includes the faired data tables for the series, listed by model number and selected hull form parameters, including L_P/B_{PX} , $L_P/\nabla^{1/3}$ and β_S . Conditions in which the residuary resistance had to be corrected for transitional flow are underlined. Approximately 1/3rd of the data in the series, mainly at the aft LCGs and lightest beam loadings, had to be corrected.

In each table, baseline trim τ_{BL} , residuary resistance to weight ratio $\frac{R_R}{\Delta}$ and mean wetted length-to-LCG ratio $\frac{L_M}{L_{CG}}$ are given at regular intervals of volume Froude number F_V . Each table includes three data series representing the three LCGs tested. In the original development of the series, static trim was set at 0, 2 and 4 degrees by varying LCG at each displacement. This meant that for a given model, the LCG changed slightly with changes in displacement; however the variation in LCG about the average value is only 1% of the length of the hull, so only the average position is given in the tables.

$L_P/\nabla^{1/3}$ is used as the primary loading parameter instead of beam loading or bottom loading because the series was originally tested at consistent values of $L_P/\nabla^{1/3}$. Table 3 includes most currently used planing coefficients (for instance, $A_P/\nabla^{2/3}$ and C_Δ) for each model in the series, enabling designers to locate the appropriate model in whichever way they prefer.

Series Plots

Appendix B includes the series plots, listed by model number. As with the data tables, some selected form coefficients are provided with the plots, the rest are available in Table 3. On each plot, baseline trim τ , residuary resistance to weight ratio

$\frac{R_R}{\Delta}$, and mean wetted length-to-LCG ratio $\frac{L_M}{L_{CG}}$ are plotted as a function of volumetric Froude number, F_V . Each plot includes three curves representing the three LCGs tested, plotted from the faired data tables.

PORPOISING

Porpoising is a coupled oscillation in heave and pitch that occurs at high speeds and high trim angles. In extreme cases, this instability makes the boat impossible to operate. During the original tests of Series 50, many runs exhibited porpoising, especially at the aft LCG. When porpoising occurred, the test engineers applied damping to the model to get a steady state trim and resistance. They later went back with a special apparatus to observe the onset of porpoising. In practice, damping can't be applied so designers must avoid conditions that will cause porpoising.

During porpoising tests, the model was free-to-trim and heave, but fixed in surge, sway, roll and yaw. The model was towed from the longitudinal center of gravity, unlike resistance tests in which it was towed from amidships. The radius of gyration of the model was set to be 0.25LWL for all cases, a typical value for most planing craft. In order to set up an initial perturbation, the model was held at a distance of 50mm above its typical running position during the acceleration phase of the run and then dropped as it reached speed. If the oscillations damped out, it was considered stable.

These special porpoising tests were run for seven selected models of the series. For each model, there was a limiting speed over which porpoising occurred. This speed decreases during conditions with light beam loadings, high speeds and high static trim angles (aft LCG). At the time Series 50 was done, no convenient means of plotting porpoising stability data had been developed and a number of different methods were tried, focusing on the loading conditions and the speeds.

Later, it became clear to researchers that porpoising could be characterized as a function of a critical trim angle above which porpoising will occur. Day and Haag (1952) found that for a prismatic planing hull, the critical trim angle was lower at small values of lift coefficient (high speeds, light loadings), and was dependent on deadrise (Savitsky, 1964).

Over 140 runs were made to estimate the onset of porpoising in Series 50. Porpoising limit lines have been developed here by only taking those data points in which the height of the pitch oscillations was between 1 and 4 degrees. This range is consistent with the onset of porpoising, and consists of approximately 60 data points. Figure 11 summarizes the critical trim angle of Series 50 as a function of volumetric Froude number, which collapsed this data set better than alternatives such as $\sqrt{C_L/2}$. Two lines are provided, one for 7-degree deadrise and one for 13 degree deadrise. The following formulae can be used to estimate the porpoising limit:

Porpoises when:

$$\tau_H > \frac{35}{F_V^{1.5}} \text{ for } \beta_5 > 13$$

$$\tau_H > \frac{18}{F_V^{1.2}} \text{ for } \beta_5 < 7$$

It is important to note that these formulae are based entirely on the porpoising inception tests of Series 50, a hull with warp, rocker and taper. For hulls that are not similar to Series 50, other references should be consulted, such as Savitsky, 1964, Clement and Blount 1963.

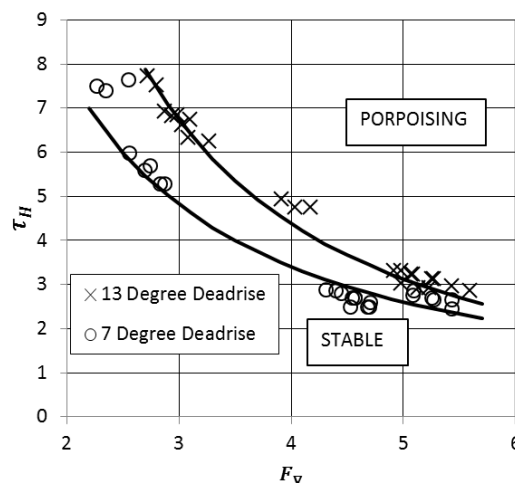


Figure 11: Porpoising Limit Lines for Series 50

USE OF SERIES DATA

The following sections describe the use of the Series 50 charts, and data tables. Appendix C contains example calculations using this procedure.

Use of Series Charts in Appendix B

1. Calculate non-dimensional parameters. The series is most easily entered using the volumetric coefficient $\frac{L_P}{\nabla^{1/3}}$ and the length-beam ratio of the planing surface, L_P/B_{PX} . However, it can also be entered using C_Δ or $A_P/\nabla^{2/3}$
2. Locate closest hull using the table of principal characteristics in Appendix A.
3. Read off the R_R/W , L_M/L_P and τ_{BL} from the plots over a range of F_V . It will be necessary to interpolate to the correct LCG.
4. Expand the data to full-scale for each speed
 - Speed (m/s), $V = F_V \sqrt{g \nabla^{1/3}}$
 - Mean Wetted Length (m), $L_M = \left(\frac{L_M}{L_P}\right) L_P$
 - Surface Area (m²), $S = 0.962 \left(\frac{L_M}{L_P}\right) L_P B_{PX}$
 - Reynolds Number, $Re = \frac{VL_M}{\nu}$
 - Friction Coefficient, $C_F = \frac{0.075}{(\text{LOG}_{10} Re - 2)^2}$

Note: The Schoenherr line was used to determine the residuary resistance from the model test data. At full-scale Reynolds numbers, the Schoenherr and ITTC lines are nearly identical, and ITTC is used here for its simplicity.

- Correlation allowance, $C_A = 0$ (Blount and Fox, 1976)
- Resistance (N), $R_{THULL} = \left(\frac{RR}{W}\right)W + (C_F + C_A) \frac{1}{2} \rho V^2 S$
- Full Scale Baseline Trim (deg) $\tau_{BL} = \text{Model } \tau_{BL}$

5. Check for porpoising
Porpoises when:

$$\tau_H > \frac{35}{F^{1.5}} \text{ for } \beta_5 > 13$$

$$\tau_H > \frac{18}{F^{1.2}} \text{ for } \beta_5 < 7$$

Interpolate between these values of deadrise.

Use of Data Tables in Appendix A

Use of the data tables is identical to use of the standard series charts, with the exception that the manual process of reading the residuary resistance to weight ratio, mean wetted length and baseline trim angle is replaced by a computerized interpolation routine, which is described below:

1. Find four models with bounding values of $\frac{L_P}{\nabla^{1/3}}$ and $\frac{L_P}{B_{PX}}$.
2. For each of the four models, R_R/W , L_M/L_P and τ_{BL} must be first interpolated to the correct LCG $\frac{LCG}{L_P}$. Simple linear interpolation is recommended for all of these procedures to prevent anomalies caused by curve fitting.
3. For the two pairs of models with matching values of $\frac{L_P}{\nabla^{1/3}}$, interpolate to the correct $\frac{L_P}{B_{PX}}$.
4. For the two remaining data sets, interpolate to the correct $\frac{L_P}{\nabla^{1/3}}$.
5. Expand the data to full scale and check for porpoising using Steps 4 and 5 of the series charts procedure.

It is not recommended to extrapolate beyond the limits of the series.

ADJUSTMENTS FOR WIND, WAVES, APPENDAGES, THRUST LINE

Wind, appendages and thrust line have a large effect on resistance, trim and wetted length of planing craft. Lift forces not only reduce the effective weight that the hull must support, but produce pitching moments resulting in a shift in the effective LCG. The purpose of this section is to explain the process for determining the effective displacement and LCG that the hull itself must support, with corrections for wind, appendages and thrust line. These methods are not specific to Series 50, but are included to illustrate how these corrections must be made to develop accurate predictions. Hadler (1966)

developed a thorough procedure for including these effects on prismatic planing hulls, including the propeller pressure forces on the bottom of the hull. The following procedure is simplified, including only the most significant components, to illustrate the process and allow for quick engineering calculations.

Planing hulls usually have either conventional inboard propulsion, outboard motors, Z-drives or surface propellers. Each of these propulsion systems has different attributes. The following framework is developed so that any type of propulsion means may be substituted.

Figure 12 shows a diagram of the forces. The total resistance is the sum of all of the resistance components, which usually includes hull, wind, appendages, and trim flaps. The horizontal component of the propeller thrust must overcome this.

$$R_T = \sum R_i = R_{THULL} + R_{WIND} + R_{APPENDAGE} + R_{FLAP} + \dots$$

The effective displacement is the weight that the hull must carry, which is the total weight minus any vertical forces due to appendages $L_{APPENDAGE}$, trim flaps L_{FLAP} , or vertical component of propeller thrust, T_Y .

$$W_E = W - \sum L_i = W - T_Y - L_{APPENDAGE} - L_{FLAP} + \dots$$

The effective LCG is equal to the original LCG plus the effect of any pitching moments. Bow-up pitching moments make the effective LCG farther aft. All models were towed horizontally at a distance above the waterline of $L_P/80$. Pitching moments are created by (1) any horizontal force that does not act along this tow line, and (2) any vertical force that does not pass through the LCG.

$$LCG_E = LCG - \frac{\sum M}{W_E}$$

Where,

LCG is the longitudinal center of gravity measured forward of the transom (m)

LCG_E is the effective hydrodynamic LCG (m)

W_E is the effective weight of the boat (N)

$\sum M$ is the sum of the pitching moments (N-m)

- All moments due to horizontal forces are taken about the vertical position of the tow point ($\frac{L_P}{80}$ above the static waterline)
- All moments due to vertical forces are taken about the LCG
- Bow up moments are positive
- Changes in moment arm with trim are neglected in this analysis for simplicity, but can be added with suitable sine and cosine corrections

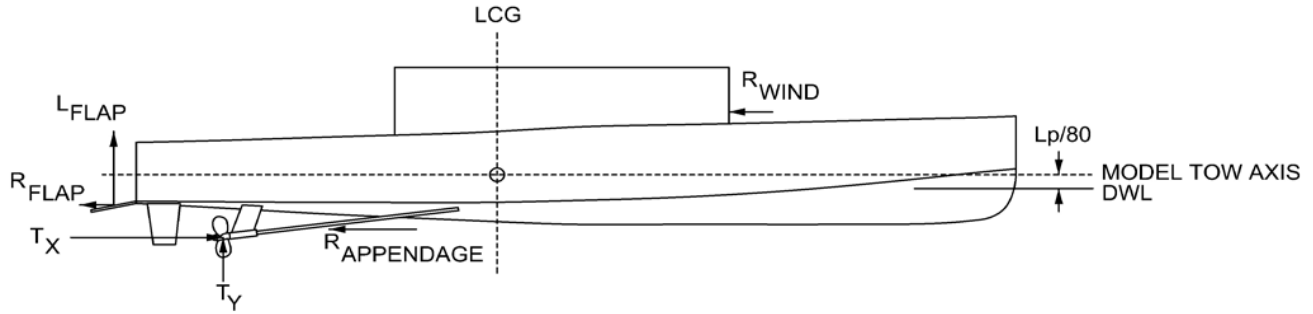


Figure 12: External forces acting on planing hull. Moments taken about intersection of LCG and model tow axis.

Propulsion Thrust

The horizontal component of propeller thrust is equal to the total resistance:

$$T_X = R_T$$

For submerged propellers, if the shaft angle, ε is taken with respect to the baseline, the vertical component of the propeller thrust is:

$$T_Y = R_T \tan(\varepsilon + \tau_{BL})$$

For surface propellers and some outboard motors, the lift generated by the propulsor can be equal to the thrust (Scherer, 2011). The operators will have control over the magnitude of this vertical component by adjusting the drive in the same manner as trim tabs. If this is the case, T_Y may be iterated (within the limits of the surface drive) until optimum resistance is reached.

For both submerged and surfaced propellers, the magnitude of the thrust along the shaft line, which is usually used in propeller calculations is:

$$T_P = \frac{R_T}{\cos(\varepsilon + \tau_{BL})}$$

For the present analysis, the horizontal and vertical components of propeller thrust, T_X and T_Y are taken as acting at the location of the propeller hub. This is in contrast to Savitsky's (1964) method, which uses a magnitude of the thrust and the perpendicular distance from the thrust line to the center of gravity to determine pitching moment from thrust. When all of the thrust is directed along the shaft line, the proposed method and Savitsky's method are equal; however, the present method permits the addition of extra vertical lift force from surface propellers.

Inboard Appendages

Appendages can create both a resistance and a vertical lift force. Gregory and Beach (1979) conducted full-scale resistance tests on a variety of appendage configurations for an inboard 10m boat with a 0.5m propeller. The configurations tested included shaft angles from 7.5 to 15 degrees, single struts and V-struts. On average, the resistance for a single-screw set of appendages with rudder can be estimated as follows:

$$R_{AP} = C_{DP} \frac{1}{2} \rho V^2 \frac{\pi D^2}{4}$$

Where,

D is the propeller diameter (m)

V is the speed of the boat (m/sec)

ρ is the water density

C_{DP} is the appendage drag coefficient = 0.071-0.076

The lift that the appendages generated varied with Reynolds number and at the highest speeds (where the appendage lift would have an effect), the appendage lift coefficient varied from negative 0.01 to positive 0.005, very small when compared to the drag.

Although Gregory and Beach did not measure the location of the center of pressure of the appendages, it would be a safe assumption to say that the drag force acts about 0.2D above the propeller hub, because the shafts and struts are above the propeller hub.

The appendage drag equation is normalized by propeller disc area. In early stage design, the diameter may be unknown. It is usually around 4%-5% of the length of the boat, although the diameter and the number of screws is dictated by cavitation criteria. Blount and Fox (1976) provide a thorough overview of propeller design for small craft.

Outboard Lower Units

Limited test data are available on the resistance of outboard lower units; however, Scherer (2011) has published a thorough method of estimating the resistance of outboard lower units, including hand calculations for non-cavitating, non-ventilating gearcase lift and drag, as well as experimental results for surface piercing outboards.

Still Air Resistance

Still-air wind resistance can be estimated by the following formula:

$$R_{WIND} = C_{DA} \frac{1}{2} \rho_A V^2 A_A$$

Where,

A_A is the vertical projected frontal area

ρ_A is the density of air (dry air is 1.25 kg/m³ at 10° C)

V is the boat speed

C_{DA} is the aerodynamic drag coefficient

Still air drag coefficients. C_{DA} vary from 0.5 to 0.7 for typical planing boats (Faltinson, 2005). The still air wind resistance can be taken as acting at the centroid of the vertical frontal area.

Many hulls, such as tunnel-hull catamarans can produce significant aerodynamic lift. For boats such as Series 50, this component is negligible and is not considered in this analysis.

Trim Flaps

Savitsky and Brown (1976) provide a method for estimating the effect of trim flaps.

$$L_{FLAP} = 0.046 s_F c_F \delta \frac{1}{2} \rho V^2$$

$$R_{FLAP} = 0.0052 L_{FLAP} (\tau + \delta)$$

Where,

s_F is the athwartships span of the flap (m)

c_F is the fore-aft chord length of the flap (m)

δ is the flap deflection (deg)

τ is the trim angle (deg)

The drag force may be taken as acting at the center of the flap. Savitsky and Brown (1976) found that the lift force due to the flap occurs at approximately 0.6 hull beams forward of the trailing edge of the flap. This location is usually somewhere on the bottom of the hull, forward of the flap. The position of the center of lift force is a result of the interaction between the flap and the hull – the flap causing an increase in pressure on the bottom of the hull. There is a small correction for the variation of this centroid with the ratio of flap span to beam, which is not included here.

Added Resistance in Waves

When operating in a seaway, there is an added increment of resistance. Although this was not tested for Series 50, Hoggard and Jones' (1980) regression covers nearly the same range of parameters as the Series 50 and will be a close estimate of the effect.

$$\frac{R_{AW}}{W} = 1.3 F_V \left(\frac{H_{1/3}}{B_{PX}} \right)^{0.5} \left(\frac{L_P}{\nabla^{2/3}} \right)^{-2.5}$$

Where,

$\frac{R_{AW}}{W}$ is the ratio of added resistance in waves to weight

$H_{1/3}$ is the significant wave height of the sea state (m)

Range of Applicability:

$$C_{\Delta} = 0.15 \text{ to } 1.27$$

$$L_P/B_{PX} = 2.82 - 6.43$$

$$\beta = 0^\circ - 24^\circ$$

$$\frac{H_{1/3}}{B_{PX}} = 0.13 - 0.77$$

$$V/\sqrt{gL_P} = 0.3 - 1.8$$

Calculation Procedure

The following procedure can be followed to calculate the effects of wind resistance, appendages and propeller thrust.

Step 1: Bare Hull

Use the calculation procedure shown earlier to estimate the resistance using the weight of boat, W and the LCG from the series charts or tables.

Step 2: Additional Components

Compute the resistance and lift components due to wind, appendages, trim flaps, and other components and add them to hull resistance to estimate total resistance.

$$R_T = \sum R_i = R_{HULL} + R_{WIND} + R_{APPENDAGE} + R_{FLAP} + \dots$$

Step 3 Propeller Thrust

The horizontal component of propeller thrust is equal to the total resistance.

$$T_X = R_T$$

If a conventional submerged propeller is used, the thrust is directed along the shaft line and the vertical component is:

$$T_Y = R_T \tan(\varepsilon + \tau_{BL})$$

Step 4: Effective Displacement

The effective displacement is equal to the weight of the boat minus any lift forces developed by the propeller thrust or appendages. This is the weight that the hull supports.

$$W_E = W - \sum L_i = W - T_Y - L_{APPENDAGE} - L_{FLAP} + \dots$$

Step 5: Sum Moments

Bow-up moments are taken as positive. The moment arm for lift forces is the horizontal distance to the LCG. The moment arm for resistance forces is the vertical distance from where the force is applied to a point $L_P/80$ above the static waterline (where Series 50 was towed from).

Step 6: Effective LCG

$$LCG_E = LCG - \frac{\sum M}{W_E}$$

Step 7: Iterate

Repeat Step 1 (hull resistance and trim) with LCG_E and W_E

Repeat Steps 2-6 using original LCG and W , but using the resistance and trim values calculated at the effective conditions.

Process is converged when the new effective LCG and effective weight are within 1-2% of the values on the previous iteration. It usually takes 2-3 iterations to achieve this.

An example showing how to apply the calculation procedure for appended hulls is provided in Appendix C.

CONCLUSIONS

Series 50 is the first and the largest planing hull standard series tested in the United States. Its main strength is the broad range of test conditions, including length-to-beam ratio, deadrise, bottom loading and LCG. This breadth enables the series to be used to rapidly explore the design space for a wide variety of

planing craft. The secondary strength of the series is that it incorporates warp, rocker, and taper. These features are present on many real boats, yet their effects are not fully understood today. The data from the series may be incorporated into future analyses to determine the magnitude of these effects.

The primary weakness of the series has been the presence of transitional flow during some of the runs with large beam and aft LCG. The resistance data for runs in which there was suspected transitional flow have been corrected using the approximation $R_R \approx \Delta \tan \tau$, typically employed for the resistance prediction of prismatic planing hulls, substantially improving the accuracy of the series.

The series has been re-analyzed and put into a format familiar to today's planing boat designers: design plots for hand calculations and faired data tables for lookup programs, to estimate mean wetted length, trim and residuary resistance to weight ratio, allowing the data to be rapidly expanded to any scale ratio. Additionally, means of estimating porpoising stability have been provided.

Estimates for the effects of wind, thrust line, and appendages have been given within a general framework that allows calculations to be made for a variety of propulsion methods, including inboard propulsion, surface piercing propellers or outboard motors. This process builds on the work of Hadler (1966) and Savitsky and Brown (1976). The means of propulsion has a significant effect on running trim and planing characteristics, and must be considered early on in design. The advantage of having a rapid calculation procedure such as Series 50 is that a designer can immediately see the effects of adjustments, such as varying angle of trim tabs.

ACKNOWLEDGMENTS

The author would like acknowledge Kyle Manning, former undergraduate student at Stevens Institute of Technology, who in 2008 carefully and accurately digitized all 180 pages of the Series 50 tank data, making this research possible.

REFERENCES

- Blount, D. and Fox, D. "Small-Craft Power Prediction." *Marine Technology*, Vol. 13, No.1, Jan 1976, pp. 14-45.
- Clement, E. P. and Blount, D.L. "Resistance Tests of a Systematic Series of Planing Hull Forms." *SNAME Transactions* pp 491-579, 1963.
- Davidson, K.S.M. "Growing Importance of Small Models for Studies in Naval Architecture." *SNAME Transactions*, 1941.
- Davidson, K.S.M. and Suarez, A. "Tests of Twenty Related Models of V-Bottom Motor Boats – U.S.E.M.B. Series 50." Report No. 170. Experimental Towing Tank, Stevens Institute of Technology, Hoboken, NJ, 1941.
- Day, J.P. and Haag, R.J. "Planing Boat Porpoising." A Thesis Submitted to Webb Institute of Naval Architecture, May 1952.
- Faltinson O. *High Speed Marine Vehicles*. Cambridge University Press, 2005.
- Froude, W. "Admiralty Experiments upon Forms of Ships and upon Rocket Floats." *Naval Science*. Vol. 4. pp 37-51, 262-264, 1875.
- Gertler, M. "Reanalysis of the Original Test Data for the Taylor Standard Series." David Taylor Model Basin Report No. 806, 1954.
- Gregory, D. and Beach, T. "Resistance Measurements of Typical Planing Boat Appendages." David Taylor Naval Ship Research and Development Center Report No. DTNDRDC/SPD-0911-01, 1979.
- Hadler, J. B. "The Prediction of Power Performance on Planing Craft." *SNAME Transactions* 1966.
- Hoggard, M. and Jones, M. "Examining Pitch, Heave, and Accelerations of Planing Craft Operating in a Seaway." Presented to High Speed Surface Craft Symposium, Brighton, England, June, 1980.
- ITTC – Recommended Procedures "Testing and Extrapolation Methods - High Speed Marine Vehicles Resistance Test" 7.5-02-05-01. Effective Date 2002
- Lewis, E.V. *Principles of Naval Architecture – Volume II – Resistance, Propulsion and Vibration*. Section 9 High-Speed Craft and Advanced Marine Vehicles. Pp93-105. Society of Naval Architects and Marine Engineers, 1989.
- Metcalf, B. "Resistance Tests of a Systematic Series of U.S. Coast Guard Planing Hulls." Carderock Division, Naval Surface Warfare Center, NSWCCD-50-TR-2005/063 December, 2005.
- Savitsky, D. and Ross, E. "Turbulence Stimulation in the Boundary Layer of Planing Surfaces – Part II Preliminary Experimental Investigation." Report No. 444. Experimental Towing Tank, Stevens Institute of Technology, Hoboken, NJ, 1952.
- Savitsky, D. "Hydrodynamic Design of Planing Hulls." *Marine Technology*, pp71-95. SNAME, October 1964.
- Savitsky, D. and Brown, P. "Procedures for Hydrodynamic Evaluation of Planing Hulls in Smooth and Rough Water." *Marine Technology*, Vol. 13, No. 4. pp 381-400, Oct. 1976
- Savitsky, D. "The Effect of Bottom Warp on the Performance of Planing hulls." Chesapeake Power Boat Symposium, Annapolis, MD, Society of Naval Architects and Marine Engineers, 2012.
- Savitsky, D. Datla, R. DeLorme, M. "Inclusion of whisker spray drag in performance prediction method for high-speed planing hulls." *Marine Technology*, 2006.
- Scherer, J.O. "Hydrodynamics of Surface-Piercing Outboard and Sterndrive Propulsion Systems." 11th International Conference on Fast Sea Transportation FAST 2011, Honolulu, Hawaii, USA, September 2011.
- Taylor, D.W. *Speed and Power of Ships*. United States Shipping Board. Revised Volume 1933.
- Wong, L.J. and Suarez, A. "Resistances of V-Bottom Motor Boats – Tests of Twenty Related Models – U.S.E.M.B. Series 50." Report No. 153. Experimental Towing Tank, Stevens Institute of Technology, Hoboken, NJ, 1941.

APPENDIX A: SERIES 50 FAIRED TABULATED DATA

Note: Underlined R_R/W are approximated based on $\frac{R_R}{W} = \tan\tau_H$

Model 2727 $L_P/\nabla^{1/3} = 8.4-8.9$ $L_P/B_{PX} = 8.5$ $\beta_5 = 20^\circ$

F_V	LCG=44% L_P			LCG=30% L_P			LCG=23% L_P		
	R_R/W	L_M/L_P	τ_{BL}	R_R/W	L_M/L_P	τ_{BL}	R_R/W	L_M/L_P	τ_{BL}
1.25	-	-	-	-	-	-	-	-	-
1.50	0.031	0.94	1.0	0.066	0.76	3.7	0.122	0.53	7.4
1.75	0.036	0.92	1.3	0.074	0.73	3.8	0.132	0.49	8.0
2.00	0.043	0.91	1.5	0.082	0.70	4.1	0.139	0.46	8.4
2.50	0.062	0.91	1.6	0.096	0.63	4.7	0.142	0.40	8.9
3.00	0.081	0.90	1.9	0.102	0.57	5.2	<u>0.136</u>	0.35	8.7
3.50	0.095	0.84	2.4	0.098	0.50	5.5	<u>0.122</u>	0.33	7.8
4.00	0.103	0.74	3.1	0.087	0.45	5.5	<u>0.106</u>	0.31	6.7
4.50	0.104	0.65	3.6	<u>0.077</u>	0.41	5.2	<u>0.093</u>	0.30	5.9
5.00	0.097	0.60	3.9	<u>0.073</u>	0.40	4.7	<u>0.084</u>	0.29	5.4
5.50	0.089	0.57	3.8	<u>0.074</u>	0.40	4.3	<u>0.078</u>	0.28	5.1

Model 2728 $L_P/\nabla^{1/3} = 8.4-8.9$ $L_P/B_{PX} = 6.95$ $\beta_5 = 13^\circ$

F_V	LCG=44% L_P			LCG=28% L_P			LCG=20% L_P		
	R_R/W	L_M/L_P	τ_{BL}	R_R/W	L_M/L_P	τ_{BL}	R_R/W	L_M/L_P	τ_{BL}
1.25	-	-	-	-	-	-	-	-	-
1.50	0.026	0.95	1.0	0.072	0.67	4.0	0.135	0.44	8.4
1.75	0.031	0.93	1.3	0.077	0.64	4.1	0.143	0.39	9.0
2.00	0.037	0.91	1.5	0.081	0.60	4.4	0.146	0.37	9.2
2.50	0.050	0.90	1.6	0.084	0.52	4.9	0.139	0.33	8.7
3.00	0.064	0.87	1.8	0.082	0.46	5.1	<u>0.123</u>	0.31	7.6
3.50	0.076	0.81	2.1	0.076	0.41	5.0	<u>0.105</u>	0.30	6.5
4.00	0.081	0.74	2.6	0.069	0.38	4.6	<u>0.087</u>	0.29	5.5
4.50	0.075	0.67	2.9	0.063	0.37	4.2	<u>0.074</u>	0.27	4.7
5.00	0.061	0.61	3.1	0.061	0.36	3.8	<u>0.066</u>	0.26	4.3
5.50	0.049	0.57	3.0	0.059	0.35	3.4	<u>0.063</u>	0.25	3.9

Model 2729 $L_P/\nabla^{1/3} = 8.4-8.9$ $L_P/B_{PX} = 6.0$ $\beta_5 = 10^\circ$

F_V	LCG=44% L_P			LCG=27% L_P			LCG=19% L_P		
	R_R/W	L_M/L_P	τ_{BL}	R_R/W	L_M/L_P	τ_{BL}	R_R/W	L_M/L_P	τ_{BL}
1.25	-	-	-	-	-	-	-	-	-
1.50	0.024	0.96	1.0	0.071	0.61	4.2	0.152	0.42	9.4
1.75	0.028	0.92	1.3	0.075	0.57	4.5	0.161	0.38	9.7
2.00	0.034	0.90	1.5	0.079	0.53	4.8	0.160	0.35	9.6
2.50	0.048	0.87	1.7	0.084	0.46	5.2	<u>0.142</u>	0.30	8.5
3.00	0.058	0.83	2.0	0.084	0.40	5.3	<u>0.117</u>	0.27	7.1
3.50	0.061	0.74	2.4	0.078	0.36	4.9	<u>0.098</u>	0.26	6.0
4.00	0.061	0.64	2.8	<u>0.069</u>	0.34	4.4	<u>0.082</u>	0.26	5.1
4.50	0.059	0.56	3.1	<u>0.061</u>	0.32	3.9	<u>0.072</u>	0.24	4.5
5.00	0.060	0.53	3.0	0.055	0.31	3.5	<u>0.066</u>	0.21	4.1
5.50	0.064	0.51	2.9	0.054	0.30	3.2	<u>0.062</u>	0.19	3.9

Model 2730 $L_P/\nabla^{1/3} = 8.4-8.9$ $L_P/B_{PX} = 5.1$ $\beta_5 = 7^\circ$

F_V	LCG=44% L_P			LCG=25% L_P			LCG=17% L_P		
	R_R/W	L_M/L_P	τ_{BL}	R_R/W	L_M/L_P	τ_{BL}	R_R/W	L_M/L_P	τ_{BL}
1.25	-	-	-	-	-	-	-	-	-
1.50	0.024	0.96	1.1	0.077	0.53	4.8	0.158	0.35	10.0
1.75	0.030	0.92	1.4	0.078	0.48	5.0	0.159	0.33	10.0
2.00	0.036	0.89	1.5	0.080	0.44	5.2	0.154	0.30	9.6
2.50	0.047	0.84	1.7	0.082	0.39	5.2	<u>0.133</u>	0.27	8.1
3.00	0.055	0.77	1.9	<u>0.079</u>	0.36	4.9	<u>0.109</u>	0.25	6.5
3.50	0.060	0.68	2.2	<u>0.072</u>	0.34	4.4	<u>0.088</u>	0.24	5.3
4.00	0.060	0.60	2.5	<u>0.064</u>	0.32	3.9	<u>0.072</u>	0.24	4.5
4.50	0.053	0.54	2.6	<u>0.058</u>	0.31	3.4	<u>0.061</u>	0.23	3.9
5.00	0.042	0.52	2.5	<u>0.054</u>	0.30	3.1	<u>0.056</u>	0.23	3.6
5.50	<u>0.034</u>	0.50	2.4	<u>0.049</u>	0.30	2.8	<u>0.052</u>	0.22	3.3

Model 2731 $L_p/\nabla^{1/3} = 8.4-8.9$ $L_p/B_{PX} = 4.4$ $\beta_5 = 5^\circ$

F_V	LCG=44% L_P			LCG=23% L_P			LCG=16% L_P		
	R_R/W	L_M/L_P	τ_{BL}	R_R/W	L_M/L_P	τ_{BL}	R_R/W	L_M/L_P	τ_{BL}
1.25	-	-	-	-	-	-	-	-	-
1.50	0.021	0.95	1.0	0.107	0.42	6.4	0.184	0.30	11.1
1.75	0.029	0.90	1.3	0.103	0.39	6.2	0.179	0.26	10.9
2.00	0.036	0.86	1.5	0.098	0.37	5.9	0.166	0.23	10.1
2.50	0.047	0.80	1.8	<u>0.085</u>	0.33	5.2	<u>0.129</u>	0.21	7.7
3.00	0.056	0.73	1.9	<u>0.073</u>	0.31	4.6	<u>0.095</u>	0.21	5.6
3.50	0.062	0.64	2.1	<u>0.065</u>	0.29	4.0	<u>0.074</u>	0.21	4.4
4.00	0.064	0.56	2.3	<u>0.059</u>	0.28	3.5	<u>0.062</u>	0.21	3.8
4.50	0.062	0.49	2.2	<u>0.053</u>	0.27	3.1	<u>0.056</u>	0.20	3.4
5.00	0.057	0.45	2.1	<u>0.048</u>	0.25	2.8	<u>0.053</u>	0.18	3.1
5.50	0.054	0.43	2.0	<u>0.047</u>	0.23	2.5	<u>0.055</u>	0.16	2.8

Model 2732 $L_p/\nabla^{1/3} = 6.7-7.1$ $L_p/B_{PX} = 6.0$ $\beta_5 = 20^\circ$

F_V	LCG=44% L_P			LCG=34% L_P			LCG=27% L_P		
	R_R/W	L_M/L_P	τ_{BL}	R_R/W	L_M/L_P	τ_{BL}	R_R/W	L_M/L_P	τ_{BL}
1.25	0.042	0.96	1.4	0.068	0.83	4.2	0.115	0.66	7.3
1.50	0.050	0.94	2.0	0.076	0.80	4.4	0.127	0.62	8.0
1.75	0.059	0.93	2.3	0.085	0.77	4.8	0.135	0.58	8.6
2.00	0.067	0.93	2.5	0.094	0.73	5.3	0.140	0.53	9.1
2.50	0.080	0.90	2.8	0.104	0.64	6.1	0.140	0.46	9.3
3.00	0.087	0.83	3.7	0.101	0.57	6.3	<u>0.129</u>	0.43	8.5
3.50	0.089	0.74	4.6	0.090	0.52	6.1	<u>0.112</u>	0.41	7.3
4.00	0.087	0.66	4.8	0.081	0.49	5.6	<u>0.096</u>	0.40	6.3
4.50	0.084	0.62	4.4	0.076	0.49	5.1	<u>0.085</u>	0.39	5.8
5.00	0.080	0.60	4.0	0.073	0.48	4.7	<u>0.075</u>	0.37	5.2
5.50	-	-	-	-	-	-	-	-	-

Model 2733 $L_p/\nabla^{1/3} = 6.7-7.1$ $L_p/B_{PX} = 4.9$ $\beta_5 = 13^\circ$

F_V	LCG=44% L_P			LCG=33% L_P			LCG=25% L_P		
	R_R/W	L_M/L_P	τ_{BL}	R_R/W	L_M/L_P	τ_{BL}	R_R/W	L_M/L_P	τ_{BL}
1.25	0.036	0.98	1.5	0.070	0.78	4.5	0.123	0.58	8.2
1.50	0.043	0.93	2.1	0.076	0.74	4.8	0.145	0.53	9.3
1.75	0.050	0.90	2.5	0.082	0.69	5.2	0.155	0.48	9.8
2.00	0.058	0.88	2.7	0.087	0.63	5.6	<u>0.157</u>	0.44	9.8
2.50	0.068	0.83	3.0	0.092	0.54	6.1	<u>0.143</u>	0.38	8.8
3.00	0.069	0.74	3.5	<u>0.088</u>	0.49	5.8	<u>0.119</u>	0.36	7.4
3.50	0.064	0.65	3.9	<u>0.080</u>	0.46	5.2	<u>0.094</u>	0.37	6.1
4.00	0.058	0.59	4.0	<u>0.070</u>	0.45	4.7	<u>0.077</u>	0.36	5.1
4.50	0.054	0.58	3.7	<u>0.063</u>	0.44	4.3	<u>0.070</u>	0.35	4.7
5.00	0.048	0.57	3.4	<u>0.057</u>	0.43	4.0	<u>0.063</u>	0.35	4.3
5.50	-	-	-	-	-	-	-	-	-

Model 2734 $L_p/\nabla^{1/3} = 6.7-7.1$ $L_p/B_{PX} = 4.3$ $\beta_5 = 10^\circ$

F_V	LCG=44% L_P			LCG=31% L_P			LCG=23% L_P		
	R_R/W	L_M/L_P	τ_{BL}	R_R/W	L_M/L_P	τ_{BL}	R_R/W	L_M/L_P	τ_{BL}
1.25	0.034	0.98	1.3	0.074	0.72	4.8	0.145	0.51	9.3
1.50	0.041	0.95	2.0	0.080	0.66	5.3	0.167	0.45	10.4
1.75	0.046	0.91	2.3	0.086	0.61	5.7	<u>0.172</u>	0.41	10.6
2.00	0.050	0.88	2.6	0.091	0.56	5.9	<u>0.165</u>	0.38	10.0
2.50	0.055	0.79	2.9	<u>0.094</u>	0.49	6.0	<u>0.133</u>	0.36	8.2
3.00	0.056	0.70	3.3	<u>0.087</u>	0.45	5.5	<u>0.105</u>	0.33	6.5
3.50	<u>0.054</u>	0.61	3.6	<u>0.072</u>	0.43	4.7	<u>0.083</u>	0.31	5.3
4.00	<u>0.049</u>	0.56	3.5	<u>0.059</u>	0.42	4.0	<u>0.069</u>	0.30	4.5
4.50	<u>0.045</u>	0.55	3.1	<u>0.054</u>	0.41	3.7	<u>0.061</u>	0.31	4.1
5.00	<u>0.041</u>	0.54	2.9	<u>0.050</u>	0.39	3.4	<u>0.055</u>	0.30	3.7
5.50	-	-	-	-	-	-	-	-	-

Model 2735 $L_p/\nabla^{1/3} = 6.7-7.1$ $L_p/B_{PX} = 3.6$ $\beta_5 = 7^\circ$

F_v	LCG=44% L_p			LCG=29% L_p			LCG=21% L_p		
	R_R/W	L_M/L_P	τ_{BL}	R_R/W	L_M/L_P	τ_{BL}	R_R/W	L_M/L_P	τ_{BL}
1.25	0.041	0.91	2.1	0.082	0.62	5.3	0.166	0.46	10.6
1.50	0.043	0.90	2.2	0.095	0.57	6.0	0.177	0.42	11.0
1.75	0.044	0.88	2.3	0.101	0.52	6.2	0.172	0.38	10.7
2.00	0.044	0.83	2.6	<u>0.101</u>	0.49	6.2	<u>0.158</u>	0.36	9.7
2.50	0.045	0.73	3.0	<u>0.091</u>	0.46	5.7	<u>0.121</u>	0.33	7.4
3.00	0.046	0.64	3.2	<u>0.077</u>	0.43	4.9	<u>0.094</u>	0.30	5.8
3.50	0.046	0.57	3.2	<u>0.064</u>	0.41	4.1	<u>0.076</u>	0.29	4.9
4.00	<u>0.043</u>	0.54	3.0	<u>0.053</u>	0.40	3.5	<u>0.064</u>	0.29	4.2
4.50	<u>0.038</u>	0.54	2.7	<u>0.046</u>	0.40	3.2	<u>0.054</u>	0.29	3.6
5.00	<u>0.034</u>	0.53	2.5	<u>0.041</u>	0.40	2.9	<u>0.048</u>	0.30	3.2
5.50	-	-	-	-	-	-	-	-	-

Model 2736 $L_p/\nabla^{1/3} = 6.7-7.1$ $L_p/B_{PX} = 3.1$ $\beta_5 = 5^\circ$

F_v	LCG=44% L_p			LCG=27% L_p			LCG=19% L_p		
	R_R/W	L_M/L_P	τ_{BL}	R_R/W	L_M/L_P	τ_{BL}	R_R/W	L_M/L_P	τ_{BL}
1.25	0.031	0.95	1.4	0.091	0.57	5.9	0.183	0.39	11.5
1.50	0.037	0.88	2.1	0.110	0.52	6.8	0.189	0.34	11.7
1.75	0.041	0.81	2.5	0.115	0.48	6.9	0.178	0.31	10.9
2.00	0.044	0.76	2.7	<u>0.110</u>	0.44	6.7	<u>0.156</u>	0.29	9.5
2.50	0.047	0.65	2.9	<u>0.088</u>	0.39	5.5	<u>0.109</u>	0.27	6.6
3.00	0.050	0.58	3.0	<u>0.071</u>	0.36	4.5	<u>0.082</u>	0.27	5.0
3.50	0.051	0.52	3.0	<u>0.060</u>	0.34	3.9	<u>0.069</u>	0.26	4.4
4.00	0.046	0.49	2.8	<u>0.052</u>	0.34	3.4	<u>0.059</u>	0.26	3.9
4.50	0.038	0.47	2.5	<u>0.046</u>	0.34	3.0	<u>0.048</u>	0.26	3.2
5.00	<u>0.032</u>	0.46	2.3	<u>0.043</u>	0.32	2.8	<u>0.041</u>	0.25	2.8
5.50	-	-	-	-	-	-	-	-	-

Model 2737 $L_p/\nabla^{1/3} = 5.8-6.2$ $L_p/B_{PX} = 4.9$ $\beta_5 = 20^\circ$

F_v	LCG=44% L_p			LCG=36% L_p			LCG=30% L_p		
	R_R/W	L_M/L_P	τ_{BL}	R_R/W	L_M/L_P	τ_{BL}	R_R/W	L_M/L_P	τ_{BL}
1.25	0.056	0.96	2.2	0.079	0.86	4.8	0.124	0.71	8.2
1.50	0.068	0.95	2.9	0.092	0.82	5.5	0.146	0.65	9.3
1.75	0.078	0.93	3.5	0.106	0.77	6.3	0.158	0.60	10.1
2.00	0.087	0.90	3.9	0.117	0.71	7.0	0.163	0.55	10.6
2.50	0.100	0.81	4.9	0.127	0.62	7.8	0.156	0.48	10.4
3.00	0.106	0.71	5.8	0.119	0.55	7.6	<u>0.138</u>	0.45	9.2
3.50	0.105	0.63	6.2	0.105	0.51	6.8	<u>0.117</u>	0.44	7.7
4.00	0.100	0.60	5.8	0.096	0.50	6.2	<u>0.102</u>	0.43	6.8
4.50	0.093	0.59	5.1	0.090	0.50	5.7	<u>0.092</u>	0.42	6.3
5.00	-	-	-	-	-	-	-	-	-
5.50	-	-	-	-	-	-	-	-	-

Model 2738 $L_p/\nabla^{1/3} = 5.8-6.2$ $L_p/B_{PX} = 4.0$ $\beta_5 = 13^\circ$

F_v	LCG=44% L_p			LCG=35% L_p			LCG=28% L_p		
	R_R/W	L_M/L_P	τ_{BL}	R_R/W	L_M/L_P	τ_{BL}	R_R/W	L_M/L_P	τ_{BL}
1.25	0.055	0.96	2.4	0.084	0.79	5.4	0.144	0.61	9.6
1.50	0.062	0.93	3.1	0.097	0.73	6.2	0.168	0.56	10.9
1.75	0.070	0.89	3.7	0.108	0.67	7.0	0.179	0.52	11.4
2.00	0.077	0.84	4.2	0.115	0.61	7.5	<u>0.178</u>	0.48	11.1
2.50	0.085	0.73	5.1	<u>0.118</u>	0.52	7.8	<u>0.158</u>	0.43	9.7
3.00	0.082	0.63	5.5	<u>0.107</u>	0.48	7.1	<u>0.128</u>	0.39	8.1
3.50	0.076	0.56	5.5	<u>0.093</u>	0.46	6.1	<u>0.103</u>	0.37	6.7
4.00	0.070	0.54	5.0	<u>0.083</u>	0.44	5.5	<u>0.091</u>	0.36	6.0
4.50	0.067	0.53	4.6	<u>0.076</u>	0.42	5.2	<u>0.086</u>	0.35	5.7
5.00	-	-	-	-	-	-	-	-	-
5.50	-	-	-	-	-	-	-	-	-

Model 2739 $L_p/\nabla^{1/3} = 5.8-6.2$ $L_p/B_{PX} = 3.5$ $\beta_5 = 10^\circ$

F_V	LCG=44% L_P			LCG=33% L_P			LCG=26% L_P		
	R_R/W	L_M/L_P	τ_{BL}	R_R/W	L_M/L_P	τ_{BL}	R_R/W	L_M/L_P	τ_{BL}
1.25	0.050	0.97	2.1	0.084	0.74	5.6	0.155	0.56	10.3
1.50	0.057	0.92	2.8	0.094	0.67	6.5	0.173	0.49	11.3
1.75	0.061	0.87	3.4	0.102	0.62	6.9	0.174	0.45	11.2
2.00	0.064	0.82	3.8	<u>0.106</u>	0.57	7.0	<u>0.164</u>	0.41	10.4
2.50	0.065	0.71	4.3	<u>0.104</u>	0.51	6.6	<u>0.132</u>	0.37	8.2
3.00	0.065	0.63	4.4	<u>0.090</u>	0.47	5.8	<u>0.105</u>	0.35	6.6
3.50	0.062	0.58	4.3	<u>0.073</u>	0.45	4.9	<u>0.085</u>	0.34	5.6
4.00	0.056	0.55	3.9	<u>0.063</u>	0.45	4.3	<u>0.072</u>	0.34	4.9
4.50	0.050	0.54	3.6	<u>0.058</u>	0.44	4.0	<u>0.063</u>	0.34	4.3
5.00	-	-	-	-	-	-	-	-	-
5.50	-	-	-	-	-	-	-	-	-

Model 2740 $L_p/\nabla^{1/3} = 5.8-6.2$ $L_p/B_{PX} = 3.0$ $\beta_5 = 7^\circ$

F_V	LCG=44% L_P			LCG=32% L_P			LCG=24% L_P		
	R_R/W	L_M/L_P	τ_{BL}	R_R/W	L_M/L_P	τ_{BL}	R_R/W	L_M/L_P	τ_{BL}
1.25	0.047	0.96	2.3	0.092	0.67	6.1	0.178	0.49	11.4
1.50	0.053	0.89	3.0	0.106	0.59	6.9	0.195	0.43	12.2
1.75	0.056	0.82	3.6	0.111	0.53	7.1	<u>0.187</u>	0.40	11.6
2.00	0.058	0.75	3.9	0.109	0.49	6.9	<u>0.165</u>	0.39	10.1
2.50	<u>0.060</u>	0.65	4.1	<u>0.093</u>	0.44	5.9	<u>0.116</u>	0.38	7.1
3.00	<u>0.059</u>	0.59	4.0	<u>0.074</u>	0.43	4.8	<u>0.085</u>	0.36	5.4
3.50	<u>0.055</u>	0.56	3.7	<u>0.059</u>	0.43	4.0	<u>0.069</u>	0.34	4.6
4.00	<u>0.049</u>	0.54	3.4	<u>0.051</u>	0.43	3.6	<u>0.061</u>	0.35	4.1
4.50	<u>0.043</u>	0.53	3.1	<u>0.047</u>	0.42	3.3	<u>0.053</u>	0.35	3.6
5.00	-	-	-	-	-	-	-	-	-
5.50	-	-	-	-	-	-	-	-	-

Model 2741 $L_p/\nabla^{1/3} = 5.8-6.2$ $L_p/B_{PX} = 2.5$ $\beta_5 = 5^\circ$

F_V	LCG=44% L_P			LCG=30% L_P			LCG=22% L_P		
	R_R/W	L_M/L_P	τ_{BL}	R_R/W	L_M/L_P	τ_{BL}	R_R/W	L_M/L_P	τ_{BL}
1.25	0.042	0.94	2.2	0.110	0.59	7.1	0.198	0.44	12.1
1.50	0.048	0.86	3.1	0.117	0.52	7.6	0.200	0.39	12.1
1.75	0.051	0.78	3.5	0.114	0.48	7.5	0.182	0.36	11.0
2.00	0.052	0.72	3.6	0.106	0.44	6.8	<u>0.153</u>	0.35	9.3
2.50	<u>0.052</u>	0.62	3.5	<u>0.084</u>	0.41	5.3	<u>0.100</u>	0.36	6.2
3.00	<u>0.050</u>	0.57	3.4	<u>0.067</u>	0.41	4.3	<u>0.075</u>	0.37	4.8
3.50	<u>0.046</u>	0.55	3.1	<u>0.055</u>	0.41	3.7	<u>0.064</u>	0.37	4.2
4.00	<u>0.041</u>	0.54	2.9	<u>0.046</u>	0.41	3.2	<u>0.053</u>	0.35	3.6
4.50	<u>0.036</u>	0.53	2.6	<u>0.040</u>	0.40	2.8	<u>0.043</u>	0.34	3.0
5.00	-	-	-	-	-	-	-	-	-
5.50	-	-	-	-	-	-	-	-	-

Model 2742 $L_p/\nabla^{1/3} = 5.3-5.6$ $L_p/B_{PX} = 4.3$ $\beta_5 = 20^\circ$

F_V	LCG=44% L_P			LCG=37% L_P			LCG=32% L_P		
	R_R/W	L_M/L_P	τ_{BL}	R_R/W	L_M/L_P	τ_{BL}	R_R/W	L_M/L_P	τ_{BL}
1.25	0.070	0.96	2.7	0.094	0.86	5.6	0.142	0.72	9.3
1.50	0.087	0.93	3.8	0.116	0.81	6.9	0.170	0.64	10.9
1.75	0.101	0.89	4.7	0.131	0.74	7.9	0.181	0.59	11.6
2.00	0.112	0.84	5.6	0.140	0.68	8.6	0.180	0.55	11.8
2.50	0.123	0.74	6.7	0.140	0.59	9.0	0.163	0.49	10.9
3.00	0.121	0.65	7.0	0.122	0.54	8.3	<u>0.140</u>	0.45	9.3
3.50	0.112	0.60	6.8	0.103	0.52	7.4	<u>0.120</u>	0.43	7.9
4.00	0.104	0.59	6.2	0.092	0.50	6.7	<u>0.109</u>	0.43	7.3
4.50	0.098	0.56	5.8	0.087	0.48	6.1	<u>0.096</u>	0.40	6.8
5.00	-	-	-	-	-	-	-	-	-
5.50	-	-	-	-	-	-	-	-	-

Model 2743 $L_p/\nabla^{1/3} = 5.3-5.6$ $L_p/B_{PX} = 3.5$ $\beta_5 = 13^\circ$

F_V	LCG=44% L_P			LCG=36% L_P			LCG=30% L_P		
	R_R/W	L_M/L_P	τ_{BL}	R_R/W	L_M/L_P	τ_{BL}	R_R/W	L_M/L_P	τ_{BL}
1.25	0.070	0.96	3.1	0.100	0.78	6.4	0.153	0.64	10.4
1.50	0.086	0.90	4.2	0.119	0.71	7.7	0.174	0.58	11.7
1.75	0.097	0.83	5.2	0.130	0.64	8.5	0.182	0.53	11.9
2.00	0.103	0.75	6.0	0.134	0.58	8.9	<u>0.178</u>	0.49	11.5
2.50	0.103	0.63	6.7	0.128	0.50	8.5	<u>0.156</u>	0.43	9.8
3.00	0.093	0.56	6.5	<u>0.111</u>	0.47	7.4	<u>0.126</u>	0.39	8.1
3.50	<u>0.084</u>	0.53	6.0	<u>0.095</u>	0.46	6.3	<u>0.103</u>	0.37	6.9
4.00	<u>0.081</u>	0.51	5.5	<u>0.086</u>	0.43	5.9	<u>0.093</u>	0.35	6.3
4.50	<u>0.075</u>	0.49	5.2	<u>0.077</u>	0.41	5.4	<u>0.085</u>	0.34	5.8
5.00	-	-	-	-	-	-	-	-	-
5.50	-	-	-	-	-	-	-	-	-

Model 2744 $L_p/\nabla^{1/3} = 5.3-5.6$ $L_p/B_{PX} = 3.0$ $\beta_5 = 10^\circ$

F_V	LCG=44% L_P			LCG=35% L_P			LCG=28% L_P		
	R_R/W	L_M/L_P	τ_{BL}	R_R/W	L_M/L_P	τ_{BL}	R_R/W	L_M/L_P	τ_{BL}
1.25	0.064	0.95	3.1	0.103	0.74	6.8	0.176	0.58	11.6
1.50	0.076	0.87	4.3	0.120	0.66	7.8	0.196	0.52	12.8
1.75	0.083	0.80	5.1	0.129	0.60	8.3	0.195	0.48	12.5
2.00	0.087	0.72	5.7	<u>0.131</u>	0.54	8.4	<u>0.179</u>	0.45	11.3
2.50	0.088	0.61	6.0	<u>0.120</u>	0.48	7.7	<u>0.138</u>	0.40	8.6
3.00	<u>0.083</u>	0.54	5.7	<u>0.100</u>	0.45	6.5	<u>0.110</u>	0.37	7.1
3.50	<u>0.075</u>	0.51	5.1	<u>0.082</u>	0.43	5.5	<u>0.094</u>	0.34	6.3
4.00	<u>0.066</u>	0.49	4.7	<u>0.075</u>	0.42	5.1	<u>0.084</u>	0.35	5.7
4.50	<u>0.060</u>	0.49	4.3	<u>0.068</u>	0.41	4.7	<u>0.078</u>	0.33	5.2
5.00	-	-	-	-	-	-	-	-	-
5.50	-	-	-	-	-	-	-	-	-

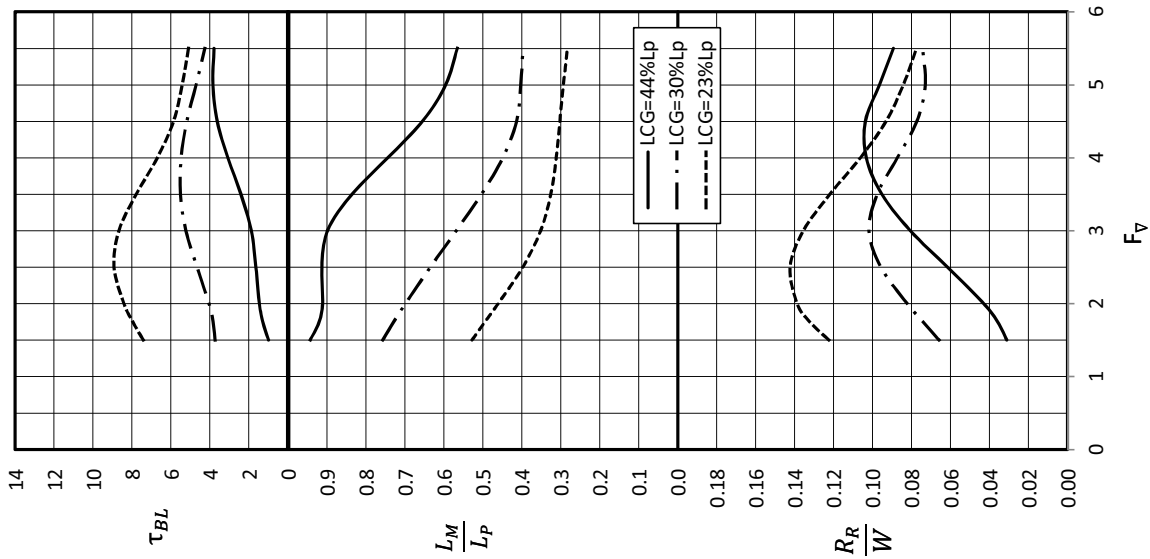
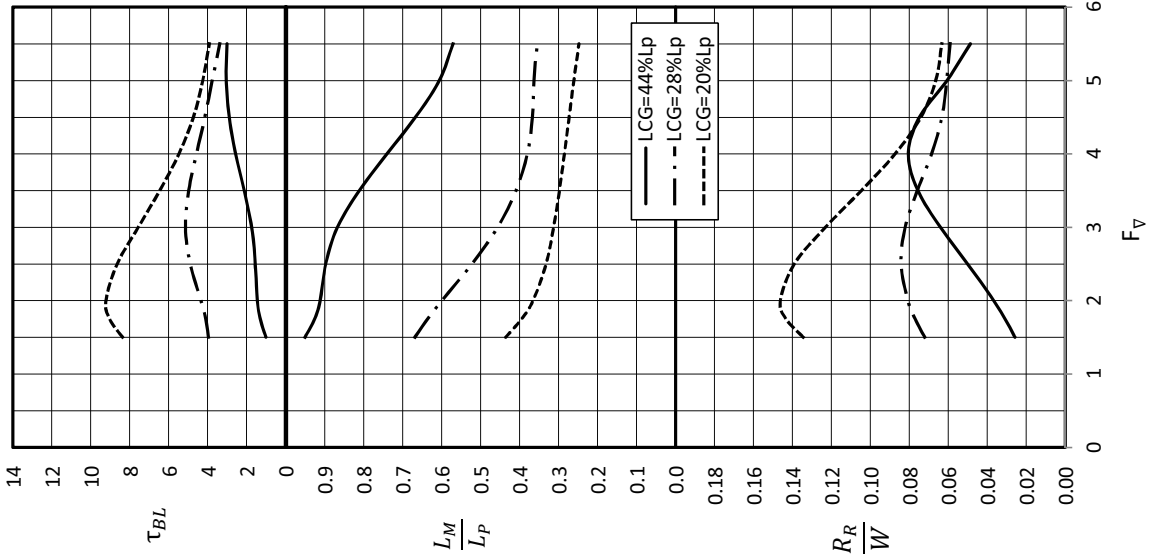
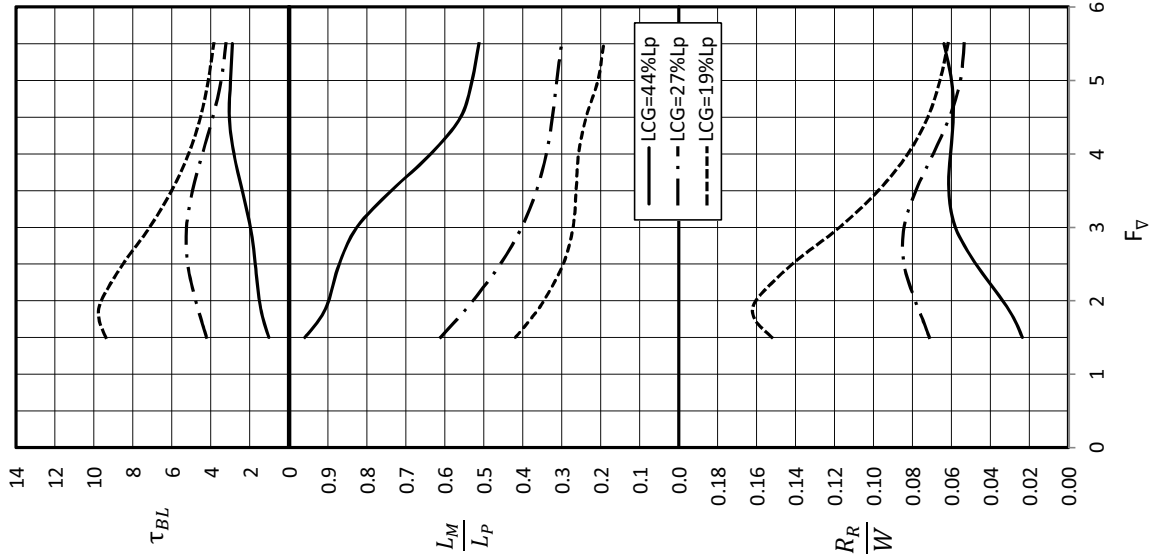
Model 2745 $L_p/\nabla^{1/3} = 5.3-5.6$ $L_p/B_{PX} = 2.6$ $\beta_5 = 7^\circ$

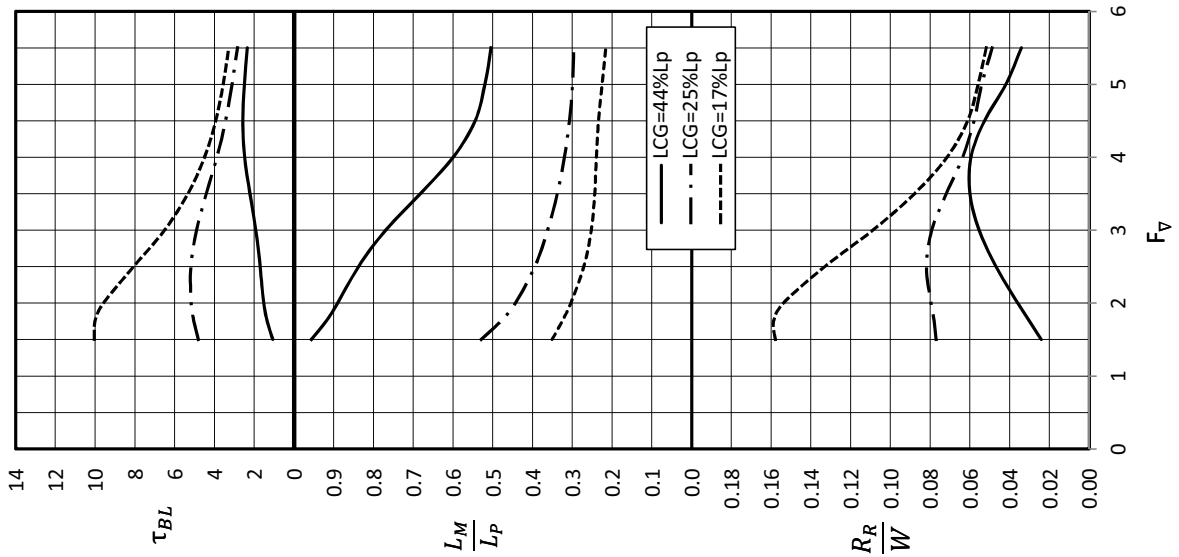
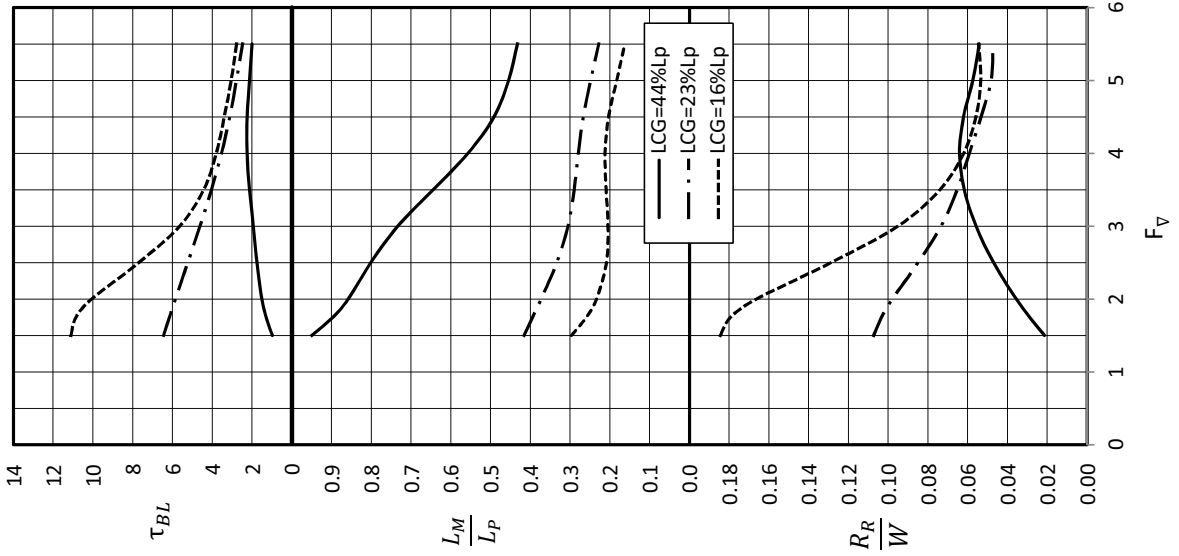
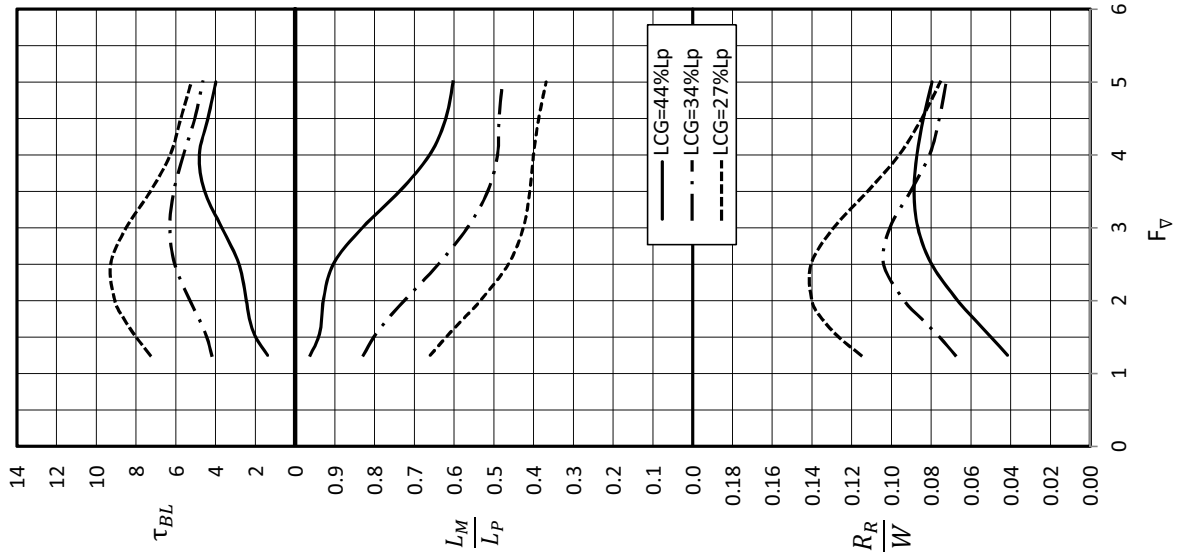
F_V	LCG=44% L_P			LCG=33% L_P			LCG=26% L_P		
	R_R/W	L_M/L_P	τ_{BL}	R_R/W	L_M/L_P	τ_{BL}	R_R/W	L_M/L_P	τ_{BL}
1.25	0.059	0.93	3.0	0.104	0.68	6.9	0.191	0.53	12.2
1.50	0.067	0.85	4.0	0.120	0.60	7.9	0.203	0.46	12.8
1.75	0.072	0.78	4.6	0.123	0.55	8.0	0.188	0.42	11.7
2.00	0.075	0.71	5.0	<u>0.117</u>	0.52	7.5	<u>0.159</u>	0.40	9.9
2.50	<u>0.074</u>	0.61	5.0	<u>0.094</u>	0.49	6.0	<u>0.110</u>	0.36	6.9
3.00	<u>0.066</u>	0.57	4.5	<u>0.073</u>	0.47	4.9	<u>0.086</u>	0.34	5.6
3.50	<u>0.058</u>	0.56	4.0	<u>0.059</u>	0.45	4.1	<u>0.076</u>	0.33	5.1
4.00	<u>0.053</u>	0.54	3.7	<u>0.054</u>	0.44	3.8	<u>0.069</u>	0.32	4.7
4.50	<u>0.050</u>	0.54	3.5	<u>0.048</u>	0.44	3.4	<u>0.062</u>	0.31	4.2
5.00	-	-	-	-	-	-	-	-	-
5.50	-	-	-	-	-	-	-	-	-

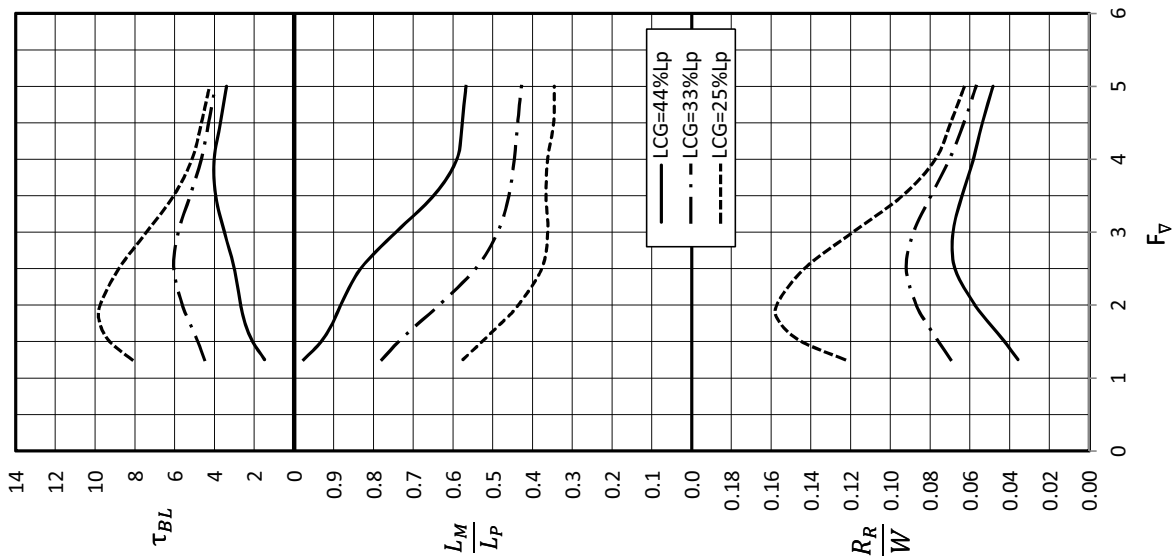
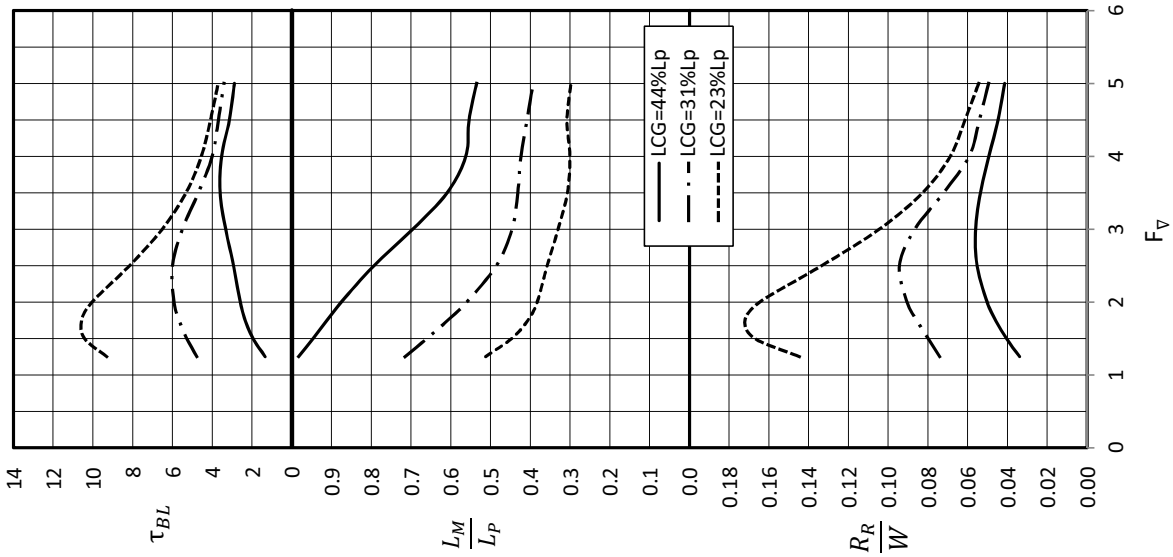
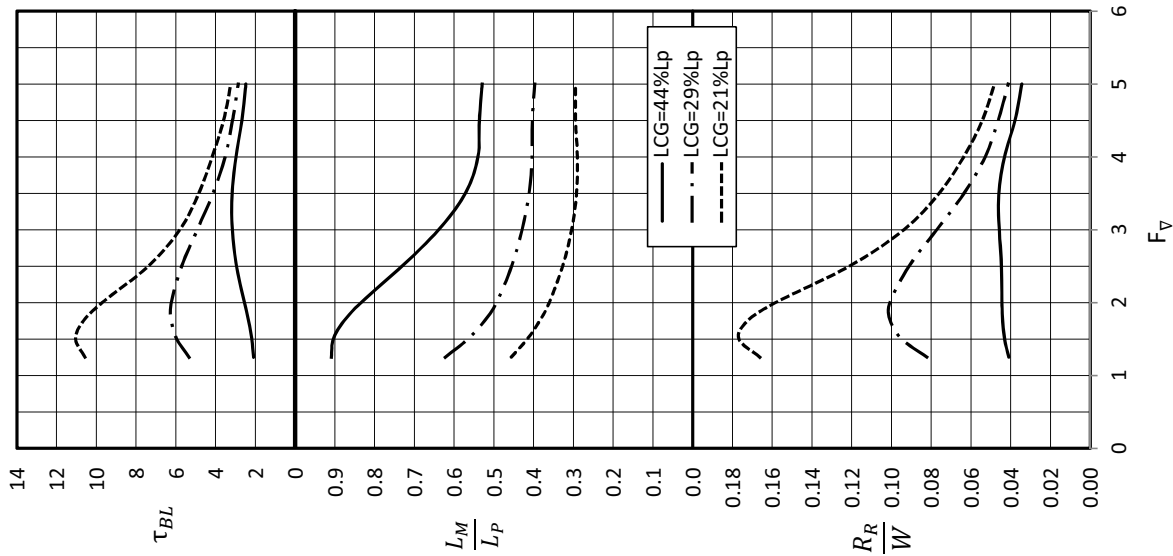
Model 2746 $L_p/\nabla^{1/3} = 5.3-5.6$ $L_p/B_{PX} = 2.2$ $\beta_5 = 5^\circ$

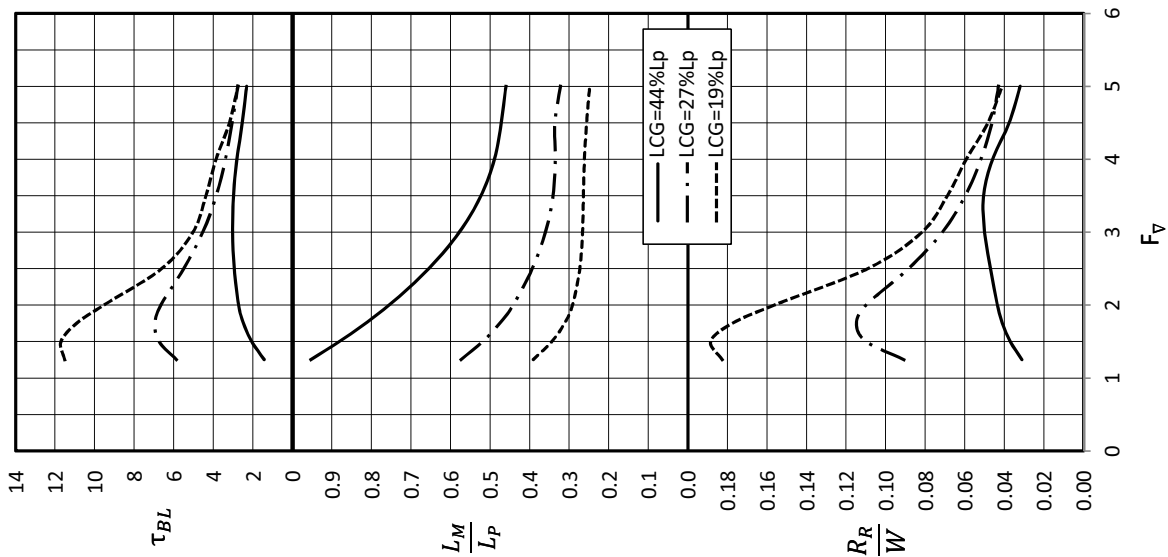
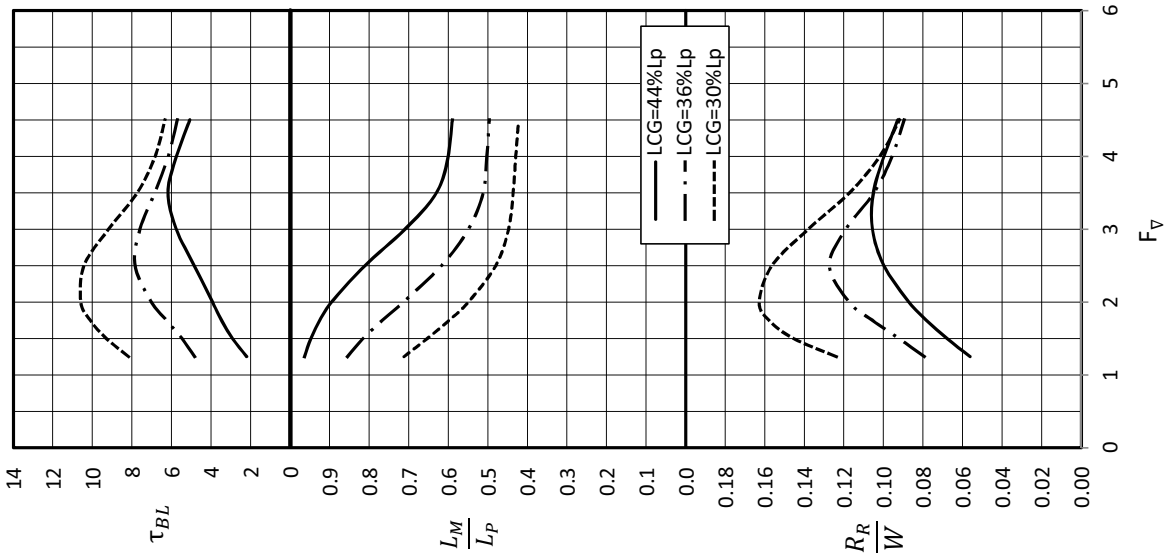
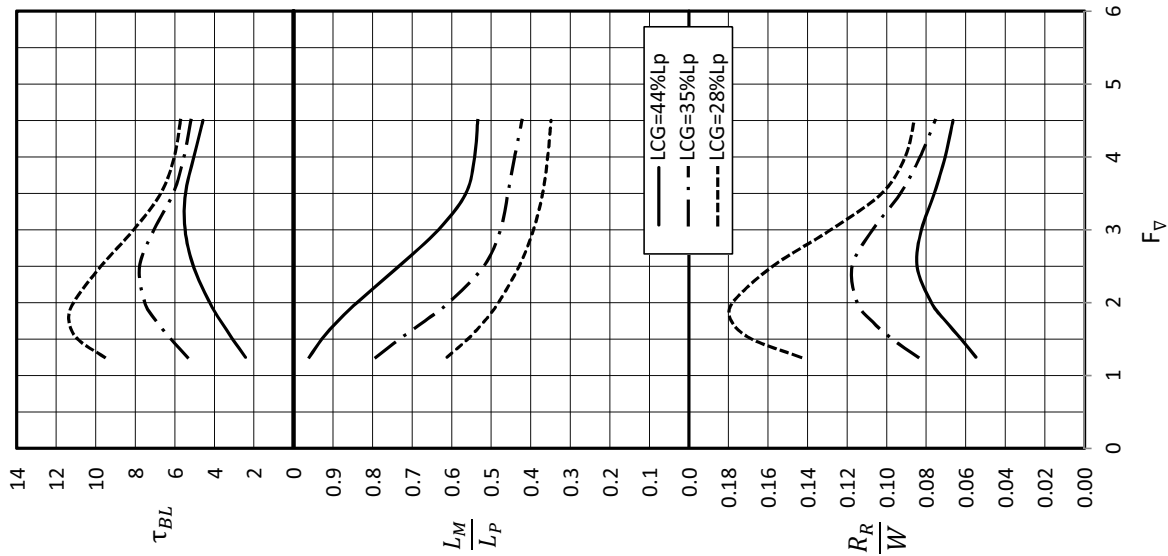
F_V	LCG=44% L_P			LCG=32% L_P			LCG=25% L_P		
	R_R/W	L_M/L_P	τ_{BL}	R_R/W	L_M/L_P	τ_{BL}	R_R/W	L_M/L_P	τ_{BL}
1.25	0.056	0.92	2.9	0.113	0.60	7.3	0.201	0.48	12.6
1.50	0.059	0.83	3.9	0.126	0.54	8.0	0.199	0.42	12.4
1.75	0.062	0.75	4.3	0.124	0.49	7.8	0.175	0.38	10.9
2.00	0.062	0.69	4.3	<u>0.113</u>	0.46	7.1	<u>0.145</u>	0.35	9.0
2.50	<u>0.060</u>	0.61	4.0	<u>0.085</u>	0.43	5.4	<u>0.102</u>	0.31	6.4
3.00	<u>0.056</u>	0.57	3.8	<u>0.066</u>	0.39	4.4	<u>0.079</u>	0.29	5.1
3.50	<u>0.049</u>	0.54	3.5	<u>0.054</u>	0.37	3.8	<u>0.065</u>	0.30	4.4
4.00	<u>0.044</u>	0.50	3.1	<u>0.045</u>	0.37	3.2	<u>0.055</u>	0.31	3.8
4.50	<u>0.040</u>	0.47	2.9	<u>0.039</u>	0.37	2.8	<u>0.052</u>	0.28	3.6
5.00	-	-	-	-	-	-	-	-	-
5.50	-	-	-	-	-	-	-	-	-

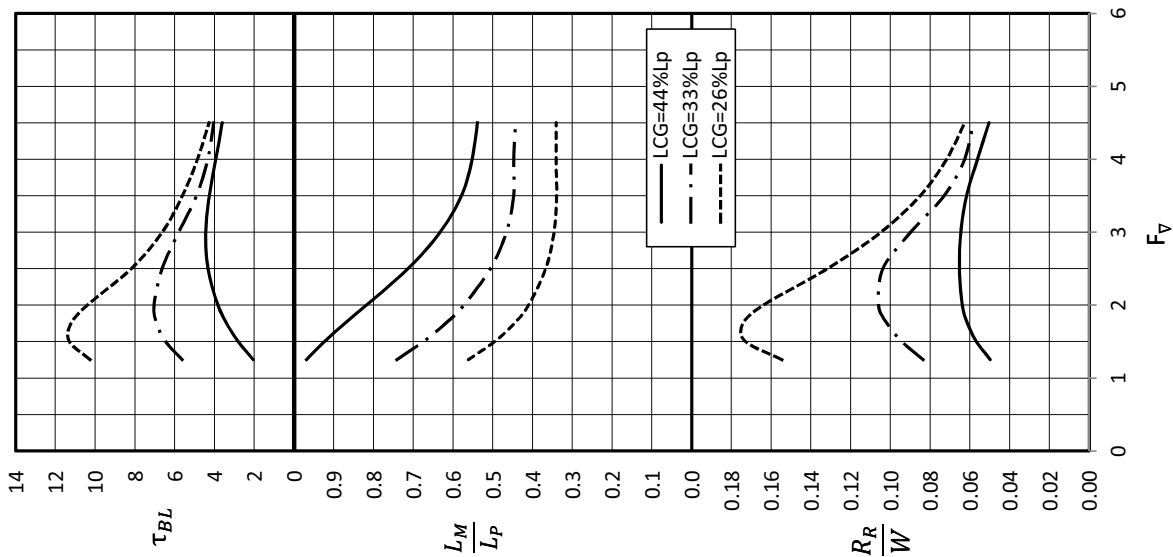
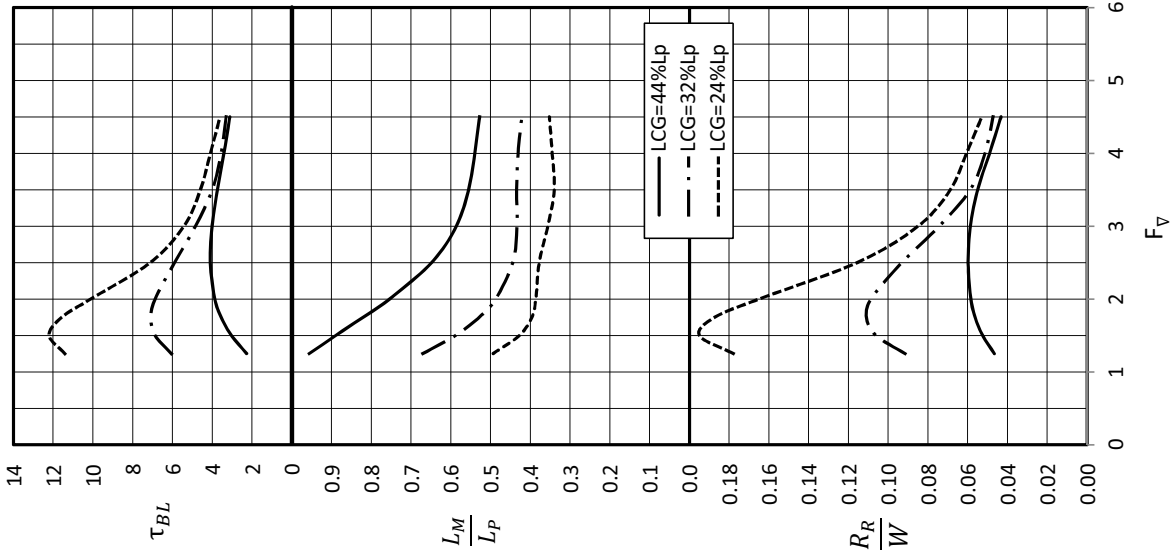
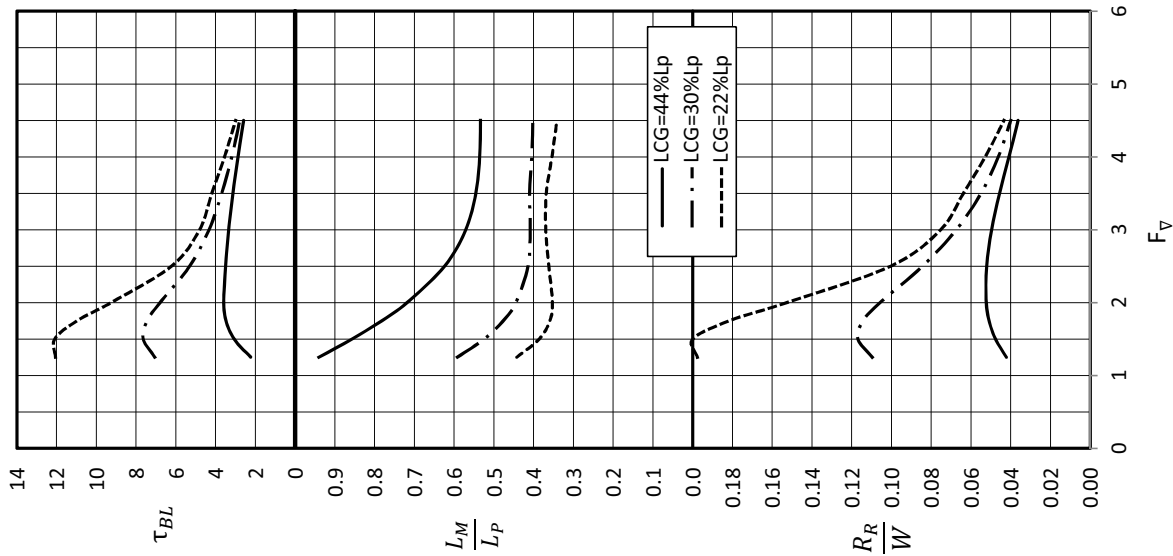
APPENDIX B - SERIES 50 DATA

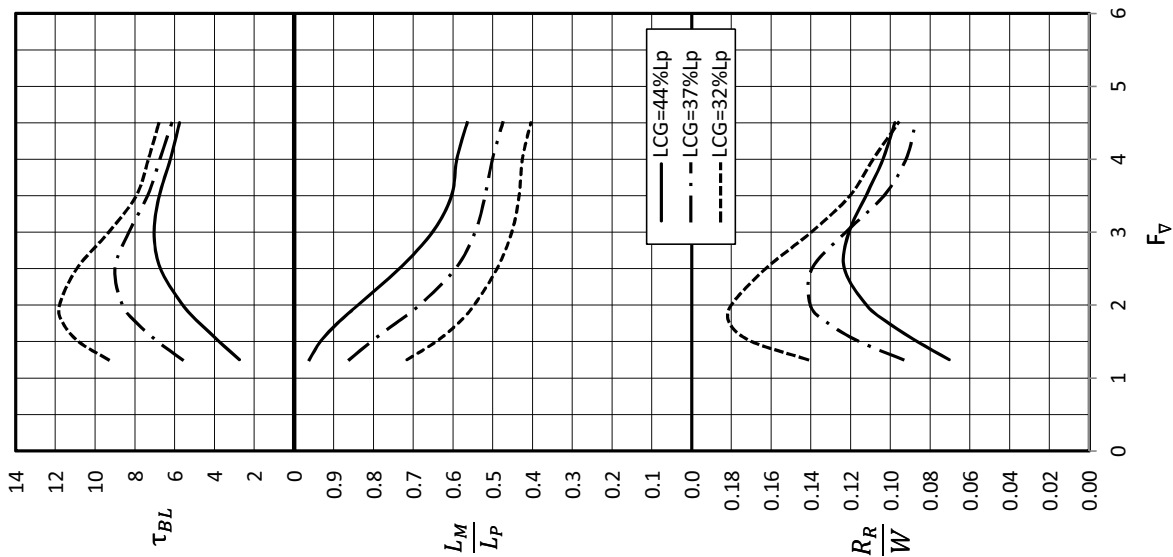
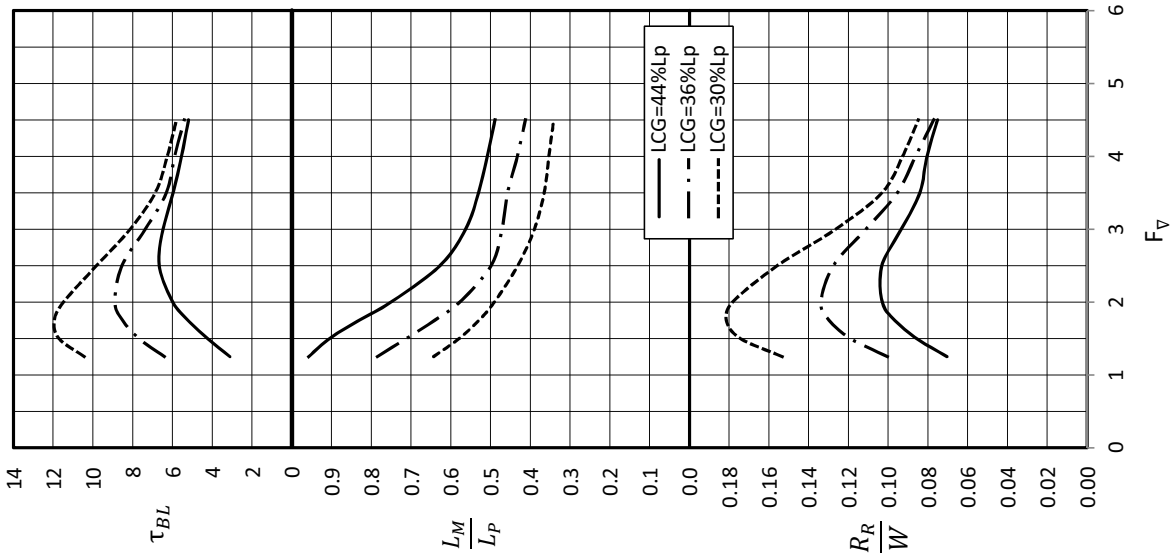
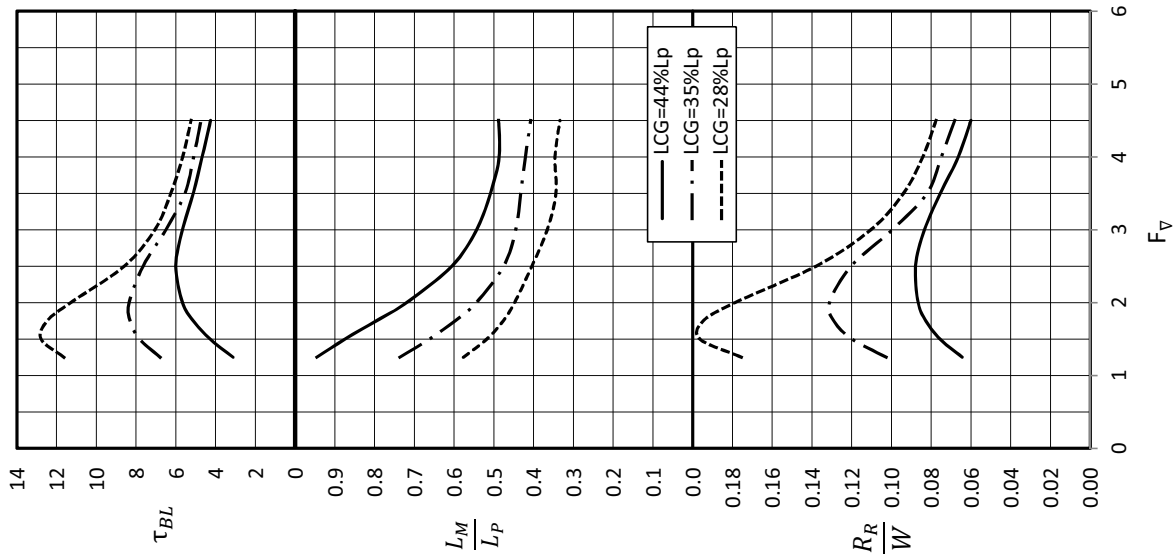


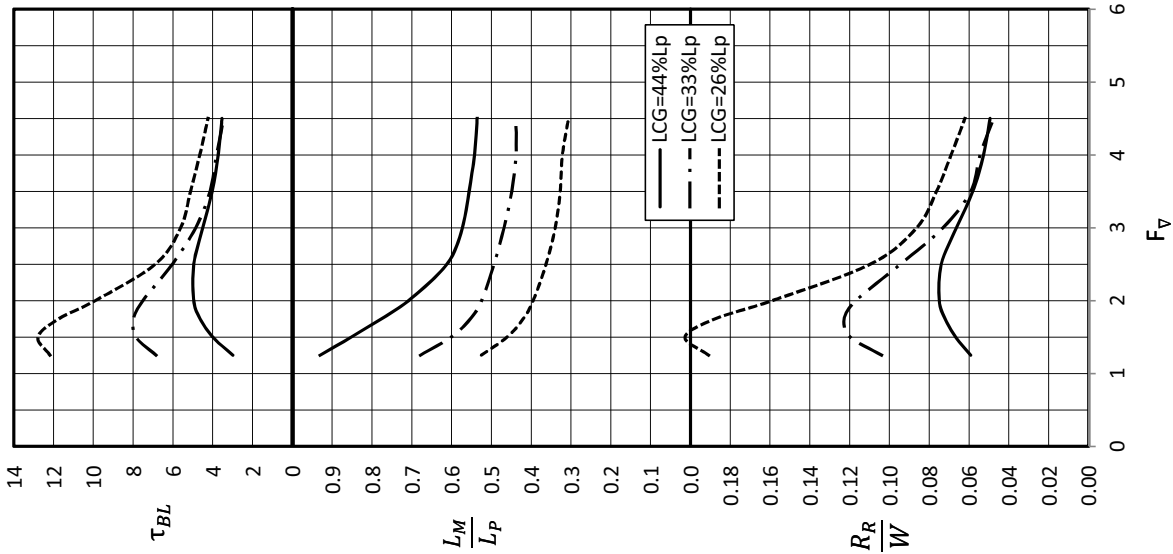
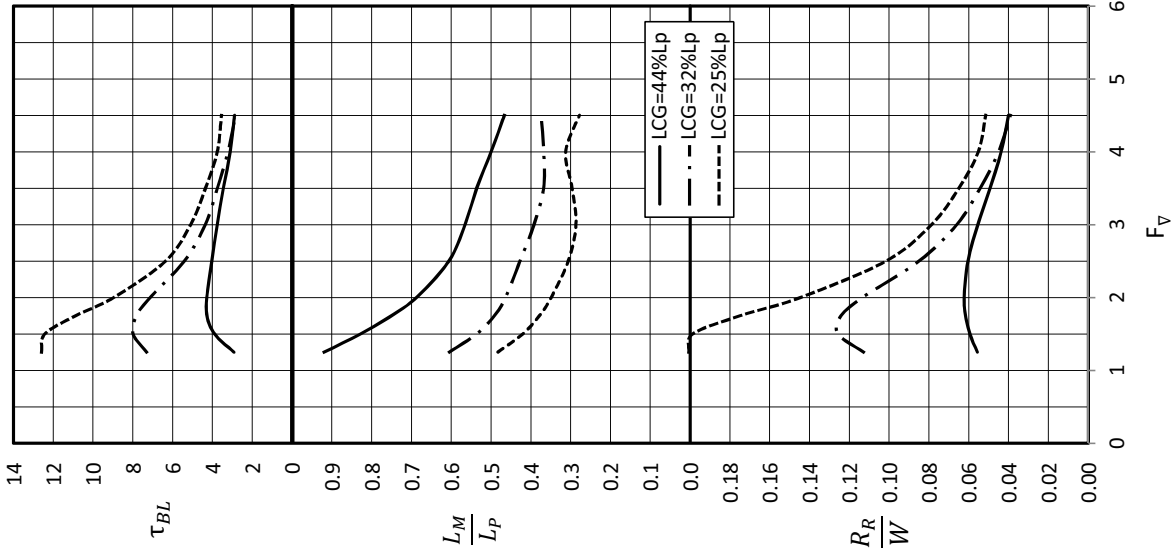












APPENDIX C: SAMPLE CALCULATIONS

This appendix includes sample calculation for the use of the standard series charts. The procedure for using the data tables is identical with the exception that the residuary resistance to weight ratio, mean wetted length and baseline trim are interpolated from the data tables instead of read off the graphs

Given:

Displacement Mass, Δ	= 75,000 kg
Speed, V	= 40 knots (20.6m/sec)
Max Chine Beam, b_{PX}	= 6 m
Planing Length, L_P	= 25m
LCG	= 9m

Non-Dimensional Parameters:

Displacement Force	$W = \Delta g$	$W = 75,000 \text{ kg} * 9.81 \text{ m/s}^2 = 736,000 \text{ N}$
Volume	$\nabla = \frac{\Delta}{\rho}$	$\nabla = \frac{75,000 \text{ kg}}{1025 \text{ kg/m}^3} = 73.2 \text{ m}^3$
Volumetric Coefficient	$\frac{L_P}{\nabla^{1/3}}$	$\frac{L_P}{\nabla^{1/3}} = \frac{25 \text{ m}}{(73.2 \text{ m}^3)^{1/3}} = 5.97$
Length-Beam Ratio:	$\frac{L_P}{b_{PX}}$	$\frac{L_P}{b_{PX}} = \frac{25}{6} = 4.16$
LCG-Length Ratio	$\frac{LCG}{L_P}$	$\frac{LCG}{L_P} = \frac{9}{25} = 36\%$
Volume Froude Number:	$F_{\nabla} = \frac{V}{\sqrt{g\nabla^{1/3}}}$	$F_{\nabla} = \frac{20.6}{\sqrt{9.81 \text{ m/s}^2 (73.2 \text{ m}^3)^{1/3}}} = 3.21$

Enter Charts:

Look for chart of hull with similar volumetric coefficient, length-beam ratio and find the closest LCG-Beam ratio. Alternately, interpolate from data tables. Model 2738 has a load condition with $\frac{L_P}{b_{PX}} = 4.0$ and $\frac{L_P}{\nabla^{1/3}} = 5.8-6.2$, which is very close. Using the curves for $\frac{LCG}{L_P} = 35\%$, at a volume Froude number of 3.21 yields the following:

Residuary Resistance to Weight Ratio	$\frac{R_R}{W} = 0.10$
Mean wetted length	$\frac{L_M}{L_P} = 0.47$
Baseline trim angle	$\tau_{BL} = 6.8 \text{ degrees}$

Calculate Resistance and EHP:

$$L_M = \left(\frac{L_M}{L_P}\right) L_P = 0.47 * 25 \text{ m} = 11.8 \text{ m}$$

$$S = 0.962 \left(\frac{L_M}{L_P}\right) L_P b_P = 0.962 * 0.47 * 25 \text{ m} * 6 \text{ m} = 67.8 \text{ m}^2$$

$$Re = \frac{VL_M}{\nu} = \frac{20.6 \text{ m/s} * 11.8 \text{ m}}{1.1892 \times 10^{-6} \text{ m}^2/\text{s}} = 2.04 \times 10^8$$

$$C_F = \frac{0.075}{(LOG_{10} Re - 2)^2} = \frac{0.075}{(LOG_{10} 2.04 \times 10^8 - 2)^2} = 0.00188$$

Assume correlation allowance, $C_a = 0$

$$R_T = \left(\frac{R_R}{W}\right) W + (C_F + C_a) \frac{1}{2} \rho V^2 S = 0.10 * 736,000 \text{ N} + (0.00188 + 0) \frac{1}{2} 1025 \text{ kg/m}^3 (20.6 \text{ m/s})^2 67.8 \text{ m}^2$$

$$R_T = 73,600 \text{ N} + 27,700 \text{ N} = 101,300 \text{ N}$$

$$EHP = R_T V = 101,300 \text{ N} * 20.6 \text{ m/s} = 2,090,000 \text{ Nm/s} = 2,090 \text{ kW}$$

Porpoising Check:

$$\tau_{BL} = 6.8 \text{ degrees}. \tau_{0.25} = -0.83 \text{ (From Table 2 Model 2738) Therefore, } \tau_H = 6.8 - 0.83 = 6.0 \text{ degrees}$$

$$\beta_5 = 13.2 \text{ degrees (From Table 2 Model 2738) Therefore, the large deadrise porpoising equation applies.}$$

$$\text{Porpoises when } \tau_H > \frac{35}{F_{\nabla}^{1.5}} = 6.1 \text{ degrees}$$

This hull is on the verge of porpoising. A designer should consider moving LCG forward or adding trim tabs to be safe.

Wind, Appendage, and Thrust Corrections

In the following example, the wind, appendage and thrust corrections are added to the bare-hull results of the previous example, for a standard twin-screw inboard propelled boat. Small changes in moment arms for wind and appendage drag due to trim are neglected for simplicity.

Given:

Hull:

Hull, load condition and speed is the same as the previous example.

Displacement Force, W	736,000N
Speed, V	20.6m/sec
Max Chine Beam, b_{PX}	6 m
LCG	9m

Thrust Line:

Shaft angle, ε	7°
Hub Location	2m ahead of transom
	1.5 m below waterline.

Wind:

Frontal Area, A_A	40 m ²
Center of Frontal Area	3m above waterline

Appendages:

Type	Twin-Screw Inboard
Propeller Diameter, D	1.25 m

Flap:

Two Flaps	
Span, s_F	1m
Chord, c_F	0.5m
Deflection, δ	5°

Step 1: Bare Hull

See previous example using charts.

Bare-Hull Resistance, R_T	101,300N
Baseline trim angle, τ_{BL}	6.8°

Step 2: Additional Components

Still Air Resistance

Assume aerodynamic drag coefficient, $C_{DA} = 0.6$

Assume no aerodynamic lift

$$R_{WIND} = C_{DA} \frac{1}{2} \rho_A V^2 A_X = 0.6 \frac{1}{2} 1.25 \frac{kg}{m^3} \left(20.6 \frac{m}{s}\right)^2 (40m^2) = 6400 N$$

Center of projected frontal area is 3m above waterline, or $3m - \frac{L_P}{80} = 2.69m$ above the model tow line.

Wind produces a bow up pitching moment of $+(6400N)(2.69m) = +17,200 Nm$ (positive bow up)

Inboard Appendages

Assume appendage drag coefficient, $C_{DP} = 0.071$

Assume no appendage lift

$$R_{AP} = C_{DP} \frac{1}{2} \rho V^2 \frac{\pi D^2}{4} = 0.071 \frac{1}{2} 1025 \frac{kg}{m^3} \left(20.6 \frac{m}{s}\right)^2 \frac{\pi (1.25m)^2}{4} = 18700 N \text{ per shaft } \times 2 \text{ shafts} = 37,400 N \text{ total}$$

Assume appendage resistance acts at 0.2 D above propeller hub.

$(1.5m - 0.2 (1.25m)) = 1.25m$ below waterline, or $1.25m + \frac{L_P}{80} = 1.56m$ below model thrust line.

Appendages produce a bow-down pitching moment of $-(1.56m)(37,400N) = -58,300 Nm$ (negative bow down)

Trim Flaps

$$L_{FLAP} = 0.046 s_F c_F \delta \frac{1}{2} \rho V^2 = 0.046 (1m)(0.5m)(5^\circ) \frac{1}{2} \left(1025 \frac{kg}{m^3}\right) \left(20.6 \frac{m}{s}\right)^2 = 25,000N \text{ per flap} = 50,000 N \text{ total}$$

$$R_{FLAP} = 0.0052 L_{FLAP} (\tau + \delta) = 0.0052 (25,000N)(6.8^\circ + 5^\circ) = 1500 N \text{ per flap} = 3000 N \text{ total}$$

Assume flap resistance does not create a pitching moment because it is small in magnitude and close to the DWL.

Flap lift acts at 0.6 beams (or 3.6m) forward of trailing edge of flap.

The location of flap lift with respect to the LCG is

$$LCG + Flap Chord - Center of Lift = 9m + 0.5m - 3.6m = 5.9m \text{ aft of LCG.}$$

Trim flaps produce a bow-down pitching moment of $-(50,000N)(5.9m) = -295,000 Nm$ (negative bow down)

Total Resistance

$$R_T = \sum R_i = R_{HULL} + R_{WIND} + R_{APPENDAGE} + R_{FLAP} = 101,300N + 6,400N + 37,400N + 3000 N = 148,100N$$

Step 3: Propeller Thrust

$$T_X = R_T = 148,100 N$$

For conventional inboard propulsion, the propeller thrust is directed along the shaft line; therefore,

$$T_Y = R_T \tan(\varepsilon + \tau_{BL}) = 148,100N \tan(7^\circ + 6.8^\circ) = 36,400 N$$

Horizontal component of propeller thrust acts at 1.5m below waterline, or $(1.5m + \frac{L_P}{80}) = 1.82m$ below model thrust line
 Horizontal component of propeller thrust produces a bow-up pitching moment of $+(1.82m)(148,100N) = +269,500 Nm$
 Vertical component of propeller thrust acts 2m ahead of transom, or 7m aft of LCG
 Vertical component of propeller thrust produces a bow-down pitching moment of $-(7m)(36,400N) = -254,800 Nm$

Step 4: Effective Displacement

The effective displacement is equal to the weight of the boat minus any lift forces developed by the propeller thrust or appendages.

$$W_E = W - \sum L_i = W - T_Y - L_{APPENDAGE} - L_{FLAP} = 736,000N - 36,400N - 0 - 50,000N = 649,600N$$

Step 5: Sum Moments

Positive moments are bow up

Still air resistance	+ 17,200 Nm
Twin-Screw Appendages	-58,300 Nm
Horizontal Propeller Thrust	+269,500 Nm
Vertical Propeller Thrust	-254,800 Nm
Trim Flap	-295,000 Nm
Total	-321,400 Nm

Step 6: Effective LCG

$$LCG_E = LCG - \frac{\sum M}{W_E} = 9m - \frac{-321,400Nm}{649,600N} = 9.49m$$

Step 7: Iterate

Enter standard series charts with $\frac{LCG_E}{L_P}$ and $\frac{L_P}{\nabla_E^{1/3}}$

$$\frac{LCG_E}{L_P} = \frac{9.49}{25} = 38\% \quad \nabla_E = \frac{W_E}{\rho g} = \frac{649,600N}{1025 \frac{kg}{m^3} \cdot 9.81 \frac{m}{s^2}} = 64.6 m^3 \quad \frac{L_P}{\nabla_E^{1/3}} = \frac{25 m}{(64.6 m^3)^{1/3}} = 6.2$$

Both of these parameters are still within the range of applicability of Model 2738. Bare-hull results:

Residuary Resistance to Weight Ratio	$\frac{R_R}{W} = 0.095$
Mean wetted length ratio	$\frac{L_M}{L_P} = 0.5$
Baseline trim angle (deg)	$\tau_{BL} = 6.5 \text{ degrees}$
Resistance (N)	$R_T = 89,400 N$
Effective Horsepower (kW)	$EHP = 1840 kW$

The appendage drag and moment calculations from steps 2-6 are repeated, using the original weight and LCG for computation of moments, but the resistance and trim values from the hull calculated using the effective LCG and effective weight.

Drag		Lift		Moments	
R_{HULL}	89,400 N	W	736,000 N	M_{RWIND}	+17,200 nm
R_{WIND}	6,400 N	T_Y	32,600N	$M_{RAPPENDAGE}$	-58,300 Nm
$R_{APPENDAGE}$	37,400N	L_{FLAP}	50,000 N	M_{TX}	+238,000 Nm
R_{FLAP}	2900 N	W_E	655,000 N	M_{TY}	-247,700 Nm
R_T	136,100 N			M_{LFLAP}	-295,000 Nm
				LCG_E	9.48m

Effective displacement, W_E and effective center of gravity, LCG_E are nearly identical to the values used in the 2nd iteration, therefore no more iterations are necessary.

$$\text{Effective Horsepower with Appendages (kW)} \quad EHP = (136,100N)(20.6 m/s) = 2800,000W = 2,800 kW$$

Appendage Example Conclusion

Two iterations were required to converge on a solution including the effects of wind and appendages. The total resistance (with wind, appendages, flaps, etc) is 136,100 N and the effective horsepower is 2800 kW. The hydrodynamic trim trim, $\tau_H = \tau_{BL} + \tau_{0.25} = 5.7 \text{ degrees}$ -- below the porpoising limit of 6.1 degrees. This hull should be stable. Also, the trim tabs provide added ability to adjust trim.

Discussion

Roger Compton, Member

Mike's undergraduate thesis was a nautical version of "A Brief History of the World" as it applied to high-speed motorboats. Comprising two volumes, it still holds the record for the lengthiest Webb thesis. Small, high-speed motorboats was – and still is- Mike's passion. It is great to see him acknowledge some great names of the past and their contributions – Ken Davidson, Gene Clement, Don Blount, as well as J.P. Day and R.J. Haag. It is also great to see him collaborate with some real giants in the field of planing boat technology like Dan Savitsky and Jacques Hadler. Refocusing our attention on the results of extensive and carefully conducted experimental investigations like Series 50 using one meter-long models, and on the results of Day and Haag's Webb thesis with even smaller models in the days before electronic dynamometry and computer-based data acquisition and analysis, is an important service to today's small boat designers. "Yes, Virginia, there can be meaningful and relevant experimental results from carefully-conducted small model tests and without Microsoft or Apple!"

As Mike made all of the edits that I suggested, I have no technical questions to pose at this time. Great job, Mike, and keep up the good work at USNA.

Dejan Radojic, Member

During the last few decades Series 50 was regarded to be somewhat obsolete due to:

- A. The manner in which it was originally presented – stemming from the well-known Taylor Standard Series for high speed (displacement) ships, and
- B. The hull form, which if applied solely for the planing regime, has changed since the Series 50 was tested.

Recognizing these problems, the author re-analyzed Series 50 data and presented it similarly to that of Series 62. The author should be congratulated for that, as the re-analysis was not as simple as it may look (problems with the transitional flow were evident and large number of measured data had to be approximated or recalculated).

Nevertheless, the evaluation of wetted area should probably be additionally described, as errors in its value might introduce error in frictional resistance. Consequently, author's discussion on this subject (in the first place impact on extrapolated results etc.) is most welcome.

Then comes question regarding presentation of the results; mathematical representation is omitted, as the re-analyzed data are presented only in tabular and graphical format. Adequate mathematical models (e.g. regression techniques) for evaluating residuary resistance and dynamic trim are missing, and, without them, computer usage as well. Mathematical modeling would also fair the data and probably give new insight into some relationships which, due to usual scatter of the data, can't be

seen in the present format. Also, ranging of the displacements of +/-10% is relatively large, as well as variations about all mean curves. This prevents the published (averaged) data from being used for future mathematical models.

Concerning the above-mentioned problems, the author has re-surfaced Series 50 to the professional community, hence should be congratulated for that too. The revamped Series 50 enables a slightly different viewpoint to its hull form and probably application too. Namely, although it is obsolete for purely planing regime, Series 50 could be attractive for the semi-planing or semi-displacement regimes (up to $F_{NV} \approx 3$ or $F_{NL} \approx 1$), as it has a warped bottom with negative keel angle and deep forefoot. This enables placement of less inclined propeller shafts, so the propeller tunnels extensively used nowadays might be avoided. Still, Series 50 should be compared, from the resistance viewpoint, to other semi-planing or semi-displacement hull forms as for instance NTUA, NPL etc.

It should be noted that the Series 50 hull form looks similar to that of contemporary ski-boats whose characteristics are small behind-the-boat wave-wake. This might imply that Series 50 hulls produce relatively small wake, but that yet has to be proved.

Finally I would like to congratulate the author again on his interesting and useful paper and to encourage him to produce the mathematical models suitable for programming.

Jacques B. Hadler, Member

The authors have done the small boat profession a great service by restoring an old small boat systematic series (Series 50) that had fallen into disuse. In the process they have corrected some of the deficiencies, used more modern nomenclature, and presented the results in a graphic form for easier use.

Although the authors have done a great deal of work to achieve the goal of bringing this series into the modern boat design world, I consider it incomplete. Today the professional world is almost totally computer literate, thus the resulting graphic work should be digitized for direct calculation on computers like other aspects of the boat design process. As an example I cite the propeller B-Series. The open water test results were first presented in graphic form to be used in predicting the power performance of propellers similar to the series propellers. In the late 1960's the test data was corrected for any test deficiencies, the data re-graphed using modern propeller nomenclature and digitized. Insofar as I know there are few, if any, that use the graphic form of the data in making propeller performance predictions today.

In closing, I encourage the authors to complete the fine work that they have started.

Author's Closure

The author would like to thank the three discussers for their insightful comments. The two main suggestions that they have made are to (1) amplify the discussion on how wetted area is determined, and the impact that errors in its value may have on extrapolated results and (2) present the data in a digital format that enables computerized computations. These are addressed as follows:

Wetted Area

Figure AR-1 shows a typical under-water photograph of a planing hull. The bottom of the model is striped at regular increments to facilitate reading the wetted lengths at the keel and the chine. At planing speeds, the flow separates cleanly off the chines and the transom, resulting in no side wetting. The wetted portion of the hull is illuminated in the photo, and the spray root appears as a dark shadow. Since the spray root line is fairly straight, the bottom area may be estimated as follows:

$$S = \frac{L_K + L_C}{2} G = L_M G$$

Where,

- L_K = Keel Wetted Length
- L_C = Chine Wetted Length
- L_M = Mean Wetted Length
- S = Surface Area
- G = Girth from chine-to-keel-to-chine

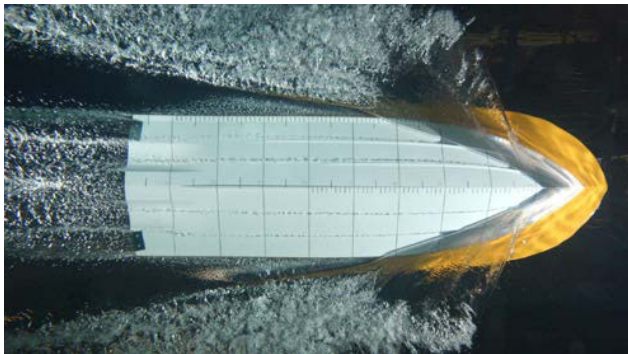


Figure AR-1: Typical Under-Water Photograph of Planing Boat (Courtesy of Davidson Laboratory)

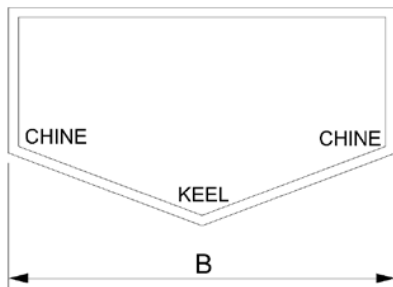


Figure AR-2: Cross-Section through Planing Hull

The girth from chine-to-keel-to-chine can be seen in Figure AR-2. Typically the girth is greater than the beam, B because of the deadrise. Savitsky (1964) gives the wetted area of prismatic planing hulls, $S = L_M \frac{B}{\cos \beta}$, where β is the deadrise angle.

Series 50 is not prismatic because it has taper and warp. The wetted surface area of Series 50 is determined by integrating the bottom area of the 3-D model of the hull. Figure AR-3 is a plot of cumulative area versus wetted length for the parent hull of the series. The data show a linear trend ($S = 0.962L_M B_{PX}$) up until the region of the bow, where there is a change in slope because of how narrow the bow is. For a planing hull, the bow is typically out of the water, and therefore additional complexity of the wetted surface relation to account for the bow was not justified.

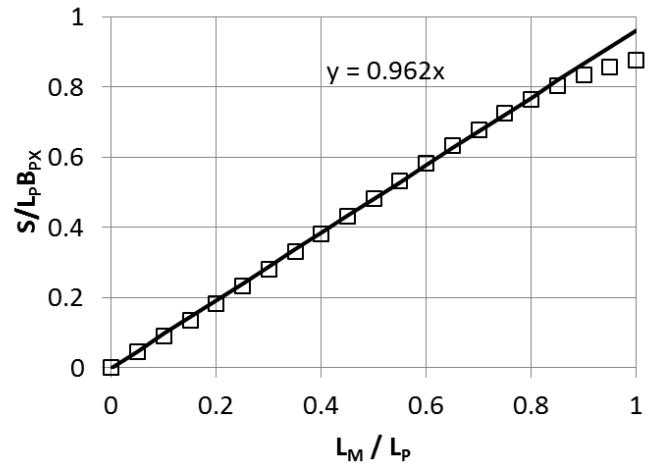


Figure AR-3: Plot of Cumulative Area

Dr. Radojic requested that I discuss the effects of errors in wetted surface area on the full-scale predictions. To illustrate the effects of errors in measurement of wetted surface area on the total resistance, start with the following equation describing the resistance expansion process:

$$\frac{R_{T,S}}{W} = \frac{R_{T,M}}{W} + \frac{R_{F,M}}{W} \left(\frac{C_{F,S}}{C_{F,M}} - 1 \right)$$

Where subscripts S and M represent Ship and Model. R_T is total resistance, R_F is frictional resistance and C_F is the friction coefficient. If an error in the wetted surface area, δS , is introduced, the equation becomes:

$$\frac{R'_{T,S}}{W} = \frac{R_{T,M}}{W} + \frac{R_{F,M}}{W} \left[1 + \delta S / S \right] \left(\frac{C_{F,S}}{C_{F,M}} - 1 \right)$$

The effect of errors in the wetted surface area depends on the friction coefficients of ship and model and also the percentage of resistance that is frictional. If a large portion of the total

resistance is frictional, errors in wetted surface have larger effects. Figure AR-4 was developed by assuming typical values of $C_{F,S} = 0.002$ and $C_{F,M} = 0.003$ and varying the percentage of model frictional resistance to total resistance. The figure shows that when frictional resistance is 50% of the total (a typical fraction for a planing hull running at optimum trim), a 10% error in wetted surface area results in only a 2% error in ship resistance. The figure shows that while it is important to measure the large variations in wetted surface area that occur on planing craft, extreme measurement precision is not necessary.

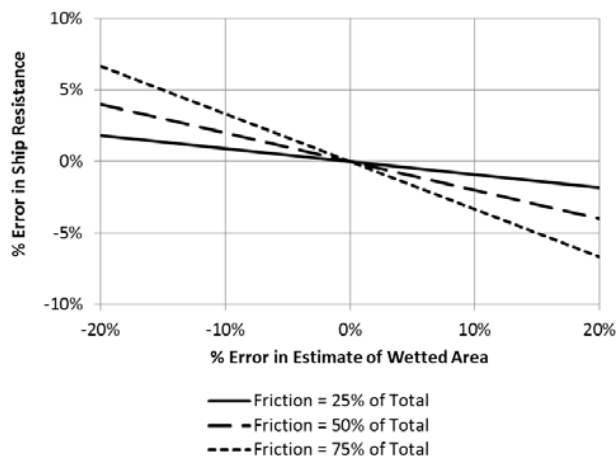


Figure AR-4: Error in ship resistance versus error in wetted surface area for various fractions of friction resistance to total resistance. Assumptions ($C_{Fm} = 0.003$, $C_{Fs} = 0.002$).

Computerized Format

Two of the reviewers pointed out the importance of presenting the series in a way that enables computer automation. The tabular presentation of the data readily enables an automated computerized lookup procedure. The advantages to developing a regression model of the series are the reduced number of terms, when compared to the full data tables, and the ability to smooth the data in multi-dimensional space.

In the months since the presentation of this paper at the SNAME Annual Meeting, the author has been contacted by Dejan Radojicic, and together they have been working with a team of students and recent graduates from the University of Belgrade, Serbia to develop a mathematical model for the Series 50.

